Dendritic Cells in Head and Neck Cancer Microenvironment : From Mechanisms to Biomarkers

Caroline Hoffmann

▶ To cite this version:

HAL Id: tel-02317812

https://theses.hal.science/tel-02317812

Submitted on 16 Oct 2019

UNIVERSITÉ PARIS-SACLAY

UNIVERSITÉ PARIS SUD

Comprendre le monde,
construire l'avenir

Dendritic Cells in Head and Neck Cancer Microenvironment: From Mechanisms to Biomarkers

Thèse de doctorat de l'Université Paris-Saclay préparée à l'Université Paris Sud

École doctorale n°582 CBMS (Cancérologie : biologie – médecine-santé)

Spécialité de doctorat: aspects moléculaires et cellulaires de la biologie

Thèse présentée et soutenue à Paris, le 08 octobre 2019 par

Caroline Hoffmann

Composition du Jury :

Eric Deutsch
UMR 1030 Radiothérapie moléculaire
Institut Gustave Roussy, Villejuif   Président

Marc Dalod
U1104 - Centre d'immunologie de Marseille
LUMINY (CIML)   Statut, Établissement (– Unité de recherche)   Rapporteur

Bénédicte Manoury
INSERM U1151-CNRS UMR 8253
Institut Necker Enfants Malades, Paris   Rapporteur

Marie-Carolyne Dieu-Nosjean
U1135 - Centre d'immunologie et de maladies infectieuses,
GH Pitié Salpetrière, Paris   Examinateur

Nicolas Manel
INSERM U932, Institut Curie, Paris   Examinateur

Vassili Soumelis
INSERM U932, Institut Curie, Paris   Directeur de thèse

Thèse de doctorat

TABLE OF CONTENTS

PREFACE

Why a Head and Neck surgeon studies dendritic cells and tumor microenvironment?

I have so frequently been asked this question during my PhD that I thought to introduce this work with an answer. Precision medicine and immunotherapy were the main axis of research and innovation in the last two decades in the field of oncology. Immunotherapy has radically changed the prognosis of melanoma patients. The benefit is however limited to a minority of patients in most other solid tumors, including head and neck squamous cell carcinomas (HNSCC), with only 13 to 15% of overall response rates to PD-1 blockade, the most advanced immunotherapy to date (1). The efforts on predictive biomarkers for immunotherapy have reached clinical impact with the example of PDL1 companion test for PD-1 blockade (2). However, this is far from precision medicine in which our goal would be to have a complete ID of each cancer including its histological features, but also genomic alterations and phenotyping of its immune and non-immune microenvironment. This ID would allow us to propose a personalized treatment according to tumors aggressiveness and to the presence of genomic and immune actionable targets. Technological advances allow us to obtain such tumor ID by large screening techniques, but for obvious economic reasons and also to impact our patient outcomes we need to identify the best biomarkers to be screened and the appropriate combinations of treatment reaching efficacy while limiting toxicity. For example, despite theoretical justification, monotherapies targeting a specific genomic alteration failed to improve patient's outcome so far (3).

Head and neck cancer surgery already offers precision medicine with customized resection of tumors for each patient, and is the most efficient treatment to date (4). This is at cost of removing essential anatomical structures leading to functional impairments and their important negative impact on patients' quality of life. Also, adjuvant treatments like radiotherapy or chemotherapy are often required and add to the global treatment toxicity. Despite those heavy treatments, a non-negligible number of our patients will present early and severe recurrences, because of resistance to all those conventional treatments. We are, to date, unable to predict such poor outcomes and additionally don't know how to treat them efficiently. This is how a head and neck surgeon enters Vassili Soumelis' team in the U932 Immunity and Cancer unit, with the objectives of identifying high-risk patients and better understanding dendritic cells (DC) biology to gain insight on how to better exploit the therapeutic potential of this key cell type for anti-tumor immune response.

In this manuscript a short introduction of the head and neck cancer field will be followed by the state of the art on DC activation in general and in cancer in particular. The results section

will present a paper showing that MMP2 has a great potential to become a clinical-grade prognosis biomarker for resectable oral cavity cancers (OCSCC), with the prospect of biomarker driven treatment intensification trials, and a second paper giving a new perspective on DC activation programs and their functional impact, with the prospect of guiding innovation and treatment combinations in immunotherapy. Another great approach to decipher cancer biology and the resistance mechanisms to immunotherapy are window-of-opportunity trials in which pre-and post-treatment samples allow intra-patient comparison of treatment effects, in addition to the comparison of responders and non-responders, to identify predictive biomarkers. We will be, with Christophe Le Tourneau, the principal investigators of such trial with M7824, a bifunctional fusion protein targeting tumor growth factor beta (TGF-β) and programmed cell death protein ligand 1 (PDL1), funded by Merck and GSK. I prepared the protocol of this investigator sponsored study and will lead its translational research. The synopsis of this trial is available in Annex 5.2.

Art is about opening possibilities, possibilities links to hope, we all need hope.
The music of strangers: Yo-yo Ma and The Silk Road Ensemble
Same applies to Science

LIST OF ABBREVIATIONS

AIM2	Absent In Melanoma 2
APC	Antigen presenting cells
AS DC	Axl+Siglec6+ DC
CARD	Caspase recruitment domain
cDC	Conventional dendritic cells, or myeloid dendritic cells
CDP	Common DC progenitors
CDS	Cytosolic DNA sensors
cGAMP	Cyclic-GMP-AMP
cGAS	cGAMP synthase
CLR	C-type lectin receptor
CR	Complement receptors
CRD	Carbohydrate recognition domain
CyTOF	cytometry by time of flight
DAI	DNA-dependent Activator of IFN regulatory factors
DAMP	Damage associated molecular pattern
DC	Dendritic Cells
DC-SIGN	DC-specific ICAM3-grabbing non-integrin
DNGR-1 or Clec9a	DC NK lectin group receptor-1
ECM	Extracellular matrix
ENE	Extradodal extension
FcR	Fc receptors
GM-CSF	Granulocyte-Macrophage Colony-Stimulating Factor
GO	Gene Ontology
HMBG1	High-mobility Box 1
HNSCC	Head and neck squamous cell carcinoma
HPV	Human Papilloma Virus
HSP	Heat shock proteins
ICOSL	Inducible T cell costimulatory ligand
IDO	Indoleamine 2,3-dioxygenase
IFN	Interferon
IHC	Immunohistochemistry
IL	Interleukin
ITAM	Immune-receptor tyrosine-based activation motifs
ITIM	Immune-receptor tyrosine based inhibitory motifs
Jak	Janus kinase
LPS	Lipopolysaccharide
LT	Lymphotoxin
MBL	Mannose-binding-lectin
MDA5	Melanoma differentiation-associated gene 5
MHC	Major Histocompatibility Complex
Mincle	Macrophage-inducible C-type lectin
MMAC	Mono-macrophages
Mo-DC	Monocyte derived dendritic cells
NFkB	Nuclear factor kappa-light chain enhancer of activated B cells
NLR	NOD-like receptors
OCSCC	Oral cavity squamous cell carcinoma
PAMP	Pathogen associated molecular pattern
PBMCs	Peripheral Blood Mononuclear Cells
PD1	Programmed cell death protein 1
pDC	Plasmacytoid dendritic cells
PDL1	Programmed cell death protein ligand 1

PNI	Perineural invasion
Pre-DC	DC precursors
PRR	Pattern recognition receptors
RAGE	Receptor for advanced glycation end products
RIG	Retinoic acid-inducible
RLR	RIG-1-like receptors
RNAseq	RNA sequencing
SCC	Squamous cell carcinoma
STAT	Signal transducer and activator of transcription
STING	Stimulator of interferon genes
TCGA	The Cancer Genome Atlas
Tfh	T follicular helper
TGF	Tumor growth factor
Th	T helper
TLR	Toll like receptor
TMB	Tumor mutational burden
TME	Tumor microenvironment
TNF	Tumor Necrosis Factor
TNFRSF	Tumor Necrosis Factor superfamily receptor
TNFSF	Tumor Necrosis Factor superfamily
Treg	Regulatory T cell
TREM	Triggering receptor expressed on myeloid cells
TSLP	Thymic stromal lymphopoietin
UICC	Union for International Cancer Control
VE	vascular embols

INTRODUCTION

1. INTRODUCTION

1.1 Head and neck squamous cell carcinoma

1.1.1 Epidemiology, Current practice and place of immunotherapy

Head and neck cancers represented 64 690 new cases in 2018 in the USA and were responsible for 13 740 disease-related deaths (5). The present thesis is limited to the most frequent type of head and neck cancers that are Head and Neck squamous cell carcinoma (HNSCC). Four main anatomical locations are involved: oral cavity, oropharynx, larynx and hypopharynx, which altogether encompass a heterogeneous group with regard to risk factors, treatment modalities and prognosis. There are 3 main risk factors for HNSCC: tobacco, alcohol and human papilloma virus (HPV). Tobacco and alcohol are risk factors for all 4 locations, although with different degrees of importance. This epidemiology explains the predominance of males among HNSCC patients (72% in 2018, USA) (5). HPV is a risk factor for the occurrence of cancer in the oropharyngeal lymphoid tissues (tonsil and base of tongue). HPV-positive oropharyngeal cancers are associated to an increased radio-chemo-sensitivity and to better prognosis as compared to the other HNSCC (6). Although HPV has also been identified in around 10% of the 3 other locations, its role and impact are still debated.

Most human cancers are classified according to the TNM stage: "T" describes the primary tumor extension and ranges from T1 (smallest) to T4 (largest); "N" describes the regional lymph node status and ranges from N0 (no invaded lymph node) to N3 (worse lymph node extension); "M" describes the metastatic status as being M0 (no distant metastasis) or M1 (one or several distant metastasis). The different combinations of TNM stages are gathered according to their prognostic value into 4 Union for International Cancer Control (UICC) stages ranging from I (earliest cancers) to IV (most advanced cancers). Treatment algorithms for HNSCC are rather complicated, because they take into account the tumor precise location and size, with detailed analysis going beyond the TNM stage. Here, only the treatment algorithm of primary OCSCC will be exposed, for a better understanding of the article in the result section 3.2. OCSCC are treated by primary surgery, with the obvious exception of unresectable tumors that undergo primary radio-chemotherapy, or chemotherapy alone in the case of distant metastasis (7). After surgery, the clinical and imaging information gathered in the pre-operative period are analyzed together with the histopathological parameters defined on the operative specimen, in order to determine the post-operative course. The major risk factors are T3 or T4 stage, N2 or N3 stage, presence

of extranodal extension and positive surgical margins. Minor risk factors are N1 stage, the presence of perineural invasion and/ vascular embols, the latter being defined by the presence of cancer cells in the lumen of vessels (8). HPV status, differentiation index and mitotic index are not validated risk factors and do not influence treatment decision. Based on their health status, their age and these clinical prognostic parameters, our patients undergo close surveillance, adjuvant radiotherapy, adjuvant chemo-radiotherapy or adjuvant radiotherapy combined with cetuximab, the only targeted therapy validated to date.

With this standard of care, around 25% of primary resectable OCSCC patients will present with recurrence within 2 years (9), (10), (11). Only 25% to 50% of these recurrences will be eligible for a salvage surgery, the best therapeutic option in this setting (12), (13), (14). More than 50% of these patients will die within the following 2 years despite treatment for their recurrent disease (11), (15). These outcomes, associated to the fact that we are to date unable to predict which patient will present with such severe recurrence, were the starting point our work on OCSCC biomarkers (Results section 3.2).

Nivolumab and Pembrolizumab are anti-PD1 immunotherapies that are part of the standard of care for second line chemo-resistant recurrent and advanced tumors, since 2017 and 2018 respectively, as a result of the CheckMate-141 (16) and Keynote-040 trials (17). In this setting the overall response rates were 13.3% and 14.6%. It is important to mention that some unexpected prolonged responses were observed that had never been observed so far with chemotherapy or targeted therapy regimens. However, these response rates remain limited and way beyond those observed in melanoma, which prompt us to better understand how to manipulate patients' immune system. Immunotherapies are currently under evaluation in multiple clinical settings, with various treatment schedules, and with various targets, molecules and treatment combinations. Since immunotherapy is expected to initiate or boost the anti-tumor immune response, it is likely that it should be more efficient if the treatment is initiated in the presence of the tumor, rather than after its removal. Anti-cancer treatments given before surgery are defined as neoadjuvant treatments. Specifically, for stage III and IV untreated OCSCC, the ongoing worldwide phase III trial KEYNOTE-689 is evaluating the benefit of short neoadjuvant pembrolizumab followed by surgery and post-operative treatment with pembrolizumab plus radio-chemotherapy.

Neoadjuvant chemotherapy has failed to show benefit in unselected stage III or IV HNSCC, possibly to the lack of power in a heterogeneous population undergoing multi-modalities treatments (18), (19). If we were able to identify aggressive OCSCC at the time of diagnosis, we may be able to evaluate the interest of neoadjuvant treatments in this selected population. Our remaining task would be to define which treatment would be the most

appropriate, by the mean of predictive biomarkers. The estimation of the expected response rate to PD-1 blockade was also one of the questions we tempted to address in this work.

1.1.2 Molecular drivers and pharmaceutical targets

The molecular drivers of HNSCC are separated according to HPV status. HPV proteins inhibit the tumor suppressors p53 and pRb and are considered as the molecular events initiating HPV-associated cancers. The carcinogenesis of HPV negative cancers include molecular events cumulating from benign mucosal hyperplasia, to dysplasia and eventually to cancer, which encompass among others losses of heterozygosity at loci 9p21, 3p21, 17p13 p53 mutation, Cyclin D1 amplification, PIK3CA amplification or mutation, and pTEN inactivation (20). Altogether HNSCC are mainly associated to the loss or inhibition of tumor suppressor genes, which are more difficult to target than driver oncogenes. This observation explains the absence of efficient targeted therapy to date for HNSCC. Ongoing developments to target mutant p53 might change the game in the next years (21). Some of the different targeted therapies and immunotherapies approved or under evaluation in HNSCC are represented in Fig 1.
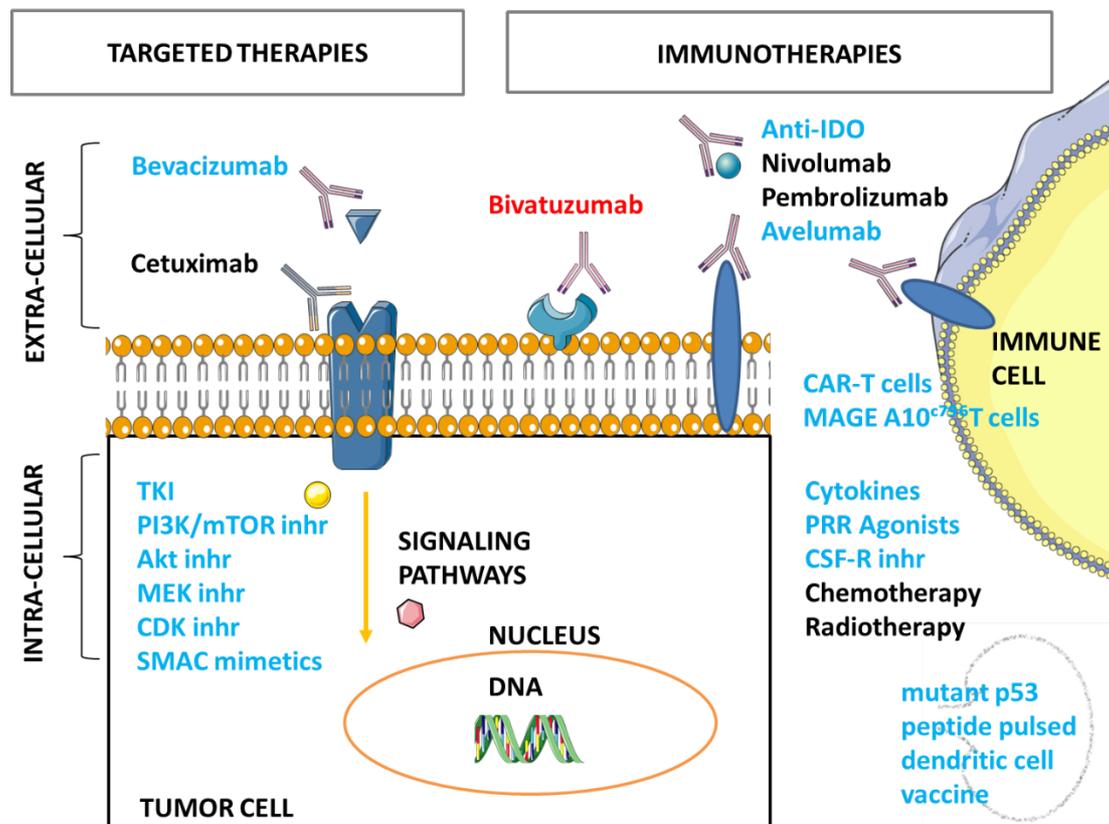
Fig 1- Selection of targeted therapies and immunotherapies for HNSCC. Color legend: Black: approved treatments, Blue: under evaluation, Red: evaluation stopped for absence of

efficacy. CAR: chimeric antigen receptor. Chemotherapy and Radiotherapy appear here because they may act as adjuvants for the immune system.

1.1.3 Molecular classifications and lack of biomarker

The molecular classification of HNSCC is largely ignored by the clinicians, because of the absence of a consensus in this field, with 4 to 6 proposed molecular classes, and above all because those molecular classes did not have any relevant clinical impact (22), (23), (24), (25). De Cecco et al. published the largest analysis to date, based on 1386 tumor and 138 healthy samples. They identified 6 molecular classes: "classical" HPV-negative, 2 "basal" classes, 1 "mesenchymal", 1 "immuno-reactive", 1 "atypical HPV-positive" grouped with HPV-negative "HPV-like" tumors. Interestingly, single cell analysis of OCSCC has recently shown that the transcriptome of cancer cells was similar in the mesenchymal and the basal tumors, and that it was the frequency of fibroblasts that explained the different signatures identified by bulk RNA sequencing. Basal and mesenchymal tumors are respectively poorly and highly infiltrated by fibroblasts.

In the absence of prognostic or theragnostic impact of the molecular classifications, many individual biomarkers or signatures have been proposed for OCSCC, but again, none of them has been implemented in clinical practice (26). One explanation is that many published studies did not follow the REMARK criteria (27) that is a checklist of methodological requirements aimed at increasing the quality of biomarker studies, to eventually promote clinical translation. Despite hundreds of reports, few have reached a sufficient level of evidence by combining multivariate analysis and the presence of a validation cohort. Levels of evidence for tumor marker studies range from 1 (highest) to 5 (lowest) (Table 1) (28) (29). Dunkel et al. proposed the CD44lowHIF1ahigh signature quantified by immunohistochemistry (IHC) with a level of evidence of 2b, but restricted to stage I OCSCC (30). A study on OCSCC data from The Cancer Genome Atlas (TCGA) and 2 independent datasets from Gene Expression Omnibus (GEO) identified in multivariate analysis a seven-CpG-based methylation signature predicting overall survival (31). However, this signature was not confronted to all major clinical and histopathological parameters cited in 1.1.1. The same caveat appeared in a study that proposed a histomorphometric-based image classifier of nuclear morphology, established in a retrospective cohort of OCSCC patients from a single institution, randomly divided in a discovery and a validation cohort (32).

Level of evidence	Study type
1a	Systematic review of prospective controlled study
1b	Individual prospective controlled study
2a	Systematic review of prospective-retrospective studies
2b	Individual prospective-retrospective using samples banked prospectively in the context of a clinical trial or register
3	Large retrospective studies
4	Small retrospective studies, Case series
5	Expert opinion, pilot studies

Table 1 – Levels of evidence according to the study type for biomarker identification

1.1.4 Concept of tumor microenvironment

Tumor microenvironment (TME) is defined as the cellular environment in which tumor cells are surrounded by blood vessels, immune cells, fibroblasts, and the extracellular matrix (ECM) (33). This concept integrates the work of geneticists, immunologists and biologists working on non-immune cells. Concerning the immune microenvironment of tumors, the TCGA data was used to propose a pan-cancer classification, by mining immune gene expression in bulk RNA sequencing data from tumor samples. Six immune groups of cancer have been proposed: C1 "Wound healing", C2 "INF-γ dominant", C3 "Inflammatory", C4 "Lymphocyte depleted", C5 "Immunologically quiet" and C6 "TGF-β dominant" (34). HNSCC were mainly "INF-γ dominant", although the classical molecular class, and to a lower extended the mesenchymal and the atypical classes, were also found in the "wound-healing" group. Almost none of the HNSCC samples were classified in the C3 to C6 groups. This classification allows a first level of resolution of the immune landscape of cancers, but lacks further resolution for each individual cancer. A study dedicated to HNSCC using 280 TCGA samples found that these tumors had the highest regulatory T cell (Treg) to CD8+ T cells ratio as compared to other cancers. However this ratio was higher in inflamed "immune high" tumors than in the non-inflamed "immune low" tumors suggesting that inflamed tumors might also have the highest level of immunosuppression (35). These 2 studies have the interest of analyzing large cohorts of patients, but the extrapolation of immune gene expression into estimated "real" immune infiltration is imperfect. Chakravarthy et al. showed that the deconvolution of methylation data is more accurately correlated to flow cytometry data than RNA data (36). They were able to show that inflamed HNSCC were enriched in CD8+T cells, B cells and Treg, when non-inflamed tumors were enriched in fibroblast and neutrophils. With the idea of understanding the link between cancer cell genomic alteration and the immune infiltration of tumors, they compared the driver mutations between inflamed and non-inflamed tumors and found few and minor statistically significant differences. This observation highlights the complexity of the TME.

1.2 Dendritic cells

1.2.1 Basics on dendritic cells and immunology

1.2.1.1 Basic concepts of the immune system

The immune system is aimed at protecting the host from pathogens, while respecting auto-antigens. It is composed of the two innate and adaptive interplaying systems. The innate immune system is composed by cells, such as macrophages and NK cells, which have the capacity to defend the host from pathogens recognized rapidly with, in the general case, a broad specificity, by pattern recognition receptors (PRR) that recognize non-self conserved microbial molecules or altered-self molecules, and have phagocytic or cytotoxic capacities. The adaptive immune system provides pathogen-specific responses, such as antibody production by B cells or T-cell mediated cytotoxicity, after cell selection via antigen-specific receptors among a large repertoire. The efficiency and the specificity of the adaptive immune response are at the cost of more complexity, the need of more cell-cell interactions and an increased delay in the response. The adaptive immune system is well known for its capacity of developing a memory against those antigens, which is the basis for vaccination. However, some innate immune cells such as NK cells may also develop memory, in the context of infection or cancer (37). Those 2 systems interplay via the antigen presenting cells (APC), which can internalize antigens from their microenvironment, to process them into peptides, to link them to major histocompatibility complex (MHC) molecules, and to present the peptide-MHC complex at the membrane to T cells. Those complexes will be recognized by the CD4+ or CD8+ T cells that have a receptor matching each specific combination of peptide-MHC. Upon activation CD4+ T cells expand and become effector T helper (Th) cells (38), specialized in coordinating the responses of the other adaptive cells that are the antibody-producing B cells and the cytotoxic CD8+ T cells, which primary function is to kill infected cells.

1.2.1.2 Discovery and definition of dendritic cells

DC are hematopoietic cells that represent 0,1-0,5% of white blood cells (39) and are also found in most tissues, among which the oral and intestinal mucosa (40). DC were first described in 1973 by Ralph Steinman when he identified large stellate cells from mouse spleen among the cells that were adherent to the glass surfaces *in vitro* (Fig. 2) (41). He

pursued a lifelong research on those cells that he described in 1978 as "100 times more effective than other major cell subclasses--i.e., B and T lymphocytes and macrophages" to stimulate primary mixed leukocyte reaction in mice, as measured by the increase in cell proliferation (42). Their increased capacity to activate T cells as compared to other antigen presenting cells was confirmed in humans in 1982 (39). The gross function of DC is now well established: DC circulate in blood and patrol into tissues were they constantly sample their surrounding environment by endocytosis and a process called macropinocytosis that allows them to capture antigens (43). In the presence of some activating signals, which will be described in greater details in this thesis, DC become activated and mature, and are able to migrate to the T cell-rich paracortex in lymph nodes. There, they present MHC-peptide complex to T cells, as well as membrane-bound costimulatory molecules, they secrete soluble modulating molecules, and finally activate the T lymphocytes that bear the matching TCR, a process called "T cell priming" (44). DC are described as the most potent cells to bridge the innate and adaptive immune responses.

Fig 2. Dendritic cell passport, DC picture from Steinman RM (41)

1.2.1.3 Dendritic cell functions

In the absence of abnormal antigen or activating signals, cells are loaded with self-antigens. They do not induce an adaptive immune response, even by the small fraction of mature T

cells that are specific for those antigens and persisted after thymic selection, because of the requirement of additional activating signals to eventually activate T cells. This system protects the host from autoimmunity. These mechanisms have been summarized by the three signal theory required to activate T cells: APC will provide the first signal by presenting the peptide-MHC complex, the second signal by membrane bound costimulatory molecules such as CD80/CD86 that bind CD28 on T cells, and the third signal by soluble priming cytokines (Fig 3) (45).
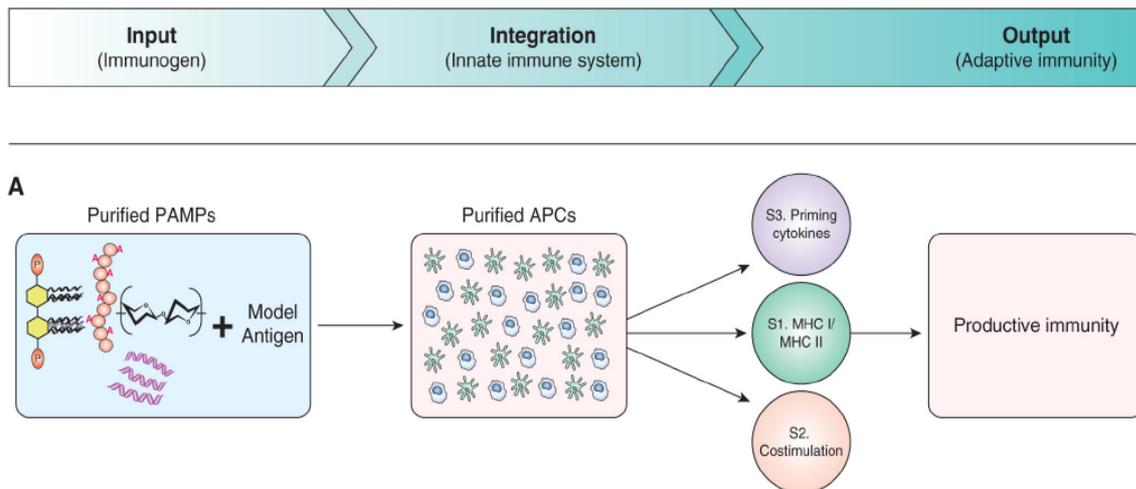

Fig 3 – The three signal theory linking the innate and adaptive immune systems (adapted from (46)

DC main functions are to provide those 3 signals, but they also participate to immune cell recruitment by the production of chemokines. Another specificity of DC, as compared to other APC, is to migrate from peripheral tissues were they captured antigens to the lymph nodes were they activate the T lymphocytes, under the control of the CCR7/CCL19-CCL21 axis (47). To deliver the first signal, that is antigen presentation, DCs internalize antigens by endocytosis, phagocytosis or micropinocytosis. Endocytosis is mediated by many different types of DC-receptors (detailed in section 1.2.1.5), that initiate the formation of clathrin-coated endocytic vesicles. Phagocytosis is also mediated by specific receptors and allows the internalization of particulate antigens, such as pathogens, apoptotic and necrotic bodies. Macropinocytosis is dependent on the cytoskeleton and not on receptors. It allows to sample large amounts of fluid that contains the soluble antigens (43). The uptaken antigens are processed into proteolytic peptides in the endosomes, and are eventually associated to MHC class I or MHC class II molecules (48), and presented at the plasma membrane. Peptide-MHC class I complexes will lead to direct CD8+ T cell activation, a process named "cross-presentation", first described by Bevan in 1976 (49). Peptide-MHC class II will lead to CD4+

T helper cell activation. According to the other DC molecules corresponding to signal 2 and signal 3 molecules, the CD4+ T cells will fine tune their final function, a process named T helper cell polarization, a concept first described by Mosmann in 1987 (50) . Since then, many different T helper profiles have been described and are presented in Fig 4 (38), (51), (52), (53), (54). The different T helper profiles correspond to different predominant transcription factors that induce the production of specific sets of cytokines, appropriate for the clearance of specific pathogens (intracellular, extracellular, parasites...), via their effect on surrounding immune and non-immune cells.
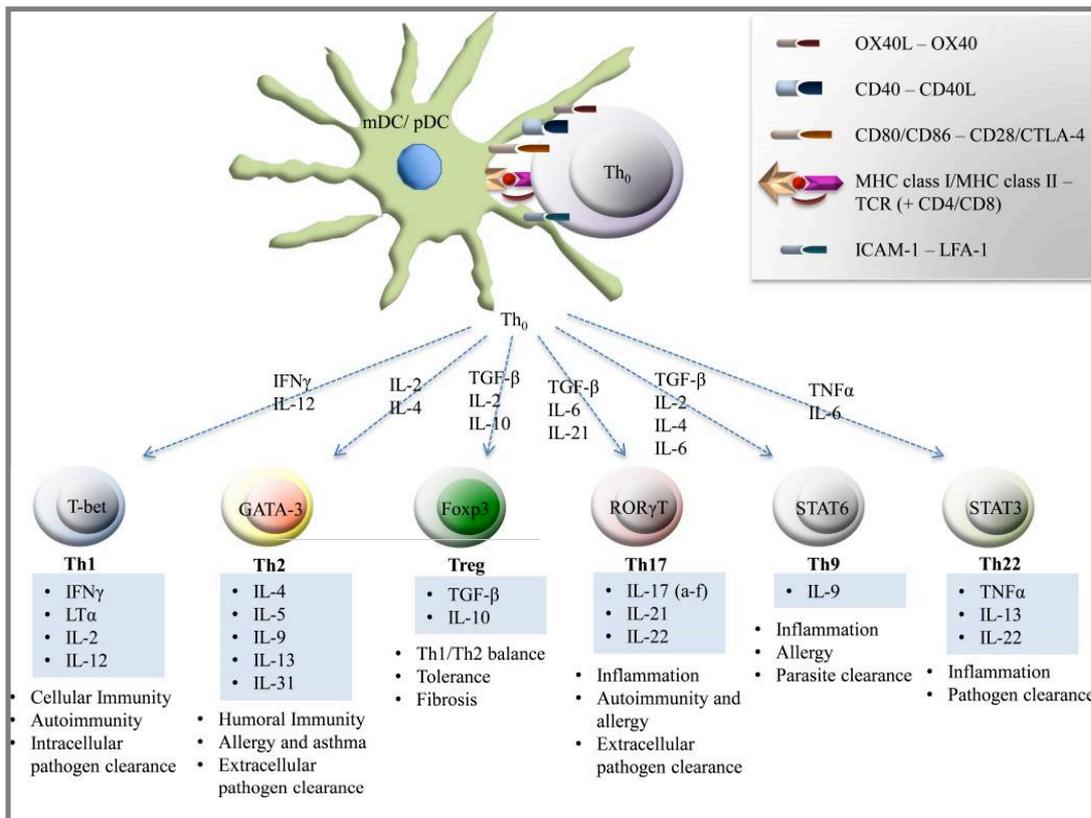
Fig 4 – CD4 T helper cell polarization according to the signals delivered by DC (54)

It is now clear that the role of DC and of our immune system in general is not restricted to infection and the detection of pathogens, but is also implied in human diseases like auto-immunity (55), cancer (56), asthma and allergies (57), atherosclerosis (58), bone diseases (59), and in the medicine-induced challenge that is transplantation (60), (61).

1.2.1.4 DC subsets

The identification of DC subsets, their markers, phenotype and function is still an evolving

field, which began in 1992 when Vremec and Shortman identified in the spleen and in the thymus of mice the CD8+ DC, using DC-enriched cell suspensions and 30 color FACS panels (62). Since then, many teams have contributed to the identification of the mice and human DC subsets in various tissues, including four recent landmark papers having been published between 2017 and 2019, that used the novel single-cell technologies to enrich the current knowledge on human blood DC (63) (64) (65) (66). The field will probably further evolve in the future by the study of tissue-infiltrating DC both at steady-state and in pathological contexts. Mouse DC biology has also bought a lot to the field, and the correspondence between mouse and human DC subsets is available in Annex 5.1.

(i) Ontogeny

DC in the periphery arise from a common DC progenitors (CDP) of the bone-marrow. Both in humans and mice, CDP differentiates first into plasmacytoid dendritic cells (pDC) or conventional (or "myeloid") DC precursors named "pre-DC". It was long debated if pDC gave rise to pre-DC or if they were two different subsets (67), since pre-DC express most pDC markers such as CD123, CD303 and CD304. Pre-DC may now be distinguished by their expression of CD33 and CX3CR1 (63). The early separation of pDC and pre-DC has been recently confirmed by barcoding technology (68). Pre-DC further differentiate into cDC1 and cDC2 the 2 main subsets of conventional DC.

(ii) Subsets markers

As mentioned above, peripheral blood DC subsets classification is still a matter of debate. To try to clarify the state of knowledge, I performed a comparison of the human DC subsets markers presented in table 2, using the markers identified by unsupervised analysis of blood DC by single-cell sequencing and confirmed by flow cytometry, or large-scale single-cell phenotyping by cytometry by time of flight (63), (64), (65), (66). These four studies have consensual data regarding cDC1 and pDC. Villani et al. described a 4 new DC subsets: DC2, DC3, DC4 and DC5 (64). The 3 other studies in part redefined the annotation of these subsets. DC2 indeed corresponded to cDC2 but require both BDCA1 and CD5 expression for their precise identification. DC3 were in fact corresponding to a mix of classical monocytes and CD5 negative cDC, referred as cDC3 by Dutertre et al. (65). DC4 were corresponding to non-classical monocytes, as shown by Dutertre et al. and Günther et al. using different technical approaches (65) (66). The DC5 (or AS-DC for AXL+ SIGLEC6+) subset was mainly composed of pre-DC (63), (65), (66). Most markers are not subsets-specific or even DC-specific, which explains why multi-marker strategies are required to

identify or purify DC and DC subsets (Results section 3.1). The different DC subsets may be identified in blood and in peripheral tissues, although with variations in proportions (Fig 5) (65).

See et al. labelling	cDC1	cDC2	Not described				Appear, but not studied	pre-DC for CD123+ & some pre-cDC2 for CD123lo *	pDC
Villani et al. labelling	DC1 CLEC9A+	DC2 CD1C+	DC3 CD1C+			Excluded by gating	DC4 CLEC9A- CD1C-	DC5 AS DC	DC6 pDC
Dutertre et al. labelling	cDC1	cDC2	Classical monocytes	cDC3 CD163-	cDC3 CD163+ CD14-	cDC3 CD163+ CD14+	Non-classical monocytes	Pre-DC, pre-cDC2 and AXL+cDC2	pDC
Günther et al. labelling	cDC1	Appear, but not detailed					Non-classical monocytes	Pre-DC	pDC
HLA-DR	+ +	+ +	+	+ +	+ +	+ +	+	+ +	+ +
CD4	+	+					+	+	+
CD11c	+	+	+	+	+	+	+	-	-
BDCA1 / CD1c	-	+ + +		+ +	+ +	Weak	-	-	-
BDCA2 / CD303	-	-	-				-	+ + (pre-cDC2)	+ +
BDCA3 / CD141	+	-	-				-	-	-
BDCA4 / CD304	-	-	-				-	+	+ +
CD123	-	-	-				-	2 populations / + +	+ +
SIGLEC6	-	Weak / +	-				-	+	weak
AXL	-	Weak / +	Weak / +	Weak / +	Weak / +		-	+	-
CLEC9A	+ +	- -	- -				- -	- -	- -
CD163	weak	weak	+	-	+	+	-	-	-
CD36	-	-	+				-	-	+
CD32B	-	+ + (CD32)	- / + (CD32)				-	-	-
CD5		+		-	-	-		+ +	
IntegrinB7		+	+						
CD200R		+							
CD271 (NGFR)								+	
CD182 (CXCR2)								+	
CD14		-	+ +	-	-	+	-		
CD16			-				+ +		
CD85d							+ +		
CD88	-	-	+	-	-	-	+ +		
CD89	-	-	+	-	-	-	+		
FceRIa	+	+ +	-	+	+	+	-		
HLA-DQ	+	+	-	+	+	+	-		
CD85g									+ +
CD1d		+ +							
BTLA	+ +								
CD135	+ +								
CD22								+ +	
CD169								+ +	
CD74	+	+							
CD109					+				
CD206						highest			
TLR2						highest			
TLR4						highest			

Table 2 – DC subsets markers comparison between the 4 publications of See et al.

(63), Villani et al. (64), Dutertre et al. (65), and Günther et al. (66). Cells in grey are for expressed markers (+), cells in light grey are for weakly expressed markers (weak), cells in white are for absent markers (-) or undetermined (empty cells). Markers and signs (+/-) in red are consistent between See et al. and Villani et al. publications, and those in black have not been reported in one or the other publication. Markers in green were reported in the study of Dutertre et al. and those in purple in the study of Günther at al.
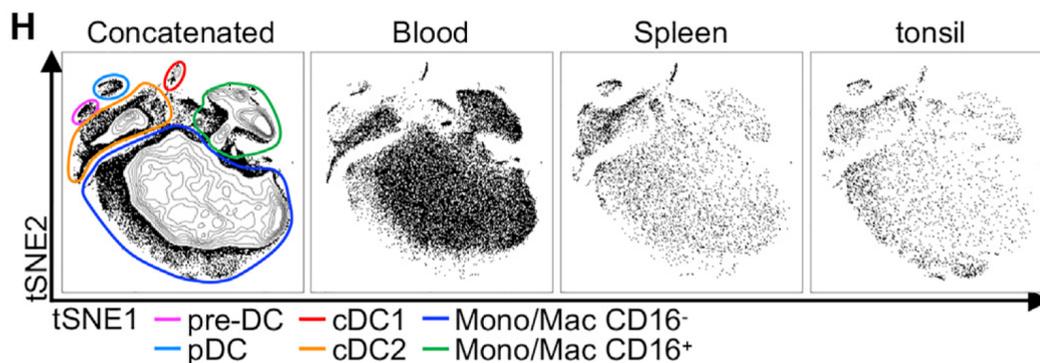

Fig. 5 Adapted from Dutertre et al. (65). Tissue distribution of monocytic cells and DC subsets in the human blood, spleen and tonsil analyzed by cytometry by time of flight.

(iii) cDC

cDC subsets presentation

cDC include all DC subsets except pDC and pre-DC. They express high levels of MHC-II molecules and CD11c+. The 2 main populations of dendritic cells, now labeled cDC1 and cDC2, were identified in 2000 (69) . cDC1 express CLEC9a and BDCA3 and are considered as the optimal subset for cross-presentation (70), when cDC2 express BDCA1 and preferentially activate CD4 T cells. Since the use of those markers to identify both subsets in flow cytometry, most researcher could observe a subset of BDCA3-BDCA1- cells, which was in general not further studied, as it is often the case for double-negative populations. Single-cell sequencing showed recently that they corresponded to a homogenous subset at the transcriptomic level in blood, labelled cDC4 by Villani et al. (64). They have also been described in benign tonsils and oropharyngeal cancer (71). However, as stated above, those cells have the highest similarities with non-classical monocytes (65). Villani et al. also proposed that cDC2 corresponded in fact to 2 subsets, DC2 and DC3, recognizable by their differential expression of CD32b (Table 1) (64). However, at the protein level CD32

expression appears more as a continuum and CD32b cannot be specifically used for cell sorting, in the absence of specific antibody available. Thus, the evidence of the existence of those 2 subsets and their differential function was still unclear. The recent papers of Dutertre at al. (65) and Günther et al. (66) confirmed that the cDC2 compartment is more heterogenous than the cDC1 compartment. Dutertre et al. propose a third class of DC, labeled cDC3, expressing BDCA1 but not CD5, and composed of a continuum of cells distinguishable by their expression of CD163 and CD14 (Table 2). Langerhans cells are one other DC subset and are found in the skin. As we could not identify them in the normal upper airway mucosa or in head and neck cancer tissue, they were not part of the scope of the present thesis and will not be further detailed.

cDC1

Human cDC1 or their mouse CD8a+ (blood and lymphoid tissue) or CD103+ (peripheral tissue) counterparts appear to be highly effective at performing cross-presentation (72), (73), as compared to other DC subsets, and are therefore ideal targets for anti-cancer vaccine, among other therapeutic uses. Human cDC1 can be identified by their expression of XCR1 and CLEC9A, and by their higher expression of BDCA3 as compared to other DC and cell types expressing this marker (74), (Results section 3.1). They are not potent inducers of regulatory T cells *in vitro*, which seems to be one of the functional difference with their mouse counterpart (75). The main transcription factors involved in cDC1 development and function are IRF8 and Batf3 (76). Mouse biology has improved a lot our understanding of cDC1, by the mean of cDC1-deficient mice that may be obtained by knock-out of *Irf8, Batf3, Nfil3, Id2*, and *Bcl6* (77). Steady-state human and mouse cDC1 express TLR3 at higher levels than cDC2 (74), and TLR8 but only mouse and not human cDC1 express TLR9 (70), (78). The high expression of TLR3 is of importance for cross-presentation in response to viral infection (79). In the lymph nodes cDC1 are sporadically dispersed in the T cell area, in line with their preferential role of direct CD8 T cell activation (80).

cDC2

On the other hand cDC2 are the main DC subset in the sense that they outnumber cDC1 in most tissues (80), (81), (Results section 3.1), (Fig 5). cDC2 are less efficient than cDC1 for cross-presentation, but similarly efficient at activating CD4 T cells and inducing the various Th polarization described in section 1.2.1.3 (Fig 4) (82). At steady-state, they are considered as regulators of the Treg/Th17 homeostasis in the barriers sites that are lung and intestinal tissues (83). They express the transcription factors *IRF4* and *ZEB2* and *IRF8*, but at lower levels than cDC1. Patients with autosomic recessive IRF8 mutations have a complete lack of classical and non-classical monocytes, pDC and cDC (76), (84). However, *IRF8*-deficiency

affected cDC1 and pDC but not cDC2 development in a model of human induced pluripotent stem cell differentiation (85). They express both the surface and intra-cellular TLR 1 to 8 (86) and are able to recognize most pathogens but those recognized by TLR9. cDC2 also overexpress ITGAM as compared to cDC1, a molecule implied in phagocytosis (74). In the lymph nodes cDC2 are clustered in the interfollicular area, in line with its preferential role of direct CD4 T helper cell activation (80).

(iv) Mo-DC, CD14+DC and inflammatory DC

Beside the cDC subsets presented above, another CD11c+ DC subset derived from CD14+ monocytes in humans (in Ly6C+ monocytes in mice) is restricted to secondary lymphoid tissues and peripheral tissue (87). This subset is labeled "Mo-DC" for monocyte-derived DC or sometimes CD14+DC or inflammatory DC in the cases were they are induced by some inflammation, which is not always easy to demonstrate in human (88), (89). They can be produced *in vitro* by stimulating for 5 days monocytes with GM-CSF and IL-4 (90). Mo-DC are efficient at promoting an inflammatory microenvironment, at antigen-uptake, antigen-presentation and cross-presentation (91), but their ability to migrate to lymph nodes is limited (81). We may thus hypothesize that *in vivo* Mo-DC interact with T cells preferentially locally in inflammatory peripheral tissues. It is important to mention that the terms CD14+DC and inflammatory DC are very confusing. A subset of blood cDC from healthy human expresses CD14, is closer to DC than to macrophages at the phenotypic and transcriptomics level, and was recently labeled CD14+CD163+ cDC3 (65). Whether HLA-DR+ CD11c+ BDCA1+ CD14+ cells identified in human inflammatory tissues arise from monocytes or are a subset of cDC3 remain to be elucidated. A simple flow cytometry approach determining their expression of the DC markers FceRIa and HLA-DQ as opposed to the monocyte markers CD88 and CD89 could address this question.

(v) pDC

Our team has recently reviewed in detail pDC phenotype and function, and I contributed to the chapter describing the state of knowledge on the role of pDC in cancer. This publication (92) is available in Annex 5.3. pDC were identified in 1958 by Lennert K and Remmele as a cell having the morphological features of a plasma cell, and located in the T cell area in lymph nodes (93). It was not until 1997 (94) that they were identified as a DC subset, and until 1999 that their main feature, that is a high efficiency at producing type I interferon (IFN) after stimulation, was described (95), (96). Their mouse equivalent was discovered in 2001 (97), and they match most human pDC features, although some differences in markers and cytokine production have been observed (92). As shown in the Table 1, steady-state pDC

express HLA-DR, CD4, CD303/BDCA2, CD304/BDCA4, CD123 (IL3 receptor), and CD36, but they do not express CD11c or CD1c/BDCA1 or AXL. Human pDC express the intracellular receptors TLR7 and TLR9 for the detection of single-stranded viral RNA and DNA respectively, but do not express TLR3 (98). They have a functional cyclic-GMP-AMP (cGAMP) synthase - Stimulator of IFN genes (cGAS-STING) pathway for cytosolic DNA sensing and type I IFN induction. pDC are less efficient than the other DC subsets at performing endocytosis or phagocytosis (99). pDC present antigens to CD4 T cells and can also perform cross-presentation (100). pDC also express surface receptors, among which cytokine-receptors for IL-3, IL-10, GM-CSF, TGF-β or TNF-α, which can induce pDC maturation or modulate TLR-induced maturation (92). In summary, pDC is the first subset to differentiate from other DC subsets during hematopoiesis and is specialized in the production of type I IFN after activation, mostly by viruses.

1.2.1.5 Dendritic cell receptors and signaling pathways

DC express at steady-state or upon activation different families of receptors that may be separated into 3 groups: PRR that are receptors for the direct recognition of pathogens and danger signals, receptors for indirect sensing of infection and inflammation, and the remaining receptors that serve the other DC functions and homeostasis. The first two groups will be detailed below, since they initiate the maturation process detailed in sections 1.2.2 and 1.2.3, and because some of their ligands were used in the manuscript presented in the result section 3.1.

(i) Pattern-Recognition Receptors

The direct recognition of pathogens and danger signals occurs via PRR that recognize pathogen-associated molecular pattern (PAMP) and damage-associated molecular pattern (DAMP) (Table 3). PAMP are small molecular motifs conserved within microbes. DAMP are molecules that are undetectable by the immune system at steady-state, but become exposed after cell stress or cell death (101). Well-known DAMP include high-mobility Box 1 (HMGB-1) and adenosine triphosphate (ATP). The main receptors for PAMP and DAMP recognition, as well as their natural or pharmaceutical ligands, are listed in Table 3. PRR include the family of Toll-like receptors (TLR), C-type lectin receptor (CLR), Cytosolic sensors that include cytosolic DNA sensors (CDS), NOD-like receptors (NLR) and RIG-1-like receptors (RLR), and DAMP receptors (Fig 6).
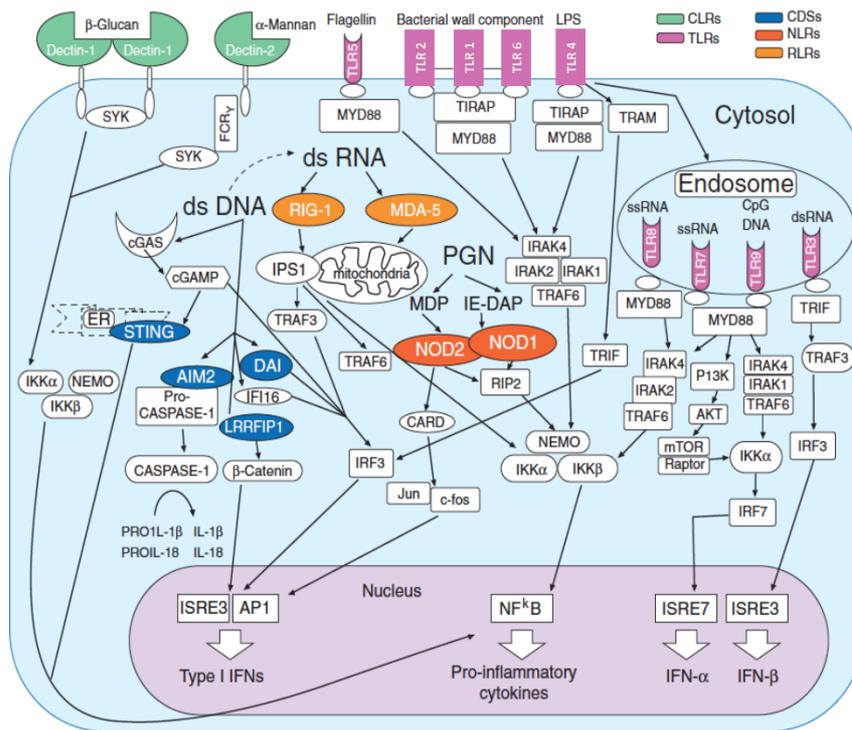
Figure 6. Signaling pathways associated to PRR, adapted from Shekarian et al. (102) (in particular, the TLR represented by a purple rectangle have been modified from the original figure, since they was a typing error so that they were all labelled TLR5)

Receptor	Ligand	Localization	Pathway	PRR agonist in clinical trial
TLR				
TLR1:TLR2 heterodimer	Lipomannans (mycobacteria), Lipoproteins Lipoteichoic acids (Gram-positive bacteria), Cell-wall b-glucans (bacteria & fungi), Zymosan (fungi), HKLM, HKSA, PAM3, HMGB1	Plasma membrane	MyD88/MAPK/ NFkB	Amplivant
TLR2:TLR6 heterodimer	Lipomannans (mycobacteria), Lipoproteins Lipoteichoic acids (Gram-positive bacteria), Cell-wall b-glucans (bacteria & fungi), FSL-1	Plasma membrane	MyD88/MAPK/ NFkB	-
TLR3	Double-stranded RNA (viruses), Poly I:C	Endolysosome	TRIF/TRAF3/ IRF3	PolyI:C, Rintatolimod, Hiltonol
TLR4	LPS (Gram-negative bacteria) Lipoteichoic acids (Gram-positive bacteria) HMGB1	Plasma membrane	MyD88/MAPK/ NFkB, TRAM/TRIF/ IRF3	LPS, GSK1572932A, G100, MPL(AS15)
TLR5	Flagellin (bacteria)	Plasma membrane	MyD88/MAPK/ NFkB	CBLB502
TLR7	Single-stranded RNA (viruses), Flu	Endolysosome	MyD88/MAPK/ NFkB	Imiquimod
TLR8	Single-stranded RNA (viruses), R848	Endolysosome	MyD88/MAPK/ NFkB	Imiquimod, Resiquimod, MEDI9197, Motolimod
TLR9	DNA with unmethylated CpG (bacteria and herpesviruses)	Endolysosome	MyD88/MAPK/ NFkB	CpG, CMP-001, MGN1703, SD-101, 1018ISS, Agatolimod
TLR10	Unknown	Plasma membrane	MyD88/MAPK/ NFkB	-
CLR				
Dectin-1 (CLEC7A)	Zymosan, b-glucan, HKCA, Curdlan, Mycobacteria	Plasma membrane	CARD9/NFkB	-
Dectin-2 (CLEC6A)	a-mannan, Mycobacteria	Plasma membrane	CARD9/NFkB	-
Mincle (CLEC4E)	Carbohydrate patterns (Fungi), trehalose dimycolate (Mycobacteria), SAP130 (dead cells)	Plasma membrane	CARD9/NFkB	-
DNGR-1 (CLEC9A)	Carbohydrate patterns (Fungi), F-actin (necrotic cells)	Plasma membrane	Syk kinases and cross-presentation	-
Clec2 (CLEC1B)	Podoplanin	Plasma membrane	Required for DC motility	-
CLECSF8 (CLEC4D)	a-mannan, trehalose dimycolate (Mycobacteria)	Plasma membrane	CARD9/NFkB	-

DCIR	Carbohydrate patterns (fungi)	Plasma membrane	ITIM inhibitory motif	-
MICL (CLEC12A)	Carbohydrate patterns (Fungi), uric acid, proteinaceous ligands (necrotic cells)	Plasma membrane	ITIM inhibitory motif	-
DEC-205	Keratin at acid pH only ((103)	Plasma membrane	Endocytic receptor	-
MMR	mannose, fucose, N-acetylglucosamine, glycolipid antigens (lipoarabinomannan)	Plasma membrane	Endocytic receptor	-
DC-SIGN	fucosylated glycans, mannose structures	Plasma membrane	ICAM-2 and ICAM-3 for T cell activation	-
MBL	glycan-associated mannose	Soluble		-
Cytosolic sensors				
NOD-like receptor	Peptidoglycans: IE-DAP (NOD1 / gram negative bacteria), MDP (bacteria)	Cytoplasm	RIP2/MAPK/ NFkB	-
AIM2	Cytosolic DNA, Flu		Caspase-1	-
ZBP1 (or DAI)	Cytosolic DNA		TBK1/IRF3/ NFkB	-
NLRP/NALP receptors	cell damage (eg. by toxins), downstream purinergic P2 receptors	Cytoplasm	CARD/ Caspase-1	-
RIG-1-like receptors	Short double-stranded RNA, 5' single-stranded RNA (RIG-1) (viruses), Long double-stranded RNA (MDA5), Flu	Cytoplasm	IPS1/TRAF3/ IRF3	BO-112 (MDA5)
cGAS	Cytosolic DNA	Cytoplasm, Endoplasmic reticulum	TBK1/IRF3/ NFkB	MIW815 (ADU-S100), MK-1454
Other DAMP receptors				
RAGE	HMGB1	Plasma membrane	MAPk/NFkB	-
TREM-1	TREM-1 ligand, soluble TREM-1, HMGB1	Plasma membrane	ERK/c-Fos/c-Jun/AP1, NFkB	-
P2X receptors	Extra-cellular ATP	Plasma membrane	Inflammasome	-

Table 3. PRR expressed by DC: classification, natural and pharmaceutical ligands, and corresponding signaling pathways. NFkB: Nuclear factor kappa-light chain enhancer of activated B cells

TLR

Jules Hoffmann was awarded in 2011 the Nobel Prize in Physiology or Medicine for the discovery in 1996 of the host-defense role of Toll receptor in adult fly. Similar receptors discovered in mammalians were called Toll-like receptors. There are 13 different TLR, but only 10 are expressed in humans (TLR1 to TLR10), whereas 12 are expressed in mice (TLR 1 to TLR 9 and TLR11 to TLR13, that will not be further detailed). Those 10 TLR of a broader specificity as compared to the antigen receptors of the adaptive immune response and have the advantage of being able to recognize PAMP that cover most pathogenic microbes. TLR3, TL7/8 and TLR9 are in the endocytic vesicles, whereas the other TLR1, TLR2, TLR4, TLR5 and TLR6 are located at the plasma membrane. They are expressed by DC, but also many other immune cell types, stromal cells, epithelial cells and even cancer cells. TLR signal through 2 main pathways: the MyD88 and the TRIF signaling pathways (104). After ligand binding, all TLR but TLR3 engage MyD88 adaptor molecule, that recruits IRAK proteins, which in turn recruit TRAF6. Upon phosphorylation, TRAF6 is dissociated from the receptor complex and binds TAK1 (TGF-β activated kinase), TAB1 and TAB2 to form a complex in the cytosol. This complex phosphorylates the kinases IkB which leads to the translocation of the transcription factor NFkB to the nucleus. In parallel TAK1 activates mitogen-activated protein (MAP) kinases signaling cascades leading to nuclear translocation of CREB and AP1. AP1 and NFkB activate the transcription of genes coding for cytokines, chemokines, MHC class II and costimulatory molecules. TLR3, but also TLR4, activate the TRIF signaling pathway. TRIF recruits TBK1 and TRAF3, and TRAM in the case of TLR4 activation. These complexes phosphorylate interferon regulatory factors (IRF) IRF3 and IRF7, which activate together with CREB the expression of interferon and a sub-class of interferon-inducible genes such as IFN-I, CXCL10 and CCL5. TRIF can also bind TRAF6 and induce cytokine production similarly to the MyD88 pathway. Finally, TLR7, TLR8 and TLR9 also induce interferon inducible genes via TRAF6 and IRF7, but without TRIF (105) (Fig 7). Eventually, these activation pathways are regulated by other autocrine and paracrine molecules, such as IFN-I itself (106), (105).
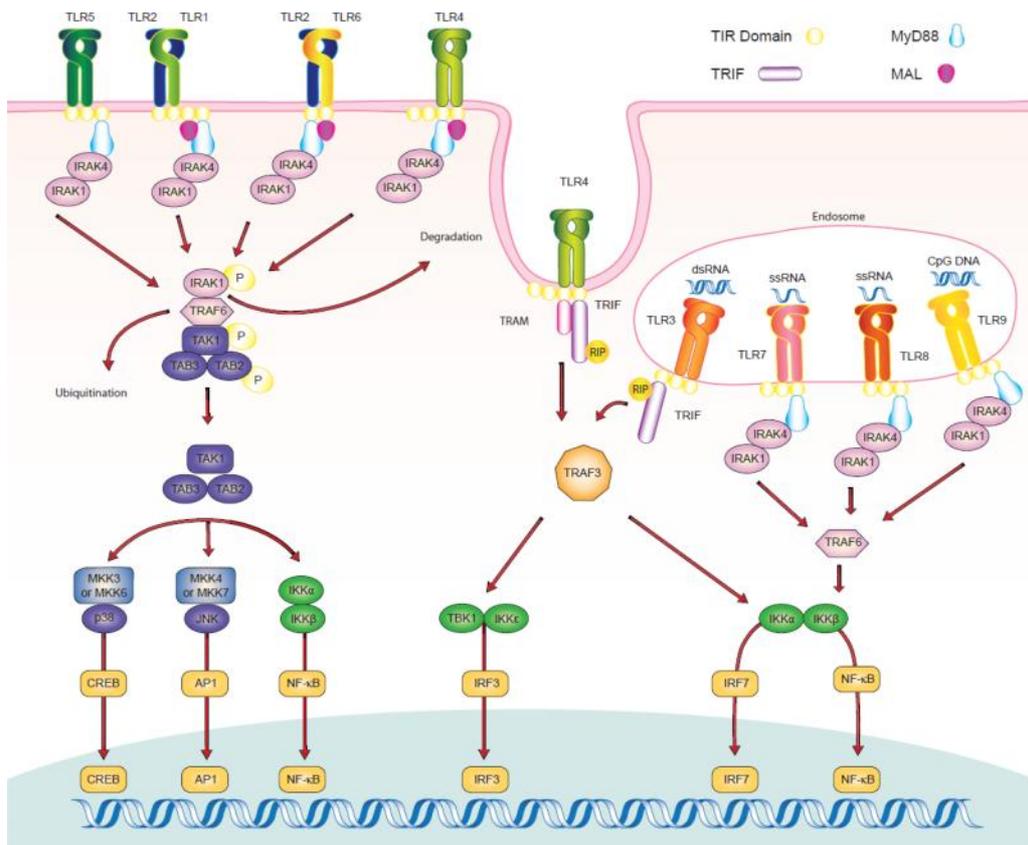
Fig 7- TLR signaling pathways (105).

CLR

C-type lectin receptors recognize mostly glycan structures of pathogens via their carbohydrate recognition domain (CRD). Only CLR having or cooperating with immune-receptor tyrosine-based activation motifs (ITAM) activate signaling cascade that primarily engage Syk kinases to eventually activate NFkB and gene transcription. The ITAM-signaling CLR are Dectin-1, Dectin-2, macrophage-inducible C-type lectin (Mincle), DC NK lectin group receptor-1 (DNGR-1) (also known as Clec9A), Clec-2 and CLECSF8. DNGR-1 is preferentially expressed on cDC1 and does not induce an inflammatory response despite its ITAM motif, but rather participates to the process of cross-presentation. Other CLR, such as DC immunoreceptor (DCIR) and myeloid inhibitory c-type lectin-like receptor (MICL) have immune-receptor tyrosine based inhibitory motifs (ITIM) that inhibit the immune response (40), (107). Other CLR are mainly involved in endocytosis and phagocytosis, such as MMR (CD206) (108), and DEC-205 (109), (110). DC-specific ICAM3-grabbing non-integrin (DC-SIGN) is a CLR that activates T cell by via ICAM-3 binding (111). Finally, mannose-binding-lectin (MBL) is a soluble CLR that undergoes conformational changes upon carbohydrate binding. It participates to host defense by direct inhibition of pathogen entry into the cell, opsonization, or activation of the complement cascade (112).

Cytosolic sensors

In addition to TLR and CLR that are primarily sensors of extracellular pathogens, DC express several families of cytosolic sensors of intra-cellular microbial products detailed in Table 2. A first family is composed of nucleotide-binding oligomerization domain (NOD)-like receptors (NLR), which are also expressed in macrophages and epithelial cells. NLR recognize peptidoglycans from bacteria, which have entered the cell by as a result of infection or by endocytosis. NLR have a caspase recruitment domain (CARD) for intra-cellular signaling. Upon activation, they induce NFkB activation via CARD/RIP2/TAK1/IKK signaling, similarly to TLR (113). Absent In Melanoma 2 (AIM2) and Z-DAN-binding protein 1 (ZBP1) also known as DNA-dependent Activator of IFN regulatory factors (DAI) are 2 other members of the NLR-family and recognize cytosolic DNA. AIM2 signals through caspase-1, to eventually induce pyroptosis (114). DAI also activates TBK1, IRF3 and leads to type I IFN production, but its knock-down does not significantly reduce the final amount of type I IFN produced upon activation (115), (116).

Another related family is the NLRP family that has a pyrin domain instead of the CARD domain. There are 14 NLRP identified in humans. NLRP3 is the best characterized, and its signaling leads to the formation of a multiprotein complex labelled the "inflammasome". It is activated upon cell damage such as membrane pores induced by toxins, or by activation of the purinergic P2 receptors like P2X7, which are receptors for extra-cellular ATP. Unlike NOD-1 and NOD-2, the inflammasome does not activate NFkB, but induces the production of inflammatory cytokines and death of infected cells (114).

A third family is composed of retinoic acid-inducible gene (RIG)-like receptors (RLR). RIG-1 and melanoma differentiation-associated gene 5 (MDA5) are members of this family and recognize respectively short and long double-stranded RNA produced by viruses within the cell (as opposed to TLR3, TLR7 and TLR8 that recognize extracellular viral RNAs) (113). RLR also harbor CARD domains, which activate the downstream mitochondrial antiviral signaling protein (MAVS), TRAF proteins and eventually TBK1 and IRF3, as previously described for TLR3.

The fourth family is composed by the cGAS-STING pathway. At steady-state, host DNA is restricted to the nucleus. Cytosolic DNA sensors therefore detect pathogen-derived DNA during viral, microbial or protozoan infection or host DNA in pathological conditions like cancer. STING is activated by cGAMP upon cytolosic DNA sensing by cGAS. This induces STING trafficking from the endoplasmic reticulum to perinuclear vesicles, the recruitment of TBK1 and the phosphorylation of IRF3, leading to the transcription of type I IFN (117).

Other DAMP receptors

DAMP receptors recognize cell and tissue damage signals, such as ATP, HMGB1, S100 proteins, heat shock proteins (HSP). Some receptors presented above, such as DNGR-1, are DAMP receptors. The purigenic receptors that recognize extra-cellular ATP are part of the inflammasome cited above in the cytosolic sensor paragraph. Other DAMP receptors include receptor for advanced glycation end products (RAGE) and triggering receptor expressed on myeloid cells-1 (TREM-1). Both receptors are located at the plasma membrane and recognize HMGB1, which is a DNA chaperone located in the nucleus at steady state, released in the extra-cellular compartment after cell death. RAGE also recognizes advanced glycation end products, S100 proteins, amyloid beta peptide and beta sheet fibrils. It signals with TLR4 to eventually activate MAP kinases and NFkB (101). TREM-1 also binds soluble TREM-1, a molecule obtained by alternative splicing or MMP cleavage of TREM-1 transcript, and TREM1-ligand, a molecule less characterized. TREM-1 harbors an ITAM motif, and activates ERK, c-Fos, c-Jun and NFkB (118). Among other HSP receptors, LDL receptor related protein 1 (also named CD91) recognizes HSPgp96 and leads to DC maturation (119).

(ii) Receptors for indirect sensing of infection and inflammation

DC may indirectly sense infection and inflammation and undergo a maturation process by the stimulation of inflammatory cytokine receptors, Fc receptors by immune complexes, or Tumor Necrosis Factor (TNF) superfamily ligands and receptors (TNFSF and TNFRSF). DC express receptors for most cytokines spontaneously or upon activation. The cytokines are secreted directly by the pathogens or indirectly by surrounding activated immune cells. Many inflammatory mediators have been described as DC activators in various contexts, such as type I IFN, TNF-α, IL-1β and prostaglandin E2 (PGE2) in infection (48), TNF-α, IL-6, PGE2 and IFN-β in cancer (120), and TNF-α, IL-1, IL-6, GM-CSF, and thymic stromal lymphopoietin (TSLP) in auto-immunity and inflammatory diseases (55). On the other hand, DC activation may be downregulated by anti-inflammatory factors such as IL-10, TGF-β, VEGF or retinoic acid (121). Cytokine receptors mainly signal through the Janus kinase (Jak)–signal transducer and activator of transcription (STAT) pathway (122), although some cytokines have other signaling pathways (123). Jak kinases phosphorylate cytokine receptors upon activation, and STAT proteins may then bind phosphorylated cytokines receptors via their SH2 domain. Phosphorylated STAT may then induce or repress gene transcription. There are 4 different JAK kinases and 7 different STAT proteins that permit a certain specificity of the cytokine signaling pathways, such as the unique IL-4/STAT6 pathway. Jak-STAT signaling, and particularly STAT1, STAT3 and STAT5, are of importance

in DC development (124). Importantly for the present work on DC activation, STAT proteins regulate different transcription programs in differentiated DC. For example, STAT3 and STAT5 may collaborate during DC maturation, as shown for TSLP-DC (125) or may antagonize each other to regulate the immune response, as shown with the IL-21/STAT3 – GM-CSF/STAT5 competition (126). Cytokine receptors may also signal through the MAP kinase pathways. Several cytokines signal through the same pathways and still induce different effects, suggesting that specificity may be due to a precise combination of the level of activation of each pathway (122), or by changes in the STAT sensitive genes in the different cell types and states (127). DC also express receptors for growth factors, some of which being considered as cytokines, such as GM-CSF, and able to induce DC maturation (122).

Beyond receptors for soluble cytokines and growth-factors, DC express several TNFSF and the receptor CD40 (TNFRSF5) that are involved cell-cell communication and DC-T cell cross-talk in particular, and are upregulated on various cell types during inflammation (128). Many of these molecules have been associated with a costimulatory function and have entered the field of the targetable positive checkpoints, such as CD40-CD40L, OX40-OX40L(TNFSF4), CD30-CD30L(TNFSF8), 4-1BB-4-1BBL(TNFSF9), HVEM-LIGHT(TNFSF14). DC maturation induced by CD40 binding of CD40L expressed on T cells was shown in 1994 by Caux et al. using cord blood derived Langherhans cells (129). All DC subsets express lymphotoxin beta receptors (LTbR) that binds lymphotoxin beta (LT-β) and LIGHT. Since DC also produce LT-β, this interaction is involved in an autocrine loop regulating DC proliferation (130).

DC may sense immune complexes or specific antibodies via their Fc receptors (FcR). All DC subsets express FcgRI (CD64), FcgRIIA and B (CD32a, CD32b), and FcgRIII (CD16). FcR binding induces DC maturation (131). All FcR but FcgRIIB harbor an ITAM motif that has the activating properties described above for CLR and induces antibody-dependent phagocytosis. FcgRIIB harbors an ITIM inhibitory motif, which activation inhibits the production of inflammatory cytokines in DC via downstream signaling through Src kinases and phospholipase C gamma (132). FcgRIIA and FcgRIIB counterbalance their opposite effect and their expression participates in the regulation of DC maturation (133). However, the role of ITAM and ITIM signaling in DC seems more complex than in other lymphoid cells: ITAM-related cytokine secretion inhibition has been described in mouse pDC during murine CMV infection (134) or after CpG stimulation (135), and ITIM-dependant IFN-I genes expression (136). It remains possible that such paradoxical effect may also occur downstream Fc receptors.

DC can detect pathogens coated with complement via their complement receptors CR3 and CR4. However, most studies on the activating role of complement in DC have been conducted with *in vitro* with Mo-DC, and the observation made on complement-induced maturation and CR upregulation during maturation need to be confirmed in primary DC (137).

Finally, chemokine receptors are also part of the indirect sensing of inflammation. Immature DC may be recruited from blood into inflammatory sites by the chemokines CCL2 (MCP-1), -3(MIP1a), -4(MIP-1b), -5(RANTES), -7(MCP-3), -8(MCP-2), -17(TARC), -18, -20(MIP-3a), -22(MDC) and CXCL13 (138).

1.2.2 DC maturation

1.2.2.1 General concept of maturation

In the early 1980's, the ability of DC to activate T cells and the high levels of expression on CMH-II by DC were established. Nussenzweig observed that the response of unprimed T cells to syngeneic DC mixed leukocyte reaction was 10-times weaker than with allogeneic cells (139). This was the first indirect evidence that some variations in DC maturation states could have functional consequences on the level of mixed T cell activation. The concept of DC maturation was first described in 1985 on Langherhans skin DC (LCs) by Schuler et al.: they described that fresh epidermal LCs were poorly efficient at activating T cells, but increased this ability by 10 fold after 3 days of *in vitro* culture without other stimulation, and that this "maturation" process was associated to some visible changes such as the disappearance of Birbeck granules (140). The same year, the importance of DC in the activation of unprimed and memory T helper cells was demonstrated (141). Shortly after the first description of T helper polarization (50), the concept of APC costimulatory molecules arose in 1988 when Weaver et al. observed that the absence or presence of IL-1 produced by macrophages induced Th1 and Th2 helper T cells respectively (142). DC failed to produce IL-1 (143), but other costimulatory molecules were identified in the 90's, such as ICAM-1 (CD54) (144), and CD80 (145). The receptors initiating DC maturation were described in section 1.2.1.5. Maturation is a global process that involves many changes in the transcriptomic programs, the expression of surface molecules including MHC molecules (146), the secretion of cytokines (147) and chemokines, and changes in cell shape, which occur prior or during the migration to the lymph nodes (148), (149), and finally the associated changes in function. Steinman stated that he preferred the term "maturation" to "activation",

since the latter seems to reduce the process to a limited number of on-off events, when maturation corresponds to a larger scale differentiation process, more comparable to the differentiation of blasts of the bone marrow into peripheral blood cells (44). First, we will describe the general changes occurring during DC maturation. Secondly, in chapter 1.2.2.2, we will overview the different shades of maturation and their functional impact. More details on DC states in the context of cancer will be given in chapter 1.2.3.

(i) MHC molecules trafficking and antigen presentation

Immature DC present very few MHC II-peptide complexes because they are poorly efficient at degrading internalized antigens as a consequence of the low efficiency of proteases and cathepsin B (150), (151). In parallel, MHC-II molecules are sequestered in the lysosomes and unable to bind peptides (152), (153), because of the presence of the li-chain that occupies the peptide binding site, which needs to be degraded by cathepsin S (154), (155). In parallel, immature DC have a strong antigen capture capacity that persists until a signal initiates the process of maturation. Among the cascade of molecular events occurring upon maturation, several participate in the increase of antigen presentation. First, the synthesis of MHC class II increases (156). Second, the acidification of the endosomes and lysosomes activates the above mentioned enzymes and leads to the formation of CMH-peptide complexes (48). Lastly, those complexes traffic to endosomal vesicles, where they colocalize with costimulatory molecules and MCH-I before being presented together at the cell surface (157). All this machinery occurs rapidly within the first hours of activation, and is limited in time to the initial phase of maturation, before a downregulation of these processes (150). Conversely, the regulation of MHC-I, involved mainly in self-antigen presentation, but also in cross-presentation, seems stable over time (48). In parallel, mature DC lose their high antigen-capture capacity (158).

(ii) Membrane-bound costimulatory molecules

T cell costimulation corresponds to the 2nd and 3rd signals described in section 1.2.1.3. Membrane bound molecules costimulatory molecules deliver the second signal to T cells, as opposed to soluble cytokines that deliver the third signal. Upon activating receptors binding, DC up-regulate more or less costimulatory molecules, such as the well-known members of the B7 family CD80 and CD86, used in most experiments to define DC activation or maturation. CD80 and CD86 are ligands for the activation molecule CD28 on T cells (45). CD28 binding on naïve CD4 T cells, simultaneously with MHC-II-peptide-TCR binding,

promotes T cell proliferation, cytokine production and cell survival. In the last decades, many other costimulatory molecules have been described: members of the TNF super family described in 1.2.1.5 (CD40, OX40L, CD30L, 4-1BBL, HVEM, LIGHT, GITRL, CD70), other members of the B7 family (inducible T cell costimulatory ligand (ICOSL), B7-H6, B7H7), members of the SLAM family (CD48, CD150, Ly9, NTBA, CD84) (159), (160), (161). The immune activation resulting from the upregulation of costimulatory molecules is regulated in two ways: the presence of an inhibitory receptor on T cell for a specific DC costimulatory molecule, or the upregulation of co-inhibitory molecules on DC. The first case is illustrated by CD80 and CD86 that may bind the inhibitory receptor CTLA-4 on T cells, the latter molecule having been the first targeted negative immune-checkpoint in immuno-oncology (162). The second case corresponds to the negative-checkpoint ligands expressed on DC, such as PDL1, PDL2, B7H3, B7H4, VISTA/B7H5, HVEM, PVR, NECTIN2, CD200 or TIM3 (159), (160), (161). The classification of those molecules as mainly costimulatory or coinhibitory is not always trivial, and some difference have been observed in the field between mice and human biology, e.g. PDL2 that has a costimulatory role in mice and a coinhibitory role in human (163). In 1999 Bleijs et al. also described a costimulatory role for integrins: T cell proliferation and polarization was modulated by the level of interaction between the LFA-1 complex (CD18/CD11a) and the intercellular adhesion molecules (ICAM) ICAM-1 (CD54), ICAM-2 (CD102), ICAM-3(CD50) in an antigen-presenting cell-free system (164). The costimulatory role of integrins expressed on DC has since then been confirmed (165).

(iii) Cytokine and Chemokine production

One of the important effect of the downstream signaling of PRR and the other receptors for indirect sensing of inflammation described in chapter 1.2.1.5 is the transcription of genes coding for inflammatory cytokines via the transcription factors *NFkB, IRF, STAT, CREB* or *AP1* (166). Simulated DC will produce a certain combination of cytokines, usually classified as immunostimulatory (IL-12, IL-6, IL-1β, IFN-a, IFN-β) or immunosuppressive (IL-10, TGF-β). The various combination of cytokines produced upon DC activation depend on the stimuli *in vitro*, and on the integration of stimuli in *in vivo* contexts. The cytokines produced by activated DC will in turn bind their own receptors in an autocrine manner and allow positive or negative feedback loops. For example, IFN-β was essential for TLR3 and TLR4 induced upregulation of CD80, CD86 and CD40 (167). In another study, IL-15 together with IFN-a and IFN-β induced autocrine DC activation and stimulated in vivo naïve CD8 T cell proliferation, but not CD4 T cells (168). Conversely IL-10 may suppress DC maturation in an autocrine manner (169).

DC cytokines will also act on surrounding cells and provide the 3rd signal to T cells. This third signal has been considered as the main regulator of Th polarization. Typically, DC derived IL-12 and IFN-γ induce Th1 polarization, IL-4 induces Th2 and IL-10 and TGF-β induce regulatory T cells (Treg) (Fig 4) (54). However, IL-4 stimulates DC production of IL-12, providing a negative feedback loop in Th2 environment (170). Cytokine production is not only controlled by the stimuli but may be influenced by the DC subsets. For example, GM-CSF activated mouse cDC1 and cDC2 promote Th1 and Th2 T cell polarization respectively, depending on IL-12 levels (171).

(iv) Migration and cell shape

Maturation-induced migration and changes in cell shape are important features specific of DC as compared to other antigen-presenting cells such as tissue-resident macrophages. Upon maturation, tissue-resident DC will migrate by the afferent lymphatics to the draining lymph node together with developing cell projections (158). These afferent-lymph derived DC are usually labelled "migratory DC", as opposed to lymphoid tissue resident DC. In the lymph node, DC will interact with T cells in the paracortical zone and initiate the adaptive immune response. It is assumed that migratory DC do not recirculate in the efferent lymph vessel and blood. The migration from the tissue to the lymph node is under the control of the CCR7/CCL19-CCL21 axis (47), (172), (173). DC upregulate CCR7 upon maturation, under the control of NFkB (174). CCR7+DC will be attracted into the lymphatics by the chemokine CCL21, produced by lymphatic endothelial cells, and will follow a gradient of CCL21 to eventually get into the lymph node areas (175).

With regard to subset specificity, all DC have the ability to become migratory DC, although it is still debated for mouse Mo-DC and data on human Mo-DC are scarce (176), (177). cDC2 preferentially migrate in the interfollicular area, as a results of the expression of EBI2 expression (178).

Concerning stimuli specificity, under some specific conditions, such as TSLP-induced maturation, DC may also upregulate CXCR5 and migrate to B cells zone of lymph nodes under the control of CXCL13, were they participate to the activation of follicular helper T cells (Tfh) (179), (180). These last examples illustrates how different stimuli induce different shades of maturation and here of migration, which will favor DC interaction with a specific cell type, which in turn will determine the final functional output.

Mature DC will develop cell protrusions via actin cytoskeleton modifications that favor DC-T interaction in the lymph node (181). The PRR signaling pathways control the cellular pools of actin: upon activation the Arp2/3-dependent front pool of actin allowing antigen capture will

be downregulated while the mDia1-dependent rear pool of actin allowing cell locomotion will be upregulated (158). CCR7 downstream signaling (182) and MHC class II invariant chain (183) will also participate to the regulation of the actin cytoskeleton, making a link between antigen-presentation and migration. In parallel, trans-endothelial migration itself promotes DC maturation (148), (184).

1.2.2.2 Maturation patterns

(i) Concept of various maturations

All the modifications described in the former chapter are part of DC maturation process. However, there are some variations in the quality and quantity of the molecules involved that correspond to the various DC maturation states described in literature, such as fully mature, TLR-induced, immunogenic, tolerogenic, semi-mature, or homeostatic (Fig 8). Those differences in maturations are important to describe because of their functional impact on both the innate and the adaptive immune responses. They are therefore implied in the physiopathology of many diseases, from autoimmunity to cancer. The role of DC in auto-immunity was discovered in 1983, when Knight et al. transferred DC from autoimmune encephalomyelitis-bearing animals to healthy ones, and observed in the latter the appearance of the disease, driven by the induction of auto-reactive T cells (185). This experiment illustrates how a specific context of DC maturation, here being encephalomyelitis, induces a reproducible effect on the adaptive immune response.

The main dichotomy found in literature on DC maturation states classifies DC as immunogenic if they lead to a predominant effector T cell response or tolerogenic if they lead to a predominant regulatory T cell response. This separation happens upon priming, when naïve T cells integrate the signals from the combination of membrane-bound and soluble costimulatory molecules present at the DC-T immune (186). Grossly, immunogenic DC are typically associated to membrane-bound costimulatory molecules and the cytokines IL-12 and IL-1β, whereas tolerogenic DC are associated to the membrane-bound coinhibitory molecules and IL10, TGF-β and TNF, or even no cytokines (187), (188), (189), (190). This is of course a simplistic view, omitting other T cell modulating signals, such exosomes (191). We will overview so called immunogenic DC and tolerogenic DC, but will not go into details about homeostatic maturation, which exists at steady-state and implies self-antigen presentation for peripheral self-tolerance (172), (192). Although being a fascinating function of DC, homeostatic maturation has no direct link to the inflammation-induced maturation that is detailed here in order to better understand the specific context of cancer inflammation.

It is important to mention that not only the context may induce immunogenic or tolerogenic

DC, but also the different DC subsets within the same context (193). For example, in mice atherosclerosis, cDC1 promote atheroprotective Treg responses, to the contrary of CCL17+ cDC2 that inhibited Treg maintenance (194). The same observation was made in lung were CD103+DC become tolerogenic while CD103-DC are immunogenic after allergen or TLR ligand stimulation (195).
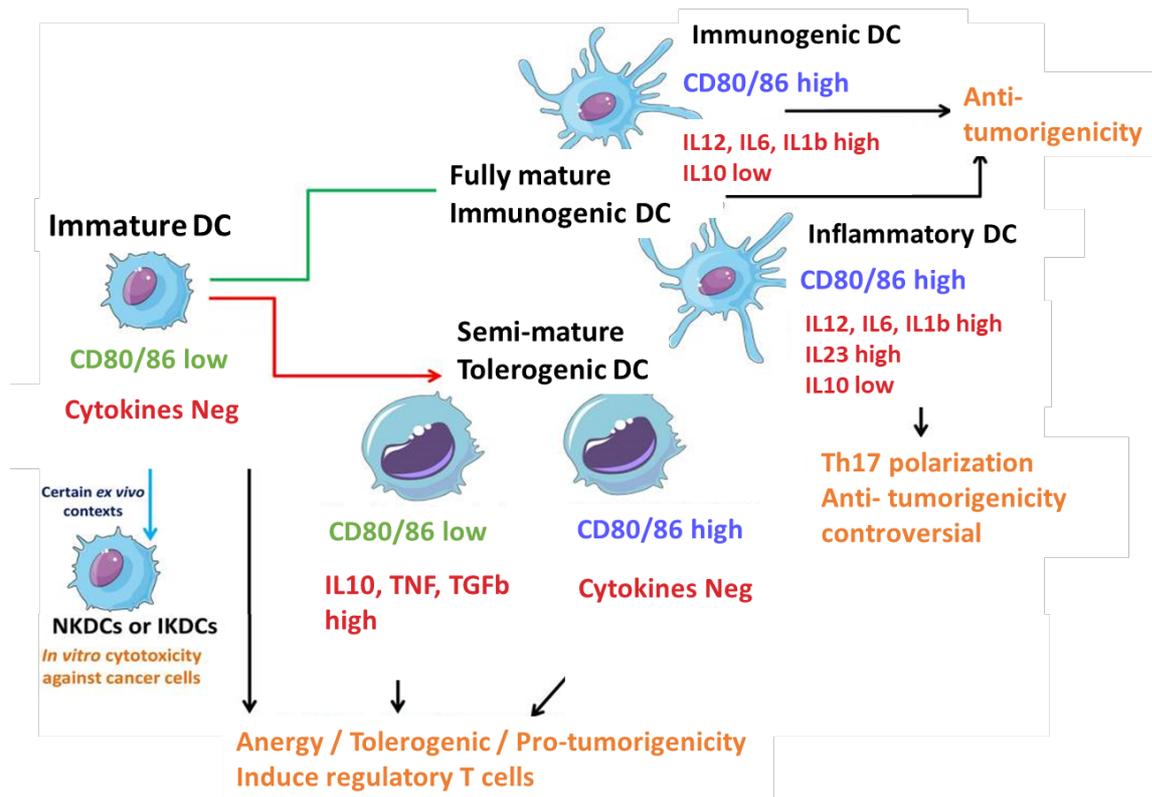

Fig 8 – Features of immature and of the different types of mature DC and their impact on the immune response, here applied to the anti-tumor immune response. Adapted from Dudek et al. (187).

(ii) Immunogenic DC

Immunogenic DC are defined by their ability to prime CD4 and eventually CD8 T cells towards a cytotoxic effector immune response, and may also include DC that promote Tfh and B cells activation towards a humoral immune response. The typical induction of immunogenic DC refers to DC stimulated by a "non-self" entity, which will prime T cell harboring the specific TCR for this "non-self" antigen, as it is the case for acute infection. One of the most broadly corresponding experimental model uses lipopolysaccharide (LPS) to stimulate TLR4 on DC. This typically leads to the upregulation of MHC-II, CD80, CD86 and

IL12p40 production, which in turn induce naïve CD4 T cell proliferation and IFNg production (196). DC IL-12 production may then be increased through CD40L-CD40 DC-T cell interaction (197), for up to 16 hours (198).

Not only the stimuli themselves, but their duration and intensity are important for the induction of immunogenic DC (199). Besides the stimuli, the tissue of origin may modulate the immunogenic potential of DC. This observation is of major importance for vaccination strategies. For example, Stary et al. showed that both R848-based synthetic adjuvants particles and a mucosal route, as opposed to a systemic route, where necessary to obtain a prolonged immunity after vaccination against Chalmydia Trachomatis (200). The same observation was made for anti-cancer vaccine by Sandoval, Tartour et al., in 2 mouse models of orthotopic head and neck and lung cancers: tumor growth was inhibited after vaccination by intranasal route and not intramuscular route (201).

(iii) Tolerogenic DC

The concept of tolerogenic DC appeared in 1979 when Mitchison introduced the idea that Langherans cells could be exploited to increase host versus graft tolerance to prevent graft rejection, which was still a major challenge at that time (202). Since then, the term has been used in many different contexts, *in vitro*, *ex vivo* and in vivo and is a rather large concept that engulfs all cases that eventually induce a predominant regulatory T cell response and immunosuppression. It also includes the specific case of self-tolerance, when this regulatory response is induced by the presentation of normal self-antigens, as in the thymus (203), the mesenteric lymph nodes (204) and even the periphery (205), that will not be further detailed in this thesis. Importantly, a regulatory T cell response can also be induced by immature DC, further enlarging this field (192), (206), (207), (208), (209). When considering stimulated DC that have a tolerogenic function, another term frequently used is "semi-mature" which in general corresponds to the presence of some, but not all, features of activation (187). The absent features are considered as the cause of this immunosuppressive response. This term is confusing because it may be understood as the results of an aborted maturation process, whereas it is not the only context lead to tolerogenic DC. It is also questionable, since a comprehensive measurement of all DC membrane-bound and secreted molecules is not routinely performed: we cannot exclude that DC inducing a tolerogenic output have in fact undergone as much change as the immunogenic DC, but qualitatively different.

The main characteristics of tolerogenic DC are a low or intermediate expression of costimulatory molecules (210), an increased or predominant secretion of IL-10 (206), and the

polarization of CD4 T cells towards a regulatory T cell response (208). IL-10 secretion favors Treg polarization (211), but also inhibits antigen presentation by DC though its inhibitory effect on proteases in the endosomes (151). Another type of tolerogenic DC corresponds to DC expressing the same levels of MHC-II and costimulatory molecules CD80/CD86 than control immunogenic DC, but that do not secrete IL-12 not IL-10. This type of DC may be induced by paracrine DC stimulation with inflammatory cytokines without PRR stimulation, as shown *in vitro* and in vivo using in chimeric TLR4-/- TLR4+/- chimeric mice (196). In this experiment, CD80+/CD86+ semi-mature DC failed to produce IL-12p40 but could induce clonal T cell proliferation at a similar level than TLR4+/+ control DC. However, they failed to promote INF-γ or IL-4 production by T cells. The regulatory phenotype of expanded T cells was not analyzed (196).

Tolerogenic DC can be induced *in vitro* by siRNA silencing CD80, CD86 (212), CD40 (213) or IL-10 (214), or by anti-inflammatory factors such as vitamin A, vitamin D3 (215), prostaglandin E2, IDO, IL10 (216), TGF-β (217), retinoids (218), hepatocyte growth factor (219), E-cadherin disruption (220), and vasoactive intestinal peptide (221). For all these tolerogenic inducers, the tolerogenic phenotype of DC was experimentally confirmed by the observation of a regulatory T cell response. Various mechanisms are engaged in each case to eventually obtain the tolerogenic function. For example, Vitamin D3 inhibited NFkB p65 phosphorylation, skewed the production of CCL17 towards CCL22, a regulatory T cell attracting chemokine, down-regulated HLA-DR, CD80, CD86 and CD40 on cDC2, as compared to unstimulated DC. The final read-out was that it augmented the suppressive effect of CD4 T cells in mixed leukocyte reaction, as shown by the decrease in IFN-γ production (215). However, some experiments performed with the tolerogenic inducers listed above were not performed with sorted human primary cDC, but with *in vitro*-generated Mo-DC, and in some cases the stimuli were given during Mo-DC differentiation, so that their effect on cDC remains to be shown. M-CSF is another example of a molecule that induces semi-mature DC: it efficiently induced the upregulation of MCH-II molecules synthesis and their presentation at the plasma membrane, but without stabilizing them sufficiently to eventually induce T cell activation, thus resulting in a final inhibitory effect (222).

Ex vivo, DC co-culture with murine pulmonary stromal cells also induces a tolerogenic phenotype, corresponding to a decreased MCH-II expression, an increase in IL-10 and prostaglandin E2 secretion, and a suppression in T proliferation, despite the unchanged levels of CD80, CD86 and CD40. In this model, TGF-β is in part responsible for this DC phenotype (189).

Tolerogenic DC have also been observed in vivo. In 3 mouse models of cancer, Gerner et al.

showed that tumor infiltrating DC expressed similar levels of costimulatory molecules than dermal DC, but that they were poorly efficient at antigen uptake, thus leading to inefficient at MHC-II-peptide complex presentation, and poor T cell response in the draining lymph node (223). Similarly, in the study of Iliev et al. (224), mouse DC from mesenteric lymph nodes induced more Treg differentiation that spleen DC (8.9% vs 3.2%) in the presence of OVA. Conditioning spleen DC with intestine epithelial cell-derived supernatant increased the Treg polarization up to 9.1%, showing the importance of the soluble microenvironment, and of TGF-β and retinoic acid in this case, in the induction of tolerogenic DC. Another factor engaged in the regulatory response is the DC: T cell ratio. In the same study, the authors showed that the decrease of DC:T cell ratio from 1:1 to 1:64 dramatically increased the induction of CD4+Foxp3+ Treg after co-culture (225).

The induction of tolerogenic DC upon stimulation is not restricted to specific receptors. TLR activation induces mainly immune responses as seen in the previous paragraph 1.2.2.2 (ii), but can also induce tolerogenic responses, as seen with Zymosan (226) or *Yersinia pestis*, that signal through TLR2 and Dectin1, and TLR6 respectively (227). Tolerogenic DC may also overexpress the inhibitory Fc receptor FcgRIIb (CD32b), as observed in human quiescent rheumatoid arthritis (228) and in cancer (71).

Tolerogenic DC play a role in many different diseases. Their presence in cancer TME is thought to favor immunosuppression and tumor immune-evasion (188) (see section 1.2.3.3). To the contrary, their absence or insufficient effect causes auto-immunity or augments atherosclerosis (229). Tolerogenic DC thus have a therapeutic potential in auto-immune and inflammatory diseases, and to augment graft lifespan after transplantation.

1.2.3 DC in cancers

1.2.3.1 Tumor-infiltrating DC

DC are key players of the anti-tumor immune response. As described for infection, DC will be recruited and activated by danger signals occurring upon tumor-induced tissue-damage (230). At the initiation of tumor-induced inflammation, DC recruitment from blood into tumor is controlled by the chemokines that may be secreted by the epithelial cells and/or the resident innate immune cells (117), (231). DAMP present in tumors are released by the tumor cells or the normal cells from the underlying tissue that undergo non-apoptotic cell deaths, such as necrosis or necroptosis. Necroptosis is a sub-type of regulated cell death in which the plasma membrane is irreversibly permeabilized and has been shown to happen during treatment by chemotherapy or radiotherapy (232). It is also named "immunogenic cell death" because of its potential to initiate anti-tumor response (233), (234). DC will uptake abnormal tumor-derived antigens (230), and present them to T cells in the tumor draining lymph node after DC maturation and migration (235). As soon as DC have been recruited into the tumor, an efficient immune response is therefore possible. The existence of tumors are obvious proofs that these responses are insufficient. Deciphering tumor infiltrating DC will add knowledge to the complex network of biological events that underlie tumor immune escape.

All main DC subsets described in blood (chapter 1.2.1.4) are found in cancer tissue, to the exception of pre-DC / AS-DC (71). Additionally, tumors are inflammatory tissues and are infiltrated by CD14+DC / Mo-DC (236), (237). In tonsil SCC, cDC1, cDC2, cDC4 (or BDCA1-BDCA3-DC) and pDC represent altogether 1.2 +/- 0.8% of CD45+ cells, as compared to 0.7%+/-0.2% in benign tonsil, and cDC1 was the less frequent DC subset (71). In the same study, the proportion of cDC/pDC ratio was increased in the tumor. These data cannot be extrapolated to the other locations of HNSCC, because tonsil cancer occur by definition in a secondary lymphoid organ and not (or not only) in upper-aero-digestive tract mucosa. In early lung adenocarcinoma, cytometry by time of flight (CyTOF) analyses showed that cDC2 and cDC1 represented 4 % and 0.25% of CD45+ cells respectively. The frequencies of cDC2 were equivalent to the one observed in paired normal lung, whereas the frequencies of cDC1 were significantly decreased (237). These variations of proportions are interesting with regard to the differential recruitment of subsets, but do not reflect the overall density of cDC subsets in tumor tissue, since the frequencies of CD45+ cells are increased in tumors as compared to juxtatumors. We will review the evidence of cDC anti- and pro-tumorigenic function in cancer. The role of pDC will not be detailed as it is presented in Annex 5.3.

1.2.3.2 cDC in cancer: teammates of the anti-tumor immune response

cDC1, the cross-presenting DC subset, are considered as the most efficient cell subset to induce an effector CD8 cytotoxic response, since the experiments performed with tumor-bearing Batf3-deficient mice models (77), (223), (238). This superiority of cDC1 to cross-present antigens from necrotic cells has been confirmed in human (72) (239) (240). Additionally, cDC1 were shown to be, at the RNA level, the main source of the major T cell attracting cytokines *CXCL9* and *CXCL10* in a mice model of melanoma, as compared to cDC2, Mo-DC, macrophages, stroma and tumor cells (241). This observation remains to be confirmed in human cancer. cDC1 of human malignant tonsil upregulated *CXCL10* as compared to cDC1 from benign tonsil, but the levels of *CXCL10* transcripts were not compared across subsets (71). Given the very low number of tumor infiltrating cDC1, it seems rather unlikely that CXCL9 and CXCL10 secretion is limited to cDC1 in human tumors. Beyond cross-presentation human cDC1 can also produce inflammatory cytokine IL-12 (72). Finally, in the line with the protective role of cDC1 in the context of cancer, tumor highly infiltrated by cDC1 have been associated to good prognosis in multiple cancers, and in the TCGA analysis of HNSCC in particular (70).

Cytotoxic anti-tumor CD8+ response is not only due to cDC1 and cross-presentation. First, human cDC2 may also cross-present (242). Second, cDC1 and cDC2 prime CD4 T cells, whom support to CD8 T cells has been shown essential in B16 and B78 melanoma mice models (243), (244), (245), (246). Third, cDC2 overexpress CCL22 and CCL17, two chemokines attracting more immature DC and CD4 T cells into tumors (237). Four, they secrete inflammatory cytokines, as shown by MARS-seq single-cell transcriptomics of the immune infiltrate of an early lung adenocarcinoma and its paired juxtatumor tissue. Two DC clusters corresponding to cDC1 and cDC2 were identified. cDC2 were shown to secrete the inflammatory cytokines IL-6, IL-8 and IL-1β at a similar level than CD14+ monocytes. The same cytokine profile was observed in normal lung tissue, supporting that the immunogenic potential of DC was maintained in tumor tissue (237). cDC2 have been also been shown to be an important source of IFN-β, a cytokine that promotes cDC1 cross-presentation (247), (248). Five, the ability of cDC2 in transporting tumor-antigen to the lymph node was confirmed in a mice model of melanoma: the percentages of antigen-positive cDC1 and migratory cDC2 in the tumor draining lymph node were of 10-15% and ~3% respectively (249). Finally, cDC2 are also important for the anti-tumor immune response occurring locally in tertiary lymphoid structures (TLS). Both cDC1 and cDC2 overexpressed LT-β, a cytokine associated with TLS (237). The analysis of tumor tissue sections confirmed that DC colocalized with TLS and T cells. This observation was in the line with the former analysis by

Dieu-Nosjean et al. of mature DC-LAMP+ DC in TLS from 74 early non-small cell carcinomas lung cancer (NSCLC) samples (250). High DC-LAMP+/TLS tumors identified patients with a better prognosis, supporting the beneficial role of tumor-infiltrating DC in the spontaneous anti-tumor response. Since both studies used DC-LAMP to identify DC by immuno-histo-chemistry (IHC), the presence of DC-LAMP negative cDC2 in other area of the tumor and their functional status was not analyzed.

1.2.3.3 cDC in cancer: opponents of the anti-tumor immune response

Having described how DC may protect the host against abnormal tumor tissue in a very similar manner as in infection, there is also an extensive literature supporting the tolerogenic role of tumor infiltrating DC (56). Tolerogenic tumor infiltrating DC are considered as pro-tumorigenic, either by remaining passive and not initiating an efficient immune response, or even by expressing factors that counteract the function of surrounding anti-tumor immune cells.

As described in section 1.2.2.2, tolerogenic tumor-infiltrating DC may be recognized by their low levels of expression of the costimulatory molecules CD40, CD80 and CD86, their low secretion of pro-inflammatory cytokines, and their increased production of IL-10 and TGF-b as shown in mice (251), (252) and human DC (253). TGF-β and IL-10 promote Treg polarization and anergy of antigen-specific effector T cells (251), (252), (253), (254). IL-10 blocking was able to restore DC responsiveness (254). In this line, other studies showed that IL-10 deficient DC were more immunogenic and able to induce sustained anti-tumor Th1 responses than control DC (255).

Tumor DC-derived indoleamine 2,3-dioxygenase (IDO) is another factor responsible for T cell immunosuppression (71), (256). IDO is an enzyme that depletes tryptophan available for surrounding cells and is recognized as a strong immunosuppressor; in particular mice IDO+DC downregulated CD3zeta chain in CD8 T cells, resulting in impaired cytotoxic effector function (257).

Tumor cDC2 have also been categorized as tolerogenic because of their poor ability to present MCH-II-tumor-antigen complex to T cells spontaneously; a soluble peptide restimulation was required to restore adequate antigen presentation (243), (244).

The overexpression of negative checkpoints ligands on DC was also reported to inhibit T cell response (258), (259), (260). In human tonsil cancer, cDC2 overexpressed the negative checkpoints PDL1, PDL2, and LAG, the genes associated to the GOTerm 'Immune response_IL-10 signaling pathway', and downregulated 2 GOTerms associated to NFkB activation as compared to cDC2 from benign tonsil, supporting the idea of tumor-induced

immunosuppression (71). Again, this might be specific to cancers developing in the lymphoid organ that is the tonsil.

Given the evidences of the presence of tolerogenic DC in cancer, the next question would be to ask which factors are responsible for this phenotype. One mechanism is a DC-Treg loop: tolerogenic DC promote Treg that in turn promote tolerogenic DC by downregulating CD80 and CD86 on DC after TCR engagement via CTLA-4 (261). Also, DC and Treg derived IL-10 reduce DC expression of MHC-II, costimulatory molecules and secretion of IL-1β, IL-6, IL-12 and TNF (169). IL-10 is the TME may also be produced by macrophages, and similarly inhibit the production of IL-12 by DC, as shown for CD103+ DC in a mice model of mammary carcinoma (262). IL-10 exerts its tolerogenic effect on DC by inhibiting TLR, TNF-α, and IFN-γ signaling in DC (169).

Besides IL-10, other DC tolerogenic inducers were identified in tumors, such as mesenchymal Stromal Cell-Derived Extracellular Vesicles (263), PGE2 (264), VEGF (265), CSF-1 (266), GDF-15 (267), RANKL (268). It is important to mention that Mo-DC and not primary DC were used in these 6 studies (263) (264) (265), (266), (267), (268).

Finally, abnormalities in metabolisms induced by the hypoxic TME is also a factor that may promote tolerogenic DC. *In vitro* experiments using a peptide-pulsed Mo-DC co-cultured with CD8+Tcells showed that lactic acid decreased the ability of Mo-DC to produce IL-12, but not IL-10, and inhibited CD8+T cell proliferation (269). In a mouse model of ovarian cancer, tumor infiltrating DC activation was inhibited by a XBP1-dependant triglyceride biosynthetic program induced by the tumor micro-environment (270).

Altogether, these data support the presence of tolerogenic DC in tumors, but e*x vivo* data from human tumor infiltrating DC compared to normal-tissue resident DC, and on TME-derived tolerogenic factors are sparse.

1.2.3.4 cDC in cancer: 2 sides of the same coin

It seems difficult to conciliate the important number of evidences supporting the anti- and pro-tumorigenic effect on cDC. NFkB is an important factor in the regulation of DC maturation and subsequent function. Although initially associated to the host protection, NFkB may also act as a mediator of anti-inflammatory functions, as reviewed by Pires et al. in "NF-kappaB: Two sides of the same coin", hence the title of this paragraph. In human, there are some evidence that tumor infiltrating DC harbor simultaneously immunogenic and immunosuppressive features. Michea, Noël et al. performed transcriptomic analysis of triple negative breast cancer APC and showed that the Gene Ontology (GO) Terms, 'chemokine

activity', 'cytokine activity', 'cytokine receptor binding' and 'IL-10 signaling' were shared by cDC2s and CD14+, supporting the simultaneous expression of pro and anti-inflammatory cytokines (236). Using a similar approach in human tonsil cancer, cDC1 were shown to simultaneously upregulate the genes associated to the GO Terms pro-inflammatory 'Immune response_IFN-alpha/beta signaling via JAK/STAT' and 'Immune response_T regulatory cell-mediated modulation' including the negative immune checkpoint *LAG3* (71).

Similarly, in the same study, BDCA1-BDCA3- DC (cDC4) overexpressed both immunostimulatory genes as *IRF1* or *STAT1* and the immunosuppressive *IDO1*. IDO that is considered as a strong immunosuppressive factor is also in fact required for DC maturation, chemokine secretion and chemokine receptor expression, thus moderating the negative role of IDO on DC in the TME (271). PGE2 induced tolerogenic DC (264), but was also able to rescue the impairment in CCR7/CCL19 upregulation on DC caused by prostate cancer cell line-derived factors (272).

In summary, DC are protective against cancer, but the complex biological network present in the TME also limits their full immunogenic potential. Combined therapeutic approaches counteracting the different factors inducing tumor tolerance are required and would need to be selected on fine analysis of human DC subsets in each specific context.

1.2.3.5 DC as therapy

Given their key role in anti-tumor immune response, several approaches using DC as a therapeutic tool have been proposed and tested. DC may be used directly as a cell therapy. In this case, autologous DC (or monocytes) are obtained by leukapheresis and modulated (and/or differentiated), expanded and pulsed or fused with specific targets *in vitro*, before being injected to patients (273). Such treatments have been proposed for cancer and auto-immune diseases (NCT02618902). One example is the sipuleucel-T vaccine that obtained approval for prostate cancer (274). DC cell therapy is limited by its cost, but also by the fact that the DC activation phenotype obtained *in vitro* may not be stable during cell transfer limiting the efficacy. A recent meta-analysis including 6 clinical trials testing DC pulsed with prostate-specific membrane antigen in metastatic castration-resistant prostate cancer patients failed to show a benefit on survival (275). Several trials with combination therapies are ongoing with sipuleucel-T (NCT03024216, NCT01818986) and other DC-based vaccines in other indications (NCT02479230). Sipuleucel-T is produced with PBMC cultured with tumor peptide but does not isolate one or several APC subtypes. To the contrary, other phase I trials tested DC vaccination with specific DC subsets, which were injected intra-

nodally, in HLA-A*0201 patients presenting with metastatic chemo-resistant melanoma expressing gp100. A first trial used autologous sorted blood pDC activated overnight with IL-3 and subsequently with FSME-IMMUN (a vaccine against tick-born encephalitis) and then loaded with tumor peptide (276). Another phase I trial successfully achieved vaccination with 3 to 10 million sorted autologous CD1c positive primary DC. cDC were cultured overnight in X-Vivo with human serum and GM-CSF for maturation, and then loaded with the tumor peptide shortly before injection (277). As observed with checkpoint blockade, 4 out of 14 patients presented prolonged clinical responses in this phase 1. A phase 3 trial is currently testing a vaccine made of autologous sorted pDC and cDC in melanoma (NCT02993315). A phase 1 trial is currently testing personalized vaccines using autologous DC pulsed with autologous whole tumor cell lysate and injected intra-nodally in patients with advanced solid tumors and high tumor mutation burden (NCT03671720).

An alternative approach to cell therapy is the DC targeting in vivo via activating receptors and pathways. We will only detail here the current clinical use of PRR and TLR agonists, as an introduction for the study presented in result section 3.1. However, other activators are being used or under evaluation such as cGAS-STING pathway activators (278), (279), (280) (NCT02723955), DEC-205 ligands (NCT02166905) (207), DC-SIGN ligands (40), and aluminum salts or saponins that activate the NLRP3 inflammasome (281). These activators may be used either as adjuvants for peptide-based vaccine or may be applied on or injected in tumors. It must be kept it mind that these adjuvants may also interact directly with other cells types, such as cGAS-STING activators that have a direct effect on T lymphocytes (282). Imiquimod (R848) is a TLR7/8 ligand used routinely for basal cell carcinoma. Salmon et al. showed an optimal anti-tumor effect by activating cDC1 with a cocktail FLT3L and Poly I:C combined to anti-PDL1 in a B16 melanoma mice models (238). In the same model, Desch et al. further showed that Poly I:C activated cDC1 and R848 activated cDC2, and that both were able to induce a cytotoxic T cell response (284). A similar approach with intra-target lesion injection of FLT3 and Poly I:C, combined with 2Gy radiation therapy, was used in a pre-clinical model and in a phase I clinical trial including patients presenting with treatment-resistant indolent non-Hodgkin's lymphomas (NCT01976585) (283). In both mice and human, accumulation of intra-tumoral cDC1 and cDC2 was observed with this in situ vaccination strategy. Another study in mouse models of fibrosarcoma, lung carcinoma and B16 melanoma, showed that peri-tumoral injections of CpG-ODN controlled tumor growth and that this effect was mediated by NK cells and CD8 T cells. The presence of mature migratory DC was demonstrated, but the possible role of CD4 T helper cells as an intermediate for CD8 T cell activation was not studied (285). In mouse models of colon and kidney cancers, weekly peri-tumoral CpG injections associated to radiotherapy could achieve

complete cure of established tumors and even induce an abscopal effect on simultaneous untreated contralateral tumors (286). That said, CpG is a TLR9 ligand, and TLR9 is not expressed on the same DC subsets in mice and in human, limiting the straightforward clinical translation of these results. Finally, a study in advanced melanoma patients showed promising results and an overall response rate of 38% with TriMixDC-MEL and ipilimumab. TriMixDC-MEL combines Mo-DC-based cell therapy with a TLR4 signaling by coelectroporating constitutively activated TLR4, CD40L and CD70 (287).

In addition to pharmaceutical TLR agonists, chemotherapy and radiotherapy are also able to promote DC recruitment and maturation. In several mice model of solid cancers, Ma et al. demonstrated that anthracycline-based chemotherapy induced the recruitment of cDC2 into tumors and that it was due to ATP binding on DC purinergic receptors, ATP having been released by dying tumor cells (288). In colon, lung and melanoma mouse models, radiotherapy induced the upregulation of CD70 and CD86, but not of MHC-II, on cDC2 and induced a CD8+ T cell mediated anti-tumor immune response. CD4+T cell were dispensable in this study (289). Radiotherapy was shown to activate the immune system in multiple ways, such as the activation of the cGAS-STING pathway, the induction of chemokine production and the upregulation of integrins (290). In this line, dozens of clinical trials are currently evaluating various combinations of radiotherapy and immunotherapy in many different cancer types (291). However, radiotherapy also has immunosuppressive effects, and in particular was shown to down-regulate CD80 and CD86 and DC (292).

OBJECTIVES

2. OBJECTIVES OF THE THESIS

DC biology is now a knowledge-rich field, particularly in mouse DC and human blood DC biology. As presented in the introduction, some debate remains on DC maturation states. Moreover in vivo mouse models and even some clinical trials have shown that DC are a highly valuable target for immunotherapy in cancer and other diseases, and that DC maturation state is the key for DC-based treatment efficacy. Knowledge on human HNSCC tumor infiltrating DC is scarce and does not allow to anticipate how to modulate tumor DC as therapy.

The objective of my thesis was to describe in a high-resolution approach the molecular state of tumor infiltrating DC and their relation to the tumor microenvironment.
We wanted to address several questions:
- Which DC subsets infiltrate HNSCC and in which proportions?
- What is their expression of maturation marker and of positive and negative immune checkpoints?
- What is the relationship between tumor infiltrating DC frequencies and states and the other tumor immune subsets?
- Which mechanisms shape DC maturation states in the TME?
- Are there patterns of tumor immune infiltration?
- What is the association between tumor immune cell infiltration and the soluble TME?
- Which TME parameters are associated to prognosis?
- Can we identify potential therapeutic targets and/or theragnostic markers?

To do so, we took advantage of the human clinical samples available at the Institute Curie, provided by the surgical oncology and the pathology departments, from surgical specimens of willing patients. We analyzed DC subsets, their maturation markers and checkpoint expression, other myeloid cell subsets, and T cell subsets in primary HNSCC by flow cytometry. In parallel, we completed our biobank of tumor-derived secretome that had been initiated several years ago in our team, to obtain multiplex analysis of soluble molecules relevant to multiple cancer pathways. I wanted to obtain paired flow cytometry and soluble TME data to perform integrated analysis. This joint DC-focused and multiparametric approach of the TME was the starting point to understand HNSCC DC in their tumor context.

We developed a multicolor flow cytometry antibody panel optimized for DC subsets and I took advantage of the expertise of the clinical immunology team of Olivier Lantz for the T cell

antibody panel. First, I discovered the difficulty of working the limited resource that are fresh human tumor samples. Then, I had to handle the analysis of the medium throughput data obtained by immuno-monitoring. For this reason, I trained to use the recent Qlucore software, aimed at helping non-bioinformatician researchers to explore sequencing data. I thought to apply to my flow cytometry dataset the methods that are usually dedicated to RNA sequencing analysis, such as unsupervised analyzes and clustering. With this approach, I have been able to identify an important role for the frequency of CD3+ T cell in the "structure" of my dataset. With this observation and the extensive literature available on the role of tumor infiltrating T cells, I finally selected this parameter for the supervised analyzes. I was then able to observe that DC subsets in CD3 high inflamed tumors presented with a constant pattern of high PDL1 and very low ICOSL expression. This pattern was opposed to blood DC and to DC from non-inflamed tumor, that had an intermediate expression of ICOSL and a low expression of PDL1.

This observation lead me to use a valuable resource of the team created by Maximilien Grandclaudon aimed at elucidating DC phenotype and T cell modulation after DC exposure to many different stimuli *in vitro* (293). The initial scope of this database was the mathematical modelling of cell-cell communication. I approached it in a new way, with the perspective of PDL1 and ICOSL, the 2 molecules identified from tumor samples. Doing so, I identified 2 opposite patterns of matured DC, which we labelled "secretory" and "helper". Transcriptomic analysis of sorted HNSCC samples allowed us to confirm the relevance of this new classification of DC maturation state in human tissue. The corresponding manuscript that will soon be submitted is presented in the results section 3.1.

In parallel, I could obtain paired flow cytometry data and soluble data for 18 samples. I was able to confirm the expected association of T cell infiltration with the levels of soluble CXCL9 and CXCL10. This observation was important to validate this original primary-tumor derived secretome approach. Comparison of tumor and juxtatumor tissue revealed many deregulated proteins that were all candidate biomarkers. I used my medical skills to select the best clinical setting to pursue with prognosis biomarker discovery and identified soluble MMP2 as a predictive of poor prognosis in oral cavity cancer patients. I designed a large validation cohort to confirm this finding. My objective then was not only to validate the value of MMP2, but also to evaluate if there was a relation between patients' prognosis and the expected response rates to immunotherapy by measuring genes of a published predictive signature. This biomarker study based on an unsupervised analysis of primary tumor secretome has been submitted to Clinical Cancer Research and is presented in the results section 3.2.

RESULTS

3. RESULTS

3.1   PDL1 AND ICOSL DISCRIMINATE HUMAN SECRETORY AND HELPER DENDRITIC CELLS

Article available at https://doi.org/10.1101/721563

Abstract

Dendritic cells (DC) are described as immature at the steady state, with a high antigen capture capacity, turning into a mature state with a strong T cell stimulatory capacity upon activation. Using 16 different stimuli *in vitro* (130 observations), we describe two states of human activated dendritic cells. PDL1highICOSLlow "secretory DC" produced large amounts of inflammatory cytokines and chemokines but induced very low levels of T helper (Th) cytokines following DC-T co-culture; conversely PDL1lowICOSLhigh "helper DC" produced low levels of secreted factors but induced high levels of Th cytokines characteristic of a broad range of Th subsets. Secretory DC were phenotypically identified in T cell inflamed primary head and neck squamous cell carcinoma. RNAseq analysis showed that they expressed a typical secretory DC signature, including CD40, PVR, IL1B, TNF, and CCL19. This novel and universal functional dichotomy of human DC opens broad perspectives for the characterization of inflammatory diseases, and for immunotherapy.

PDL1 AND ICOSL DISCRIMINATE HUMAN SECRETORY AND HELPER DENDRITIC CELLS

AUTHORS

Caroline Hoffmann [1,2,3], Floriane Noel[1,2]*, Maximilien Grandclaudon[1,2]*, Paula Michea[4,5], Aurore Surun[6,7], Lilith Faucheux[8,9,10], Philemon Sirven[1,2], Olivier Lantz[1,2,11], Juliette Rochefort[10,12], Jerzy Klijanienko[1,13], Charlotte Lecerf[1,14], Maud Kamal[1,14], Christophe Le Tourneau[1,14,15], Maude Guillot-Delost[1,2,11], Vassili Soumelis[1,2,16].

* Equal contribution to the work

AUTHORS AFFILIATIONS

1. Paris-Saclay University, Paris, France
2. INSERM Unit U932 research unit, Immunity and Cancer, Paris, France
3. Institut Curie, Department of Surgical Oncology, Paris & Saint-Cloud, France
4. Inserm U1068 - CNRS UMR7258 - AMU UM105 - Institut Paoli Calmette
5. University Aix-Marseille
6. SIREDO Cancer Center (Care, innovation and research in pediatric, adolescents and young adults oncology), Institut Curie, Paris, France
7. Paris Descartes University, Sorbonne Paris Cité, Paris, France
8. INSERM UMR-1153, ECSTRRA team, Statistic and epidemiologic research center Sorbonne Paris Cité, Paris, France
9. Hospital St Louis, Immunology & Histocompatibility Laboratory, Paris, France
10. University of Paris, Paris, France
11. Center of Clinical Investigation, CIC IGR-Curie 1428, Paris, France
12. INSERM U1135, Cimi Paris, and Odontology department, Hospital Pitié Salpêtrière, Paris, France
13. Department of pathology, Institut Curie, Paris, France
14. Department of Drug Development and Innovation (D3i), Institut Curie, Paris & Saint-Cloud, France
15. INSERM U900 research unit, Saint-Cloud, France
16. Institut Curie, Clinical immunology department, Paris, France. Last author current address is "9".

INTRODUCTION

Dendritic cells (DC) have a key role in initiating and polarizing the immune responses, including anti-tumor immunity (1). Immature DC patrol in tissues and have a low expression of costimulatory molecules. Following antigen stimulation, they mature and acquire a strong T cell stimulatory capacity (2). So far, mature DC have been classified as immunogenic when they induced T effectors and secreted IL12 and IL1b, or tolerogenic when they induced regulatory T cells and secreted IL-10, TNF and TGFb, or no cytokines (3), (4), (5), (6). In cancer, it is considered that factors derived from the tumor microenvironment induce tolerogenic DC (7), (8), (9). However, most studies have been realized using a limited number of stimuli, mostly in mice models or *in vitro* with human monocyte-derived DC (10), (11), (12). Furthermore, the phenotype and function of tissue infiltrating DC in human remains largely unknown. Our aim was to decipher the mechanisms regulating DC phenotypes and to understand their associated function, with a physiopathological relevance in human cancer.

RESULTS

To determine the phenotypic heterogeneity of DC infiltrating cancer tissue and its relation to the other immune cell types, we analyzed by flow cytometry 22 fresh head and neck squamous cell carcinoma (HNSCC) samples. Here, we show that the frequencies of tumor infiltrating CD3 T cells were positively associated to the frequencies of DC and to PDL1 expression on CD11c+HLA-DR+ cell subsets, and negatively associated to the frequencies of neutrophils and of ICOSL expression on the same cells (Fig1). We used 2 different antibody panels analyzing T cell subsets (Fig S1A) and myeloid cells subsets (Fig 1A, 1B). In the myeloid panel, CD45+, Lineage- (CD3, CD19, CD56) cells were analyzed by their expression of CD11c and HLA-DR. The double positive population was separated into four populations by their expression of CD14 and BDCA1, and included the monocytes and macrophages (MMAC), the CD14+DC, the cDC2 (BDCA1+CD14-) and the double negative population enriched in cDC1 (cDC1e) (Fig S1B). Plasmacytoid DC were gated as CD11c-, HLA-DR+, CD123+. We extracted a total of 434 parameters. We found a large variation of CD3 infiltration across tumors ranking from 1% to 61% (Fig 1C). In order to identify the parameters associated to tumor inflammation, we defined 3 groups of equivalent sizes labeled "CD3 High" (n=8), "CD3 Int" (n=6), and "CD3 low" (n=8). To avoid bias, we used a sub-list of 81 non-redundant parameters among the 434 measured, meaning that each population was expressed only in percentage of its parental population (Table 1). CD3 high

tumors were significantly enriched in cDC2, cDC1e, pDC and in PDL1 expressing MMAC and cDC1e. Conversely, CD3 low tumors were enriched in Lin-DR- cells (mainly neutrophils, see Fig S1C), macrophages, and ICOSL expressing CD11c+HLA-DR+ cells (Fig 1D, 1E, 1F). The levels of expression of PDL1 and ICOSL in the four CD11c+HLA-DR+ subsets were highly correlated in all tumor samples (Fig S1D). CD11c+HLA-DR+ cell subsets in CD3 low tumors expressed intermediate levels of PDL1 and ICOSL and were closer to the expression observed on their blood counterparts than the same subsets in CD3 high tumors, which upregulated PDL1 and downregulated ICOSL (Fig 1E). Thirteen out of the 16 significant parameters were obtained from the myeloid cell panel (Fig 1D), showing that there were fewer variations in the percentages of the various T cells subsets related to CD3 infiltration levels. For example, the proportion of regulatory T cells among the CD4+ T cells were 34%, 35% and 41% in the CD3 High, Int and Low groups respectively. Finally, to determine if any combined parameter, ratio or clinical variable was highly efficient at discriminating the 3 groups, we performed an elastic net model including the all the 434 parameters and 14 clinical parameters (Table 2). We found that the intermediate expression of ICOSL on CD11c+HLA-DR+ cell subsets was highly characteristic of the CD3 low group (Fig S1E). Only parameters directly linked to T cell infiltration (percentages of T cell subsets in live cells) were found in the high CD3 group. In summary, we showed that CD3 inflamed tumors were more infiltrated by DC subsets that expressed higher levels of PDL1 than in non-inflamed tumors, and that PDL1 and ICOSL expressions on DC and macrophages were opposed (Fig 1D, Fig S1D).

To identify candidate stimuli that could be responsible for the PDL1/ICOSL expression patterns and to further understand the subsequent functional implications, we took advantage of a DC-T cell dataset from Grandclaudon et al. (13). We used the existing data on primary blood CD11c+HLA-DR+ DC and generated supplementary experiments and analysis. Briefly, blood DC were activated for 24 hours by 16 different types of perturbators and analyzed for their expression of 29 surface markers (n=154 data points), and their secretion of 32 chemokines and cytokines (n=130 data points). The remaining cells were co-cultured with allogenic naïve CD4 T cells for 6 days and we measured the expansion fold. After 24h of restimulation by anti CD3/CD28 we measured 17 T helper cytokines (Fig 2A). We confirmed the anti-correlation of PDL1 and ICOSL expression (Fig2B). Three main groups of responses were observed: (i) PDL1high and ICOSLlow, like on *ex vivo* cDC2 from inflamed tumors; (ii) PDL1low and ICOSLhigh, and (iii) medium-like PDL1 low and ICOSL low (Fig 2B). Co-expression of both PDL1high and ICOSLhigh was a rare profile and was not observed for very high expression levels. ICOSL expression was null when PDL1 expression reached its highest levels. We used an unsupervised approach by t-SNE of the

29 surface markers to verify that PDL1 and ICOSL were relevant markers to discriminate the various DC phenotypes observed *in vitro*. We observed that PDL1 high cells clustered together and were distinct from ICOSL high cell clusters and from PDL1 low ICOSL low cluster, the latter including most Medium-DC conditions (Fig 2C). The DC perturbators inducing a majority of PDL1 high ICOSL low cDC2 were R848, Zymosan, HKSA and HKLM, while the ones inducing a majority of ICOSL high PDL1 low cDC2 were TSLP, GM-CSF and Flu (Fig 2C, Table 3). To pursue the analysis of the different functions of these DC phenotypes, we defined 4 groups of activated DC by their PDL1 and ICOSL expression (Fig 2B). First, we analyzed the 29 surface markers in these 4 groups and in Medium-DC: PDL1 High ICOSL low DC co-expressed PVR, PDL2, Nectin2, CD54, and CD40, with Spearman correlation coefficients of 0.8, 0.75, 0.66, 0.64 and 0.62 respectively (Fig2D, 3E, Table 4). ICOSL high PDL1 low DC did not have any correlated molecule with a Spearman correlation coefficient superior to 0,5.

Next, we analyzed the secretion of 32 DC derived cytokines and chemokines, and 17 T helper cytokines secreted by naïve CD4 T cells after 6 days of co-culture (Fig 3A, Table 5, Table 6). PDL1 high ICOSL low secreted the largest amount of most cytokines measured, such as TNF-α, IL-1a, IL-1b, IL1-RA, IL-6, IL-10, IL-12p40, IL-23, IL-27, CCL19, BCA1, MIP1a, as compared to both PDL1 low ICOSL high DC and to Medium DC, but they did not induce more secretion of T helper cytokines by naïve CD4 T cells than Medium-DC (Fig 3B). Conversely, it was the PDL1 low ICOSL high DC that induced the highest activation of T cells as measured by the high expression of most CD4 T helper cytokines after co-culture, without a clear T helper polarization (Fig 3A, 3B, S3A, S3B). Therefore, we labeled PDL1 high ICOSL low DC the "secretory DC" and PDL1 low ICOSL DC the "helper DC", both being different activated profiles, distinct from previously described tolerogenic DC. "Helper" DC increased very significantly the secretion of Th2 cytokines, IL-10, IL-3 and IL-9 by the CD4 T cells as compared to "secretory" DC, whereas IL-2 and IFNg were only mildly increased. There was no significant difference for Th17 cytokines. T cell proliferation was increased by both "secretory" and "helper" DC as compared to medium DC (Fig S3C).

To further characterize the changes occurring during DC activation in the context of cancer, we performed RNA sequencing of cDC2 sorted from HNSCC or blood and identified 882 differentially expressed genes (DEG): 639 increased in tumor cDC2 and 243 in blood cDC2 (Fig 4A, Table 7 for donors characteristics and Table 8 for DEG). Due to the minimal number of cells required for this experiment, inflamed tumors highly infiltrated by DC were necessarily selected (Fig S4A). In parallel, we compared transcriptomics data of cDC2 activated with pRNA, a TLR7/8 ligand expected to induce "secretory" DC or GM-CSF a

"helper" DC2 inducer (Fig 4B) from GSE89442 (14). Using both comparisons of the stimuli together and towards unstimulated blood cDC2, we defined the "secretory" and "helper" signatures including 1473 and 1277 genes respectively (Fig 4C, Table 9). Among the 639 genes upregulated during tumor-induced maturation, 135 (21%) were shared with the "secretory" signature and only 64 (10%) with the "helper" signature, the 440 (69%) remaining genes being tumor-specific (Fig 4D). Using supervised lists of genes coding for checkpoints and maturation markers (Fig 4E left, Table 10), cytokines and chemokines (Fig 4E center, Tables 11 & 12), and of the NFkB pathway (Fig 4E right, Table 13), we confirmed that tumor cDC2 shared the majority of the genes with the pRNA "secretory" condition (Fig 4F). cDC2 overexpressed *CD274*/PDL1, and several other "secretory" specific markers identified previously at the protein level, such as *PDCD1LG2*/PDL2, PVR, *IL1B, IL12B, IL23A, TNF,* and *CCL19*, and also other negative checkpoints such as *IDO1, IDO2, and HAVCR2*/TIM3*,* and the migration marker *CCR7*.

Since the concept of immature versus mature DC, and their respective roles in immune regulation, attempts have been made to identify classes of mature DC, such as "fully mature", "immunogenic", "inflammatory", "semi-mature", "tolerogenic" (3). These suffer from several limitations: 1) they lack a clear and consensual definition, 2) they lack universality and specificity, i.e many DC do not fall into any of these categories or may fall into multiple. In this study, we report on a novel classification of human activated DC that mature either as "secretory" DC or as "helper DC", recognizable by their opposed PDL1 and ICOSL expression. Each phenotype is induced by some specific stimuli, but not restricted to a single receptor pathway (Table 3). Tumor infiltrating cDC2 in inflamed HNSCC have the phenotypic signature of "secretory" DC. In blood and in non-inflamed HNSCC, DC have an immature phenotype (Fig 5). These observations have several applications for immunotherapies modulating DC in cancer and inflammatory diseases, such as DC stimuli used directly, or for DC-based vaccines, or even for standard cancer treatment that will increase danger signals in the tumor microenvironment. For example in cancer, the stimuli inducing "secretory DC" should be used in combination with anti-PD(L)1 antibodies, when it is not planned in some upcoming trials (NCT02320305, NCT03742804, NCT02180698), and the stimuli inducing "helper DC" could be used to increase the T cell response via polyfunctional Th cytokine profiles.

METHODS

Human samples and patient characteristics

Fresh samples of HNSCC tumor tissues and blood of untreated patients with head and neck cancers were obtained from the pathology department of the Institut Curie hospital in accordance with the ethical guidelines, with the principles of Good Clinical Practice and the Declaration of Helsinki, and with patients consent. Patient characteristics for the flow cytometry cohort (Fig.1) and RNAseq cohort (Fig.3) are summarized in Supplementary Tables 2 and 7, respectively. Fourteen of 22 the patients of the FACS cohort were included in the clinical trial SCANDARE NCT03017573.

Single-cell suspensions

Tumor tissues were mechanically and enzymatically digested in CO2-independent medium (Gibco) containing 5% FBS (HyClone). Enzymatic digestion consisted of three rounds of 15 min of incubation with agitation at 37 °C, separated by pipetting, with 2 mg/ml collagenase I (C0130, Sigma), 2 mg/ml hyaluronidase (H3506, Sigma) and 25 µg/ml DNAse (Roche). The samples were filtered on a 40-µm cell strainer (Fischer Scientific) and were diluted in PBS 1X (Gibco) supplemented with EDTA 2 mM (Gibco) and 1% de-complemented human serum (BioWest). After centrifugation, cells were suspended in the same medium and were counted by trypan blue before being assessed by flow cytometry or sorted. PBMC were isolated from blood samples using FICOLL (GE Healthcare) gradient centrifugation.

Antibodies, flow cytometry and cell sorting

Single-cell suspensions from digested tumor and from blood were stained with antibodies (Table 14) for 15 min at 4°C. After washing step, cells were analyzed or sorted directly, immediately after having added DAPI (Miltenyi Biotec) for dead cells exclusion. Flow cytometry phenotyping was performed on BD LSRFortessa Analyzer. Cell sorting for the RNA-seq experiment were performed on BD FACSAria III using the purity and low-pressure mode, and a 100-µm nozzle. DC subsets and MMAC were sorted in Eppendorf tubes containing TCL buffer (Qiagen) supplemented with 1% β–mercaptoethanol (SIGMA) before RNA extraction, as decribed in Michea P, Noël F et al. (15).

In vitro analysis

Material and methods are described in detail in the resource paper from Grandclaudon et al. (13). As compared to the resource paper containing 118 data points for primary blood CD11c+HLA-DR+ cells (referred to as bDC), we generated supplementary experiments and analysis to specifically address our question. We added 36 data points for the analysis of

surface markers (leading to a total of 154 data points) among which 12 for the analysis of DC secreted cytokines and chemokines and of the T helper cytokines (leading to a total of 130 data points). Extra data points included: Curdlan 10ug/ml (n=1), Flu (1X) (n=3), Flu(1X)+TSLP(50ng/ml) (n=3), HKSA (MOI10) (n=3), GM-CSF 50ng/ml (n=4), LPS (n=3), Medium (n=9), Poly I:C 50ug/ml (n=4), R848 1ug/ml (n=3), TSLP 50ng/ml (n=3), for a total of 29 blood donors. The antibodies used for the checkpoints and maturation markers analyzed by flow cytometry are listed in Table 4. For the DC secreted cytokines and chemokines, we measured 24 supplementary cytokines and chemokines. IL1a, IL1b, IL6, IL10, TNF-α and IL12p70 were measured by cytometry bead assay flex set (CBA) and we added the measure of IFNa. IL23 and IL28a were measured by Luminex and we added the measure of APRIL, BCA1, CCL19, CXCL11, CXCL16, CXCL9, Eotaxin2, I309, IFNb, IL12p40, IL16, IL1RA, IL27, IL29, IP10, MCP1, MCP2, MCP4, MIP1a, RANTES, TARC, TRAIL, YKL40 (Table S5). The 17 T helper cytokines were analyzed by CBA or Luminex (Millipore) (Table 6), similarly to the resource paper.

RNA extraction, sequencing and data pre-processing

Material and methods are described in detail in the resource paper (15). Briefly, single Cell RNA Purification Kit (Norgen Bioteck) was used for RNA extraction, including on-column DNase digestion (Qiagen), as described by the manufacturer's protocol. RNA integrity was controlled with a RNA 6000 Pico Kit (Agilent Technologies) in BioAnalyzer. cDNA was generated with SMARTer Ultra Low input RNA for Illumina Sequencing-HV (Clontech), following manufacturer's protocol with 14 cycles for amplification. Quality controls were performed with Qubit dsDNA high sensitivity (Thermofisher) and an Agilent Bioanalyzer using nanochip (Agilent Technologies). Multiplexed pair-end libraries 50nt in length were obtained using Nextera XT kit (Clontech). Sequencing was performed in a single batch with Illumina HiSeq 2500 using an average depth of 15 million reads. Library, sequencing and quality controls were performed by the NGS facility at the Institut Curie. Reads were mapped to the human genome reference (hg19/GRCh37) using Tophat2 version 2.0.14. Gene expression values were quantified as read counts using HTSeq-count version 0.6.1. Genes with less than one read count in at least one sample were filtered out and. The remaining raw data were normalized and analyzed using DESeq2 R package. Differentially expressed genes were obtained with an adjusted p-value of 0,10. The supervised list of genes used in Fig 4D were established by including all markers analyzed at the protein level in the *in vitro* analysis and by adding other known checkpoints and maturation markers, cytokines and chemokines from literature search. The NFkB pathway genes list was established by literature search.

Data availability. RNA-seq data that support the findings of this study will been deposited in the NCBI Sequence Read Archive (SRA).

Analysis of Flow cytometry data

We measured a total of 434 parameters including 52 cell/cell ratios. We established a sub-list of 81 non-redundant parameters, meaning that each population was expressed in percentage of its parental population. The list of 81 parameters was used in Fig 1D, and the list of 434 parameters enriched wit 14 clinical parameters was used for the elastic net model in Fig S1D. The elastic net model was performed using R software, a Lambda at 1SE, and an alpha of 0,5.

Statistical analysis

Statistical analyses of flow cytometry data (Fig1) and *in vitro* analysis (Fig2, Fig3) were performed using ANOVA or Kruskal-Wallis tests for parametric and non-parametric data respectively, with Qlucore and GraphPad Prism 8 (GraphPad Software Inc.) softwares. Data were considered significant for adjusted p-values after Tukey or Dunn's tests superior to 0.05. t-SNE was performed using Qlucore software and a perplexity of 15.

REFERENCES

1. Gardner A, Ruffell B. Dendritic Cells and Cancer Immunity. Trends Immunol. 2016;37(12):855–65.

2. Banchereau J, Steinman RM. Dendritic cells and the control of immunity. Nature. 1998 Mar 19;392(6673):245–52.

3. Dudek AM, Martin S, Garg AD, Agostinis P. Immature, Semi-Mature, and Fully Mature Dendritic Cells: Toward a DC-Cancer Cells Interface That Augments Anticancer Immunity. Front Immunol. 2013 Dec 11;4:438.

4. Li Q, Guo Z, Xu X, Xia S, Cao X. Pulmonary stromal cells induce the generation of regulatory DC attenuating T-cell-mediated lung inflammation. Eur J Immunol. 2008 Oct;38(10):2751–61.

5. Flavell RA, Sanjabi S, Wrzesinski SH, Licona-Limón P. The polarization of immune cells in the tumour environment by TGFbeta. Nat Rev Immunol. 2010 Aug;10(8):554–67.

6. Stary G, Olive A, Radovic-Moreno AF, Gondek D, Alvarez D, Basto PA, et al. VACCINES. A mucosal vaccine against Chlamydia trachomatis generates two waves of protective memory T cells. Science. 2015 Jun 19;348(6241):aaa8205.

7. Manicassamy S, Pulendran B. Dendritic cell control of tolerogenic responses. Immunol Rev. 2011 May;241(1):206–27.

8. Trojandt S, Bellinghausen I, Reske-Kunz AB, Bros M. Tumor-derived immuno-modulators induce overlapping pro-tolerogenic gene expression signatures in human dendritic cells. Hum Immunol. 2016 Dec;77(12):1223–31.

9. Zong J, Keskinov AA, Shurin GV, Shurin MR. Tumor-derived factors modulating dendritic cell function. Cancer Immunol Immunother CII. 2016 Jul;65(7):821–33.

10. Ghiringhelli F, Puig PE, Roux S, Parcellier A, Schmitt E, Solary E, et al. Tumor cells convert immature myeloid dendritic cells into TGF-beta-secreting cells inducing CD4+CD25+ regulatory T cell proliferation. J Exp Med. 2005 Oct 3;202(7):919–29.

11. Dumitriu IE, Dunbar DR, Howie SE, Sethi T, Gregory CD. Human dendritic cells produce TGF-beta 1 under the influence of lung carcinoma cells and prime the differentiation of CD4+CD25+Foxp3+ regulatory T cells. J Immunol Baltim Md 1950. 2009 Mar 1;182(5):2795–807.

12. Dalod M, Chelbi R, Malissen B, Lawrence T. Dendritic cell maturation: functional specialization through signaling specificity and transcriptional programming. EMBO J. 2014 May 16;33(10):1104–16.

13. Grandclaudon M, Perrot-Dockès M, Trichot C, Mostafa-Abouzid O, Abou-Jaoudé W, Berger F, Hupé P, Thieffry D, Sansonnet L, Chiquet J, Levy-Leduc C, Soumelis V. A Quantitative Multivariate Model of Human Dendritic Cell-T Helper Cell Communication. Available at SSRN: https://ssrn.com/abstract=3353217. Accepted in Cell in July 2019.

14. Basit F, Mathan T, Sancho D, de Vries IJM. Human Dendritic Cell Subsets Undergo Distinct Metabolic Reprogramming for Immune Response. Front Immunol. 2018;9:2489.

15. Michea P, Noël F, Zakine E, Czerwinska U, Sirven P, Abouzid O, et al. Adjustment of dendritic cells to the breast-cancer microenvironment is subset specific. Nat Immunol. 2018;19(8):885–97.

Figure 1
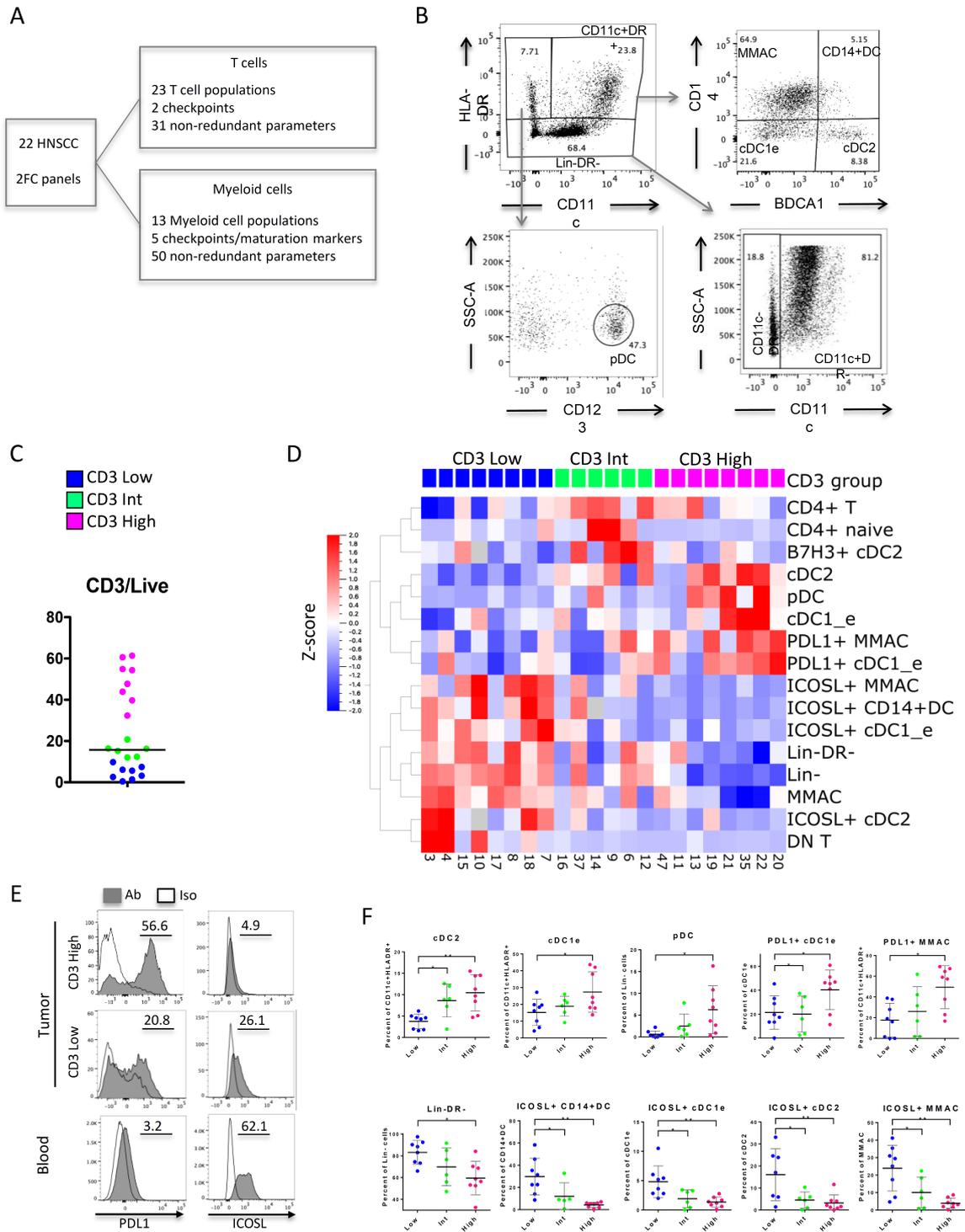
Fig1. **T cell infiltration is associated to DC infiltration and PDL1 & ICOSL expression on CD11c+HLA-DR+ cell.** Phenotypic characterization of 22 human HNSCC primary tumor-

infiltrating cells. A. Multicolor flow cytometry analysis scheme. B. Myeloid cell panel gating strategy for the CD45+CD3-CD56-CD19- compartment. C. Percentage of CD3 positive cells among live cells. D. Anova test between CD3 high, int and low, showing only the 16 significant variables among the 81 analyzed. E. Representative staining of PDL1 (right) and ICOSL (left) in CD11c+DR+ cells in a representative CD3 high tumor (top), CD3 low (middle) and blood from a healthy donor (bottom). F. Quantification of cell populations in percentages of their parental population in the 3 groups of CD3 infiltration.

Figure 2
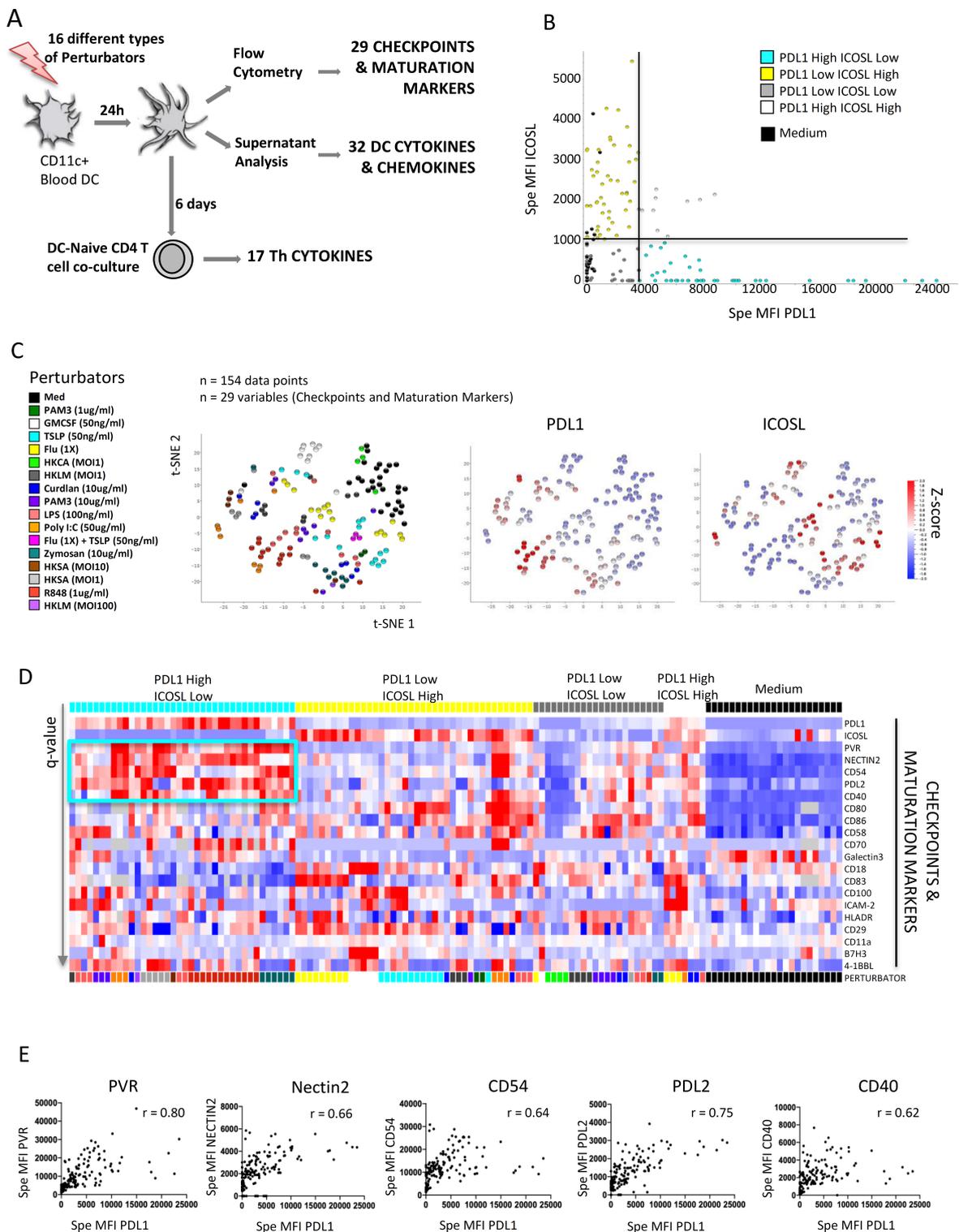
Fig 2. PDL1 and ICOSL expression on CD11c+DC were exclusive and PDL1 high DC overexpress PVR, Nectin2, CD54, CD40 and PDL2. A. Methods for the *in vitro* analysis of

primary blood DC. B. Expression of PDL1(x) vs ICOSL(y) on DC at H24. Individual tests were annotated according to their expression of PDL1 as high/low and ICOSL high/low with the thresholds of specific MFI at 3500 and 1000 respectively. C. T-SNE of the 29 surface markers colored by stimuli (left), PDL1 specific MFI (center) and ICOSL specific MFI (right) using Qlucore software. D. Heatmap representing the expression of the 29 surface markers in the 4 groups defined by PDL1 and ICOSL in "B", and in Medium condition. Multigroup comparison by Kruskal-Wallis test and Tukey post-hoc test. Only the variables significant at a p-value < 0,05 are represented and ordered by increasing q-value (max q-value = 0,046), among 130 individual experiments. E. Correlation of PDL1 (x) with PVR, Nectin2, CD54, PDL2 and CD40 (y). « r » values are Spearman correlation coefficients.

Figure 3
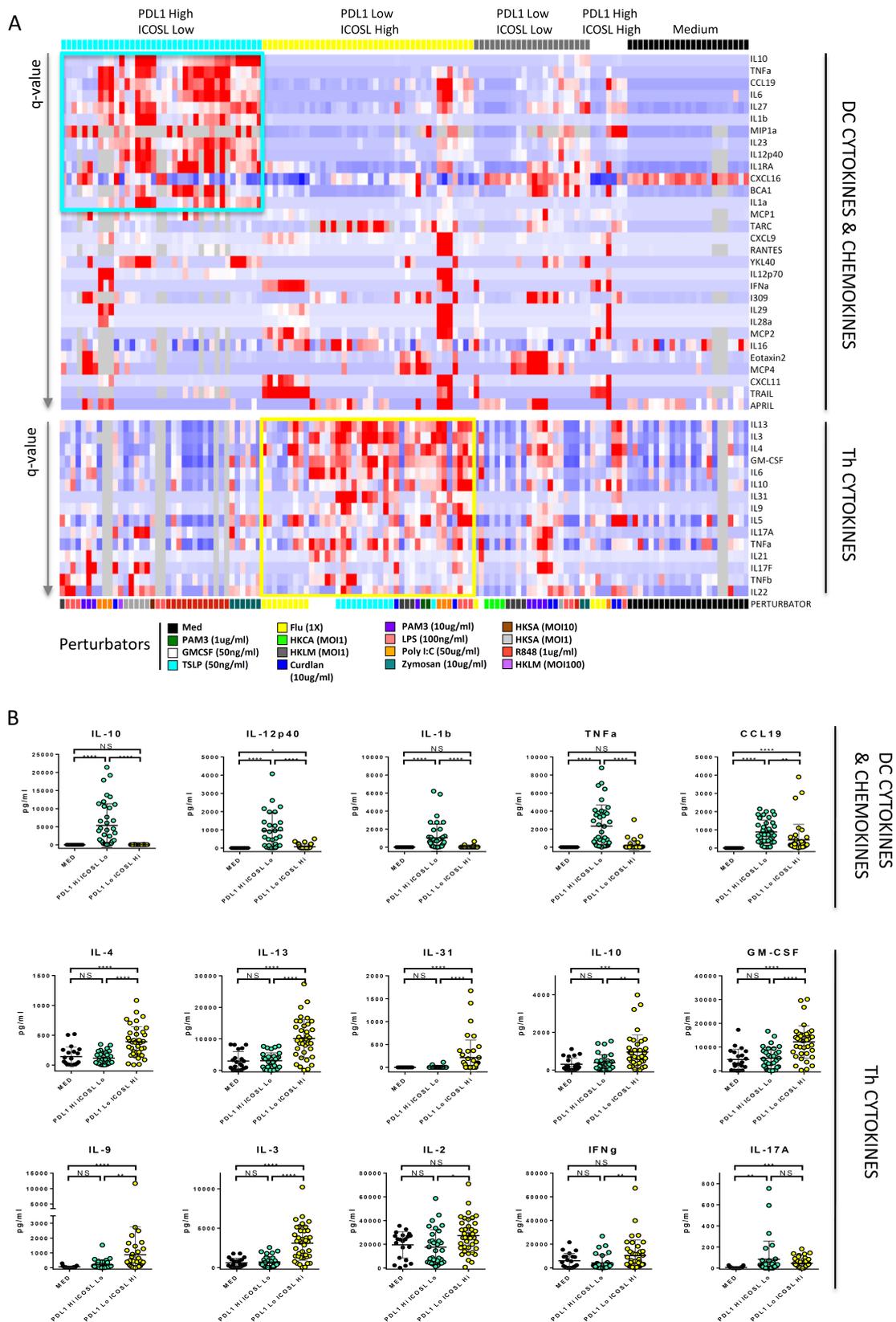
Fig 3. PDL1 and ICOSL expression pattern characterize "Secretory" and "Helper" DC.

A. Heatmaps representing the cytokines and chemokines secreted by the DC measured in H24 supernatants (top), and the CD4 T helper cell cytokines measured after co-culture (bottom) in the 4 groups defined by PDL1 and ICOSL expression and Medium condition. Only the variables significant at a p-value < 0,05 after Kruskal-Wallis multigroup comparison and Tukey post-hoc test are represented and ordered by increasing q-value (max q-value = 0,035 (top) and 0,055 (bottom)), among 130 individual experiments. Cells in grey are missing values. B. Quantification of cytokines and chemokines secreted by the DC (top row) and of the CD4 T helper cell cytokines (2 bottom rows) in the Medium, PDL1 high ICOSL low and PDL1 low ICOSL high conditions.

Figure 4
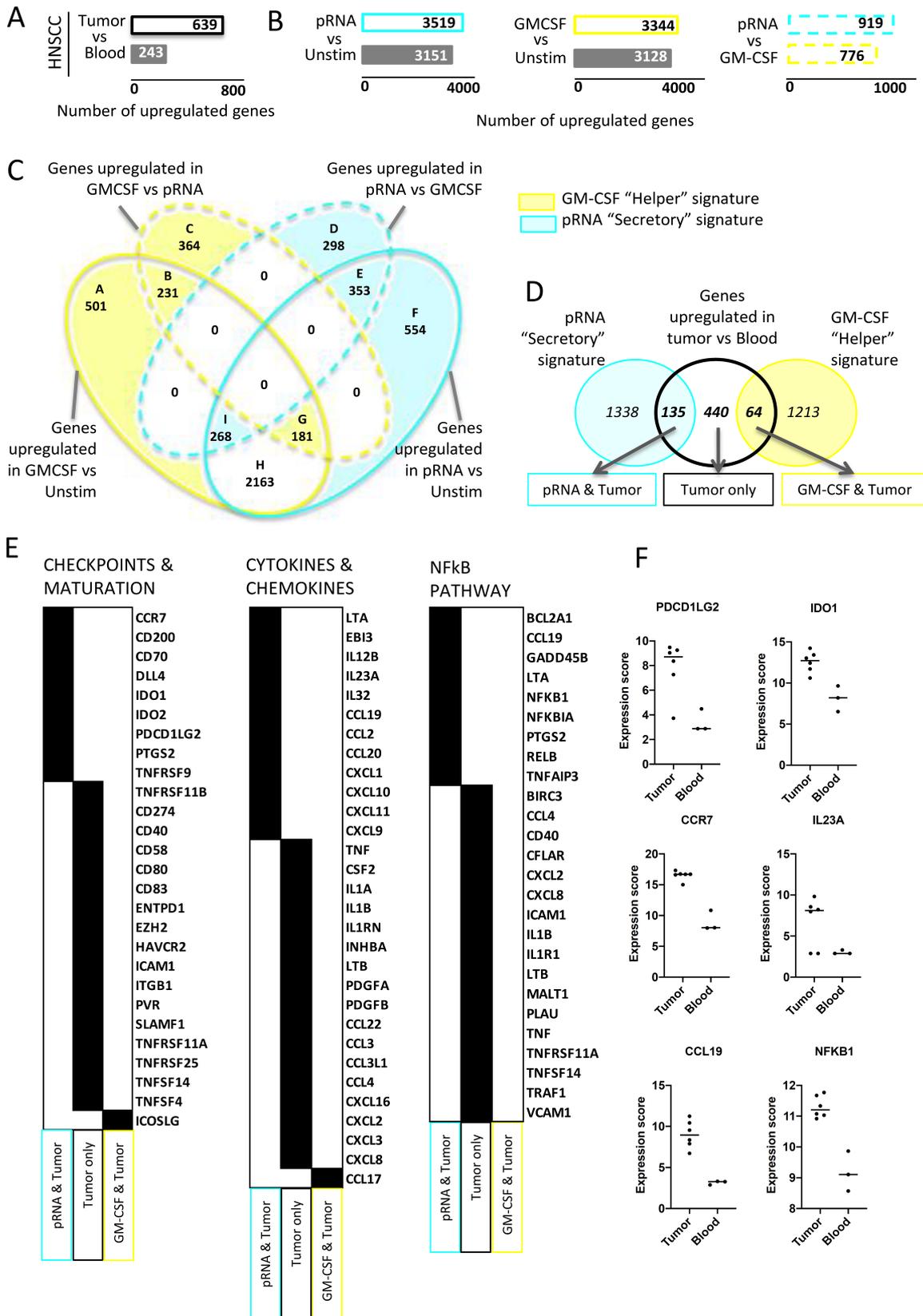
Fig4. RNAseq of tumor vs blood cDC2 confirms that T cell inflamed HNSCC are infiltrated by "secretory" DC. A. Analysis of differentially expressed genes (DEG) by

DESeq2 between HNSCC tumor (n=6) and blood cDC2 (n=3). B. Analysis of DEG from dataset GS87442 by DESeq2 between unstimulated cell and pRNA, a TLR7/8 ligand (left) or GM-CSF (center) and pRNA vs GM-CSF (right). C. Venn diagram of upregulated genes identified in "B". The blue and the yellow-colored area contain the genes of the "secretory" and "helper" signatures respectively. D. Venn diagram of the 639 tumor cDC2 upregulated genes with the "secretory" and "helper" signatures defined in "C". E. Supervised analysis of the 135 genes shared between tumor & pRNA "secretory" signature (light blue), 440 tumor specific genes (black) and the 64 genes shared between tumor & GM-CSF (yellow), using 3 gene lists: checkpoint and maturation markers (left, 148 genes), cytokines and chemokines (center, 169 genes), NFkB pathway (right, 100 genes). F. Expression of selected genes in cDC2 from tumors and blood of HNSCC patients.

Figure 5
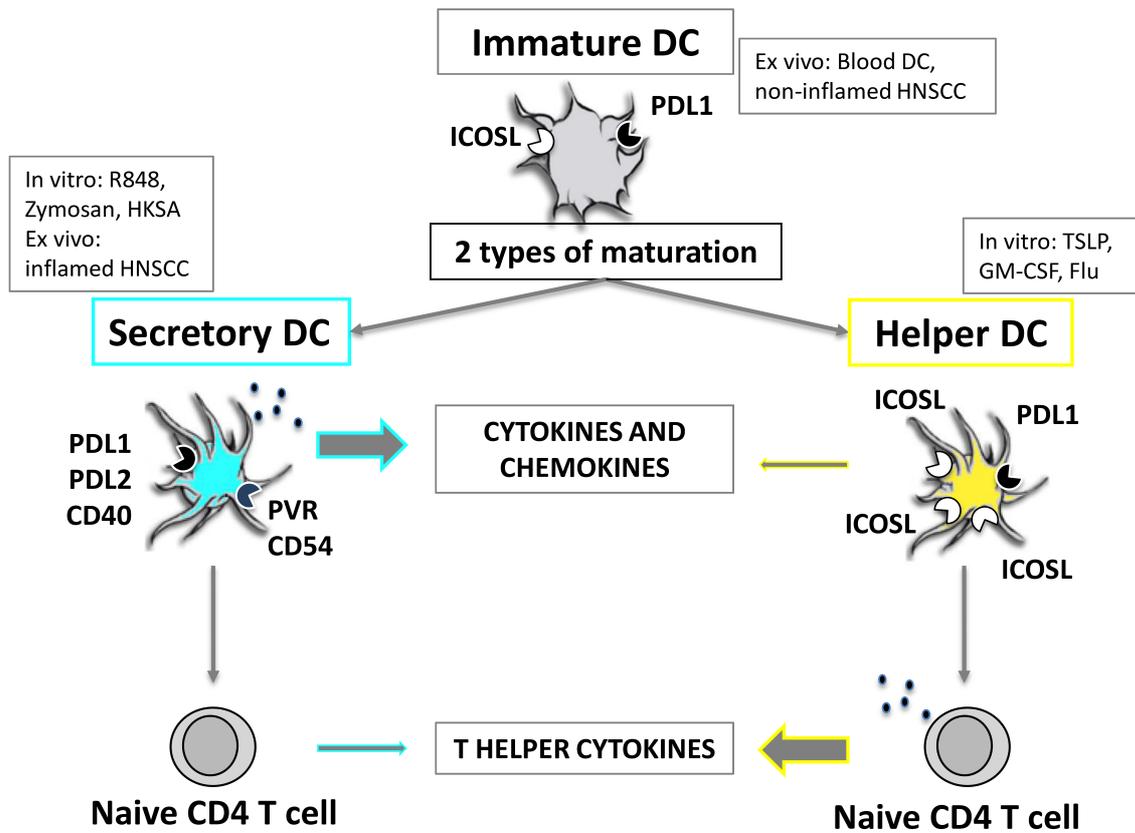
Fig.5 Schematic representation of DC activation into "helper" and "secretory" phenotypes
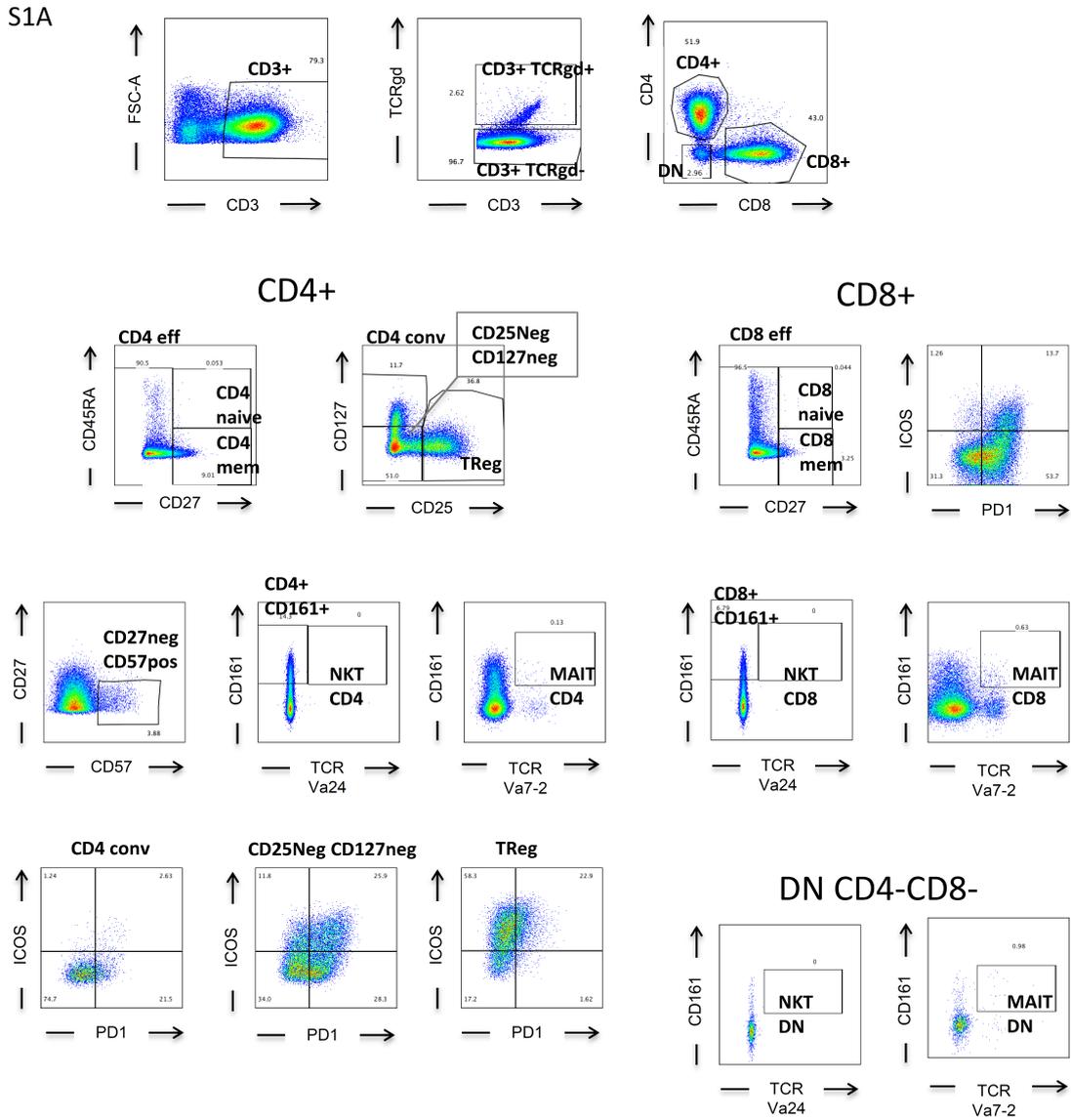
FigS1A. T cell panel gating strategy

S1B
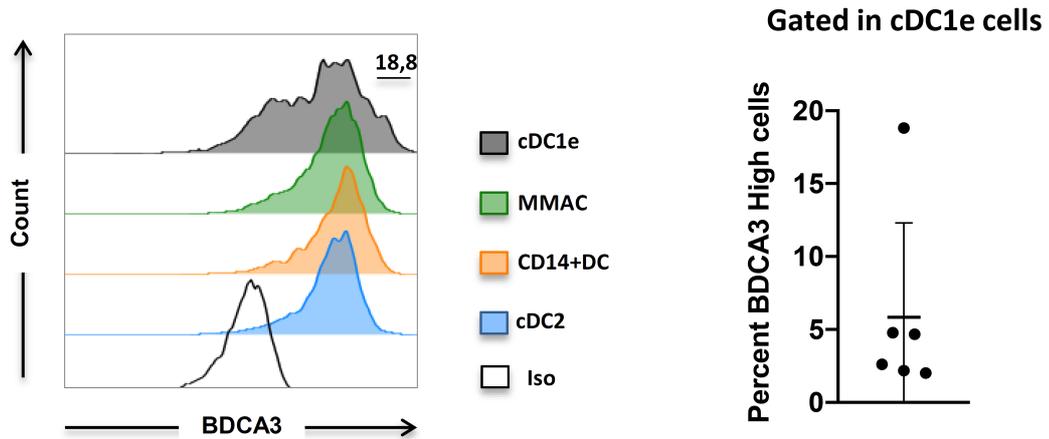
FigS1B. Left: Flow cytometry staining for BDCA3 expression in 4 cell populations in a HNSCC primary tumor. This tumor was selected for its high level of cDC1 infiltration. Right: Percentages of cDC1, gated as BDCA3 high, in the cDC1e gate (n = 6 tumors).

S1C
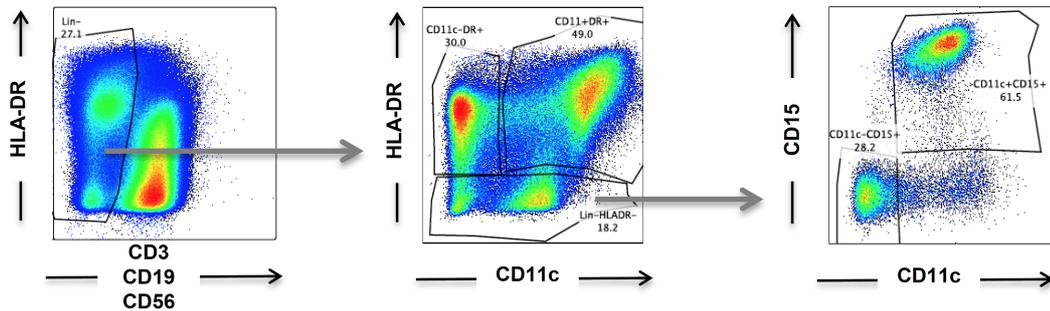
Fig S1C. Flow cytometry staining showing CD15 expression in Lin-HLADR- population. Most Lin-HLADR-CD11c+ cells are CD15+, therefore having a neutrophil phenotype.

S1D
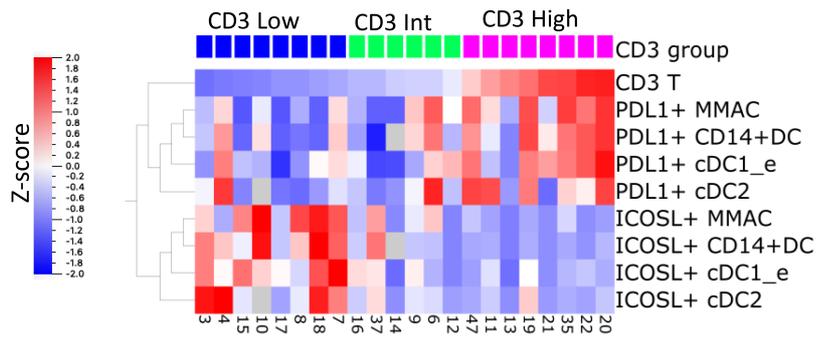
Fig S1D. Heatmap representing the expression of PDL1 and ICOSL in the 4 subsets of CD11c+HLA-DR+ cells in the 22 HNSCC samples, ordered by the level of CD3 infiltration from the lowest (left) to the highest (right).
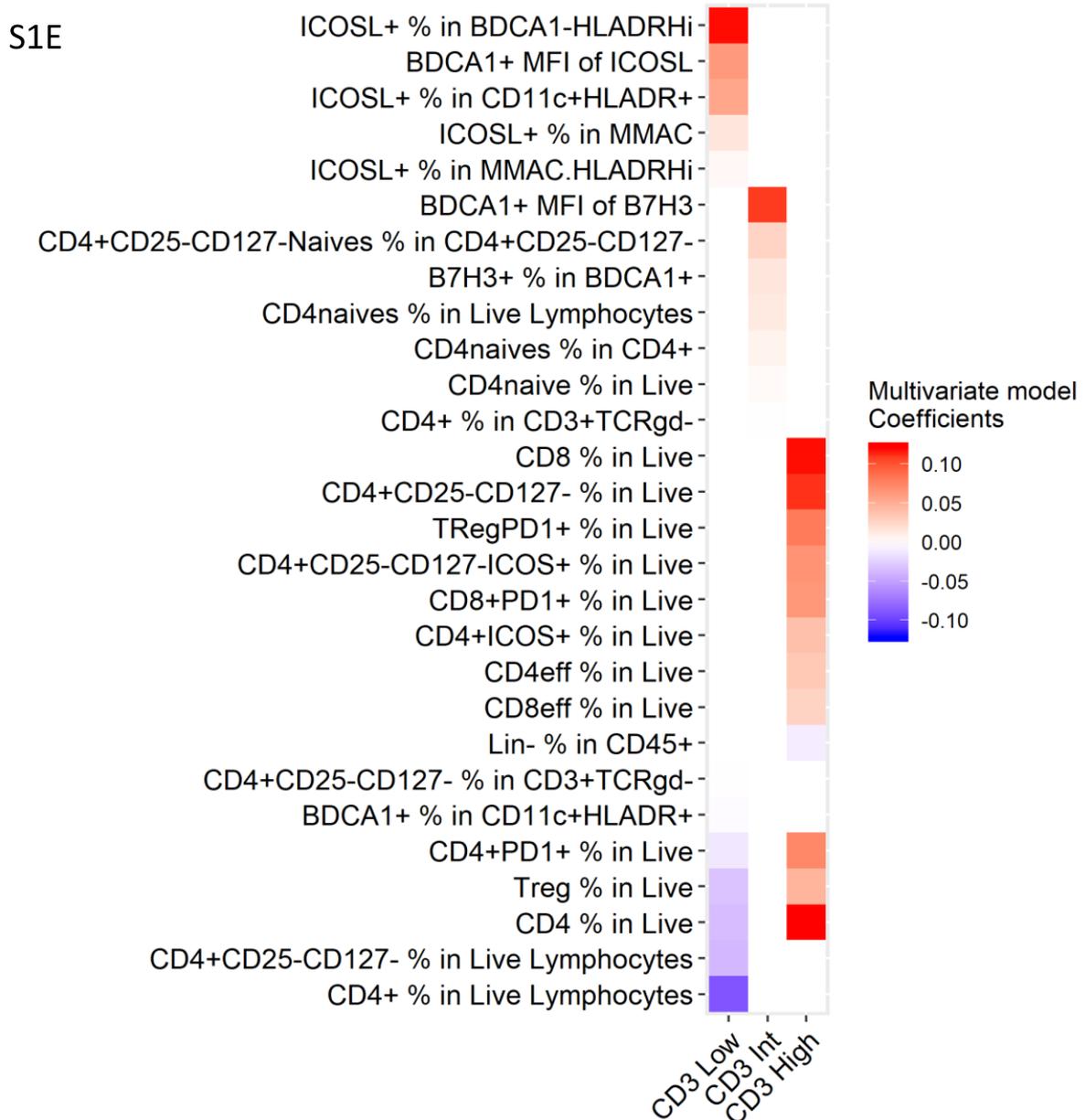
Fig S1E. Elastic net model of the 434 parameters measured by flow cytometry and 14 clinical parameters in the 22 HNSCC, showing the parameters the most representative of CD3 Low, CD3 Int and CD3 High tumors. The "Live" gate was established by selecting the live cells among a parental gate of all the cells in the FSC-A versus SCC-A graph, excluding only the debris and red blood cells. The "Live Lymphocyte" gate was established by selecting the live cells among a parental gate of cells having the FSC and SCC levels corresponding to lymphocytes only.
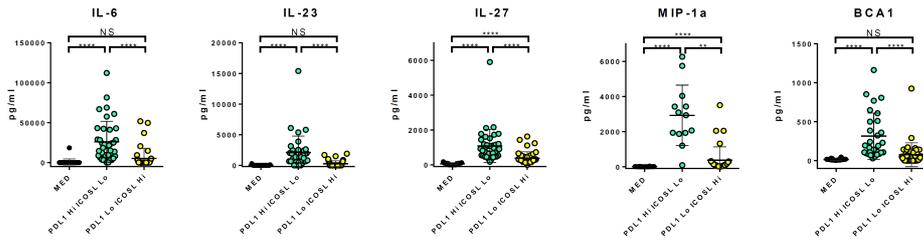
Fig S3A. Quantification of cytokines and chemokines secreted by the DC, in the Medium, PDL1 high ICOSL low and PDL1 low ICOSL high conditions.
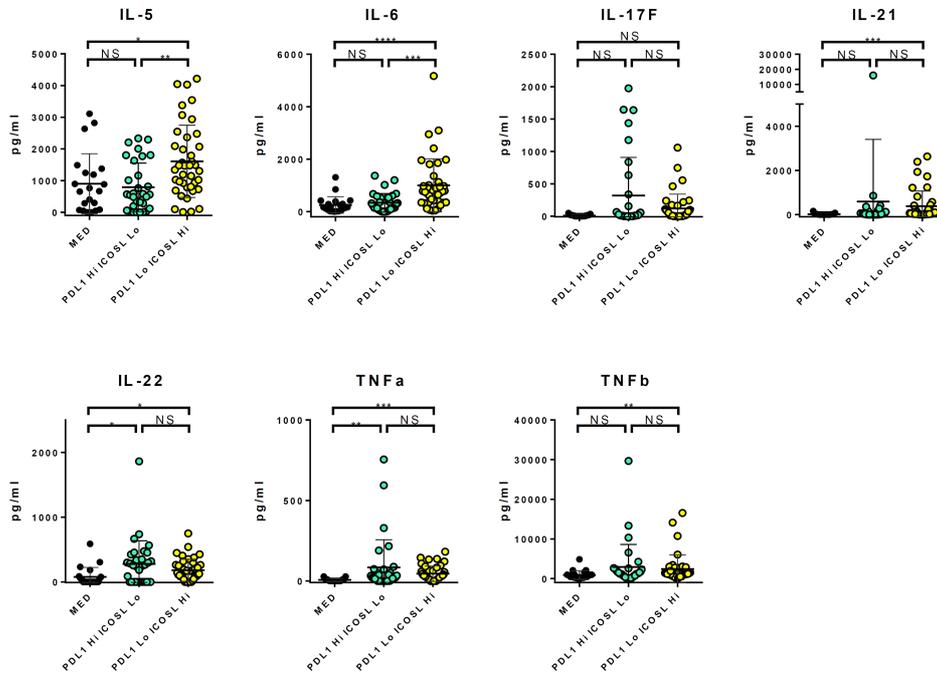
Fig S3B. Quantification of the CD4 T helper cell cytokines, in the Medium, PDL1 high ICOSL low and PDL1 low ICOSL high conditions.
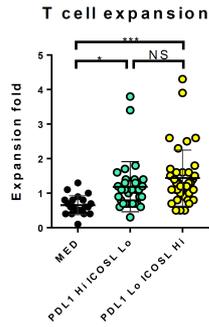
Fig S3C. T cell expansion at day 6 of DC-T co-culture in the Medium, PDL1 high ICOSL low and PDL1 low ICOSL high conditions.
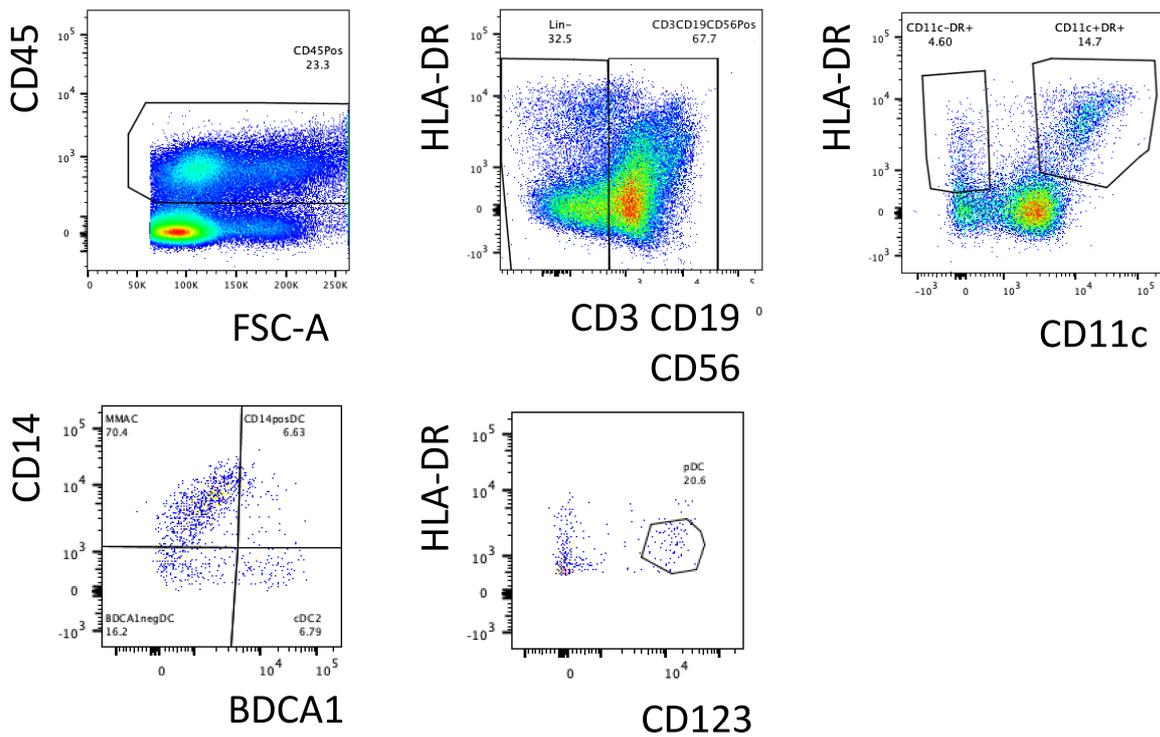
FigS4A. Flow cytometry sorting strategy for RNA sequencing of blood and tumor infiltrating cDC2, selected as CD45+, CD3-, CD19-, CD56-, CD11c+, HLA-DR+, CD14-, BDCA1+. Plots from a representative donor.

ALL TABLES ARE PROVIDED AS SUPPLEMENTARY MATERIAL.

Large tables that cannot be included fully in this manuscript are partially shown and available in a complete format at: https://doi.org/10.1101/721563

Table 1   **Cell populations analyzed by flow cytometry (Fig 1)**

Cell populations	Markers	Checkpoint / Maturation marker	Short name
T cells Panel			
CD3	CD3+		CD3 T
CD3 TCRgd	CD3+TCRgd		Gd T
CD4+	CD3+TCRgd-CD4+CD8-		CD4+ T
CD4 mem	CD3+TCRgd-CD4+CD8-CD27+CD45RA-		CD4+ mem T
CD4 naive	CD3+TCRgd-CD4+CD8-CD27+CD45RA+		CD4+ naive T
CD4 eff	CD3+TCRgd-CD4+CD8-CD27-CD45RA+		CD4+ eff T
T Reg	CD3+TCRgd-CD4+CD8-CD25+CD127int/-	PD1, ICOS	Treg
CD4conv	CD3+TCRgd-CD4+CD8-CD25-CD127+	PD1, ICOS	CD4+CD25-CD127+T
CD25NegCD127Neg	CD3+TCRgd-CD4+CD8-CD25-CD127-	PD1, ICOS	CD4+CD25-CD127- T
CD27NegCD57Pos	CD3+TCRgd-CD4+CD8-CD27-CD57+		CD4+CD27-CD57+ T
MAIT CD4	CD3+TCRgd-CD4+CD8-CD161+TCRVa72+		CD4+ MAIT
NKT CD4	CD3+TCRgd-CD4+CD8-CD161+TCRVa24-		CD4+ NKT
CD4CD161PosTCRVa24Neg	CD3+TCRgd-CD4+CD8-CD161+TCRVa24-		CD4+ CD161+ T
CD8+	CD3+TCRgd-CD8+CD4-	PD1, ICOS	CD8+ T
CD8 mem	CD3+TCRgd-CD8+CD4-CD27+CD45RA-		CD8+ mem T
CD8 naive	CD3+TCRgd-CD8+CD4-CD27+CD45RA+		CD8+ naive T
CD8 eff	CD3+TCRgd-CD8+CD4-CD27-CD45RA+		CD8+ eff T
MAIT CD8	CD3+TCRgd-CD8+CD4-CD161+TCRVa72+		CD8+ MAIT
NKT CD8	CD3+TCRgd-CD8+CD4-CD161+TCRVa24-		CD8+ NKT
CD8CD161PosTCRVa24Neg	CD3+TCRgd-CD8+CD4-CD161+TCRVa24-		CD8+ CD161+ T
DN	CD3+TCRgd-CD4-CD8-		DN T
MAIT	CD3+TCRgd-CD4-CD8-CD161+TCRVa72+		DN MAIT
NKT	CD3+TCRgd-CD4-CD8-CD161+TCRVa24-		DN NKT
Myeloid cells Panel			
CD45Pos	CD45+	B7H3, PDL1	CD45+
LinNeg	CD45+Lin-		Lin-
CD11cPosHLADRPos	CD45+Lin-CD11c+HLADR+		CD11c+DR+
BDCA1Pos	CD45+Lin-CD11c+HLADR+	B7H3, PDL1, ICOSL, CD86, CD83	cDC2
BDCA1NegHLADRLo_BDCA1Neg	CD45+Lin-CD11c+HLADR+		cDC2 DRlow
BDCA1Neg	CD45+Lin-CD11c+HLADR+	B7H3, PDL1, ICOSL, CD86, CD83	cDC1[e]
BDCA1Pos HLADRLo_BDCA1Pos	CD45+Lin-CD11c+HLADR+		cDC1[e] DRlow
CD14PosDC	CD45+Lin-CD11c+HLADR+	B7H3, PDL1, ICOSL, CD86, CD83	CD14+DC
CD14PosDC HLADRLo_CD14Pos	CD45+Lin-CD11c+HLADR+		CD14+DC DRlow
MMAC	CD45+Lin-CD11c+HLADR+	B7H3, PDL1, ICOSL, CD86, CD83	MMAC
MMAC HLADRLo_MMAC	CD45+Lin-CD11c+HLADR+		MMAC DRlow
pDC_LinNeg	CD45+Lin-CD11c-HLADR+CD123+	B7H3, PDL1, ICOSL, CD86, CD83	pDC
LinNegHLADRNeg	CD45+Lin-HLADR+		Lin-DR-
CD11cPosHLADRNeg	CD45+Lin-HLADR+CD11c+	B7H3, PDL1, ICOSL, CD86, CD83	Neutrophils[e]
CD11cNegHLADRNeg	* redundant, percent of cell not used in Fig1A	B7H3, PDL1, ICOSL, CD86, CD83	CD11c-DR-

Table 2 - Characteristics of the 22 patients whom tumors were analyzed by flow cytometry

Gender	Site	Stage_UICC	HPV	Diff_Ix	Mit_Ix	PNI	VE	OH	Tobacco	N_status	ECS	Margins
1	oral cavity	2	unknown		1	unknown	0	0	0	0	0	0
1	oral cavity	3		0	2	unknown	0	1	0	1	1	0
0	oral cavity	4	unknown		1	3 unknown	1	0	0	1	1	0
0	oral cavity	4		1	2	unknown	1	1	1	1	1	2
0	oral cavity	4	unknown		2	3	0	1	0	0	1	0
1	oropharynx	1		1	2	3	0	0	0	0	0	1
0	oropharynx	3		1	2	3	0	0	0	0	0	0
1	oropharynx	4		0	1	3	0	0	1	1	1	1
0	larynx	4	unknown		1	unknown	1	1	1	1	1	0
0	oral cavity	2		0	1	3	0	0	0	0	0	1
1	oral cavity	4	unknown		1	unknown	unknown	0	0	1	1	0 unknown
0	oral cavity	4	unknown		1	2	0	0	1	0	1	0
0	oropharynx	3		1	3	3	0	0	1	1	0	0
0	oropharynx	3		0	3	3	1	0	1	1	0	0
0	hypopharynx	4	unknown		2	3	1	1	0	1	1	0
0	larynx	4		0	2	unknown	unknown	0	0	1	1	0 unknown
0	larynx	4	unknown		2	3	0	0	0	1	0	0
0	oral cavity	1	unknown		1	1	0	0	1	1	0	0
0	oral cavity	4		0	1	2	0	0	0	0	0	0
0	oropharynx	1		0	1	3	1	1	1	1	0	0
0	oropharynx	3		0	1	3	1	1	1	1	0	1
0	oropharynx	3	unknown		3	3	0	1	1	1	0	0

...nale
...Positive
... Index: 1=well, 2=moderately, 3=poorly differentiated
...1=low, 2=intermediate, 3=high
...Positive
...Positive
...Positive
...Positive
...Positive
...Close, 2=Positive
...he 7th edition UICC

Table 3   In vitro analysis: Percentages of datapoints in each PDL1/ICOSL category per perturbator (Fig2)

Perturbators	Receptor	Total number of data points	PDL1 Hi / ICOSL Lo	PDL1 Lo / ICOSL Hi	PDL1 Lo / ICOSL Lo	PDL1 Hi / ICOSL Hi
PAM3 (1ug/ml)	TLR1 :TLR2	2	0%	100%	0%	0%
GMCSF (50ng/ml)	GMCSFR	10	0%	80%	10%	10%
TSLP (50ng/ml)	TSLPR	15	0%	87%	13%	0%
Flu (1X)	TLR7, Cytosolic sensors	16	0%	75%	6%	19%
Med		29	0%	24%	76%	0%
HKCA (MOI1)	Dectin-1	4	0%	0%	100%	0%
HKLM (MOI1)	TLR2	8	13%	38%	50%	0%
Curdlan (10ug/ml)	Dectin-1	8	25%	25%	25%	25%
PAM3 (10ug/ml)	TLR1: TLR2	8	38%	13%	50%	0%
LPS (100ng/ml)	TLR4	11	45%	27%	18%	9%
PolyIC (50ug/ml)	TLR3	8	50%	38%	0%	13%
Flu (1X) + TSLP	See Flu and TSLP	3	67%	0%	0%	33%
Zymosan (10ug/ml)	TLR2, Dectin-1	8	75%	0%	25%	0%
HKSA (MOI10)	TLR2	4	75%	0%	0%	25%
HKSA (MOI1)	TLR2	6	83%	0%	17%	0%
R848 (1ug/ml)	TLR7/8	13	92%	0%	8%	0%
HKLM (MOI100)	TLR2	1	100%	0%	0%	0%
Total number		154	44	54	46	10

Table 4   In vitro analysis: List of measured checkpoints and maturation markers and antibodies list (Fig2)

Marker	Dye	Brand	Clone	Ref
4-1BBL	APC	R&D Systems	282220	FAB2295A
B7H3	FITC	R&D Systems	185504	FAB1027F
CD100	FITC	BioLegend	A8	328406
CD11a	PerCP	R&D Systems	CR38	FAB35951C
CD18	PE	BioLegend	TS1/18	302107
CD229/ SLAMF3	APC	R&D Systems	249936	FAB1898A
CD29	AF700	BioLegend	TS2/16	303020
CD30L	PE	R&D Systems	LQI03	FAB1028P
CD40	PE-Cy7	BioLegend	5C3	334321
CD54	BV711	BD	HA58	564078
CD70	FITC	BD	Ki-24	555834
CD80	BV786	BD	L307.4	564159
CD83	PerCP/Cy5.5	BioLegend	HB15e	305320
CD86	BV650	BioLegend	IT2.2	305428
Galectin 3	AF488	R&D Systems	Polyclonal Goat IgG	IC1154G
HLA-DR	BV711	BioLegend	L243	307644
ICAM-2	FITC	BioLegend	CBR-IC2/2	328507
ICAM-3	APC	BioLegend	CBR-IC3/1	330011
ICOSL	APC	R&D Systems	136726	FAB165A
Jagged 2	APC	BioLegend	MHJ2-523	346906
LFA3 / CD58	PE-Cy5	BioLegend	TS2/9	330909
LIGHT	PE	R&D Systems	115520	FAB664P
Nectin-2	PE	BioLegend	TX31	337410
OX40L	R-PE	Ancell	ANC10G1	400-050
PDL1	PerCP-eFluor e710	eBioscience	MIH18	46-5983-42
PDL2	BV786	BD	MIH18	563843
PVR	PE	BioLegend	SKII.4	337619
SLAMF5	FITC	R&D Systems	Polyclonal Goat IgG	FAB1855F
VISTA	AF700	R&D Systems	730804	FAB71261N

Table 5   In vitro analysis: List of measured DC Cytokines and Chemokines, and corresponding genes (Fig3)

Analytes	Technology for measurements	Corresponding gene(s)
APRIL	Luminex	TNFSF13
BCA1	Luminex	CXCL13
CCL19	Luminex	CCL19
CXCL11	Luminex	CXCL11
CXCL16	Luminex	CXCL16
CXCL9	Luminex	CXCL9
Eotaxin2	Luminex	CCL24
I309	Luminex	CCL1
IFNa	CBA	IFNA1, IFNA10, IFNA13, IFNA14, IFNA16, IFNA17, IFNA2, IFNA21, IFNA22P, IFNA4, IFNA5, IFNA6, IFNA7, IFNA8
IFNb	Luminex	IFNB1
IL10	CBA	IL10
IL12p40	Luminex	IL12B
IL12p70	CBA	IL12A, IL12B
IL16	Luminex	IL16
IL1a	CBA	IL1A
IL1b	CBA	IL1B
IL1RA	Luminex	IL1RN
IL23	Luminex	IL23
IL27	Luminex	IL27
IL28a	Luminex	IL28A, IL28B, IFNL2, IFNL3
IL29	Luminex	IL29, IFNL1
IL6	CBA	IL6, IFNL1
IP10	Luminex	CXCL10
MCP1	Luminex	CCL24
MCP2	Luminex	CCL8
MCP4	Luminex	CCL13
MIP1a	Luminex	CCL3
RANTES	Luminex	CCL5
TARC	Luminex	CCL17
TNFa	CBA	TNF
TRAIL	Luminex	TNFSF10
YKL40	Luminex	CHI3L1

Table 6   **In vitro analysis: List of measured T helper cytokines (Fig3)**

Analytes	Technology for measurements
GMCSF	CBA
IFNg	CBA
IL10	CBA
IL13	CBA
IL17A	CBA
IL17F	CBA
IL2	CBA
IL21	Luminex
IL22	Luminex
IL3	CBA
IL31	Luminex
IL4	CBA
IL5	CBA
IL6	CBA
IL9	CBA
TNFa	CBA
TNFb	Luminex

Table 7   Characteristics of the 6 patients, whom tumor was analyzed by RNAseq (Fig 4)

All donors are HNSCC bearing patients			

Number of donors: 7 donors	Tumor only		n = 4
	Blood only		n = 1
	Tumor and Blood		n = 2

Patients Characteristics	Age (Mean +/- SD)			63.6 +/- 13.0
	SexRatio (%Male)			0.57
	T Stage	T3		14%
		T4		86%
		N0		14%
		N+		86%
	Localisation	Oral Cavity		71%
		Oropharynx		29%
			HPV+	50%
			nc	50%

Table 8   DESeq2 results defining DEG between Blood and Tumor cDC2 at FDR 0.1 (Fig 4A). Only the top 182 up-regulated genes in tumor cDC2 are shown, ordered by Log2 fold change.

| Blood vs Tumor cDC2 | Negative value in "log2FoldChange" column corresponds to genes increased in tumor DC (n=639) | | | | |
| | Positive value in "log2FoldChange" column corresponds to genes increased in blood DC (n=243) | | | | |

Gene	baseMean	log2FoldChange	lfcSE	stat	pvalue	padj
LTA	192.185977	-24.18002994	2.775534122	-8.711847478	2.99E-18	2.91E-15
VTN	157.4367516	-23.90123077	2.835400472	-8.429578468	3.47E-17	3.11E-14
MMP1	148.2692325	-23.80307792	2.681210637	-8.877735149	6.82E-19	8.84E-16
KRT13	92.36307357	-23.15439318	3.076947192	-7.525118807	5.27E-14	2.79E-11
GRM7	88.99226171	-23.10380436	3.231986306	-7.14848461	8.77E-13	2.99E-10
SCN7A	79.29408787	-22.94452977	3.041796641	-7.543084722	4.59E-14	2.55E-11
NGFR	57.03270815	-22.3682963	3.097158779	-7.222198764	5.12E-13	1.86E-10
NFIB	47.74269465	-22.24543238	2.843268016	-7.823895691	5.12E-15	3.51E-12
FAM111B	42.04221585	-22.05826966	3.00943924	-7.329694306	2.31E-13	9.97E-11
PTP4A3	35.01163662	-21.78194156	3.435145126	-6.340908685	2.28E-10	5.44E-08
PIEZO2	45.0227955	-21.75342772	3.110588587	-6.993347757	2.68E-12	8.70E-10
FABP3	30.70721352	-21.6243888	3.435272023	-6.294811199	3.08E-10	7.04E-08
TNIP3	30.34632966	-21.6080201	3.43528394	-6.290024487	3.17E-10	7.12E-08
CD3D	24.27874241	-21.29828492	3.435544803	-6.199390823	5.67E-10	1.12E-07
LY6D	19.48715406	-20.99020894	3.435866694	-6.109145322	1.00E-09	1.88E-07
SERPINE3	19.16122911	-20.96744551	3.43589406	-6.102471479	1.04E-09	1.93E-07
SEMA3A	18.40399438	-20.91138647	3.4359624	-6.086034723	1.16E-09	2.11E-07
SLC9C1	16.36489847	-20.74932348	3.436176549	-6.038491675	1.56E-09	2.75E-07
TNFRSF11B	666.8823832	-12.69956904	1.449184281	-8.763253373	1.90E-18	2.01E-15
CCL17	584.8680463	-12.5103139	1.312812734	-9.52939713	1.58E-21	3.08E-18
ANXA3	495.0522675	-12.26970909	1.955187377	-6.275464558	3.49E-10	7.53E-08
UBD	450.2044853	-12.13265219	1.640831891	-7.394207938	1.42E-13	6.64E-11
MMP12	4838.818207	-12.06705356	1.258279571	-9.590121181	8.80E-22	2.05E-18
AOC1	825.0120148	-12.04461395	1.604941284	-7.504706914	6.16E-14	3.12E-11
TMEM150C	382.1773824	-11.89624741	1.566796225	-7.592721512	3.13E-14	1.83E-11
IL22RA2	291.8690401	-11.50747012	1.84738187	-6.229069533	4.69E-10	9.44E-08
PLEK2	546.2385488	-11.44962357	1.798722289	-6.36542041	1.95E-10	4.73E-08
IL2RA	268.4780967	-11.38718088	2.213533639	-5.144345079	2.68E-07	2.61E-05
IL7R	2012.116529	-11.23822604	0.963932189	-11.65873095	2.07E-31	2.42E-27
CCL19	749.2118611	-11.11864844	1.522226185	-7.304202587	2.79E-13	1.16E-10
CLDN1	174.7231126	-10.76780012	2.119766081	-5.079711489	3.78E-07	3.50E-05
ADTRP	170.2071186	-10.72913966	1.670996495	-6.420803214	1.36E-10	3.50E-08
SDK2	160.2827761	-10.64242087	1.756045828	-6.060445973	1.36E-09	2.44E-07
TRPC6	150.2813353	-10.54993952	2.038446371	-5.175480534	2.27E-07	2.27E-05
GPR153	140.2214461	-10.44933479	2.130637775	-4.904322505	9.38E-07	7.98E-05
IL23A	251.4894106	-10.3303737	2.392492585	-4.317828932	1.58E-05	0.000879385
SUCNR1	119.9957245	-10.22521487	2.1305108	-4.799419404	1.59E-06	0.000122497
IL32	408.2500218	-10.21412128	1.403972907	-7.275155543	3.46E-13	1.39E-10
C10orf10	389.3010817	-10.21275875	1.730671002	-5.901039967	3.61E-09	5.62E-07
LAD1	116.8465844	-10.18727439	1.572033641	-6.480315769	9.15E-11	2.54E-08
TREML1	393.7230785	-10.1676251	1.518261714	-6.696885658	2.13E-11	6.54E-09
FAM149A	114.047924	-10.15159317	2.067713187	-4.909575096	9.13E-07	7.83E-05
TBC1D4	3884.204825	-10.14167464	1.129903892	-8.975696706	2.82E-19	4.11E-16
HPGDS	338.3984408	-10.05041691	2.683145251	-3.745759535	0.000179849	0.006320007
WTAPP1	102.0245111	-9.990875469	2.517690919	-3.968269256	7.24E-05	0.003081872
IL12B	97.78531816	-9.929962523	2.690457356	-3.690808368	0.000223543	0.00751412
ACVR1C	92.91320961	-9.855863452	2.581978948	-3.81717421	0.000134989	0.005173699
HMSD	92.07220342	-9.842746288	2.760428917	-3.565658304	0.000362944	0.010995789
MMP3	87.95702458	-9.776638641	2.630340504	-3.716871875	0.000201705	0.006879191
GNAO1	87.2769927	-9.76531096	1.840366283	-5.306177933	1.12E-07	1.23E-05
TMEM163	164.4157334	-9.716839133	2.246124862	-4.326045847	1.52E-05	0.000855415
SLC16A9	81.51766195	-9.667044205	2.266046594	-4.266039468	1.99E-05	0.001069506
RND1	80.73223032	-9.653010653	2.622297647	-3.681126994	0.000232205	0.007672642
GLYATL2	79.67936618	-9.633899678	2.517226914	-3.827187618	0.000129616	0.005039459
ITGB8	286.3715753	-9.541554022	1.625295517	-5.870657934	4.34E-09	6.58E-07
SLCO2B1	72.38085789	-9.497449667	1.832177004	-5.18369658	2.18E-07	2.19E-05
LAMP3	4814.781569	-9.202378071	1.265668863	-7.270762785	3.57E-13	1.39E-10
CNN3	56.75311726	-9.143965378	1.961326446	-4.662133322	3.13E-06	0.000226722

Gene					
ARNT2	54.73593018	-9.092697804	2.720788378	-3.341934962	0.000831966	0.020386651
NCCRP1	681.5778918	-9.055523814	1.180270358	-7.672414843	1.69E-14	1.04E-11
GPR85	52.57089166	-9.034062243	2.631786141	-3.432673386	0.000597662	0.015771776
CCL22	92217.33683	-9.030304285	0.80379546	-11.23457985	2.76E-29	1.61E-25
ITIH1	100.3943392	-9.005011583	2.347908446	-3.835333358	0.000125394	0.004914633
BCL2L14	466.0609484	-8.900222027	1.230847695	-7.230969407	4.80E-13	1.80E-10
CD80	1884.726549	-8.820421118	1.140543315	-7.733525772	1.05E-14	6.78E-12
RAPGEF4	44.52568637	-8.795850261	2.512855566	-3.50034056	0.000464664	0.013123105
C6orf223	43.85935432	-8.771619379	2.02867839	-4.323809738	1.53E-05	0.000859982
RAMP1	43.16600416	-8.750019873	2.185240432	-4.004145149	6.22E-05	0.002787957
PC	42.44246703	-8.726010354	2.490054141	-3.504345633	0.000457731	0.013085717
TMEM54	41.30376819	-8.686895995	2.650353194	-3.277637115	0.001046799	0.024322432
HSPA1B	3799.561986	-8.681835496	0.877193077	-9.897291396	4.28E-23	1.25E-19
TNF	663.0192006	-8.679321417	1.315139585	-6.599543894	4.12E-11	1.20E-08
SLCO5A1	201.6645256	-8.671707979	1.498218087	-5.788014476	7.12E-09	1.03E-06
GPR31	39.36227976	-8.617213458	2.906425472	-2.964883683	0.003027974	0.053643304
TNFSF4	245.8925554	-8.604623814	2.30337352	-3.735661516	0.000187222	0.006518692
CXCL9	651.2153886	-8.56523063	1.760239643	-4.865945762	1.14E-06	9.20E-05
LOC730101	36.9464799	-8.524817389	2.131503374	-3.999438844	6.35E-05	0.002815896
RRAD	36.60301275	-8.512836857	2.288717529	-3.71947903	0.000199634	0.006848625
CCL20	317.5104773	-8.497775513	1.569130776	-5.415594189	6.11E-08	7.20E-06
NPR1	35.96910941	-8.487691689	1.899443243	-4.468515562	7.88E-06	0.000499125
STRIP2	1270.578021	-8.476997545	1.469711564	-5.767796724	8.03E-09	1.12E-06
FAM167A	35.52128972	-8.469915908	2.54175392	-3.332311535	0.000861278	0.020713288
MMP9	445.5868786	-8.361259046	1.434702011	-5.827871561	5.61E-09	8.29E-07
GPC5	31.93804236	-8.315481034	2.489448445	-3.340290518	0.000836908	0.020464767
S100B	4573.808131	-8.288414759	1.622768769	-5.107575962	3.26E-07	3.07E-05
KRT16	31.26524752	-8.284795913	2.888944264	-2.867758999	0.004133903	0.066284993
TPX2	104.5590123	-8.274770634	2.19811145	-3.764490937	0.000166889	0.006026595
SHISA2	30.18158196	-8.23414921	3.063040986	-2.688226912	0.007183257	0.096305177
NOS1	58.2551483	-8.218598385	2.095616574	-3.921804441	8.79E-05	0.003648147
LINC00885	28.37418557	-8.144814365	2.931074723	-2.778780868	0.005456332	0.080356889
RGS16	487.4830568	-8.144136536	1.674008214	-4.865051717	1.14E-06	9.20E-05
CADM1	27.73110901	-8.112324091	2.560606705	-3.16812577	0.001534251	0.032419397
GEM	636.3052233	-8.084833306	1.256884295	-6.432440388	1.26E-10	3.41E-08
LOC399715	51.17487878	-8.031039368	2.768657519	-2.900698014	0.003723325	0.062219003
PTPRG	26.22300974	-8.030700545	2.923872696	-2.746597195	0.006021704	0.085239267
ANKRD55	123.4946849	-7.993877418	1.913817813	-4.176927064	2.95E-05	0.001466556
GCM1	85.69366161	-7.993277004	2.544073352	-3.141920808	0.001678434	0.034834977
PPP2R2B	25.45239679	-7.989501995	2.459282726	-3.248712282	0.001159287	0.026368763
CRLF2	548.6083156	-7.977855723	1.901170492	-4.196286319	2.71E-05	0.001358266
HOPX	48.76257194	-7.962190806	2.26042078	-3.52243745	0.000427598	0.012468756
FSCN1	91.96031304	-7.947922703	1.351052996	-5.882761612	4.03E-09	6.19E-07
SYNPO2	400.5965745	-7.875155353	1.610860691	-4.888787339	1.01E-06	8.51E-05
CD3E	43.51526332	-7.798687941	2.601816035	-2.997401752	0.002722916	0.050074814
TSPAN15	85.49210412	-7.792127084	1.960302758	-3.974961037	7.04E-05	0.003040882
KRT17	43.19988255	-7.787356941	2.263197505	-3.440864937	0.000579858	0.01554819
ECE1	228.2751526	-7.722182005	1.461903596	-5.282278548	1.28E-07	1.37E-05
FAM159A	21.15116069	-7.721800689	2.790040865	-2.767629961	0.005646553	0.081511623
PLAT	20.58141633	-7.68221546	2.44712289	-3.139284705	0.001693608	0.034963266
CDKN1C	346.0824497	-7.681186294	1.228836464	-6.250779919	4.08E-10	8.51E-08
PMEPA1	82.25358425	-7.680743084	2.10101446	-3.65573071	0.00025645	0.008263089
IL1A	232.9981079	-7.679454734	1.173885897	-6.541909019	6.07E-11	1.73E-08
TFAP2C	32.86919172	-7.656334711	2.808804796	-2.725833679	0.006413931	0.089488146
TARP	20.21169927	-7.655985868	2.809529395	-2.725006502	0.006430022	0.089605469
ENPP2	827.0433476	-7.648470558	1.357238543	-5.63531783	1.75E-08	2.29E-06
RASAL1	123.6817692	-7.605587966	2.146642941	-3.54301492	0.00039558	0.011740582
ANKRD33B	123.7248934	-7.569548292	1.501816541	-5.040261635	4.65E-07	4.14E-05
HSPA1A	4386.140153	-7.564723045	0.898583891	-8.418493947	3.81E-17	3.18E-14
ST8SIA1	74.60956141	-7.545006195	2.050908251	-3.67886091	0.000234278	0.007694449
ANKRD18DP	18.57020702	-7.533970346	2.627290919	-2.867581314	0.004136225	0.066284993
GJB2	18.54756601	-7.531862044	2.362743851	-3.187760722	0.001433791	0.030912647

ADORA2A	713.946437	-7.52498231	1.448483833	-5.195075111	2.05E-07	2.08E-05
LOC400043	124.7826698	-7.47613121	1.935545636	-3.862544531	0.000112212	0.004467037
FBXO27	34.54315948	-7.463845945	2.426668225	-3.075758717	0.002099677	0.041160723
C3	85.58584106	-7.459286822	1.828403017	-4.079673219	4.51E-05	0.002095758
CLEC5A	1369.060237	-7.422840042	1.264906901	-5.868289624	4.40E-09	6.58E-07
CSF2	80.75084878	-7.42021104	2.163868251	-3.429141787	0.000605493	0.015942374
AQP9	184.2271479	-7.39555054	2.301045662	-3.213995559	0.001309017	0.028646105
ANGPTL4	80.23320586	-7.388352276	2.287492835	-3.229890893	0.001238375	0.027565653
C15orf48	4214.349789	-7.383069156	0.723020279	-10.21142749	1.76E-24	6.85E-21
SEMA6B	32.53190273	-7.379462909	2.076179219	-3.554347737	0.000378918	0.011332558
CD274	517.1624031	-7.37513428	1.527187429	-4.829226681	1.37E-06	0.000107297
DLL4	16.49660837	-7.365142278	2.17814534	-3.381382382	0.000721221	0.018367515
DBNDD2	32.22117198	-7.362624566	1.640339894	-4.488474975	7.17E-06	0.000462274
MACC1	531.852583	-7.337289995	1.263770258	-5.805873299	6.40E-09	9.34E-07
PDGFA	304.8015543	-7.329553023	1.38254869	-5.301479128	1.15E-07	1.25E-05
SELM	102.43782	-7.319657065	1.863077398	-3.92879924	8.54E-05	0.003569062
CETP	52.74080552	-7.291207748	2.514992898	-2.899096754	0.003742394	0.062448186
MREG	261.4504202	-7.279919783	1.134273968	-6.418131764	1.38E-10	3.50E-08
SYNPO	15.52884859	-7.278624859	1.890652929	-3.849794295	0.000118217	0.004674183
CCR7	87788.24956	-7.261281267	0.876246936	-8.286797899	1.16E-16	8.85E-14
SH2D3A	14.89679259	-7.21716428	1.83608155	-3.93074277	8.47E-05	0.003553066
SLC7A11	220.4595814	-7.162078659	1.002355411	-7.145248658	8.98E-13	2.99E-10
ADORA2A-AS	91.48138723	-7.152112064	1.79392245	-3.986856882	6.70E-05	0.002914015
EBF4	14.19395884	-7.149711216	1.775674914	-4.02647532	5.66E-05	0.002579711
LINC00515	147.2417839	-7.130146025	1.23784142	-5.760144969	8.40E-09	1.14E-06
CMTM1	14.03877572	-7.127267707	2.543376682	-2.802285543	0.005074194	0.076466924
PDGFB	132.6951542	-7.115200041	1.644076636	-4.327778817	1.51E-05	0.000852834
CXCL11	109.2413342	-7.098256449	1.81684887	-3.906905282	9.35E-05	0.0038395
CXCL3	300.3409998	-7.087864881	1.322725847	-5.358529055	8.39E-08	9.68E-06
TULP2	393.2651457	-7.042784235	0.959015997	-7.343760955	2.08E-13	9.32E-11
GPR68	49.76794474	-7.016240952	1.602434656	-4.378488025	1.20E-05	0.00070757
CDC42EP2	99.89582287	-6.976761979	2.002817389	-3.48347384	0.000494951	0.013811278
PDCD1LG2	313.7504875	-6.971263181	1.577505208	-4.419169677	9.91E-06	0.00060642
TNFAIP6	70.62026379	-6.954943539	1.974092929	-3.52310848	0.000426517	0.012468399
PLEKHG1	128.2723548	-6.933299937	2.079431547	-3.334228504	0.000855364	0.020647035
MAP1LC3C	23.8920864	-6.932523816	2.073427632	-3.343508937	0.00082726	0.02031403
TNFRSF25	57.84927376	-6.921327416	2.445619379	-2.830091826	0.004653465	0.072082352
BIRC3	43715.80359	-6.917765844	0.781514211	-8.851746704	8.62E-19	1.00E-15
ANKRD37	126.0851928	-6.907026157	1.497832848	-4.61134643	4.00E-06	0.000281109
HCAR3	299.1339563	-6.894687771	1.367186359	-5.042975837	4.58E-07	4.11E-05
PLAU	300.1560595	-6.865076764	1.413558017	-4.856593561	1.19E-06	9.47E-05
DNAJA4	5119.311504	-6.855206011	1.243429129	-5.513145745	3.52E-08	4.24E-06
NCS1	55.04356553	-6.834663135	2.112711237	-3.235020014	0.001216342	0.02735139
F3	38.66257273	-6.832874111	2.034812047	-3.35798784	0.000785121	0.019736309
TROAP	22.29408687	-6.830680999	2.37790288	-2.872565173	0.004071541	0.065948277
POU6F1	38.71266112	-6.830171233	1.950717982	-3.501362727	0.000462885	0.013123105
NRP2	126.7781678	-6.798875772	1.176608888	-5.778365132	7.54E-09	1.07E-06
GTF2IRD1	21.46114084	-6.778225483	1.895480524	-3.575993211	0.000348901	0.010681307
LOC152225	10.94926164	-6.775349619	2.387146519	-2.838262991	0.004535979	0.070826856
DNAJB1	17434.25882	-6.771568979	0.902975844	-7.499169581	6.42E-14	3.12E-11
TLR3	151.5125527	-6.744033109	1.864160838	-3.617731352	0.000297197	0.009276854
FXYD2	10.64596909	-6.731022491	2.353316262	-2.860228606	0.004233357	0.067456118
HCAR2	312.5650563	-6.729815469	1.135082141	-5.928923757	3.05E-09	5.01E-07
CXCL8	7928.032548	-6.72569284	1.306022737	-5.149751723	2.61E-07	2.56E-05
CXCL2	392.4737585	-6.661435167	1.791410814	-3.71854134	0.000200377	0.006853934
GNLY	34.07149772	-6.652763895	2.215625813	-3.002656791	0.002676341	0.049694858
G0S2	2871.489719	-6.637810201	1.151604176	-5.763968504	8.22E-09	1.13E-06
SPP1	3494.39642	-6.629616293	1.447706647	-4.579392037	4.66E-06	0.000318086
TRAF1	1396.533229	-6.619645138	0.799308547	-8.281714438	1.21E-16	8.85E-14
IGSF3	92.55769332	-6.607969943	1.981181304	-3.335368615	0.000851864	0.020647035
TRIP10	133.0904901	-6.604302645	1.112368315	-5.937154591	2.90E-09	4.83E-07
ADRA2B	9.678713063	-6.60234495	2.258764105	-2.922990026	0.003466876	0.059084318

Table 9 **List of genes associated with the Venn diagramm comparing DEG betwenn pRNA and GMCSFat FDR 0.1 (Fig 4C).** Only 62 up-regulated genes per cluster are shown

Gene list name	A	B	C	D	E	F	G	H	I
Number of genes	501	231	364	298	353	554	181	2163	268
	DHX15	MAPRE3	FAM102B	GRAMD1B	GMIP	CRYM	ABCB1	A2M	ABHD12
	C1QL2	EXOSC4	CBX8	CLGN	CDYL2	C14orf1	ABCC3	A4GALT	ABTB2
	ABCF2	ANKH	ACER3	ADAM11	ADA	ABCC2	ADRA1B	AACS	ACE
	FOXD4L3	PPBPL2	IER5L	LOC1005074	IL15	FAM65C	AGPAT9	AAK1	ACHE
	ANKRD13C	C21orf67	ALOX15	APOBEC3B	APOL6	AKAP8	ALDH1A2	AANAT	ADAMDEC1
	ESPNL	P2RX1	GLCE	JUP	HPS1	EHF	AQP3	AARS	ADORA2A
	ARID5A	CDH2	ATP7A	C10orf47	BTG1	ASCC3	ARAP3	AATK	AGAP3
	ATP6V1B1	CKLF	C10orf125	C20orf112	C12orf56	ATP6V0A2	ARHGAP23	ABCA10	AGRN
	CEP85	HS2ST1	CLSTN3	FAM26F	DNAI2	CCDC157	ARHGAP31	ABCA6	AICDA
	FURIN	PPFIBP1	IKBIP	LOC285696	IL15RA	FAM71F2	ASAP1	ABCB6	AK8
	C14orf142	DMPK	C3orf33	CD38	CCDC80	C10orf18	ASB1	ABCF3	AKR1C1
	CXorf23	LOC652276	ERCC8	GPA33	FUT1	COQ10B	ASPHD1	ABCG2	AKR1C2
	CHST15	IGFBP6	CMTM7	FARP2	EDF1	CCDC87	ATP1B2	ABHD16B	ANKLE2
	ALDOB	C17orf57	ADORA1	ANXA4	APOBEC3F	ADPRHL1	AXIN2	ABHD4	ANKRD1
	HYOU1	SIGLECP3	LOC1001295	NIPAL3	LOC1001328	GJA3	C13orf15	ABHD6	APOO
	CPLX1	KCNK13	DLX4	GBP1P1	FAM72D	CDK4	C15orf26	ABL2	AQP9
	EHD4	MPZL3	FLJ90757	HPS3	HES4	DHX37	C19orf59	ABLIM1	ARAP2
	BTG2	CYTH4	C1orf96	CACHD1	C7orf41	BRD1	C20orf123	ACADVL	ARHGAP20
	C16orf70	EMR3	CALM2	CFD	CCL8	C11orf84	C5orf43	ACAT2	ASXL1
	FLG	PPA2	HIST1H2AL	LOC1001343	IGF2BP3	FAM175B	C7orf57	ACO1	ATF7IP2
	GMFB	PRRX2	ITGA4	LYSMD2	IRF7	FGF11	CCDC147	ACOT13	ATOX1
	ELOVL1	NCLN	GAS1	IL7	HLA-C	DNMBP	CCDC165	ACOX3	ATP10B
	C6orf211	FAM43A	CD1E	CXCL9	CHRNB2	C2CD3	CCL17	ACP2	ATP6V0D2
	CCDC57	FMNL2	CDR2L	DTX4	CXCL10	C7orf60	CD276	ACP5	B4GALT5
	C12orf5	DIRC2	C3orf21	CD300E	CBR1	C10orf111	CD9	ACSL1	BAALC
	FBXL18	PLXDC2	GPR65	LDLRAD3	IFIT1	ESF1	CECR6	ACSL3	BCL2A1
	DNAJB14	MED22	FAM95B1	GVINP1	GPR55	CSTF3	CHST1	ACTN2	BHLHE22
	CUL5	LOC1001342	EPS8	GMDS	FRK	CNTNAP2	CISH	ACTR1A	BMP10
	BTBD10	CXCR1	C17orf87	C6orf192	C7orf40	BEST4	CLEC5A	ACTR3	BTBD7
	ALG12	C19orf35	AKAP12	ANXA8L2	APOBEC3G	AFAP1-AS1	CLN8	ACVR1	BUB3
	E2F6	MMRN1	FGD4	HLA-DOA	HAPLN3	DDX31	CNRIP1	ACVR1C	C10orf92
	GRPEL2	QSOX1	KDELC2	MGC16275	KCNJ2	FOXL2	COL22A1	ACVR2A	C14orf34
	F2RL3	PDE1B	GMFG	KIAA1407	IDO2	ELOVL3	CST6	ADAM12	C15orf48
	FBXO6	PNPLA7	GPSM3	LILRA3	IFIT3	ETV7	CTGF	ADAM17	C17orf96
	GNL1	PSIMCT-1	IVNS1ABP	MAP3K8	ISG15	FJX1	CTNNAL1	ADAM19	C1QTNF1
	ACRC	ARHGAP18	ACOX2	ADAP2	ADCY9	ACBD7	CTSH	ADAM32	C21orf71
	ELAVL4	MYO1E	FXYD5	IGFBP7	HLA-A	DLD	CUX2	ADAM9	C22orf45
	BAP1	CMTM2	C11orf31	C4orf46	C20orf203	ATXN7L3B	CXCL5	ADAMTS14	C3orf64
	ACSL5	BCAN	ACPP	AGBL2	AGK	ACOT9	CYB5D1	ADAMTS7	C5orf62
	CTRC	LAYN	EFNB1	GIMAP2	FLJ31662	CLIC2	CYYR1	ADAT3	C8orf56
	DOCK10	MGAT4A	FANK1	HCG26	GTPBP1	DCUN1D1	DAB2	ADIPOR2	CAMK1G
	CD209	GALNT6	CEBPE	EEPD1	CXCL13	C8orf39	DIRAS2	ADM	CCL2
	FIGLA	POM121L9P	HHEX	LOC1001333	IFITM3	FAM102A	DLC1	ADM2	CCL20
	GLRX2	PROS1	IQSEC2	LY75	IRF1	FBXL3	DMWD	ADO	CCL7
	C11orf9	DHRS9	C2orf89	CD2AP	CBLN3	BRSK1	DNAH17	ADPRH	CCND1
	CD8B	GPR133	CIB1	EPHB4	DDX60	C9orf95	DOK6	ADRM1	CCR7
	ANXA2P2	CA2	APOBR	APOL3	ARHGAP24	ANKRD22	DUSP6	AFF2	CDCA4
	C21orf2	FAIM2	CCDC19	CPVL	CEMP1	C14orf55	ECEL1	AFF4	CELSR1
	FGD6	POLE4	HDDC2	LOC1001327	IFITM1	FABP6	ENO2	AGPAT4	CGN
	ARG2	CD1A	ARHGEF40	B3GNT4	BATF2	ARSB	EPAS1	AHCYL1	CHAC2
	ARHGEF35	CD36	ARSG	BAZ2A	BCL9L	ASB16	ETNK2	AHRR	CHMP5
	EDC4	MOBKL2A	FGL2	HLA-DPA1	HCP5	DERL1	FABP4	AHSA1	CHST7
	CDAN1	GPR56	CIDEB	ERGIC1	DENND5B	CAMSAP1	FAM135B	AIFM2	CILP2
	CTSZ	LIPA	EMR4P	GLT25D2	FLJ45340	CMKLR1	FAM40B	AK1	CKB
	ARHGEF12	CD1B	ARHGEF6	B3GNT7	BCL2L14	ASAP1-IT1	FBXO2	AK4	CLCN6
	DDIT3	LYPD3	ESYT2	GPR141	GATSL3	CRTAM	FLRT2	AKR1C3	COL17A1
	C3orf39	FAM173B	CCND3	CTSS	CHD2	C18orf8	FLT1	AKR1C4	COL5A3
	CLDN11	IL1RL2	COTL1	FFAR2	ENPP4	CCNL2	FRMD4A	AKR1CL1	CREG1
	CTTN	LOC1001288	EPHB6	GLTSCR2	FNBP1	CNGB1	GALNT4	AKT1S1	CRISPLD1
	CTSE	LDLRAP1	EHBP1L1	GIMAP8	FLJ39051	CLIC6	GAS2L3	AKT3	CTHRC1
	HECTD1	RAI1	KIAA1797	MYCBP2	KIF19	FSTL3	GGN	ALAS1	CXCL1
	EIF2C3	MYO1D	FOXJ2	IFITM2	HIVEP2	DIRC3	GGT5	ALCAM	CXCL6

Table 10 **List of 148 genes used for supervised analysis of checkpoints and maturation markers expressed at the RNA level by dendritic cells (Fig 4D)**

ANXA1	CD6	HLA-DRB9	LGALS3	TNFRSF11B
ARG1	CD63	HMGB1	LGALS9	TNFRSF12A
ARG2	CD7	HMGB2	LILRB2	TNFRSF13B
BTLA	CD70	ICAM1	LILRB4	TNFRSF13C
CCR7	CD80	ICAM2	LY9	TNFRSF14
CD101	CD81	ICAM3	MARCO	TNFRSF17
CD109	CD82	ICOS	MICA	TNFRSF18
CD200	CD83	ICOSLG	MICB	TNFRSF1A
CD209	CD84	IDO1	NECTIN2	TNFRSF1B
CD226	CD86	IDO2	NECTIN3	TNFRSF21
CD274	CD8A	ITGA4	NT5E	TNFRSF25
CD276	CD8B	ITGAL	PDCD1	TNFRSF4
CD28	CD9	ITGB1	PDCD1LG2	TNFRSF6B
CD300A	CD96	ITGB2	PTGS1	TNFRSF8
CD300C	CTLA4	JAG1	PTGS2	TNFRSF9
CD300E	DLL1	JAG2	PVR	TNFSF10
CD300LB	DLL4	KIR	PVRIG	TNFSF11
CD300LD	ENTPD1	KIR2DL1	SEMA4D	TNFSF12
CD300LF	EZH2	KIR2DL2	SIRPA	TNFSF13
CD300LG	HAVCR2	KIR2DL3	SLAMF1	TNFSF13B
CD33	HHLA2	KIR2DL5A	SLAMF6	TNFSF14
CD40	HLA-DRA	KIR2DL5B	TAP1	TNFSF15
CD44	HLA-DRB1	KIR2DS1	TAP2	TNFSF18
CD47	HLA-DRB2	KIR3DL1	TIMD4	TNFSF4
CD48	HLA-DRB3	KIR3DL2	TMEM173	TNFSF8
CD5	HLA-DRB4	KIR3DS1	TNFRSF10A	TNFSF9
CD53	HLA-DRB5	KIT	TNFRSF10B	VSIR
CD58	HLA-DRB6	LAIR1	TNFRSF10C	VTCN1
CD59	HLA-DRB7	LAIR2	TNFRSF10D	
CD5L	HLA-DRB8	LGALS1	TNFRSF11A	

Table 11   List of 117 genes used for supervised analysis of cytokines expressed at the RNA level by dendritic cells (Fig 4D)

AMH	IFNA10	IL17F	IL4
BMP10	IFNA13	IL18	IL5
BMP15	IFNA14	IL19	IL6
BMP2	IFNA16	IL1A	IL7
BMP4	IFNA17	IL1B	IL8
BMP6	IFNA2	IL1F10	IL9
BMP7	IFNA21	IL1RN	INHBA
CD27	IFNA22P	IL2	INHBB
CD40LG	IFNA4	IL20	LEP
CD74	IFNA5	IL21	LIF
CLCF1	IFNA6	IL22	LTA
CNTF	IFNA7	IL23A	LTB
CSF1	IFNA8	IL24	MIF
CSF2	IFNB1	IL25	MSTN
CSF3	IFNG	IL26	NODAL
EBI3	IFNL1	IL27	OSM
EDA	IFNL2	IL28A	PDGFA
EPO	IFNL3	IL28B	PDGFB
FASLG	IFNW1	IL29	PDGFC
FLT3LG	IL10	IL3	PRL
GDF1	IL11	IL30	TGFA
GDF10	IL12A	IL31	TGFB1
GDF11	IL12B	IL31RA	TGFB2
GDF2	IL13	IL32	TGFB3
GDF3	IL15	IL33	THPO
GDF5	IL16	IL34	TNF
GDF9	IL17A	IL36A	TSLP
GH1	IL17B	IL36B	
GHR	IL17C	IL36RN	
IFNA1	IL17D	IL37	

Table 12   List of 52 genes used for supervised analysis of chemokines expressed at the RNA level by dendritic cells (Fig 4D)

CX3CL1	CCL3	CXCL2
CCL1	CCL3L1	CXCL3
CCL11	CCL3L3	CXCL4
CCL13	CCL4	CXCL5
CCL14	CCL4L1	CXCL6
CCL15	CCL4L2	CXCL7
CCL16	CCL5	CXCL8
CCL17	CCL7	CXCL9
CCL18	CCL8	PF4
CCL19	CHI3L1	PPBP
CCL2	CHI3L2	XCL1
CCL20	CXCL1	XCL2
CCL21	CXCL10	
CCL22	CXCL11	
CCL23	CXCL11	
CCL24	CXCL12	
CCL25	CXCL13	
CCL26	CXCL14	
CCL27	CXCL16	
CCL28	CXCL17	

Table 13   List of 100 genes used for supervised analysis of the NFkB pathway (Fig

4D)

ATM	CSNK2A3	LTB	TAB2
BCL10	CSNK2B	LTBR	TAB3
BCL2	CXCL12	LY96	TICAM1
BCL2A1	CXCL2	LYN	TICAM2
BCL2L1	CXCL8	MALT1	TIRAP
BIRC2	CYLD	MAP3K14	TLR4
BIRC3	DDX58	MAP3K7	TNF
BLNK	EDA	MYD88	TNFAIP3
BTK	EDA2R	NFKB1	TNFRSF11A
CARD10	EDAR	NFKB2	TNFRSF13C
CARD11	EDARADD	NFKBIA	TNFRSF1A
CARD14	ERC1	PARP1	TNFSF11
CCL13	GADD45B	PIAS4	TNFSF13B
CCL19	ICAM1	PIDD1	TNFSF14
CCL21	IGH	PLAU	TRADD
CCL4	IKBKB	PLCG1	TRAF1
CCL4L1	IKBKG	PLCG2	TRAF2
CCL4L2	IL1B	PRKCB	TRAF3
CD14	IL1R1	PRKCQ	TRAF5
CD40	IRAK1	PTGS2	TRAF6
CD40LG	IRAK4	RELA	TRIM25
CFLAR	LAT	RELB	UBE2I
CHUK	LBP	RIPK1	VCAM1
CSNK2A1	LCK	SYK	XIAP
CSNK2A2	LTA	TAB1	ZAP70

Table 14   Antibody and Panels list for Human HNSCC and Blood FACS phenotyping and sorting (Methods)

PANELS	Figures	Number of samples	
T cells	1B, 1C, 1D, 1E, S1A		22
Myeloid cells	1B, 1C, 1D, 1E, 1F		22
BDCA3 panel	S1B		6
CD15 panel	S1C		3
RNAseq sorting	4	9 (6 Tumor + 3 Blood)	

Dye	Marker	Brand	Clone	Ref	Panel
FITC	CD14	BD	M5E2	555397	Myeloid cells
PerCP eFluor 710	PDL1	Ebiosciences	MIH1	46-5983-42	Myeloid cells
APC	ICOSL	R&D	136726	FAB165A	Myeloid cells
Alexa-700	CD3	BD	UCHT1	557943	Myeloid cells
Alexa-700	CD19	BD	HIB19	557921	Myeloid cells
Alexa-700	CD56	BD	B159	557919	Myeloid cells
APC-Cy7	CD45	BD	2D1	557833	Myeloid cells
BV605	CD83	BD	HB15e	740420	Myeloid cells
BV650	CD123	BD	7G3	563405	Myeloid cells
PE	B7H3	Biolegend	MIH42	351004	Myeloid cells
PECF594	CD11c	BD	B-ly6	562393	Myeloid cells
PC7	CD1c/BDCA1	Biolegend	L161	331516	Myeloid cells
BUV395	HLA-DR	BD	G 46-6	564040	Myeloid cells
BUV737	CD86	BD	2331 (FUN-1)	564428	Myeloid cells
BV785	CD15	Biolegend	W6D3	323043	CD15 panel
Qdot 605	CD14	Life technology	TuK4	Q10013	BDCA3 panel
BV711	HLA-DR	Biolegend	L243	307643	BDCA3 panel
Alexa 700	CD3	BD	UCHT1	557943	BDCA3 panel
Alexa 700	CD19	BD	HIB19	557921	BDCA3 panel
Alexa 700	CD56	BD	B159	557919	BDCA3 panel
APCCy7	CD45	BD	2D1	557833	BDCA3 panel
APC	BDCA-3	Miltenyi	AD5-14H12	130-113-876	BDCA3 panel
PC5	CD1a	BD	HI149	555808	BDCA3 panel
PC7	CD11c	Biolegend	Bu15	337216	BDCA3 panel
PE	BDCA-1	Biolegend	L161	331506	BDCA3 panel
Fluo 650NC	CD123	eBiosciences	6H6	95-1239-42	BDCA3 panel
FITC	Langerin	Miltenyi	MB22-9F5	130-098-349	BDCA3 panel
BV570	CD45	Biolegend	HI30	304033	RNAseq sorting
FITC	CD14	Biolegend	10.1	555527	RNAseq sorting
APC-eFluor780	HLA-DR	Ebiosciences	LN3	47-9956-42	RNAseq sorting
Alexa-700	CD3	BD	UCHT1	557943	RNAseq sorting
Alexa-700	CD19	BD	HIB19	557921	RNAseq sorting
Alexa-700	CD56	BD	B159	557919	RNAseq sorting
PECy5	CD11c	BD	B-ly6	551077	RNAseq sorting
BV650	CD123	BD	7G3	563405	RNAseq sorting
PE	CD1c/BDCA1	Biolegend	L161	331506	RNAseq sorting
APC	FceR1	Ebiosciences	AER-37	17-5899-42	RNAseq sorting
FITC	TCRgd	BD	11F2	347903	T cells
PerCP 5.5	TCRVa7.2	Biolegend	3C10	351710	T cells
APC	ICOS	Ebiosciences	ISA-3	17-9948-42	T cells
Alexa700	CD3	Biolegend	UCHT1	300424	T cells
APC Vio770	CD57	Miltenyi	TB03	130-104-197	T cells
BV510	TCR Va24	Biolegend	6B11	342918	T cells
BV605	CD27	Biolegend	O323	302830	T cells
BV650	CD127	Biolegend	A019D5	351326	T cells
BV711	PD1	Biolegend	EH12.2H7	329928	T cells
BV785	CD161	Biolegend	HP-3G10	339930	T cells
PE	CD25	BD	M-A251	555432	T cells
PE TX	CD4	Invitrogen	S3.5	MHCD0417	T cells
PC5	CD8b	Coulter	2ST8.5H7	6607109	T cells
PC7	CD45RA	Ebiosciences	HI100	25-0458-42	T cells

3.2 MMP2 AS AN INDEPENDENT PROGNOSTIC STRATIFIER IN ORAL CAVITY CANCERS

Abstract

Background: Around 25% of oral cavity squamous cell carcinoma (OCSCC) are not controlled by standard of care. Identifying those patients could offer them possibilities for intensified and personalized regimen. However, there is currently no validated biomarker for OCSCC patient selection in a pre-treatment setting. Our objectives were to determine a robust and independent predictive biomarker for disease related death in OCSCC treated with standard of care.

Patients and methods: Tumor and juxtatumor secretome were analyzed in a prospective discovery cohort of 37 OCSCC treated by primary surgery. Independent biomarker validation was performed by RTqPCR in a retrospective cohort of 145 patients with similar clinical features. An 18-gene signature (18G) predictive of the response to PD-1 blockade was evaluated in the same cohort.

Results: Among 29 deregulated molecules in a secretome analysis, we identified soluble MMP2 as a prognostic biomarker. In our validation cohort (n=145), high levels of MMP2 and CD276, and low levels of CXCL10 and STAT1 mRNA were associated with poor prognosis in univariate analysis (Kaplan-Meier). MMP2 (p = 0.001) and extra-nodal extension (ENE) (p = 0.006) were independent biomarkers of disease-specific survival (DSS) in multivariate analysis and defined prognostic groups with 5-year DSS ranging from 36% (MMP2highENE+) to 88% (MMP2lowENE-). The expression of 18G was similar in the different prognostic groups, suggesting comparable responsiveness to anti-PD-1.

Conclusion: High levels of MMP2 was an independent and validated prognostic biomarker, which may be used to select poor prognosis patients for intensified neoadjuvant or adjuvant regimens.

MMP2 AS AN INDEPENDENT PROGNOSTIC STRATIFIER IN ORAL CAVITY CANCERS

AUTHORS:

Caroline Hoffmann[1 2 3], Sophie Vacher[1 4], Philémon Sirven[1 2], Charlotte Lecerf[1 5], Lucile Massenet[1 2], Aurélie Moreira[1 5], Aurore Surun[6 7], Anne Schnitzler[1 4], Jerzy Klijanienko[1 8], Odette Mariani[1 8 9], Emmanuelle Jeannot[1 8], Nathalie Badois[1 3], Maria Lesnik[1 3], Olivier Choussy[1 3], Christophe Le Tourneau[1 5 10], Maude Guillot-Delost[1 2 11], Maud Kamal[1 5], Ivan Bieche[1 4 12]*, Vassili Soumelis[1 2 13]*.

* These authors contributed equally to this work

Corresponding author: caroline.hoffmann@curie.fr

AFFILIATIONS:

1. Paris-Saclay University, Paris, France
2. INSERM U932 research unit, Immunity and Cancer, Paris, France
3. Department of Surgical Oncology, Institut Curie, Paris & Saint-Cloud, France
4. Department of Genetics, Institut Curie, Paris, France
5. Department of Drug Development and Innovation (D3i), Institut Curie, Paris & Saint-Cloud, France
6. SIREDO Cancer Center (Care, innovation and research in pediatric, adolescents and young adults oncology), Institut Curie, Paris, France
7. Paris Descartes University, Sorbonne Paris Cité, Paris, France
8. Department of pathology, Institut Curie, Paris, France
9. Biological Resources Center, Institut Curie, Paris, France
10. INSERM U900 research unit, Saint-Cloud, France
11. Center of Clinical Investigation, CIC IGR-Curie 1428, Paris, France
12. INSERM U1016 research unit, Paris Descartes University, Faculty of Pharmaceutical and Biological Sciences, Paris, France
13. Clinical immunology department, Institut Curie, Paris, France. Current address of the author is Hospital St Louis, Immunology & Histocompatibility Laboratory, Paris, France

RUNNING TITLE: MMP2 AND PROGNOSIS IN ORAL CAVITY CANCER

KEYWORDS:

Biomarker / Metalloproteinase / Prognosis / Secretome/ Squamous cell carcinoma / Head and Neck / Oral cavity

CONFLICT OF INTEREST STATEMENT:

The authors declare no potential conflicts of interest.

STATEMENT OF TRANSLATIONAL RELEVANCE

There is currently no validated biomarker for risk-based patient stratification in oral cavity cancers, preventing the development of personalized approaches. This study started with a detailed characterization of the soluble microenvironment in human primary tumors and non-involved juxta-tumor samples. Translation to clinical biomarker was obtained by survival analyzes on our discovery cohort, and independent validation in a large (n=145) retrospective cohort. MMP2 was retained as an independent prognostic biomarker that may be measured at the protein or the RNA level to identify high-risk oral cavity cancer patients. High levels of MMP2 and the presence of extra-nodal extension defined prognostic groups that may serve biomarker-driven clinical trials for intensified neoadjuvant or adjuvant regimens. Expression of the 18G signature predictive of response to anti-PD-1 suggests possible combination trials with immunotherapy.

INTRODUCTION

Oral cavity squamous cell carcinoma (OCSSC) patients treated by primary surgery undergo post-operative surveillance, adjuvant radiotherapy, or chemo-radiotherapy, according to clinical and histopathological parameters that include disease stage, nodal involvement, extranodal extension (ENE), perineural invasion (PNI), vascular embols (VE) and resection margin status (1). Despite those numerous clinical decision parameters, around 25% of OCSCC will present an unpredictable early and/or severe recurrence (2), (3), (4). Even the local failures that are eligible to the best treatment option, that is salvage surgery (5), (6), (7), have a poor prognosis with a median overall survival ranging from 20 to 30 months (4), (8). Accurately identifying those high-risk patients would allow proposing them an intensified and risk-adjusted therapy, such as neoadjuvant chemotherapy or immunotherapy.

Neoadjuvant chemotherapy has failed to show benefit in head and neck squamous cell carcinoma (HNSCC), possibly because trials were made in unselected Stage III/IV HNSCC population (9), (10). Immunotherapy is a new treatment modality, and its interest as neoadjuvant treatment is currently being evaluated (11), (12), (13). Numerous prognostic markers have been proposed for OCSCC, but none of them has shown independent validation, and translation to clinical practice (14). In this study, we used a biology-driven exploratory strategy, in order to identify a robust predictive biomarker for early severe recurrence and disease related death in primary OCSCC after treatment by standard of care. We found MMP2 as fulfilling those criteria, and when combined to nodal involvement, providing a simple and efficient patient stratification scheme.

RESULTS

Human primary tumor secretome analysis identified 29 deregulated molecules

To identify candidate biomarkers, we chose an unbiased approach applied to human primary tumors, in order to ensure physiopathological relevance. We used a tumor explant-culture system to analyze the soluble microenvironment in a prospective discovery cohort of 37 OCSCC patients treated by primary surgery (Table S1). Fresh standardized tumor and juxtatumor (non-involved) specimens were cultured for 24h at 37°C, and we measured a panel of 49 soluble molecules relevant to multiple cancer pathways, such as immunity, chemotaxis, tumor growth, angiogenesis, and tissue remodeling. We identified 25 molecules increased, and 4 decreased, in the tumor tissue (Fig 1, Table S2). CXCL9, the metalloproteinases (MMP) MMP1, MMP2 and MMP9, plasminogen activator inhibitor (PAI-1) and resistin were among the molecules most increased in tumors, and MCP-1 (CCL2) in juxtatumors. SCF, multiple cytokines (IL-1b, TNF-α, IL-15), growth factors (GM-CSF, VEGF) and chemokines (MDC, TARC) were also increased in the tumor, as compared to juxta-tumor samples (Fig 1). The cytokines IL-9, TNFb, TSLP, IL-21 were never detected (Fig 1). This provided a global, unbiased protein level profiling of the OCSCC tumor secretome.

High levels of soluble MMP2 were associated with poor prognosis

Patients were classified as severe if they had a disease-specific survival (DSS) of less than 36 months and /or a disease-free survival (DFS) of less than 12 months and could not achieve a second remission (unsuccessful salvage procedures and/or permanent palliative treatment). Among the 29 deregulated secretome molecules, analyzed as candidate biomarkers, MMP2 was the only molecule expressed at significant higher levels among severe patients as compared to non-severe (p = 0.007) (Table S3). ROC curve defined 29.3 ng/ml as the optimal cut-off for soluble MMP2, with a sensitivity of 100% and a specificity of 71.4 % to identify severe cases (Fig2A). MMP2high tumors were associated with reduced DSS (p = 0.001), overall survival (OS) (p = 0.012) and DFS (p = 0.003) (Fig 2B).

Soluble MMP2 levels were independent of T cell infiltration

MMP degrade the extra-cellular matrix and promote tumor cell invasion (15). Tissue damage may lead to a local increase in danger signals and initiate an innate and then adaptive immune response. Thus, we hypothesized that MMP2 levels might influence T cell infiltration. Paired CD3 and CD8 T cell quantification by flow cytometry, and soluble MMP2 quantification, was available for 18 HNSCC patients. MMP2 was not significantly correlated to CD3 (r = 0.01, Spearman correlation coefficient) (Fig 2C) nor to CD8 infiltration (r = -0.13, data not shown). Conversely, CD3 and CD8 infiltration were highly correlated to CXCL9 (r = 0.78 and r = 0.79) and CXCL10 (both r = 0.66) (Fig 2C, data not shown for CD8). In the

secretome analysis of the 37 OCSCC samples, MMP2 was not correlated to CXCL9 and CXCL10 (r=0.19 and r=0.09), further supporting that MMP2 levels were not associated to T cell infiltration (Fig 2D).

RNA levels of *MMP2, CD276, CXCL10,* and *STAT1* predicted prognosis

To independently validate the prognostic value of MMP2, we measured a 30 genes panel (Table S4) by RTqPCR in a large retrospective cohort of 145 OCSCC patients treated by primary surgery. Gene panel included MMP-2, -1, -9, other immune-related genes, and a published 18-gene signature predictive of the response to anti-PD-1 immunotherapy (16). Patients' characteristics are available in Table 1. Significant variables in univariate analysis for DSS, OS and DFS are listed in Table 2. Among the clinical variables, tumor differentiation index, stage, ENE, VE and PNI were significant for both DSS and OS, while only the latter three were significant for DFS. Among the genes, high levels of *MMP2* were associated to reduced DSS, OS and DFS. High levels of *CD276* (B7-H3) and low levels of *CXCL10* and *STAT1* were also among the 5 and 11 genes associated to reduced DSS and OS, respectively (Table 2). This validated the prognostic impact of MMP2, measured by two different methods (protein and mRNA), in a large OCSCC cohort.

MMP2 RNA, ENE, PNI and stage were independent prognostic factors

To identify clinical and biological parameters significant in multivariate analysis, we performed two Cox proportional hazards models. Model 1 included all the 145 patients and all clinical and biological variables significant in univariate analysis, except PNI and VE, because of missing values in 21 patients (14%), whereas Model 2 included all significant variables, but was restricted to the 124 patients with complete data (Fig 3A, Table S5). In both models *MMP2*high was an independent prognostic factor for DSS and DFS (Model 1 DSS: p = 0.001, DFS: p = 0.006, Model 2 DSS: p = 0.034, DFS: p = 0.016). For DSS, ENE status (p = 0.006) and PNI (p = 0.020) were also significant in Model 1 and 2, respectively. For DFS, ENE status was also significant in Model 1 (p = 0.006), but *MMP2* was the only significant parameter in Model 2. For OS, *MMP2* (p = 0.015) and stage (p = 0.042) were significant in Model 1, and PNI (p = 0.01) and stage (p = 0.019) were significant in Model 2 (Fig 3A, Table S5). We defined prognostic groups using the parameters identified in multivariate analysis by the Model 1 to analyze the largest cohort of 145 patients. *MMP2*highENE+ patients had the worse DSS and DFS, as compared to *MMP2*lowENE- patients (p < 0.001), whereas *MMP2*highENE- and *MMP2*lowENE+ had an intermediate DSS and DFS (Fig 3B) (2 by 2 comparisons available in Table S6). *MMP2* status induced clinically relevant variations in survival. *MMP2*high vs *MMP2*low tumor bearing patients had a 5-year DSS of 61% versus 88% when ENE was absent, and of 36% versus 52% when ENE was

present (Table 3). *MMP2*high tumors were associated to the presence of metastatic lymph node (p = 0.031), low or intermediate mitotic index (p = 0.001) and the presence of PNI (p = 0.02) (Table S7).

MMP2 may be used as a biomarker to select patients for treatment intensification

MMP2 RNA status was an efficient prognostic biomarker as measured by ROC curves according to severity criteria, in the whole 145 patient cohort (AUC = 0.66, p = 0.003), and among the ENE negative patients (n = 106, AUC = 0.71, p = 0.003) (Fig S1). The optimal thresholds were 1.81 and 1.82, which led to high negative predictive values (NPV) of 82% and 88% respectively, but lower positive predictive values (PPV) of 41% and 36%. For 29 patients, both soluble MMP2 and *MMP2* RNA data were available, which allowed us to observe that both biomarkers were significantly correlated (Spearman r = 0.45, p = 0.016) (Fig S2), suggesting that MMP2 protein or RNA levels can be used as biomarker.

The expression of an 18-gene signature predictive of response to PD-1 blockade was similar between the different prognostic groups

The proportions of patients expected to respond to immunotherapy may vary between the prognostic groups defined above, and have consequences on the type of treatment that could be proposed in a risk-adjusted strategy. Therefore, we measured the expression of an 18-gene signature (18G) (16) that is a predictive biomarker of response to PD-1 blockade. The 18G signature is composed of a core of 17 highly correlated genes (all Spearman correlation coefficients of the 17genes > 0.455), and CD276 (Fig S3, Fig S4). 18G score was moderately increased in *MMP2*high tumors (p = 0.019) (Fig S4, Fig S5), but was similar whatever the ENE status (p=0,671) and disease stage (p = 0.513) (Fig S5). The 18G score was similar between the prognostic groups defined by *MMP2* RNA and ENE status (p=0.119), *MMP2* RNA status and Stage (p = 0.051), *MMP2* RNA and PNI statuses (p = 0.089), and stage and PNI status (p = 0.661) (Fig 3C). This suggests that various prognostic groups may show response to anti-PD-1 therapy, with implications for the design of biomarker-driven trials in untreated resectable OCSCC patient with the goal of limiting early and severe recurrences (Fig S6).

DISCUSSION

In this study, we identified MMP2 as an independent prognostic biomarker for severe outcomes in OCSCC patients treated by primary surgery.

First, we prospectively produced and analyzed tumor and juxtatumor secretomes, which revealed 29 deregulated soluble molecules, the majority of them being upregulated in the

tumor tissue. Those molecules belonged to various biological classes such as MMPs, chemokines, interleukins, adipokines and growth factors. One may consider that all these deregulated proteins reflect mechanisms of tumor progression and could be candidate biomarkers. However, only soluble MMP2 was associated to poor prognosis in our study. Primary tumor-derived supernatant is not a widely applied method for biomarker identification and data on OCSCC secretome are scarce (17) if we exclude cancer cell-line derived supernatants. A database for healthy body fluids proteome was created in 2008, highlighting the general interest for such approach (18). Here, we cannot exclude that tissue handling, although limited to the minimum in our protocol, may have induced or enhanced the production of some proteins, but this limitation was partially overcome by the comparison with paired juxtatumor supernatant. By the mean of an ultrafiltration catheter, interstitial fluid from a single HNSCC patient was analyzed and revealed 525 proteins by mass spectrometry, but the method was not applicable to juxtatumor tissue, which limited the potential to identify candidate biomarkers (19). Another difficulty is that tumor secretome needs to be produced prospectively using fresh tumor samples, which limits the access to large cohorts with sufficient follow-up in order to identify prognostic biomarkers. However, we could overcome these difficulties, and our study illustrates the added value of this approach in providing data with strong biological relevance.

For further validation, we designed a homogenous retrospective cohort of patients with the same clinical setting of resectable OCSCC treated by primary surgery and extracted tumor RNA from biobanked frozen samples to ensure the best quality of RNA (20). Univariate analysis confirmed the prognostic value of *MMP2* to predict DSS, OS and DFS. High levels of *CD276* and low levels of *CXCL10* and *STAT1* were also associated to reduced DSS and OS, but only *MMP2* remained significant in multivariate analysis. Several studies have proposed MMP2 as a prognostic biomarker for OCSCC, but all had important limitations, such as the absence of multivariate analysis (21), (22), (23), the inclusion of heterogeneous head and neck cancer patients with different tumor locations and treatments (24), (25), or retrospective cohorts with less than 60 patients (22), (23), (26), (27). Most of these studies quantified MMP2 by immunohistochemistry (IHC) through semi-quantitative methods. Our study provided unbiased and definite evidence for the independent prognostic role of MMP2, in a large homogeneous OCSCC cohort, within a multivariate prognostic model.

The biological basis explaining why MMP2 is associated with poor prognosis is well known. MMP2 degrades type IV collagen and promotes epithelial-mesenchymal transition and metastasis (15), (28). MMP may also skew the anti-tumor immune response by their effect on immune cells (29). MMP2 is secreted in an inactive form (pro-MMP2) and is activated by MMP1 (30) and MMP14 (31). Many cell types may produce MMP2, but fibroblasts seem to be the main source of this molecule in the tumor microenvironment (32), (33). From MMP

biology, we understand that a high level of MMP is a risk factor for cancer-related events, such as recurrence and disease-related death. This explains why in our study the accuracy of MMP2 as prognostic biomarker was better for DSS than for OS, both in univariate and multivariate analysis. It is well known that HNSCC patients have a reduced cancer-independent life expectancy, which explains the differences observed between OS and DSS (34). In this line, in the TCGA data, MMP2 was co-expressed with MMP1, MMP9 and MMP14 in HNSCC, but the authors did not report the impact of any MMP on OS in HNSCC (35). The absence of DSS evaluation may explain this discrepancy. Beyond prognosis, MMP were also candidate therapeutic targets in cancer, but, so far, most molecules failed in their development because of their toxicities (36). Selective inhibitors are still in development (37), (NCT03486730), as well as other drugs that have an indirect effect on MMP (38).

Clinical and histopathological parameters fail to identify around 25% of high-risk patients. Here, we propose that combining MMP2 status to those parameters would improve patients' risk stratification. MMP2-high tumor bearing patients could be proposed for an intensified therapeutic plan, as compared to standard of care. MMP2 status may be defined pre-operatively on the initial biopsy, or post-operatively if analyzed on the resection specimen (Fig S6). Pre-operative stratification would guide neoadjuvant treatment such as immunotherapy or chemotherapy, when post-operative stratification would guide adjuvant treatment. The latter setting is particularly important for ENE negative patients who may, in some cases, not be offered any adjuvant treatment. To address the question of the best (neo)adjuvant treatment option in high risk patients, we measured the expression of an 18-gene signature predictive of response to PD-1 blockade. This signature was established on a large cohort of patients treated by pembrolizumab for head and neck cancers (n=107), melanoma (n=89) and other cancers (n=119) (16). The fact that this signature was established by merging the data from 22 different types of cancers and limited to advanced and recurrent cancers might not reflect the clinical setting of the present study. However, *PDL1* and interferon gamma response genes (*STAT1, CXCL9, IDO1, HLADR, HLADQ*) were part of this 18-gene signature and were identified as predictive of response to neoadjuvant pembrolizumab in a window-of-opportunity trial including untreated head and neck cancer patients (13). Therefore, this 18G signature may be used to estimate expected response rates to PD-1 blockade of untreated OCSCC. There was no difference in expression of the 18G score among the different prognostic groups defined by our multivariate analysis for DSS, DFS and OS. In this line, using soluble CXCL9 and CXCL10 as surrogates for tumor T cell infiltration, or direct measures of frequencies of tumor-infiltrating T cells by flow cytometry, we observed that soluble MMP2 levels were not associated to T cell infiltration. Similar results were previously described for MMP2 measured by IHC in endometrial cancer (39). From these results, we may estimate that the proportion of patients expected to

respond to PD-1 blockade should be similar in the different prognostic groups, leaving immunotherapy as a valid treatment option. Patient stratification in future OCSCC trials and clinical practice would definitely benefit from robust biomarkers used in combination with clinical variables, such as our MMP2 / ENE scoring, and with predictive biomarkers for final treatment decision-making.

MATERIALS AND METHODS

Patients and cohorts

Tumor and juxtatumor samples were obtained from operative specimens from previously untreated head and neck cancer patients. Patients with previous head and neck radiotherapy or chemotherapy were excluded. Juxta-tumor samples were taken on the specimens' margins, at least 1cm away from the tumor. Three cohorts of patients treated in our anti-cancer center were included in this study. All analysis on secretome presented in Fig.1 were done on a 37 patient cohort including OCSCC patients only, with the exception of the 3 graphs of Fig1D that show the correlation of CD3 infiltration with soluble MMP2, CXCL9 and CXL10, that was done in a 18 patients HNSCC cohort. This 18 patient cohort had paired secretome and flow cytometry data available and included the following tumor locations: 8 oral cavity, 6 oropharynx, 3 larynx, 1 hypopharynx. The third cohort included 145 OCSCC patients and was used to analyze gene expression by RTqPCR and prognosis. Twenty-nine patients were in common between the n=37 and n=145 cohorts and served for the RNA versus soluble protein correlation. Patients were treated between March 2010 and October 2016, for the 37 patients cohort, between January and July 2017 for the 18 patients cohort, and between February 1991 and November 2016 for the 145 patients cohort. The clinical parameters analyzed were all binarized as follows: gender (male/female), HPV status (positive by PCR/negative), Differentiation (well differentiated or verrucous or basaloid / moderate or poor), Mitotic index (high if ≥10mitoses/field at X400, otherwise low), Perineural invasion (absent/present), Vascular embols (absent/present), Alcohol (positive if ≥30g/day), Tobacco (smoker active or former ≥2PY/non-smoker or former smoker < 2PY), Stage (I or II / III or more) using the pTNM 8th edition AJCC (40), Extranodal extension (absent/present), Margins (negative or close / positive), Age (more or less than 70). For outcomes analysis, we used 3 survivals: disease free survival, in which the censoring event was the first occurrence of recurrence, disease specific survival, in which the censoring event was the occurrence of death caused by the evolution of the cancer (to the exclusion of treatment related toxicities and post-operative complications), and overall survival. We also used a binary criteria of

severity defined as present in cases of DSS < 36 months and /or a DFS < 12 months without subsequent remission (unsuccessful salvage procedures and/or permanent palliative treatment); we considered that these criteria define the population with the most urgent need for prognosis biomarkers (41). This study was done in compliance with the principles of Good Clinical Practice and the Declaration of Helsinki. All patients signed a consent form mentioning that their operative specimens might be used for scientific purposes, and 12 of the 18 patients cohort were also included in the clinical trial NCT03017573.

Tumor and juxta-tumor secretome analysis

Fresh tumor and juxta-tumor were cut into fragments of 17.5 +/-2.5mg. Each fragment was placed in a 48-well flat bottom plate in 250µl of RPMI 1640 Medium Glutamax (Life Technologies) enriched with 10% Fetal Calf Serum (Hyclone), 100 U/ml Penicillin/Streptomycin (Gibco), 1% MEM Non-Essential Amino Acids (Gibco), and 1% pyruvate (Gibco), and incubated at 37°C with 5%CO2. After 24 hours, supernatants were filtered through a 0,22µm Millex-GP filter (SLGP033RS, Merck), diluted ½ in the same enriched RPMI Medium and stored at -80°C until the secretome analysis. The 49 analytes measured are listed in Table S2. Analytes concentrations were obtained using Milliplex Map kits used as recommended: Human MMP magnetic Bead panel 2, Human cytokine/chemokine Magnetic Bead panels I, II, III, and Human Adipocyte Magnetic Bead Panel (Millipore), a Bio-Plex 200 plate reader and the Bio-Plex Manager 6.1 software (Bio-Rad Laboratories). All analytes were measured as stored, but MMP1 and MMP9 were also measured after 1/25th dilution for the 18 HNSCC patients with paired flow cytometry data.

Analysis of CD3 and CD8 infiltration by Flow Cytometry

Details are available at (42). Briefly, single-cell suspensions were obtained from enzymatically digested tumor samples, then filtered, washed, counted and stained for 15 minutes with DAPI (Miltenyi Biotec) to exclude dead cells, CD3 (Alexa700, clone UCHT1, from BD, #557943) and CD8b (PC5, clone 2ST8.5H7, from Beckman Coulter, #6607109) antibodies, among other antibodies (data not used in the present paper), before phenotyping by flow cytometry (BD LSRFortessa Analyzer).

Gene expression analysis by Real-Time RT-PCR

Samples and RNA Extraction

Tumor and juxtatumor samples were snap-frozen in liquid nitrogen upon surgical removal after pathologist's review and were stored in the corresponding our biological resources center. Samples were sectioned using Tissue-Tek optimal cutting temperature (O.C.T)

compound to estimate the percentage of tumor cells and to remove non-malignant tissue by macrodissection if necessary. Median percentage of tumor cells was 80% (range 40-95). RNA extraction was performed on the same sample, using the miRNeasy miniKit (Qiagen) according to the manufacturer's protocol. RNA was quantified using Nanodrop spectrophotometer ND-1000 and the integrity and purity were assessed by the Agilent 2100 Bioanalyzer and RNA 6000 Nano Labchip Kit (Agilent Biotechnologies, Palo Alto, CA, USA). Total RNA was extracted from 145 OCSSC and 31 juxtatumor frozen samples from HNSCC bearing patients by using the acid-phenol guanidium method. RNA samples quality was assessed by electrophoresis through agarose gels and staining with ethidium bromide, and the 18S and 28S RNA bands were visualized under UV light.

cDNA Synthesis

RNA was reverse transcribed in a final volume of 20 µl containing 1X RT buffer, 0.01M DTT, 0.5mM each dNTP, 0.15µg/µL random primers, 100U SuperScript™ II Reverse Transcriptase (Life Technologies, Carlsbad, Californie), 20U RNasin® Ribonuclease Inhibitor (Promega, Madison, Wisconsin) and 1 µg of total RNA. The samples were incubated during 10min at 25°C 30min at 42°C, and reverse transcriptase was inactivated by heating 5min at 99°C and cooling 5min at 5°C.

PCR Amplification and quantification

All of the PCR reactions were performed using an ABI Prism 7900HT Sequence Detection system (Thermo Fisher Scientific, Waltham, Massachusetts). PCR was performed using the *Power* SYBR™ Green PCR Master Mix (Life Technologies, Carlsbad, Californie). The thermal cycling conditions comprised an initial denaturation step of 10min at 95°C followed by 50 cycles at 95°C for 15 s and 65°C for 1 min. Cycle Threshold (Ct value) was defined by the cycle number at which the increase in the fluorescence signal associated with exponential growth of PCR products started to be detected, using Applied Biosystems analysis software according to the manufacturer's manuals. For quality controls, we quantified the housekeeping gene TBP (Genbank accession NM_003194). Primers for TBP and the 30 target genes were designed with the assistance of Oligo 6.0 computer program (National Biosciences, Plymouth, MN). dbEST and nr databases were used to confirm the total gene specificity of the nucleotide sequences chosen as primers and the absence of single nucleotide polymorphisms. The primer pairs selected were unique relative to the sequences of closely related family member genes and the corresponding retropseudogenes. One of the two primers was placed at the junction between two exons or on two different exons to avoid genomic DNA contaminating. Specificity of PCR amplicons was verified by agarose gel electrophoresis. The oligonucleotide primers sequences used are shown in Table S8.

Data processing

TBP was used for each sample normalization. ΔCt value was equal to mean Ct value of the target gene minus mean Ct value of TBP. The N-fold differences per sample in target gene expression relative to TBP was equal to $2^{\Delta Ct}$. For each gene, $2^{\Delta Ct}$ values of the 31 juxtatumor samples were multiplied by a factor named "k" so that their median was equal to 1. The final values for tumor samples were equal to $k2^{\Delta Ct}$. The 30 genes of this study are listed in Table S5. To obtain a score for the 18 genes signature, we standardized each gene separately, and used those values in the formula: 18G score = (*CCR7+ HLADRB + CCL5 + CD27 - CD276 + CMKLR1 + CXCL9 + CXCR6 + HLA-DQA1 + HLA-E + IDO1 + LAG3 + NKG7 + PDCD1LG2 + PSMB10 + STAT1 + TIGIT*)/18.

Statistical Analysis

Descriptive and statistical analyses were performed using GraphPad Prism V8, Xlstat (Addinsoft), and Qlucore softwares. Paired tumor and juxtatumor secretome comparison was done by Wilcoxon test. Univariate unpaired non-parametric comparisons used Mann-Whitney tests and Kruskal-Wallis test for multigroup comparisons. All correlations used Spearman method. Optimal threshold for ROC curves was defined as the value maximizing the sum of sensitivity and specificity. Univariate survival analysis was performed on clinical parameters and biological parameters (soluble molecules or 30 genes measured by RT-PCR) categorized as high or low by cut-off at median, or at optimal threshold when specified. Log-rank tests were used for univariate analysis. For the 145 patient validation cohort, significant variables at the threshold of $p < 0.05$ were selected for the Cox proportional hazard models for multivariate analysis. Model 1 included 145 patients and all clinical and biological parameters significant in univariate analysis, but PNI and VE, because of missing values, whereas Model 2 included all significant parameters, but was restricted to the 124 patients with complete data. The heatmap representing the 18-gene signature in Fig3A was performed with Qlucore software.

SUPPORTING INFORMATION

ACKNOWLEDGMENTS

REFERENCES

1. NCCN. https://www.nccn.org/professionals/physician_gls/default.aspx.

2. Gañán L, López M, García J, Esteller E, Quer M, León X. Management of recurrent head and neck cancer: variables related to salvage surgery. Eur Arch Oto-Rhino-Laryngol Off J Eur Fed Oto-Rhino-Laryngol Soc EUFOS Affil Ger Soc Oto-Rhino-Laryngol - Head Neck Surg. 2016 Dec;273(12):4417–24.

3. Argiris A, Karamouzis MV, Raben D, Ferris RL. Head and neck cancer. Lancet Lond Engl. 2008 May 17;371(9625):1695–709.

4. Tam S, Araslanova R, Low T-HH, Warner A, Yoo J, Fung K, et al. Estimating Survival After Salvage Surgery for Recurrent Oral Cavity Cancer. JAMA Otolaryngol-- Head Neck Surg. 2017 01;143(7):685–90.

5. Ord RA, Kolokythas A, Reynolds MA. Surgical salvage for local and regional recurrence in oral cancer. J Oral Maxillofac Surg Off J Am Assoc Oral Maxillofac Surg. 2006 Sep;64(9):1409–14.

6. Sacco AG, Cohen EE. Current Treatment Options for Recurrent or Metastatic Head and Neck Squamous Cell Carcinoma. J Clin Oncol Off J Am Soc Clin Oncol. 2015 Oct 10;33(29):3305–13.

7. Liao C-T, Chang JT-C, Wang H-M, Ng S-H, Hsueh C, Lee L-Y, et al. Salvage therapy in relapsed squamous cell carcinoma of the oral cavity: how and when? Cancer. 2008 Jan 1;112(1):94–103.

8. Janot F, de Raucourt D, Benhamou E, Ferron C, Dolivet G, Bensadoun R-J, et al. Randomized trial of postoperative reirradiation combined with chemotherapy after salvage surgery compared with salvage surgery alone in head and neck carcinoma. J Clin Oncol Off J Am Soc Clin Oncol. 2008 Dec 1;26(34):5518–23.

9. Zorat PL, Paccagnella A, Cavaniglia G, Loreggian L, Gava A, Mione CA, et al. Randomized phase III trial of neoadjuvant chemotherapy in head and neck cancer: 10-year follow-up. J Natl Cancer Inst. 2004 Nov 17;96(22):1714–7.

10. Bossi P, Lo Vullo S, Guzzo M, Mariani L, Granata R, Orlandi E, et al. Preoperative chemotherapy in advanced resectable OCSCC: long-term results of a randomized phase III trial. Ann Oncol Off J Eur Soc Med Oncol. 2014 Feb;25(2):462–6.

11. Uppaluri R, Zolkind P, Lin T, Nussenbaum B, Jackson RS, Rich J. Neoadjuvant pembrolizumab in surgically resectable, locally advanced HPV negative head and neck squamous cell carcinoma (HNSCC). In: J Clin Oncol 35, 2017 (suppl; abstr 6012).

12. Ferris RL, Gonçalves A, Baxi S, Martens A, Gauthier H, Langenberg M et al. An Open-label, Multicohort, Phase 1/2 Study in Patients With Virus-Associated Cancers (CheckMate 358): Safety and Efficacy of Neoadjuvant Nivolumab in Squamous Cell Carcinoma of the Head and Neck. In: Poster LBA46, ESMO 2017.

13. Wise-Draper TM, Matthew O. Old, Francis P. Worden, Paul E. O'Brien, Ezra E.W. Cohen, Neal Dunlap, Michelle Lynn Mierzwa, Keith Casper, Sarah Palackdharry, Benjamin Hinrichs, Alfredo Molinolo, Vinita Takiar, Jonathan Mark, Alice Tang, Muhammad Kashif Riaz, John Charles Morris, Nooshin Hashemi Sadraei, Changchun Xie, Maura L. Gillison. Phase II multi-site investigation of neoadjuvant pembrolizumab

and adjuvant concurrent radiation and pembrolizumab with or without cisplatin in resected head and neck squamous cell carcinoma. In: ASCO 2018, abstract 6017.

14. Rivera C, Oliveira AK, Costa RAP, De Rossi T, Paes Leme AF. Prognostic biomarkers in oral squamous cell carcinoma: A systematic review. Oral Oncol. 2017;72:38–47.

15. Kessenbrock K, Plaks V, Werb Z. Matrix metalloproteinases: regulators of the tumor microenvironment. Cell. 2010 Apr 2;141(1):52–67.

16. Cristescu R, Mogg R, Ayers M, Albright A, Murphy E, Yearley J, et al. Pan-tumor genomic biomarkers for PD-1 checkpoint blockade-based immunotherapy. Science. 2018 12;362(6411).

17. Gromov P, Gromova I, Olsen CJ, Timmermans-Wielenga V, Talman M-L, Serizawa RR, et al. Tumor interstitial fluid - a treasure trove of cancer biomarkers. Biochim Biophys Acta. 2013 Nov;1834(11):2259–70.

18. Li S-J, Peng M, Li H, Liu B-S, Wang C, Wu J-R, et al. Sys-BodyFluid: a systematical database for human body fluid proteome research. Nucleic Acids Res. 2009 Jan;37(Database issue):D907-912.

19. Stone MD, Odland RM, McGowan T, Onsongo G, Tang C, Rhodus NL, et al. Novel In Situ Collection of Tumor Interstitial Fluid from a Head and Neck Squamous Carcinoma Reveals a Unique Proteome with Diagnostic Potential. Clin Proteomics. 2010 Sep;6(3):75–82.

20. Li J, Fu C, Speed TP, Wang W, Symmans WF. Accurate RNA Sequencing From Formalin-Fixed Cancer Tissue To Represent High-Quality Transcriptome From Frozen Tissue. JCO Precis Oncol. 2018;2018.

21. Chen C-H, Chien C-Y, Huang C-C, Hwang C-F, Chuang H-C, Fang F-M, et al. Expression of FLJ10540 is correlated with aggressiveness of oral cavity squamous cell carcinoma by stimulating cell migration and invasion through increased FOXM1 and MMP-2 activity. Oncogene. 2009 Jul 30;28(30):2723–37.

22. Fan H-X, Li H-X, Chen D, Gao Z-X, Zheng J-H. Changes in the expression of MMP2, MMP9, and CollV in stromal cells in oral squamous tongue cell carcinoma: relationships and prognostic implications. J Exp Clin Cancer Res CR. 2012 Oct 29;31:90.

23. Aparna M, Rao L, Kunhikatta V, Radhakrishnan R. The role of MMP-2 and MMP-9 as prognostic markers in the early stages of tongue squamous cell carcinoma. J Oral Pathol Med Off Publ Int Assoc Oral Pathol Am Acad Oral Pathol. 2015 May;44(5):345–52.

24. Ruokolainen H, Pääkkö P, Turpeenniemi-Hujanen T. Tissue and circulating immunoreactive protein for MMP-2 and TIMP-2 in head and neck squamous cell carcinoma--tissue immunoreactivity predicts aggressive clinical course. Mod Pathol Off J U S Can Acad Pathol Inc. 2006 Feb;19(2):208–17.

25. Gunawardena I, Arendse M, Jameson MB, Plank LD, Gregor RT. Prognostic molecular markers in head and neck squamous cell carcinoma in a New Zealand population: matrix metalloproteinase-2 and sialyl Lewis x antigen. ANZ J Surg. 2015 Nov;85(11):843–8.

26. Gontarz M, Wyszyńska-Pawelec G, Zapała J, Czopek J, Lazar A, Tomaszewska R. Immunohistochemical predictors in squamous cell carcinoma of the tongue and floor of the mouth. Head Neck. 2016;38 Suppl 1:E747-753.

27. Katayama A, Bandoh N, Kishibe K, Takahara M, Ogino T, Nonaka S, et al. Expressions of matrix metalloproteinases in early-stage oral squamous cell carcinoma as predictive indicators for tumor metastases and prognosis. Clin Cancer Res Off J Am Assoc Cancer Res. 2004 Jan 15;10(2):634–40.

28. Yokoyama K, Kamata N, Fujimoto R, Tsutsumi S, Tomonari M, Taki M, et al. Increased invasion and matrix metalloproteinase-2 expression by Snail-induced mesenchymal transition in squamous cell carcinomas. Int J Oncol. 2003 Apr;22(4):891–8.

29. Godefroy E, Manches O, Dréno B, Hochman T, Rolnitzky L, Labarrière N, et al. Matrix metalloproteinase-2 conditions human dendritic cells to prime inflammatory T(H)2 cells via an IL-12- and OX40L-dependent pathway. Cancer Cell. 2011 Mar 8;19(3):333–46.

30. Sato H, Takino T, Okada Y, Cao J, Shinagawa A, Yamamoto E, et al. A matrix metalloproteinase expressed on the surface of invasive tumour cells. Nature. 1994 Jul 7;370(6484):61–5.

31. Jobin PG, Butler GS, Overall CM. New intracellular activities of matrix metalloproteinases shine in the moonlight. Biochim Biophys Acta Mol Cell Res. 2017 Nov;1864(11 Pt A):2043–55.

32. Puram SV, Tirosh I, Parikh AS, Patel AP, Yizhak K, Gillespie S, et al. Single-Cell Transcriptomic Analysis of Primary and Metastatic Tumor Ecosystems in Head and Neck Cancer. Cell. 2017 Dec 14;171(7):1611–1624.e24.

33. Zhang Z, Liu R, Jin R, Fan Y, Li T, Shuai Y, et al. Integrating Clinical and Genetic Analysis of Perineural Invasion in Head and Neck Squamous Cell Carcinoma. Front Oncol. 2019;9:434.

34. Massa ST, Cass LM, Osazuwa-Peters N, Christopher KM, Walker RJ, Varvares MA. Decreased cancer-independent life expectancy in the head and neck cancer population. Head Neck. 2017;39(9):1845–53.

35. Gobin E, Bagwell K, Wagner J, Mysona D, Sandirasegarane S, Smith N, et al. A pan-cancer perspective of matrix metalloproteases (MMP) gene expression profile and their diagnostic/prognostic potential. BMC Cancer. 2019 Jun 14;19(1):581.

36. Zhong Y, Lu Y-T, Sun Y, Shi Z-H, Li N-G, Tang Y-P, et al. Recent opportunities in matrix metalloproteinase inhibitor drug design for cancer. Expert Opin Drug Discov. 2018;13(1):75–87.

37. Scannevin RH, Alexander R, Haarlander TM, Burke SL, Singer M, Huo C, et al. Discovery of a highly selective chemical inhibitor of matrix metalloproteinase-9 (MMP-9) that allosterically inhibits zymogen activation. J Biol Chem. 2017 27;292(43):17963–74.

38. Van Tubergen EA, Banerjee R, Liu M, Vander Broek R, Light E, Kuo S, et al. Inactivation or loss of TTP promotes invasion in head and neck cancer via transcript stabilization and secretion of MMP9, MMP2, and IL-6. Clin Cancer Res Off J Am Assoc Cancer Res. 2013 Mar 1;19(5):1169–79.

39. Jedryka M, Chrobak A, Chelmonska-Soyta A, Gawron D, Halbersztadt A, Wojnar A, et al. Matrix metalloproteinase (MMP)-2 and MMP-9 expression in tumor infiltrating CD3 lymphocytes from women with endometrial cancer. Int J Gynecol Cancer Off J Int Gynecol Cancer Soc. 2012 Oct;22(8):1303–9.

40. Amin, M.B., Edge, S., Greene, F., Byrd, D.R., Brookland, R.K., Washington, M.K., Gershenwald, J.E., Compton, C.C., Hess, K.R., Sullivan, D.C., Jessup, J.M., Brierley, J.D., Gaspar, L.E., Schilsky, R.L., Balch, C.M., Winchester, D.P., Asare, E.A., Madera, M., Gress, D.M., Meyer, L.R. AJCC cancer staging manual. 8th ed. New York: Springer; 2017.

41. Agra IMG, Carvalho AL, Ulbrich FS, de Campos OD, Martins EP, Magrin J, et al. Prognostic factors in salvage surgery for recurrent oral and oropharyngeal cancer. Head Neck. 2006 Feb;28(2):107–13.

42. Hoffmann C, Noel F, Grandclaudon M, Michea P, Surun A, Faucheux L, et al. PDL1 and ICOSL discriminate human secretory and helper dendritic cells. bioRxiv [Internet]. 2019 Aug 1 [cited 2019 Aug 2]; Available from: http://biorxiv.org/lookup/doi/10.1101/721563

43. Daneshmandi S, Pourfathollah AA, Forouzandeh-Moghaddam M. Enhanced CD40 and ICOSL expression on dendritic cells surface improve anti-tumor immune responses; effectiveness of mRNA/chitosan nanoparticles. Immunopharmacol Immunotoxicol. 2018 Sep 28;1–12.

Figure 1
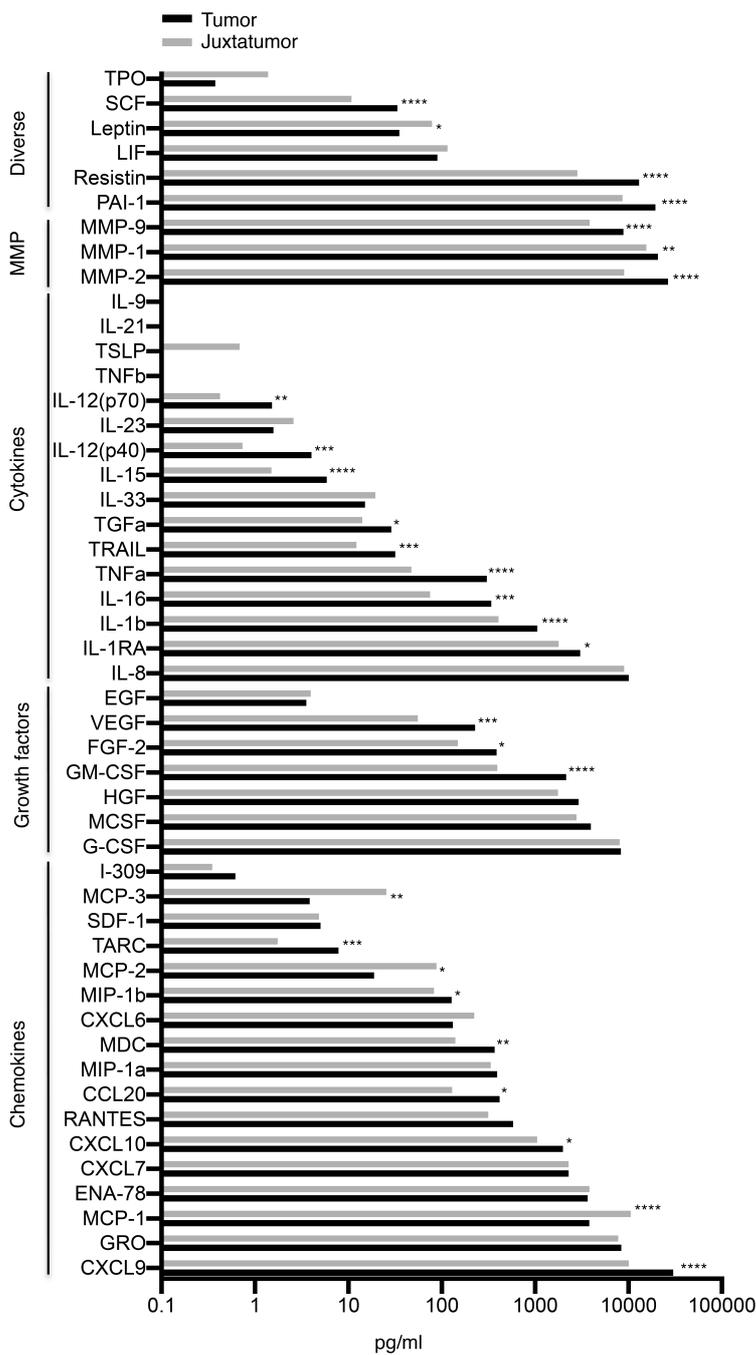
Fig 1. Tumor secretome analysis identified 29 deregulated molecules

Quantification of 49 molecules from the soluble microenvironment of 37 OCSCC and paired juxtatumor tissue. P-values obtained by Wilcoxon tests are represented by range: * < 0.05, ** < 0.01, *** < 0.001, **** < 0.0001.

Figure 2
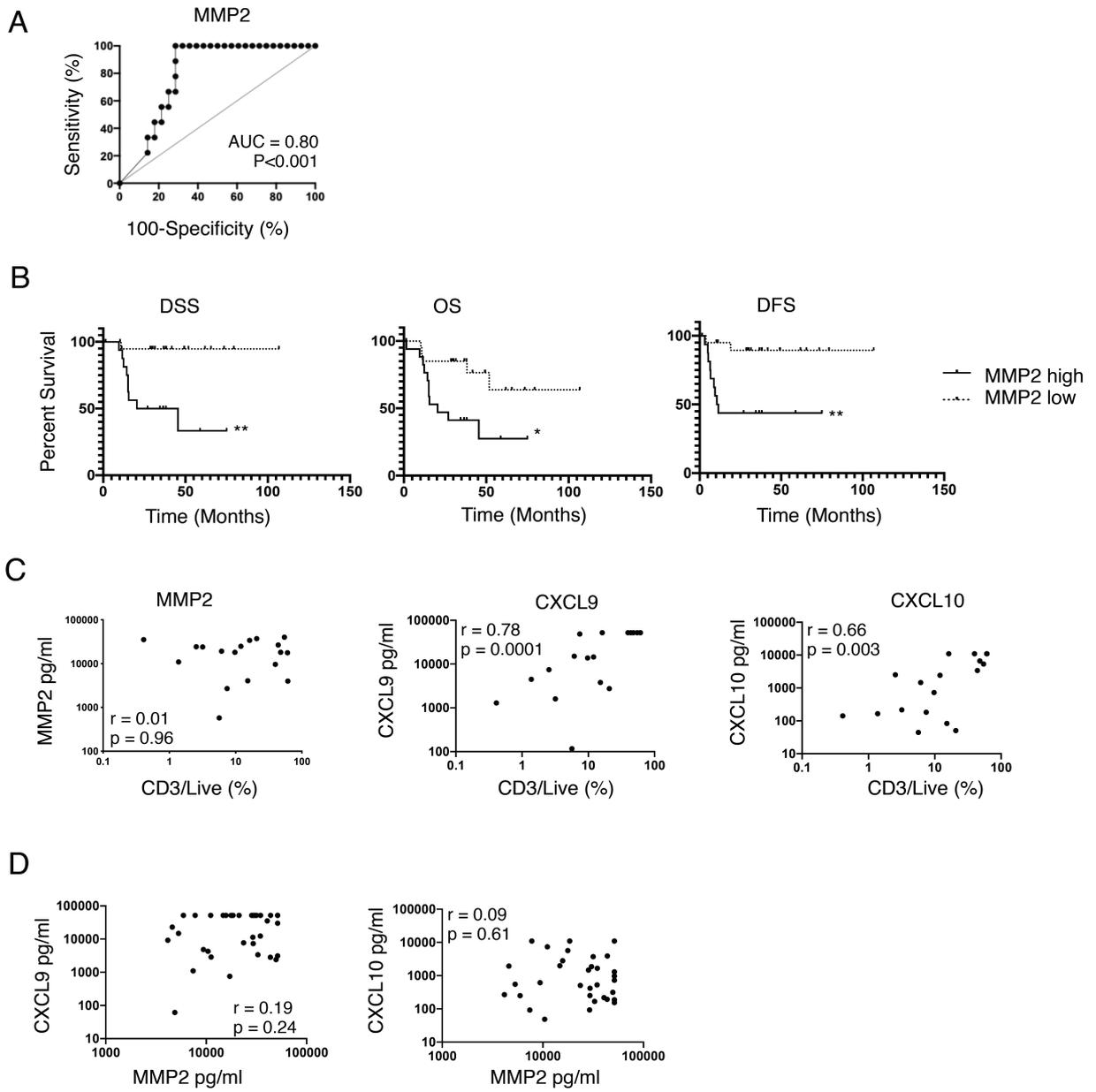
Fig 2. Soluble MMP2 is a prognostic biomarker of OCSCC, independent of T cell infiltration

A. ROC curve of soluble MMP2 for severity criteria (DSS < 36 months and /or a DFS < 12 months followed by permanent palliative treatment). The optimal threshold was 29.3 ng/ml.

B. DDS, DFS and OS survival curves according to soluble MMP2 level, define as high or low relatively to the threshold defined in "B".

C. Correlation between CD3 in live cells and soluble MMP2 (left), CXCL9 (center) and CXCL10 (right), in tumors of 18 HNSCC patients. r values are Spearman correlation coefficients.

D. Correlation between soluble MMP2 and CXCL9 (left) and CXCL10 (right), in 37 OCSCC samples. r values are Spearman correlation coefficients.

Abbreviations. OCSCC: oral cavity squamous cell carcinoma, ROC: receiver operating characteristic, DSS: disease specific survival, DFS: disease free survival, OS: overall survival, HNSCC: head and neck squamous cell carcinoma

Figure 3

A

Survival	Parameters	p-value	HR (95% CI)
DSS	MMP2	0.001	1.242 (1.091-1.414)
	ENE	0.006	2.513 (1.311-4.819)
OS	MMP2	0.015	1.175 (1.032-1.339)
	Stage	0.042	1.902 (1.023-3.536)
DFS	MMP2	0.006	1.177 (1.048-1.321)
	ENE	0.006	2.151 (1.249-3.706)

B

C
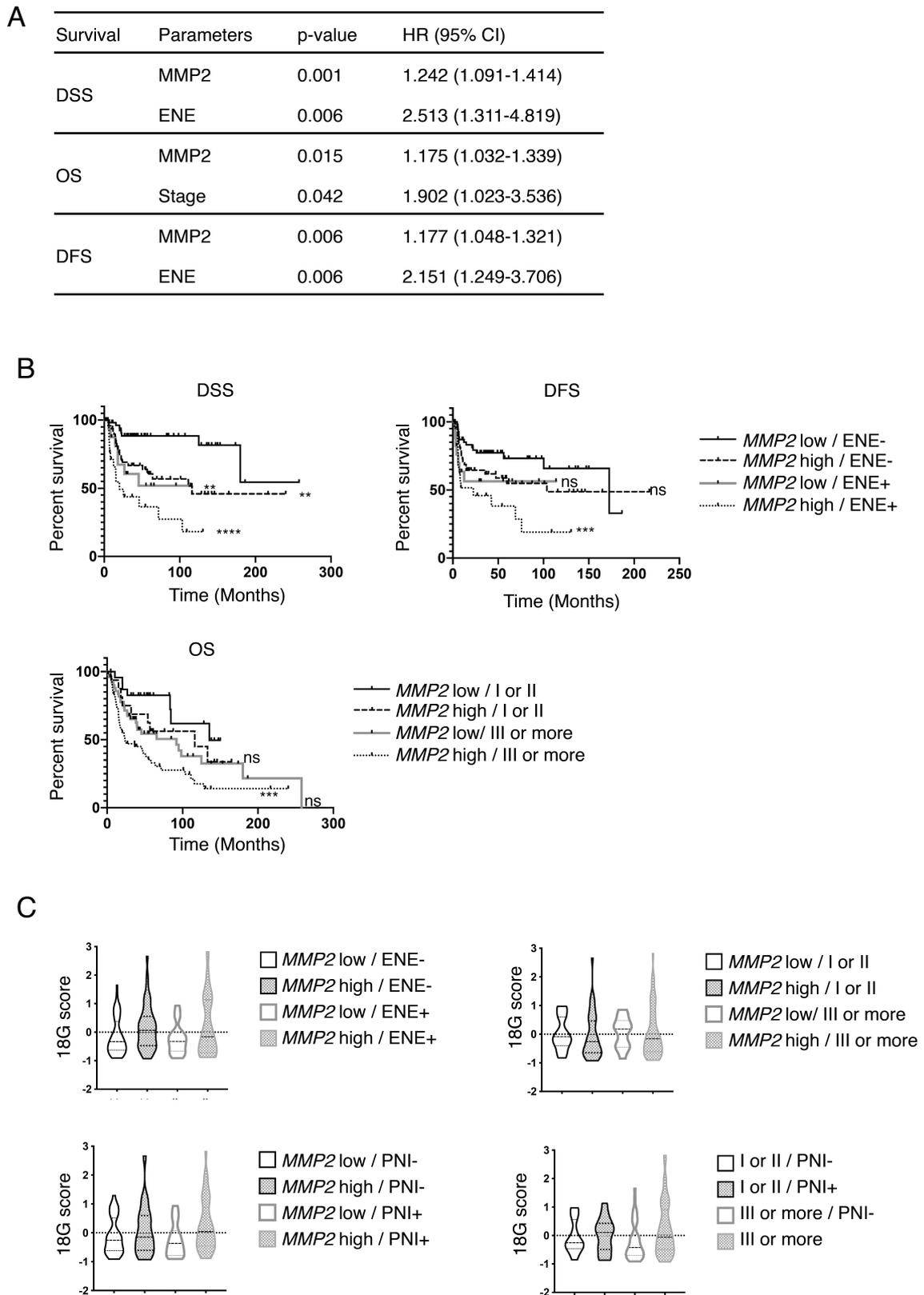
Fig 3. *MMP2*, ENE and stage define prognostic groups with equivalent expression of an 18-gene signature predictive of response to PD-1 blockade

A. Cox proportional hazards Model 1, including n = 145 patients, and all clinical and biological data significant at $p < 0.05$ in univariate analysis, excepted perineural invasion and vascular embols.

B. Survivals according to the prognostic groups defined by the Cox Model 1: DSS (top left) and DFS (top right) in the 4 groups defined by *MMP2* RNA and ENE status. OS (bottom) in the 4 groups defined by MMP2 status and Stage. P-value obtained by Log-rank tests are represented by range: $* < 0.05$, $** < 0.01$, $*** < 0.001$, $**** < 0.0001$, and relatively to the best prognosis groups that are *MMP2* low/ENE- for DSS and DFS, and *MMP2* low/Stage I or II for OS.

C. Distribution of the 18-gene signature score among the prognostic groups defined by the Cox Model 1 and 2 for DFS, DSS and OS.

Abbreviations. DSS: disease specific survival, DFS: disease free survival, ENE: extranodal extension, OS: overall survival.

SUPPLEMENTARY FIGURES

Figure S1
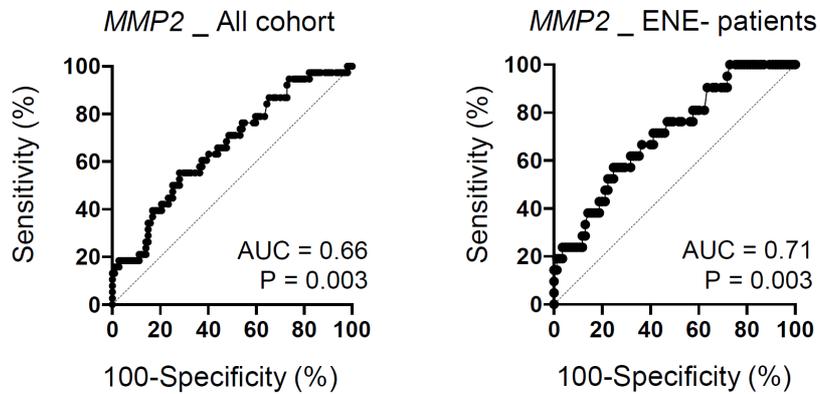
Fig S1. ROC curve of *MMP2* RNA for severity criteria in the cohort of 145 patients (left) and among the 106 patients without ENE (right).

Figure S2
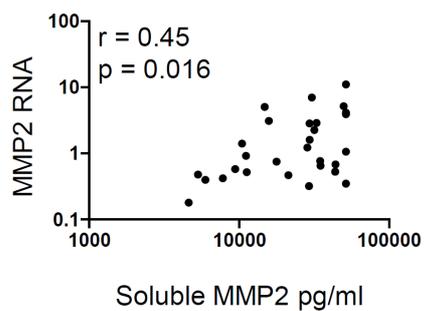
Fig S2. Correlation between soluble MMP2 and *MMP2* RNA (Spearman correlation coefficient).

Figure S3
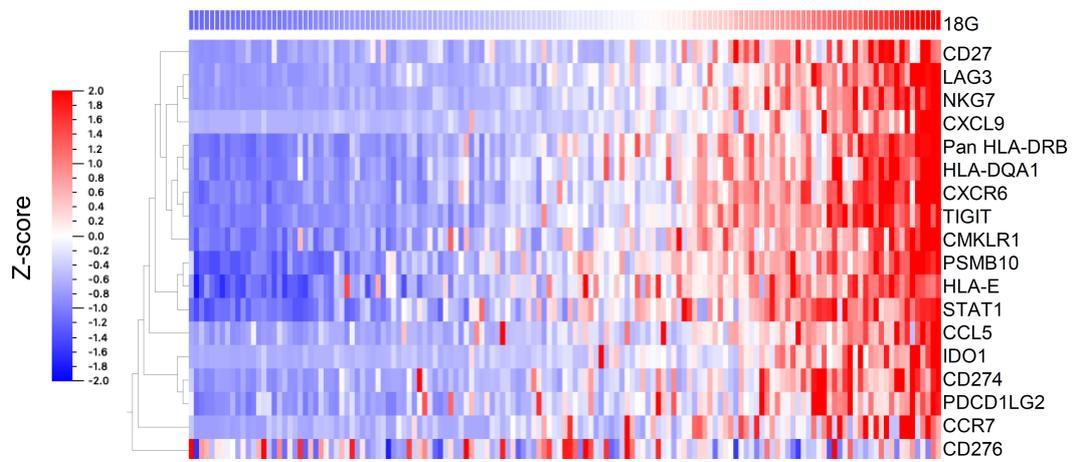
Fig S3. Heatmap representing the expression of the 18 genes of the signature ordered by the 18-gene signature score from low values (left) to high values (right). Each column represents one patient sample (n=145).

Figure S4
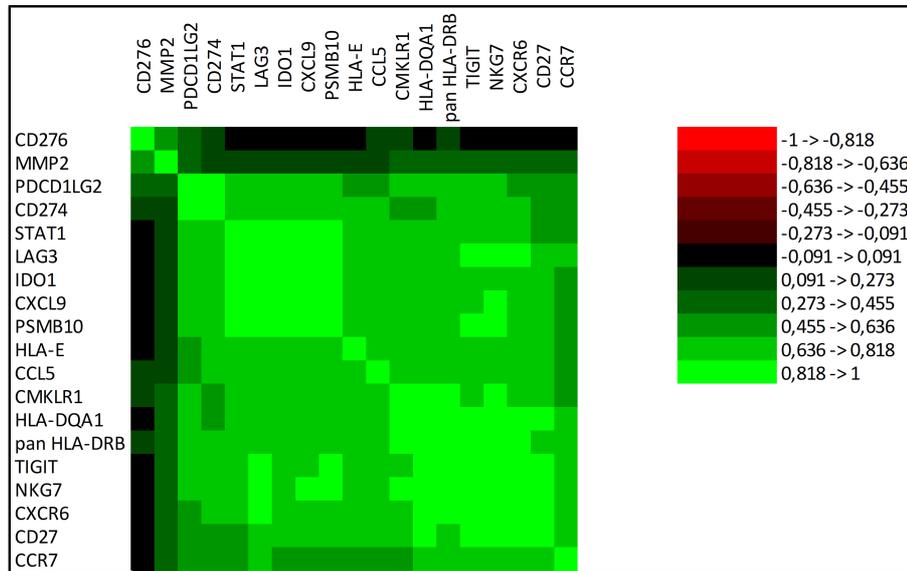
Fig S4. Correlation matrix of *MMP2* RNA and the genes of the 18-gene signature (Spearman correlation coefficient).

Figure S5
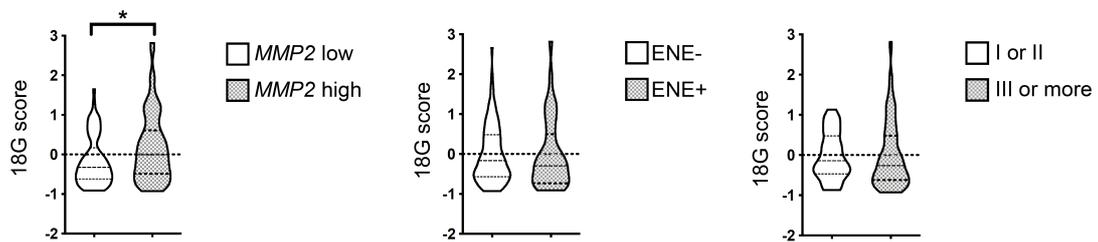
Fig S5. Distribution of the 18-gene signature score among *MMP2* RNA high and low tumors (left), absence or presence of ENE (center) and disease stage (right).

Figure S6
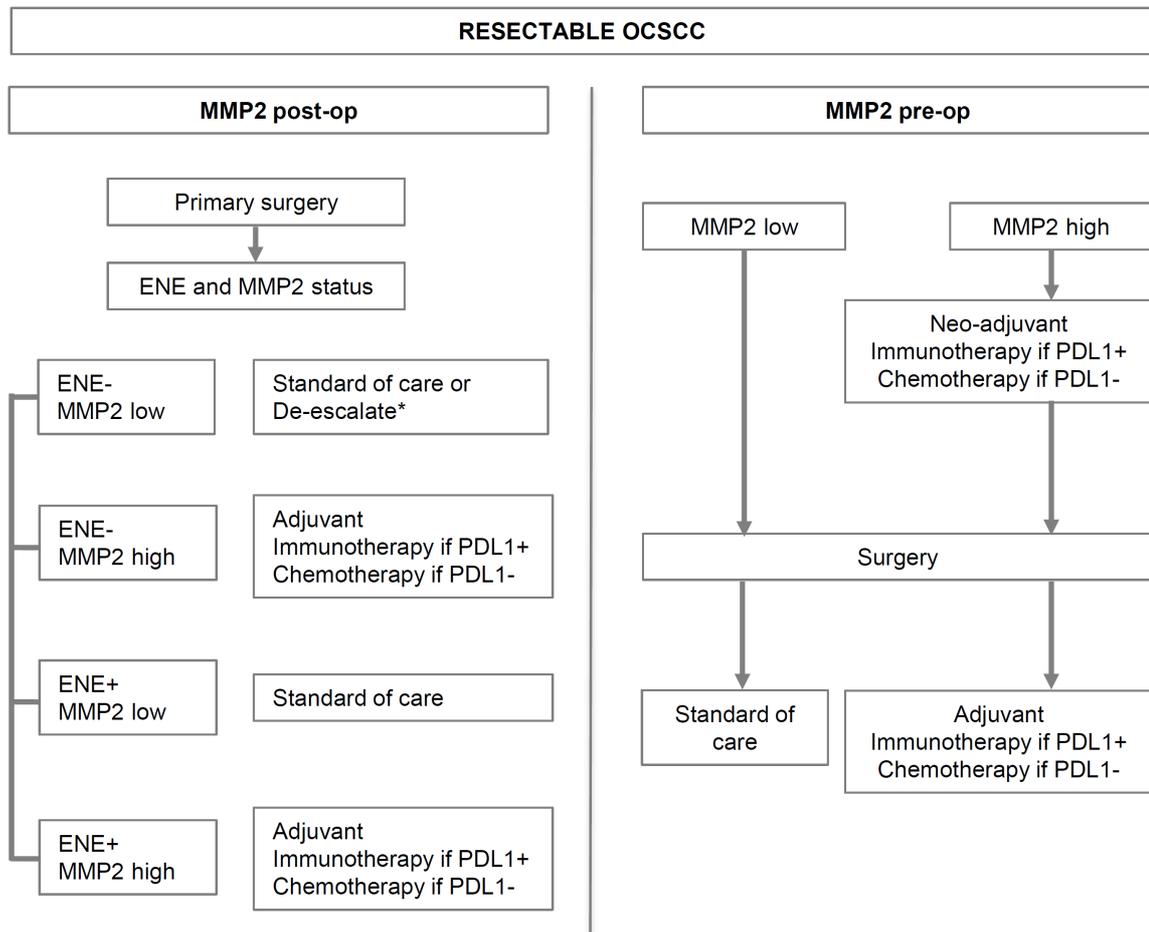
Fig S6. Flow-chart representing proposals of MMP2-driven clinical trials

TABLES

Table 1 - Patients characteristics of the RT-qPCR retrospective validation cohort (n=145)

Parameter		Percentage (n)
Gender	female	39% (57)
	male	61% (88)
Age		63.8 +/- 13.99 (mean +/- SD)
Alcohol abuse (n=121)	absent	60% (73)
	present	40% (48)
Tobacco (n=137)	non smoker	43% (59)
	smoker	57% (78)
T stage	T1	12% (18)
	T2	23% (34)
	T3	40% (58)
	T4	24% (35)
N stage	N0	51% (74)
	N1	11% (16)
	N2	16% (23)
	N3	22% (32)
Stage	I	11% (16)
	II	17% (24)
	III	20% (29)
	IVA	30% (43)
	IVB	23% (33)
Differentiation	verrucous	3% (5)
	well	70% (102)
	moderate	20% (29)
	poorly	6% (8)
	basaloid	1% (1)
Mitotic Index (n=119)	high	40% (48)
	low	33% (39)
	mid	27% (32)
Perineural invasion (n=125)	absent	48% (60)
	present	52% (65)
Vascular embols (n=126)	absent	61% (77)
	present	39% (49)
ENE	absent	73% (106)
	present	27% (39)
Margins	negative or close	83% (120)
	positive	17% (25)
HPV	negative	94% (136)
	positive	6% (9)
Adjuvant treatment	none	41% (59)
	RT	40% (58)
	RT + CT or Cetuximab	19% (27)
	curietherapy	1% (1)
Recurrence	absent	61% (88)
	local	23% (33)
	regional	19% (27)
	metastatic	13% (19)
Severity	non-severe	74% (107)
	severe	26% (38)

Numbers in brackets beside clinical parameters indicate the number of patients for which the information was available

Table 2 – Prognosis value of the clinical parameters and genes measured by RTqPCR in the validation cohort (univariate analysis, Log-Rank test)

Parameter	Mean +/- SD	Poor prognosis if	p-values per survival (Log-rank)		
			DSS	OS	DFS
Gender		ns	0.8420	0.4387	0.801
Age (</> 70)		ns	0.9460	0.9785	0.434
Alcohol		ns	0.8710	0.1860	0.848
Tobacco		ns	0.7839	0.1191	0.670
Stage		III or more	0.0120	0.0036	0.053
Differentiation		moderate or poor	0.0350	0.0434	0.117
Mitotic index		ns	0.1957	0.7066	0.928
Perineural invasion		present	< 0.0001	< 0.0001	0.0046
Vascular embols		present	0.0004	0.0002	0.0130
ENE		present	< 0.0001	0.0004	0.003
Margins		ns	0.1020	0.1484	0.193
HPV		ns	0.4950	0.4536	0.823
MMP2	1.84+/-1.75	high	0.0009	0.0140	0.0440
CD276	2.4+/-1.18	high	0.0056	0.0340	0.0870
CXCL10	18.67+/-27.62	low	0.0083	0.0008	0.0820
STAT1	3.72+/-2.35	low	0.0160	0.0007	0.1300
MMP9	8.55+/-12.93	high	0.0190	0.0880	0.0610
LAMP3	7.43+/-5.59	low	0.1500	0.0008	0.4300
CXCR6	1.22+/-0.92	low	0.6200	0.0037	0.6600
HLA-E	1.12+/-0.51	low	0.1100	0.0056	0.0810
CD274	3.3+/-3.25	low	0.2100	0.0070	0.4100
IDO1	13.98+/-20.3	low	0.0650	0.0095	0.1800
PSMB10	1.68+/-0.99	low	0.2000	0.0270	0.2800
CCR7	8.41+/-10.73	low	0.4700	0.0300	0.5900
TIGIT	3.28+/-2.8	ns	0.8800	0.0560	0.7700
CCL5	2.3+/-2.41	ns	0.7700	0.0600	0.8800
LAG3	3.04+/-3.28	ns	0.4700	0.0640	0.7900
PDCD1	2.19+/-2.17	ns	0.8500	0.0670	0.5400
CXCL9	19.04+/-30.47	ns	0.7000	0.0680	0.9800
HLA-DQA1	1.5+/-1.2	ns	0.5600	0.0850	0.7200
IL3RA	0.9+/-0.69	ns	0.6300	0.0990	0.3700
CD27	1.88+/-2.06	ns	0.7700	0.0990	0.7000
NKG7	1.83+/-2.12	ns	0.7900	0.1300	0.4700
CD3E	2+/-1.9	ns	0.8100	0.1400	0.7700
pan_HLA-DRB	1.35+/-1.04	ns	0.7000	0.1500	0.6300
PDCD1LG2	2.64+/-2.24	ns	0.3100	0.2000	0.2200
CD8A	1.74+/-2.1	ns	0.6200	0.2800	0.4000
ICOSLG	0.68+/-0.35	ns	0.9400	0.4200	0.4600
CMKLR1	1.13+/-0.8	ns	0.4200	0.4300	0.4800
MMP1	774.76+/-1051.42	ns	0.3000	0.6300	0.3500
FUT4	1.06+/-0.53	ns	0.1600	0.8600	0.4000
CD1C	0.36+/-0.42	ns	0.2300	0.9400	0.4500

Cells highlighted in grey contain significant values at p < 0.05

Table 3 - Survival durations by prognostic groups defined by the Cox Model 1

Survival	Prognostic groups	n (%)	MST (months)	2-y S	3-y S	5-y S
DSS	MMP2 high / ENE-	50 (34%)	116.07	69.19%	66.72%	60.63%
	MMP2 high / ENE+	22 (15%)	20.04	49.23%	43.76%	36.47%
	MMP2 low / ENE-	56 (39%)	not reached	88.44%	88.44%	88.44%
	MMP2 low / ENE+	17 (12%)	not reached	67.31%	60.58%	51.92%
DFS	MMP2 high / ENE-	50 (34%)	103.89	64.45%	61.87%	54.86%
	MMP2 high / ENE+	22 (15%)	22.57	45.85%	45.85%	38.21%
	MMP2 low / ENE-	56 (39%)	172.39	79.25%	77.27%	73.20%
	MMP2 low / ENE+	17 (12%)	not reached	56.31%	56.31%	56.31%
OS	MMP2 high / I or II	17 (12%)	116.07	75.00%	68.75%	56.25%
	MMP2 high / III or more	55 (38%)	23.98	49.06%	47.09%	32.96%
	MMP2 low / I or II	23 (16%)	135.43	86.96%	82.61%	82.61%
	MMP2 low / III or more	50 (34%)	91.83	71.49%	65.16%	54.47%

SUPPLEMENTARY TABLES

Table S1 - Patients characteristics of the secretome prospective discovery cohort (n = 37)

Parameter		Percentage (n)
Gender	female	32% (12)
	male	68% (25)
Age		68.31 +/- 12.81 (mean +/- SD)
Alcohol abuse (n=27)	absent	67% (18)
	present	33% (9)
Tobacco (n=34)	non smoker	50% (17)
	smoker	50% (17)
T stage	T1	14% (5)
	T2	22% (8)
	T3	32% (12)
	T4	32% (12)
N stage	N0	59% (22)
	N1	8% (3)
	N2	14% (5)
	N3	19% (7)
Stage	I	14% (5)
	II	11% (4)
	III	19% (7)
	IVA	38% (14)
	IVB	19% (7)
Differentiation	well	78% (29)
	moderate	22% (8)
	poorly	0% (0)
Mitotic Index (n=36)	high	53% (19)
	low	25% (9)
	mid	31% (11)
Perineural invasion (n=36)	absent	47% (17)
	present	53% (19)
Vascular embols	absent	59% (22)
	present	41% (15)
ENE	absent	76% (28)
	present	24% (9)
Margins	negative or close	86% (32)
	positive	14% (5)
HPV (n=21)	negative	90% (19)
	positive	10% (2)
Adjuvant treatment	none	30% (11)
	RT	54% (20)
	RT + CT or Cetuximab	16% (6)
Recurrence	absent	73% (27)
	present	27% (10)
Severity	non-severe	76% (28)
	severe	24% (9)

Numbers in brackets beside clinical parameters indicate the number of patients for which the information was available

Table S2 - Comparison of the analytes of the soluble microenvironment of 37 paired OCSCC and juxtatumor samples (Wilcoxon)

Analyte	Tumor Median (min-max)	Juxtatumor Median (min-max)	Higher in	p-value
CXCL9	35380 (61-52000)	2934 (31-52000)	Tumor	<0.0001
GM-CSF	1093 (0-10800)	105 (0-3386)	Tumor	<0.0001
IL-15	5 (0-17)	1 (0-8)	Tumor	<0.0001
MMP-2	28457 (4155-51500)	5414 (0-51500)	Tumor	<0.0001
MMP-9	10500 (783-10500)	2522 (159-10500)	Tumor	<0.0001
PAI-1	19392 (1513-34000)	4579 (61-34000)	Tumor	<0.0001
Resistin	10460 (109-24500)	1263 (27-24500)	Tumor	<0.0001
SCF	22 (0-242)	9 (0-42)	Tumor	<0.0001
TNF-α	83 (1-2402)	37 (0-330)	Tumor	<0.0001
MCP-1	1103 (163-19500)	10669 (0-19500)	Juxtatumor	<0.0001
IL-1b	843 (1-5996)	163 (0-3221)	Tumor	0.0001
IL-12(p40)	0 (0-24)	0 (0-8)	Tumor	0.0002
IL-16	143 (18-2085)	35 (0-632)	Tumor	0.0003
TARC	4 (0-87)	0 (0-15)	Tumor	0.0003
TRAIL	17 (0-238)	6 (0-136)	Tumor	0.0003
VEGF	72 (0-2399)	39 (0-228)	Tumor	0.0006
MMP-1	21000 (7281-21000)	21000 (28-21000)	Tumor	0.0024
IL-12(p70)	1 (0-14)	0 (0-2)	Tumor	0.0029
MCP-3	0 (0-52)	0 (0-519)	Juxtatumor	0.0078
MDC	198 (0-2264)	45 (0-1226)	Tumor	0.0083
TGFa	14 (0-209)	9 (0-76)	Tumor	0.0104
IL-1RA	1529 (17-10200)	311 (0-10200)	Tumor	0.0110
Leptin	12 (0-328)	22 (0-426)	Juxtatumor	0.0162
MCSF	2897 (634-27235)	2124 (24-13266)	Tumor	0.0173
MIP-1b	85 (4-517)	45 (0-262)	Tumor	0.0181
CXCL10	527 (0-11000)	106 (0-11000)	Tumor	0.0200
FGF-2	192 (29-1553)	120 (0-501)	Tumor	0.0233
MCP-2	7 (0-151)	13 (0-1037)	Juxtatumor	0.0376
CCL20	113 (0-8227)	73 (0-547)	Tumor	0.0496
HGF	2218 (115-8862)	1195 (24-7529)	ns	0.0621
RANTES	197 (4-5222)	112 (0-3188)	ns	0.0884
TSLP	0 (0-0)	0 (0-13)	ns	0.1250
IL-8	11000 (3545-11000)	11000 (2-11000)	ns	0.1324
LIF	38 (0-731)	75 (0-479)	ns	0.1579
IL-33	5 (0-135)	15 (0-136)	ns	0.2367
I-309	0 (0-7)	0 (0-3)	ns	0.2789
IL-23	0 (0-24)	0 (0-24)	ns	0.3750
GRO	12000 (236-12000)	12000 (6-12000)	ns	0.4634
TPO	0 (0-14)	0 (0-22)	ns	0.5000
TNFb	0 (0-2)	0 (0-1)	ns	0.6250
G-CSF	10500 (353-10500)	10500 (0-10500)	ns	0.6578
MIP-1a	207 (7-2100)	193 (0-2100)	ns	0.7152
ENA-78	2212 (26-23000)	2137 (0-23000)	ns	0.8231
CXCL6	65 (0-523)	69 (0-2600)	ns	0.8463
CXCL7	1813 (144-7802)	1447 (93-8201)	ns	0.8815
EGF	4 (0-13)	4 (0-27)	ns	0.9809
SDF-1	0 (0-77)	0 (0-40)	ns	1.0000
IL-21	0 (0-0)	0 (0-0)	ns	all values at 0
IL-9	0 (0-0)	0 (0-0)	ns	all values at 0

Cells highlighted in grey contain significant values at p < 0.05

Table S3 - Prognosis value of the 49 analytes measured in the tumor soluble microenvironment (Mann-Whitney)

Analyte	Non-severe Median (min-max)	Severe Median (min-max)	p-value
MMP2	17432 (4155-51500)	34839 (29414-51500)	0.0074
IL12(p70)	1 (0-14)	0 (0-2)	0.0738
EGF	0 (0-13)	7 (0-12)	0.1422
CCL20	82 (0-1160)	303 (26-8227)	0.1729
MCP2	8 (0-151)	0 (0-21)	0.1934
ENA78	2712 (26-23000)	1468 (65-11471)	0.2264
CXCL9	52000 (61-52000)	7350 (2415-52000)	0.2286
IL23	0 (0-24)	0 (0-11)	0.2501
MCP3	0 (0-52)	0 (0-0)	0.2505
IL1RA	1137 (17-10200)	2126 (421-10200)	0.2958
PAI1	19392 (1513-34000)	22582 (12431-34000)	0.3297
CXCL6	85 (0-523)	40 (5-394)	0.3365
IL1b	748 (1-3519)	1072 (88-5996)	0.4122
CXCL7	1348 (144-6613)	2251 (535-7802)	0.4325
I309	0 (0-7)	1 (0-2)	0.4392
TRAIL	17 (0-238)	20 (7-167)	0.4679
IL12(p40)	0 (0-14)	4 (0-24)	0.5056
TARC	3 (0-87)	7 (0-32)	0.5351
CXCL10	584 (0-11000)	314 (168-1863)	0.5588
GRO	10378 (236-12000)	12000 (2966-12000)	0.5810
Resistin	11045 (109-24500)	8741 (413-24500)	0.5851
MMP9	10500 (783-10500)	10500 (2806-10500)	0.6027
MMP1	21000 (7281-21000)	21000 (21000-21000)	0.6143
TPO	0 (0-14)	0 (0-0)	0.6143
RANTES	200 (4-5222)	189 (98-1565)	0.6385
Leptin	13 (0-226)	6 (0-328)	0.6957
FGF2	159 (29-1553)	250 (43-993)	0.7149
IL16	158 (18-2085)	131 (35-1464)	0.7411
IL8	11000 (3545-11000)	11000 (7858-11000)	0.7421
GCSF	10500 (353-10500)	10500 (1095-10500)	0.7496
TNFb	0 (0-2)	0 (0-1)	0.7648
IL15	5 (0-15)	6 (2-17)	0.7904
IL33	3 (0-60)	5 (0-135)	0.8068
LIF	38 (0-731)	67 (0-231)	0.8593
MIP1b	87 (4-517)	82 (31-177)	0.8595
MCP1	1103 (163-19500)	1162 (269-12495)	0.8734
VEGF	101 (0-2399)	49 (26-1072)	0.9154
SDF1	0 (0-40)	0 (0-77)	0.9215
MIP1a	214 (7-2100)	169 (60-889)	0.9295
MCSF	2918 (634-12946)	2639 (814-27235)	0.9308
SCF	25 (0-93)	21 (5-242)	0.9435
TNF-α	94 (1-2402)	75 (29-1035)	0.9584
MDC	184 (0-2264)	219 (33-1050)	0.9859
TGFa	16 (0-147)	12 (5-209)	0.9861
HGF	2218 (115-7258)	2223 (363-8862)	0.9861
GMCSF	1236 (0-10800)	946 (753-10800)	1.0000
IL21	0 (0-0)	0 (0-0)	1.0000
IL9	0 (0-0)	0 (0-0)	1.0000
TSLP	0 (0-0)	0 (0-0)	1.0000

Cells highlighted in grey contain significant values at p < 0.05

Table S4 - List of the 30 genes measured by RTqPCR

Gene	Alias(es)	Included in the 18 gene signature
MMP1		no
MMP2		no
MMP9		no
CXCL10		no
CD3E	CD3	no
FUT4	CD15	no
ICOSLG	ICOS-L	no
CD1C		no
LAMP3		no
IL3RA		no
CD8A	CD8	no
PDCD1	CD279, PD1	no
CD274	B7H1, PDL1, PDCD1L1	yes
CCR7		yes
HLADRB		yes
CCL5	RANTES	yes
CD27	TNFRSF7	yes
CD276	B7H3	yes
CMKLR1		yes
CXCL9		yes
CXCR6		yes
HLA-DQA1		yes
HLA-E		yes
IDO1	IDO	yes
LAG3	CD223	yes
NKG7		yes
PDCD1LG2	B7DC, PDL2	yes
PSMB10	LMP10	yes
STAT1		yes
TIGIT		yes

Table S5 - Multivariate Cox proportional hazards Model 2, including n = 124 patients, and all clinical and biological data significant at p < 0.05 in univariate analysis

Survival	Parameters	P value	HR (95% CI)
DSS	MMP2	0.034	1.168 (1.012-1.349)
	PNI	0.020	2.599 (1.161-5.818)
OS	PNI	0.010	2.198 (1.204-4.01)
	Stage	0.019	2.646 (1.175-5.957)
DFS	MMP2	0.016	1.162 (1.028-1.312)

Table S6 - Comparison of survivals in the prognostic groups defined by the Cox Model1

	Prognostic groups	Log-rank P value	HR (Mantel-Haenszel)		
			HR	Inf CI 95%	Sup CI 95%
DSS	MMP2 high / ENE- vs. MMP2 high / ENE+	0.0093	0.3417	0.1522	0.7671
	MMP2 high / ENE- vs. MMP2 low / ENE-	0.0022	3.228	1.524	6.834
	MMP2 high / ENE- vs. MMP2 low / ENE+	0.6203	0.7928	0.3165	1.986
	MMP2 high / ENE+ vs. MMP2 low / ENE-	<0.0001	21.49	7.226	63.94
	MMP2 high / ENE+ vs. MMP2 low / ENE+	0.1851	1.795	0.7556	4.264
	MMP2 low / ENE- vs. MMP2 low / ENE+	0.0016	0.1079	0.02715	0.4286
DFS	MMP2 high / ENE- vs. MMP2 high / ENE+	0.0317	0.4281	0.1973	0.9285
	MMP2 high / ENE- vs. MMP2 low / ENE-	0.0893	1.771	0.916	3.426
	MMP2 high / ENE- vs. MMP2 low / ENE+	0.6349	0.8029	0.3243	1.987
	MMP2 high / ENE+ vs. MMP2 low / ENE-	0.0002	5.539	2.236	13.72
	MMP2 high / ENE+ vs. MMP2 low / ENE+	0.3634	1.497	0.6273	3.57
	MMP2 low / ENE- vs. MMP2 low / ENE+	0.0705	0.3582	0.1177	1.09
OS	MMP2 high/I or II vs. MMP2 high/III or more	0.0402	0.5285	0.2873	0.972
	MMP2 high/I or II vs. MMP2 low/I or II	0.2129	1.886	0.6948	5.122
	MMP2 high/I or II vs. MMP2 low/III or more	0.653	6e-310	2e-322	infinite
	MMP2 high/III or more vs. MMP2 low/I or II	0.0004	2.8878	1.597	5.186
	MMP2 high/III or more vs. MMP2 low/III or more	0.0398	6e-310	2e-322	infinite
	MMP2 low/I or II vs. MMP2 low/III or more	0.0646	6e-310	2e-322	infinite

Inf: inferior. CI: confidence interval. Sup: infinite. Cells highlighted in grey contain significant values at $p < 0.05$

Table S7 - Clinical parameters according to *MMP2* RNA status

Parameter	Percentage (n)	MMP2 Low (n=73)	MMP2 high (n=72)	p value (Fisher)	Odd Ratio [95%CI]
Gender	female	40% (29)	39% (28)	1.0000	
	male	60% (44)	61% (44)	0.9506	
Age	mean +/- SD	63,21 +/- 13,68	63,35+/-14,39		
Alcohol abuse (n=63, n=58)	absent	59% (37)	62% (36)	0.7148	
	present	41% (26)	38% (22)		
Tobacco (n=70, n=67)	non smoker	43% (30)	43% (29)	1.0000	
	smoker	57% (40)	57% (38)		
T stage	T1 or T2	40% (29)	32% (23)	0.3876	
	T3 or T4	60% (44)	68% (49)		
N stage	N0	60% (44)	42% (30)	0.0310	2.11 [1.04; 4.35]
	N+	40% (29)	58% (42)		
Stage	I or II	32% (23)	24% (17)	0.3536	
	III or more	68% (50)	76% (55)		
Differentiation	verrucous, well, basaloid	75% (55)	74% (53)	0.8506	
	moderate, poorly	25% (18)	26% (19)		
Mitotic Index (n=63, n=56)	high	54% (34)	25% (14)	0.0015	3.48 [1.51; 8.35]
	low / mid	46% (29)	75% (42)		
Perineural invasion (n=63, n=62)	absent	59% (37)	37% (23)	0.0200	2.40[1.12; 5.28]
	present	41% (26)	63% (39)		
Vascular embols (n=65, n=61)	absent	63% (41)	59% (36)	0.7157	
	present	37% (24)	41% (25)		
ENE	absent	77% (56)	69% (50)	0.3536	
	present	23% (17)	31% (22)		
Margins	negative or close	82% (60)	83% (60)	1.0000	
	positive	18% (13)	17% (12)		
HPV	negative	93% (68)	94% (68)	1.0000	
	positive	7% (5)	6% (4)		
Adjuvant treatment	none	41% (30)	40% (29)	0.9636	
	RT	41% (30)	39% (28)		
	RT + CT or Cetuximab	18% (13)	19% (14)		
	curietherapy	0% (0)	1% (1)		
Severity	low	82% (60)	65% (47)	0.0241	2.44[1.07; 5.80]
	high	18% (13)	35% (25)		
Recurrence	absent	70% (51)	51% (37)	0.0398	
	local	30% (22)	29% (21)		
	regional	14% (10)	24% (17)		
	metastatic	7% (5)	19% (14)		

Numbers in brackets beside clinical parameters indicate the number of patients for which the information was available. Cells highlighted in grey contain significant values at p < 0.05.

Table S8 - Primer sequences

Primer Name	Primer Sequence 5' to 3'

D-ALB-U	GCTGTCATCTCTTGTGGGCTGT
D-ALB-L	ACTCATGGGAGCTGCTGGTTC
TBP-U	TGCACAGGAGCCAAGAGTGAA
TBP-L	CACATCACAGCTCCCCACCA
MMP1-U2	GGCTTGAAGCTGCTTACGAATTT
MMP1-L2	ACAGCCCAGTACTTATTCCCTTTGA
MMP2-U1	ACTGCGGTTTTCTCGAATCCA
MMP2-L1	GGTATCCATCGCCATGCTCC
MMP9-U1	CGGCTTGCCCTGGTGCAGT
MMP9-L1	CGTCCCGGGTGTAGAGTCTCTCG
CXCL10-U1	CTGACTCTAAGTGGCATTCAAGGAG
CXCL10-L1	GGTTGATTACTAATGCTGATGCAGG
CD3E-U2-Hs	AAGATGGTAATGAAGAAATGGGTGGT
CD3E-L2-Hs	TGAGGGCATGTCAATATTACTGTGGT
FUT4-U3-Hs	CTGCCATGGACCGTCTGTGT
FUT4-L3-Hs	CCCCAGCAAGCGTAGGTGA
CD274-U1-Hs	GCTGAATTGGTCATCCCAGAACTAC
CD274-L1-Hs	AAACGGAAGATGAATGTCAGTGCTAC
ICOSLG_U1_Hs	CTTCTGCAGCAGAACCTGACTGT
ICOSLG_L1_Hs	CGGTACTGACTGGATTCTCTGTGAT
CD1C-U1	GACAATGCAGACGCATCCCA
CD1C-L1	CAACTCGTCCAGCCATCCTGA
CCR7-U2	GGGGAAACCAATGAAAAGCGT
CCR7-L2	ATCTTGACACAGGCATACCTGGAA
LAMP3-U2	ACCCGAAAATCCAACCTTCTGT
LAMP3-L2	GTCAAATAGGCTCCCACTTCACTG
IL3RA-U1	ATCGCAAATTTCGCTATGAGCTT
IL3RA-L1	GGAGGTTCTGTCTCTGACCTGTTCT
HLA-class2-DRB-U2-Hs	TGCCAAGTGGAGCACCCAA
HLA-class2-DRB-L2-Hs	CAGATTCAGACCGTGCTCTCCAT
CCL5-U2	GCCCACATCAAGGAGTATTTCTACA
CCL5-L2	TTCGGGTGACAAAGACGACTG
CD27-U1-Hs	GTGCACCGAGTGTGATCCTCTT
CD27-L1-Hs	GGCCTCCAGCATCTCACTGAC
CD276-U1-Hs	AGGAGAATGCAGGAGCTGAGGA
CD276-L1-Hs	TCAGAGGCTGCAGGGCTGTC
CMKLR1-U2	TCAACCTGGCAGTGGCAGAT
CMKLR1-L2	CCCGAAAACCCAGTGGTAGTC
CXCL9-U2	ATCCACCTACAATCCTTGAAAGAC
CXCL9-L2	TCCATTCTTCAGTGTAGCAATGATTT
CXCR6-U1	GGTTCAGCAGTTTCAATGACAGCA
CXCR6-L1	CAGACCACAGACAAACACCACCAG
HLA-DQA1-U3	CTACCGCTGCTACCAATGAGGTTC
HLA-DQA1-L3	TGGGCTGACCCAGTGTCACG
HLA-E-U3	GCTACTCTAAGGCTGAGTGGAGCGA
HLA-E-L3	TTTACAAGCTGTGAGACTCAGACCCCT
IDO1-U1	TGTTTCACCAAATCCACGATCAT
IDO1-L1	CCTTCATACACCAGACCGTCTGAT
LAG3-U2-Hs	CCTTTCTCTGCTCCTTTTGGTGACT

LAG3-L2-Hs	**AATCGTCTTGGTCGCCACTGTCT**
NKG7-U1	**CCCCAGATCCAGACCTTCTTCTC**
NKG7-L1	**CCAGGCTCAGGGCACCTGTA**
PDCD1LG2-U1-Hs	**TCCTGCTAATGTTGAGCCTGGAA**
PDCD1LG2-L1-Hs	**GTCACATTGCTGCCATGCTCTATTAT**
PSMB10-U1	**CGCCCCCAAAATCTACTGCTG**
PSMB10-L1	**TGGACGCCACCATCCGTGT**
STAT1-U1	**AGCATGAAATCAAGAGCCTGGA**
STAT1-L1	**ACCATTGGTCTCGTGTTCTCTGTT**
TIGIT_Hs_U3	**CTCCCCTCGCCTCAGGAATGAT**
TIGIT_Hs_L3	**CCGTGGTGGAGGAGAGGTGACA**
CD8A-U3-Hs	**CCGGTCTTCCTGCCAGCGAAG**
CD8A-L3-Hs	**GGCGCCGGTGTTGGTGGTC**
PDCD1-U1-Hs	**TCGTCTGGGCGGTGCTACAAC**
PDCD1-L1-Hs	**AGGGCCTGTCTGGGGAGTCTAAG**

DISCUSSION AND PROSPECTS

4. DISCUSSION AND PROSPECTS

4.1 Discussion

4.1.1 DC maturation states: towards a novel classification?

In our study, we are proposing a novel classification of cDC maturation states, based on systematic *in vitro* analysis of DC-T cell features. We used 16 stimuli activating 6 different TLR, 1 CLR, cytosolic sensors and 2 cytokine receptors, covering a broad spectrum of signaling pathways, reviewed in the introduction. PRR signaling pathways have some specificities but are also very redundant as shown by the transcription factors shared by the different pathways. The exact mechanisms by which a cell will present with different outputs after stimulation by 2 different ligands binding the same receptor or a unique ligand present at different concentration or for different duration remains to be fully elucidated. Here, we could further classify our observations in 3 categories: (i) different ligands for different receptors that all induce the same phenotype (e.g. "secretory" for Zymosan/TLR2-Dectin1 and R848/TLR7/8, and "helper" for GM-CSF/GM-CSFR and Flu/TLR7-Cytosolic sensors); (ii) 2 different ligands for the same receptor that induce "secretory DC" or "helper DC" (e.g. TLR2 and the ligands HKSA and Pam3); (iii) ligand-receptor pairs that have their own specificity, such as Poly I:C/TLR3 that was one of the few stimuli with an intermediate phenotype between "secretory" and "helper", and was also unique at inducing high levels of IFN-a and IL-28. Most observations were in the first category, so that we may now ask the question of the universality of this classification.

Would any other DC stimuli induce necessarily "secretory" or "helper DC"? Are there stimuli, combinations or doses able to induce simultaneous high expression of PDL1 and ICOSL, or are these molecules exclusive at high expression levels on cDC? and what would be the associated DC and T cell outputs? Other types of stimuli and combination would need to be tested to address this question, for instance using pure cytosolic sensor activators such as cGAMP (117).

Another aspect of universality would be the impact of the DC subset, as we have seen in the introduction that the same stimuli on different DC subsets, even when both express the corresponding receptor, could have a different impact. Two years ago, in our team, we had identified functional pDC subsets after CpG or Flu stimulation, labelled "P1", "P2" and "P3", according to their final state of maturation with the same stimuli. The markers best discriminating these subsets were PDL1 and CD80. "P1" were PDL1high and CD80low and associated to an increased secretion of IFN-α, whereas "P3" PDL1lowCD80high were the

most potent activators of T cell (294), and "P2" had an intermediate phenotype. This suggest that our classification may apply to pDC, but that PDL1 and ICOSL were not the best functional subset markers in this case. However, ICOSL was also overexpressed in "P3" as compared to "P1".

As the extensive literature on DC maturation states was obtained with Mo-DC, it would also be interesting to determine if our cDC classification applies to this *in vitro*-generated subset. Finally, our dataset contained data from primary blood CD11c+ DC, composed of a majority of cDC2 and a minority of cDC1. We therefore cannot be sure if this classification would apply to cDC1 stimulated alone, especially since cDC1 do not express the same PRR than cDC2. A potential influence of cDC1 on cDC2 was also possible in our model. For instance, cDC1 express high levels of TLR3, the receptor for Poly I:C, which might explain the specificity of this stimuli described above.

Another question is the mechanisms responsible for the DC phenotypes and the T cell outputs. PDL1 and ICOSL are efficient markers to identify each functional DC state, but this does not necessarily mean that they are responsible for the effect observed on T cells. PDL1 was co-expressed with other negative checkpoints and with the integrin CD54 and the costimulatory CD40 on "secretory" DC. We did not identify any other surface marker systematically associated to ICOSL on "helper" DC. The predominance of negative signals for "secretory" DC is in line with a limited stimulation of T cells, although it remains to be demonstrated by blocking experiments. "Secretory" DC secreted high levels of IL-10 that may be responsible for the absence of stimulation of T cell cytokine production, and may also be the signal responsible for PDL1 upregulation in an autocrine manner (169). In our system, IL-10 signaling towards T cell seems to have a dominant immunosuppressive effect on IL-12 that was also produced by "secretory" DC. Additionally, although "secretory-DC"- activated naïve CD4 T cells were not able to produce more cytokines than T cell co-cultured with medium DC, they acquired higher proliferation capacity.

CD4 T helper cells promote CD8 cytotoxic activation by the secretion of cytokines but also by membrane-bound molecules that were not measured in our model, such as CD40L (245), and cDC2 may cross-present. We have not performed subsequent DC/CD8+Tcells or CD4+Tcell/CD8+Tcell functional assays and cannot further conclude on the level of CD8+T cell immunosuppression or anergy associated with "secretory DC". Finally, it is possible that some molecules not measured in our model may also play a role on the observed phenotypes, such as TGF-β (254).

Transcriptomic analysis of tumor infiltrating DC and of a public dataset of DC activated with one "secretory" and one "helper" stimuli allowed us to observe that the NFkB pathway was strongly upregulated in "secretory" DC. The transcription factors *IRF-1, -7, -8, -9* and the

STAT-1, -4, -5a were also associated to the "secretory" signature, whereas *IRF4, CREB3* and *CREB3L2* were associated to the "helper signature", and *IRF2*, *JUN*(gene for AP1) and *CREB3L1* were part of the common maturation trunk (Section 3.1, Fig4E and Table 9). Additional transcriptomic analysis of DC stimulated with some of the other stimuli of our model would help us to confirm the differential expression of the transcription factors associated with each phenotype.

Ex vivo phenotypic and transcriptomic analyses of human tumor infiltrating cDC2 showed that the cells from inflamed tumors had important similarities with our *in vitro* "secretory" DC. These results are very encouraging for the relevance of our *in vitro* model to human physiopathology. Our classification also conciliates the observations of simultaneous immunosuppressive and immunogenic features observed in various context in human and presented in the introduction (71), (236).

Former observations that lead to the existing classification of immunogenic and tolerogenic matured DC are not necessarily conflicting with the classification presented here. Two main aspects related to the experimental settings of former studies may explain how: (i) the lack of molecules analyzed, (ii) the relativity of the comparator. The added value of our model is the unbiased and systematic measurement of multiple DC and T cell outputs. Most studies presented in the introduction studied the expression of few DC membrane markers and cytokines to define immunogenic and tolerogenic DC and might have lacked a more global view. As per the relativity of the comparator, in our model, each stimuli could be compared to the classical negative control that is medium, but more importantly to multiple different positives controls that were the other stimuli, and we tended to observe the "true" highest level of expression the molecules studied. For example, a dual comparison of TSLP-DC with Medium-DC will conclude that TSLP induces an upregulation of PDL1 on DC and define the PDL1high DC. The same experiment with a supplementary condition such as R848 will conclude that PDL1 is only mildly upregulated by TSLP as compared to R848, and the TSLP-DC will become PDL1low/intermediate, whereas R848 will appear as PDL1high. This relativity shows how much the choice of one or the other positive control is impactful for the interpretation of experimental results.

4.1.2 Translation of DC "Secretory" and "Helper" patterns into a theoretical basis for the use of DC modulators in cancer and other diseases

In the introduction section 1.2.3.5, we have seen that some of the stimuli used in our *in vitro* model are also pharmaceutical compounds approved or under evaluation. They may be used to modulate DC maturation state before DC therapy, or as peptide-based vaccine adjuvants (273).

Stimuli inducing "secretory" DC, such as R848 (TLR7/8 ligand), may be proposed as candidate drugs to induce immune cell recruitment in cold tumors and DC maturation in the TME. However, our results suggest that they should not be used in cancer patients without combining them with PD(L)1 blockade, otherwise, T cell activation in the peripheral lymph node or within the tumor might be further limited. R848 is frequently used as a vaccine adjuvant, but we have not been able to identify a trial in combination with PD(L)1 blockade (NCT02126579). TLR4 activator GSK1795091 injected in tumors is under evaluation and is, to date to or knowledge, the sole Phase I/II in this category to have planned one cohort with concomitant PD1 blockade (NCT03447314). Combination with IL-10 blocking would in theory also be needed (56). Zymosan has shown some pre-clinical efficacy in a mice model of melanoma, but no clinical trial is ongoing with this compound (295). The analysis of the effect of those compounds in the human TME is required to translate our *in vitro* observations and anticipate the factors of resistance and needs for treatment combinations.

We have not observed "Helper" cDC in the HNSCC TME, but we have defined the stimuli that may induce them *in vitro*, which include GM-CSF, TSLP, Flu and low dose of Pam3. ICOSL high myeloid cells have been described to infiltrate tissues in inflammatory diseases, auto-immune disorders and in allergy (296). As stated above, we have not yet shown that ICOSL was the key molecule for T cell activation in our model, and it may well be the absence/low levels of IL-10 and inhibitory checkpoints that simply allow a final immunostimulatory signal to transit from the DC to the T cell. That said, ICOSL has previously been shown to promote T cell activation, and is unambiguously classified as a positive checkpoint (297).

Whether DC targeting in a sense that would favor "Helper" DC polarization would be beneficial or deleterious in the context of cancer remains to be shown. This question faces the dual role of ICOS/ICOSL targeting with potential anti-tumor and pro-tumor effect in the TME, which explains why both agonists and antagonists are being tested in clinical trials in the context of cancer (298). A better understanding of the factors regulating ICOSL expression in our *in vitro* model and in the HNSCC TME would help for clinical translation. ICOS is highly expressed on Treg (296), (299), (300), but ICOS+CD8 T cells are also

present in cancer tissues, although with lower percentages of expression (28), (study 3.1, data not shown). Several studies report that these ICOS+CD8 T cells are the cytotoxic T cell responsible for the spontaneous anti-tumor immune response (30), (31), and that they are the cells that increase under PD1 blockade in cases with treatment efficacy (32). In this line, ICOS was used to enhance the efficacy of CAR-T cell-based therapies (33).

In parallel, other types of stimuli, such as cytosolic sensors activating cGAMP/STING pathway are entering the clinics [NCT03010176, NCT03172936]. cGAMP is able to activate myeloid cells and upregulate MHC molecules (301), but whether it drives a "secretory", a "helper" or even an undescribed third type of activation needs to be determined in order to have a rational for the need of optimized combinations. The combination of cGAMP-nanoparticles and anti-PDL1 did not significantly enhance the anti-tumor response over cGAMP-nanoparticles alone (301), which supports the importance of increasing our knowledge in the field.

4.1.3 What favors a hot versus cold immune microenvironment?

The major T cell attracting chemokines are CXCL9 and CXCL10 (302), (303), which is consistent with our results (Results 3.2 Fig 3.C). In the introduction, we reported that cDC1 were the main source of those 2 chemokines in a mice model of melanoma, but that there was a possible discrepancy between the low number of cDC1 and the high levels of chemokines (241). *CXCL9* and *CXCL10* were also produced by human tumor infiltrating cDC2 in our study (Results 3.1 Fig 4E). This difference may be due to differences in mice and human DC biology, and/or between tumor models and spontaneous human tumors.

Interestingly, there was no correlation between tumor mutational burden (TMB) and tumor inflammation, so that is not likely that the level of neoantigens is responsible for DC/T cell recruitment into tumors (304). From the biology presented in the introduction and in the 2 studies of this thesis, DC attracting chemokines seem to vary with the PRR and cytokine signaling occurring in the TME. Fig 1 from Results 3.2 shows that many DC attracting chemokines are increased in the tumor tissue, except the MCP-1, -2, -3 that are significantly decreased. A better understanding of the relationship between those the MCP, the other upregulated CCL and the main T cells attracting chemokines CXCL9 and CXCL10 would be one way to decipher the hot and cold tumors.

4.1.4 MMP2: towards a clinical-use biomarker for OCSCC?

In the second study (3.2) we propose to use pre-operative MMP2 status or post-operative MMP2 and extranodal extension status for biomarker-driven clinical trial. The gold standard way to implement biomarkers into clinical practice is to run a prospective randomized trial comparing the biomarker-driven approach (the experimental arms were described in 3.2 Fig. S6) with the control arms treated by standard of care. The objective would be to show a benefit in survival. The preparation of randomized clinical trials includes an important statistical work aimed at defining the number of patients to include in each experimental arm. To do so, existing data is used to estimate the expected outcomes in the control arms and the expected benefit of the approach tested (305). The present study delivers valuable data to prepare such trial, and we even indirectly estimated the expected rates of responders to PD1-blockade, since it would be one of the proposed options for treatment intensification. Randomized clinical trials deliver the highest level of evidence and are the best way to obtain authorities approval and the adherence of the clinicians (306).

Another way for a biomarker to enter the clinical practice is to gather an important number of evidences from studies with lower levels of evidence. For example, clinical parameters usually enter the TNM classification by such cumulated evidences, as it was the case recently for depth of invasion in OCSCC (307). Another example is the urokinase-type plasminogen activator (uPA) and its inhibitor (PAI-1) signature for prognostic stratification of breast cancer, associated with the indication of adjuvant chemotherapy (308). This biomarker was validated after a meta-analysis merging 8377 patients from 18 datasets (309). Many studies supported the prognostic role of MMP2 in OCSSC but only 1 was performed with OCSCC patients treated by primary surgery and showed a significant result in an appropriate multivariate analysis, and included only 60 patients (310). This low number of patients is of course insufficient to reach a robust level of evidence, but on the other hand shows that MMP2 is a sufficiently powerful biomarker that it may be significant even with so few patients and events, as in our 37 patient prospective discovery cohort. Another larger study in Taiwan included 256 patients in the same clinical setting, but did not present any multivariate analysis, (311). Therefore, I am not convinced that the studies available to date would be enough for a well conducted meta-analysis.

An important prerequisite is the standardization of the biomarker testing across the different centers participating to the trial in the first case, or in the medical health system in the second case. Optimal biomarkers are defined as independent in multivariate analysis, robust with a narrow confidence interval of their hazard ratio, simple to implement in routine, reproducible within the different assessors from different laboratories and cost-efficient (312). In the present case MMP2 fulfils the first two criteria, but the technology to be used in clinical practice remains to be determined. Soluble MMP2 is an elegant way to measure directly the

protein and obtain a continuous measure, as most biological analysis in medicine, but the need for standardized fresh samples to produce tumor-derived secretome is not compatible with the simplicity criteria. RTqPCR or semi-quantitative IHC would be standard alternatives, and have shown their applicability in former studies in OCSCC (310), (311).

4.2 PROSPECTS

4.2.1 Redefining tumor infiltrating DC functional subsets: the contribution of unsupervised single cell sequencing

Single cell RNA sequencing, possibly combined to antibody-barcoding, has been a technological revolution that took place during my PhD. In section 1.2.1.4, we described 2 single-cell studies on blood DC, which highlight the added value of unsupervised analysis of data obtained from single cell transcriptomic sequencing, as compared to the historical supervised analysis of multicolor flow cytometry data. Single cell RNA sequencing allows to redefine the different subsets and/or states of the different cell types by grouping them according to their level of transcriptomic similarities. The signature of each subset may then be analyzed to (i) identify predicted surface markers that may serve to further study each subset, and need to be confirmed by flow cytometry, (ii) decipher overexpressed genes and infer cell state and function, (iii) identify potential therapeutic targets (64). Only one study analyzing in detail the innate compartment by single-cell transcriptomics of a human tumor is available to date (237). The only single-cell study available in head and neck cancer from Puram et al. included so few DC that this dataset cannot be further exploited for this cell subset (25).

In the team, and in collaboration with the Team of Pierre Saintigny in the Centre Léon Bérard, Lyon and the INRA, Lyon, we have implemented a protocol for single cell sequencing of tumor-infiltrating immune cells. The specificity of our protocol is to make an asymmetric enrichment of the various immune subsets, in order to obtain data on all cell types, but with an equivalent resolution for frequent (T cells) and rare (DC) cells types. To date, we have analyzed one OCSCC patient. Our preliminary result show that the genes that are specific to the cDC2 in the bulk transcriptomic data presented in Fig 4 of Results section 3.1 are in fact secreted by a subset of matured cDC2. Next, we will complete the analysis of our first patient sample, confirm our results in 2 other tumors and identify and confirm the surface markers of newly identified subsets, before implementing functional studies. Our objective is to obtain a comprehensive resource on the innate immune infiltrate of OCSCC patients, to be used for clinical translation.

4.2.2 The challenges of translational medicine and the contribution of window-of-opportunity trials

All experiments presented in this thesis were performed with human samples, either from cancer patients of from healthy blood donors. We believe that it is the shortest path to clinical translation. However, human sample biology has several limitations: (i) ethical issues and requirements of informed consents, (ii), synchronization of the players of the sample circuit, (iii), experimental limitations, such as the use of gene-KO models, (iv) limited access to samples and need for invasive procedures. Therefore, if working on human samples is very efficient for the identification of prognosis biomarkers, it is way more complicated for the study of the associated biological mechanisms or the identification of predictive biomarkers.

Pre- and post- treatment comparison is a basic of research on mechanism and predictive biomarkers. While mouse biologists are developing humanized mouse models (313), (314), clinicians and biologists working on human samples have developed a new way to perform such pre and post-treatment comparisons in patients: pre-operative window-of-opportunity trials. It is an optimal setting for predictive biomarker identification in human (315), (316). Such trials, as the one presented in Annex 3.2, require an excellent synchronization of the multiple teams involved, to be able to perform in a limited timeframe the neoadjuvant treatments, the surgical planning, the surveillance of adverse events, repeated imaging and other efficacy endpoints evaluation, and importantly the translational research on blood and tumor samples. Window-of-opportunity trials is a nice example of how we may overcome the limitations of human sample-based research.

4.2.3 The role of the tumor draining lymph node in the anti-tumor immune response

I introduced this thesis with the question of how a head and neck surgeon comes to immunology. I will end up this manuscript explaining what happens when a junior immunologist goes back to the operating theater. As a head and neck surgeon, I often perform therapeutic or even elective (prophylactic) neck dissection. With my new immunology perspective, I am quite puzzled to remove the lymph nodes that are supposed to contain patients' immune memory against cancer. Several studies support the role of the tumor draining lymph node for the anti-tumor immune response (235), (317), and other have shown that response to PD-1 blockade occurs in the lymph node and not in the tumor (318).

In the ongoing Keynote-689, pembrolizumab is given at D0 and D15 and surgical removal of the tumor and the draining lymph nodes is performed around day 30. Even in the cases classified as N0 by pre-operative MRI and TEP-CT, the lymph nodes are removed, as it is the standard of care. The objective is to remove the occult micro-metastasis that are eventually found in 30% of the N0 patients (319), (320).

The study of human tumor draining lymph node could give us some answers. Flow cytometry and even single cell technologies are hard to apply to lymph nodes in humans, because the markers allowing to distinguish lymph node resident DC, inflammatory migratory DC coming from the tumor tissue, inflammatory migratory DC coming from another benign inflammatory local area such as dental infection, or homeostatic migratory DC is not trivial. Deciphering tumor related and unrelated events is more robust when studying T cells, because tumor antigens can be matched with the clonal T cell with the corresponding TCR.

For the future, we may imaging that advances in micro-imaging and tagging technologies could allow us to determine precisely which lymph node needs to be removed and which one doesn't and/or which lymph node contains the pool of anti-tumor T cells clones, and could be preserved or collected and stored for T cell adoptive therapy.

ANNEX

5. ANNEX

5.1 Table of correspondences between mice and human DC subsets

Adapted from Dalod et al. (106)

5.2 Synopsis of ICING, a Phase II trial of M7824 (MSB0011359C), a bifunctional fusion protein targeting TGF-β and PDL1, in a pre-operative setting for resectable and untreated head and neck squamous cell carcinoma.

I will be with Christophe Le Tourneau the principal investigator of this trial that has just been funded by Merck and GSK and will lead the translational research.
Realized with the help of the Methods in Clinical Cancer Research Workshop and all the faculties.

		Version	1.1	Date	13.06.2018
Title	Phase II trial of M7824 (MSB0011359C), a bifunctional fusion protein targeting TGF-β and PDL1, in a pre-operative setting for resectable and untreated head and neck squamous cell carcinoma				
Abbreviated title	ICING				
Sponsor	Unicancer				
Coordinating investigators	Prof Christophe Le Tourneau, MD, PhD Head, Department of Drug Development and Innovation Institut Curie, 26 rue d'Ulm, 75005 Paris, France Christophe.letourneau@curie.fr Dr Caroline Hoffmann, MD, PhD student Department of Head and Neck Surgery Institut Curie, 26 rue d'Ulm, 75005 Paris, France Caroline.hoffmann@curie.fr				
Biostatistics	Jocelyn Gal, MSc, PhD student Epidemiology and Biostatistics unit – research center Centre Antoine-Lacassagne, 33 av de Valombrose, 06189 Nice cedex 2 Jocelyn.gal@nice.unicancer.fr				
Pharmacy	Dr Laurence Escalup Department of Pharmacy Institut Curie, 26 rue d'Ulm, 75005 Paris, France Laurence.escalup@curie.fr				
Number of centers	7	France	Yes	International	No
Indication	Histologically or cytologically confirmed squamous cell carcinoma of the oral cavity, oropharynx, larynx or hypopharynx, previously untreated, with indication of primary surgery. Patients with a diagnosis of SCCHN from unknown primary will not be enrolled.				
Primary objective	To evaluate the efficacy of M7824 (MSB0011359C), a bifunctional fusion protein targeting transforming growth factor (TGF-β) and PDL1, as measured by pathological response (PathR), given in a pre-operative setting, in resectable and previously untreated head and neck squamous cell carcinoma (HNSCC).				

Secondary objectives	1/ To evaluate the efficacy of M7824 using alternative readouts, namely:
	
	    a) . The pathological response using alternative threshold of tumor cell death as compared to the one used for primary objective
	    a) . The clinical response, as measured by to RECIST v1.1.
	    b) . The response rate, using primary endpoint criteria, by PDL1 status assessed by combined positive score (CPS) as <1 (absent), ≥ 1CPS <				

	20 (low), and ≥ 20 (high).
	c) *Note: cTNM and pTNM will be recorded to evaluate the post-treatment down-staging, but it will not be a secondary endpoint in the absence of control cohort, knowing that, from literature and study coordinators expertise, cTNM might be different from pTNM in the absence of any treatment in a significant number of patient.*
	2/ To evaluate the safety and tolerability profile of M7824
	3/ To evaluate the usefulness of having inked the tumor margins during baseline endoscopy in avoiding surgical plan changes putatively induced by tumor shrinking under therapy.
Exploratory objectives	To evaluate the pharmacodynamics value of potential biomarkers comparing pre and post-treatment blood and tumor samples
Methodology	This study is a prospective open label, multicenter, phase II, window-of-opportunity preoperative, single-agent trial.
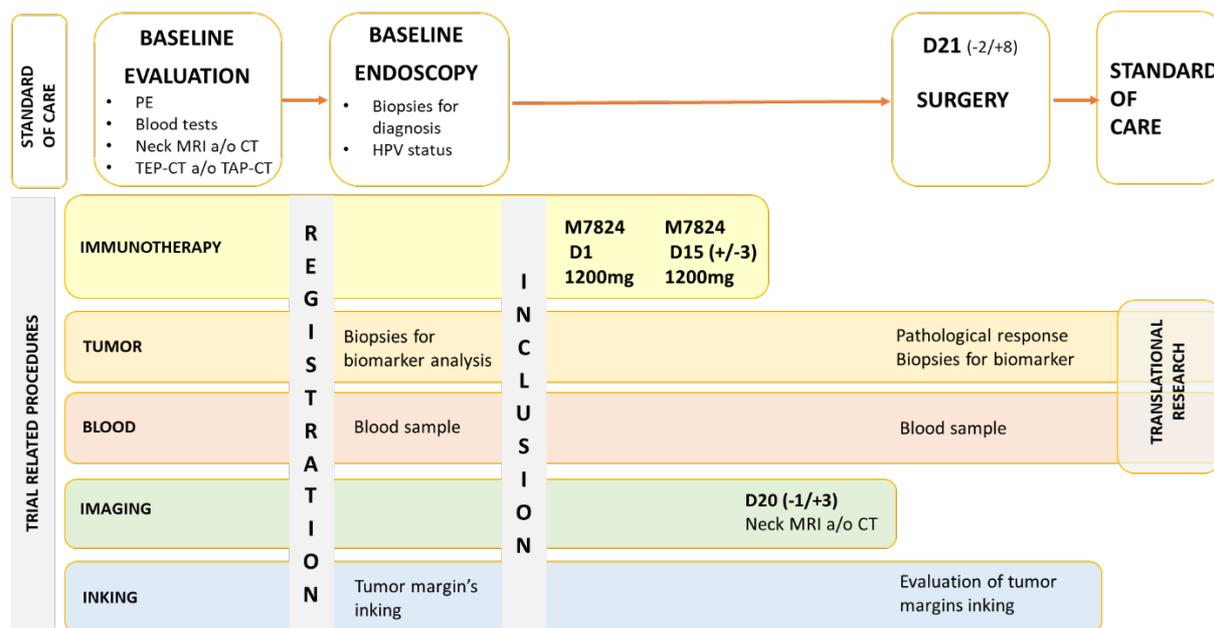
Inclusion criteria
Untreated resectable HNSCC, with an indication of upfront surgery. T2 with N1 or more, or T3 / T4 any N.

Cohort A, n = 43: Non-oropharyngeal HNSCC, or Oropharyngeal SCC that are HPV negative, or Oropharyngeal SCC that are HPV positive and smoker ≥ 10PY
Cohort B, n = 16: Oropharyngeal SCC that are HPV positive and non-smoker, or smoker < 10 PY

Registration criteria	1) Age ≥ 18 years		

Registration criteria	1) Age ≥ 18 years 2) Histologically or cytologically confirmed, or highly suspected* squamous cell carcinoma of the oral cavity, oropharynx, larynx or hypopharynx, previously untreated, with indication of primary surgery. Patients with a diagnosis of SCCHN of unknown primary are excluded. (*: In order to avoid repeated biopsies procedures under general anesthesia, patients with clinically highly suspected squamous cell carcinoma could be registered before the histological or cytological proof. In these cases, the diagnosis will be confirmed intra-operatively, during the initial panendoscopy, by frozen sections.) 3) ECOG performance status ≤ 1 4) Patients must be willing and able to comply with scheduled visits, treatment plan, laboratory tests and other study procedures 5) Patients must be affiliated to a Social Security System 6) Patient information and written informed consent form signed
Inclusion criteria	1) Histologically or cytologically confirmed squamous cell carcinoma of the oral cavity, oropharynx, larynx or hypopharynx, previously untreated, with indication of primary surgery. Patients with a diagnosis of SCCHN of unknown primary are excluded. 2) Absence of distant metastases determined by CT scan or Pet CT 3) TNM and primary tumor location-related inclusion criteria are similar in the 2 cohorts of patients, and are, according to the 7th edition AJCC: T2 with N1 or more; T3 or T4 and N. These inclusion criteria are summarized in the following table. The 7th edition of AJCC is used here in order to have a unique table for both HPV-negative and oropharyngeal HPV-positive cancer patients.

	N0	N1	N2a	N2b	N2c	N3
T1	Not eligible	Not eligible	Not eligible	Not eligible	Not eligible	Not eligible
T2	Not eligible	ok	ok	ok	ok	ok
T3	ok	ok	ok	ok	ok	ok
T4	ok	ok	ok	ok	ok	ok

Table1: Eligibility criteria according to TNM status, AJCC 7th edition.

4) Baseline radiology studies evaluating tumor primary (MRI or CT scan) must be performed within 28 days prior to registration.
5) ECOG performance status ≤ 1
6) Adequate organ and marrow function as defined below:
 . Hemoglobin ≥ 9,0 g/dL
 . Absolute neutrophil count (ANC) ≥ 1,500/mm3
 . Platelet count ≥ 100,000/mm3
 . AST and ALT ≤ 2.5 × institutional upper limit of normal (ULN);
 . Total bilirubin ≤ 1.5 × ULN;
 . Creatinine clearance > 30 mL/min as determined by the Cockcroft-Gault equation (Cockcroft and Gault, 1976)
7) Negative serology for hepatitis B and C
8) Women of childbearing potential must have a negative serum β-HCG

	pregnancy test within 7 days prior to the administration of the first study treatment and/or urine pregnancy 48 hours prior to the administration of the first study treatment. Both sexually active women of childbearing potential and males (and their female partners) patients must agree to use two methods of effective contraception, one of them being a barrier method, or to abstain from sexual activity during the study and for at least 6 months after last dose of study drugs. 9) Absence of any psychological, familial, sociological or geographical condition potentially hampering compliance with the study protocol and follow-up schedule; those conditions should be discussed with the patient before registration in the trial
Exclusion criteria	1) Primary site of head and neck carcinoma in nasopharynx, sinuses, or skin 2) Patients receiving other anti-cancer medication such as, chemotherapy, immunotherapy, biologic therapy, targeted therapy, monoclonal antibodies, hormonal therapy (other than leuprolide or other GnRH agonists) or other investigational agent within 6 months prior to the first dose of study drug and while on study treatment. 3) Patients receiving other anti-cancer non-drug therapies: radiation, or tumor embolization within 6 months prior to the first dose of study drug and while on study treatment. 4) Participation in another clinical study with an investigational product during the last 30 days 5) Uncontrolled intercurrent illness including, but not limited to, ongoing or active infection, active peptic ulcer disease or gastritis, active bleeding diatheses. 6) Patient under guardianship or deprived of his liberty by a judicial or administrative decision or any condition (e.g psychiatric illness/social/familial/geographical condition) that would limit compliance with study requirement or compromise the ability of the subject to give written informed consent 7) Current or prior use of immunosuppressive medication within 28 days before the first dose of M7824, with the exceptions of intranasal, intraocular and inhaled corticosteroids or systemic corticosteroids at physiological doses, which are not to exceed 10 mg/day of prednisone or an equivalent corticosteroid. 8) Receipt of live attenuated vaccination within 30 days prior of inclusion 9) Active or prior documented autoimmune disease within the past 2 years. NOTE: Subjects with vitiligo, Grave's disease, or psoriasis not requiring systemic treatment (within the past 2 years) can be enrolled 10) Active or prior documented inflammatory bowel disease (eg, Crohn's disease, ulcerative colitis) 11) History of primary immunodeficiency 12) History of allogenic organ transplant that requires the use of

	immunosuppressive drugs 13) Pregnant or breast-feeding women 14) Any previous treatment with an anti-PD-1/PDL1 agent 15) Any condition that, in the opinion of the investigator, would interfere with evaluation of study treatment or interpretation of patient safety or study results 16) Known positive HIV status
Treatment	**M7824** 2 infusions of M7824 will be administered on D1 and D15 Dose: 1200mg intravenously over 60 minutes Primary prophylactic administration of anti-histaminic must be administered systematically after before each infusion.
Criteria of evaluation	**Primary endpoint:** Rate of pathological response defined as tumor necrosis and/or giant cell/histolytic reaction to keratinous debris in ≥ 10% of tumor area
	Secondary endpoints: 1) **Evaluation of the efficacy of M7824 using alternative readouts:** a) The pathological response, using a threshold of 50% (PathR50), 70% (PathR70) and 90% (PathR90): will be considered as responders, the patients presenting 50% or more, 70% or more, and 90% or more, respectively, of tumor necrosis and/or giant cell/histolytic reaction to keratinous debris. b) The pathological response according to PDL1 status using CPS. c) The clinical response, as measured by to RECIST v1.1 clinical response using RECIST on CT or MRI (same imaging than as baseline). 2) The **safety profile of M7824** described using the common toxicity criteria from the NCI CTCAE v5.0 3) The **evaluation of the usefulness of having inked the tumor** margins during baseline endoscopy in avoiding surgical plan changes putatively induced by tumor shrinking under therapy will be assessed by: a. A question for the surgeon to be answered on the day of curative surgery "Would your surgical plan have been different in the absence of ink labelling?" b. Optional, if feasible: measure of the distance between current tumor front and the ink in 2 to 4 different points and take a picture. **Exploratory objectives / Translational research** Immuno-monitoring and genomic analysis will be performed on pre- and post-treatment blood and tumor samples. This multi-parametric evaluation, including dynamical changes along treatment, will allow to identify differential parameters between responders and non-responders (supervised analysis), that will be coupled to unsupervised analysis. The main axis of research will be: . Targets: TGFb & PDL1 expression

	. Immune microenvironment: immune subsets proportions, characteristics (other checkpoints expression, spatial distribution, antigen specific response…) and dynamical changes
	. Cancer cell related parameters: TMB, molecular class, checkpoint expression, RNA expression
	. Fibrosis: ECM remodeling, CAF
	. ADCC, ADCP: Fc receptors balance and polymorphism
Sample size determination	The primary endpoint is to evaluate the efficacy of M7824 (MSB0011359C) evaluated by the rate of pathological response defined as tumor necrosis and/or giant cell/histolytic reaction to keratinous debris in > 10% of tumor area. Given the differences in prognosis between oropharyngeal HPV-positive non-smokers or smoker < 10PY (1), on the potential differential drug efficacy in these 2 groups (2) (3) (4), the patients enrolled will be distributed in two distinct cohorts for statistical considerations and analysis. HPV status will be determined by p16 staining performed on the biopsies obtained during baseline endoscopy for all patients, even for non-oropharyngeal tumors. Since all trial-related interventions will be strictly similar for the 2 cohorts, the result of p16 status will not be required for the inclusion, until one of the 2 cohorts will be complete. Once 1 of the 2 cohorts will be complete, p16 status will be required for the inclusion, in no more than 7 days after the biopsy, to avoid any surgical delays.
	Cohort A: Non-oropharyngeal HNSCC, or Oropharyngeal SCC that are HPV negative, or Oropharyngeal SCC that are HPV positive and smoker ≥ 10PY
	Cohort B: Oropharyngeal SCC that are HPV positive and non-smoker or smoker < 10PY (former or active).
	M7824
	In the NCT02517398 trial evaluating M7824 in the recurrent and/or metastatic setting, in the cohort enrolling SCCHN tumors unselected for PDL1 and HPV status that were either metastatic or not amenable to local therapy with curative intent, and that progressed or recurred <6 months since the last platinum dose, an ORR of 27.9%, 13.6% and 50.0% in all, HPV-negative and HPV-positive patients respectively were reported (5). No data on the efficacy of M7824 in untreated HNSCC is available to date.
	In the same trial, an ORR of 36.5% was obtained when merging data of all HPV-associated solid cancers (6).
	In the cohort enrolling second-line metastatic non-small cell lung cancer (NSCLC) patients, an ORR of 27.5%, 40.7% and 71.4% in all, PDL1 positive (>1%), and PDL1 high (> 80%) patients respectively were reported (7).
	In 2 pre-clinical models of melanoma and triple-negative breast cancer (TNBC) bearing humanized mice, such a-PDL1-TGFBRII antibody had a significantly increased anti-tumor activity as compared to anti-PDL1 alone or even anti-PDL1 and anti-TGFBRII given as a combination (8).
	Efficacy of neoadjuvant PD-1/PDL1 targeting
	M7824 is structurally close to Avelumab for anti-PDL1 targeting (9). However, no data is available to date on the efficacy of Avelumab in

the neoadjuvant setting. In a previous window-of–opportunity trial with Pembrolizumab, an immunotherapy targeting PD-1, a 43% (95% CI: 21%-64%) pathological response rate was reported *(10)*. In the CheckMate 358 trial, 2 doses of neoadjuvant Nivolumab (targeting PD-1) induced an investigator-assessed tumor size reduction superior to 25% in 13% of the patients *(11)*. However, the extrapolation of these results is limited by the facts that Pembrolizumab and Nivolumab target PD-1 whereas M7824 targets PDL1. In addition, M7824 has antibody dependent cell cytotoxicity (ADCC) and also targets TGFb.

Estimation of M7824 minimal and target response rates
The primary endpoint is the rate of pathological response, observed in the post-treatment operative specimen, defined as tumor necrosis and/or giant cell/histolytic reaction to keratinous debris in more than 10% of the tumor area.

The minimal pathological response rate with M7824 should not be inferior to PD1/PDL1 targeting alone, measured at 43% *(10)*. To take into account the fact that this 43% rate has been determined in a small number of patients, and is necessarily associated with a large confidence interval (95% CI (21%-64%)) and given the results obtained with M7824 above-mentioned trials, we consider that a pathological response rate of 30% or less as unacceptable.
In untreated resectable HNSCC, we estimate that 1/3 of patients with HPV negative tumors present a tumor microenvironment poor in both T cells and dendritic cells, and are very unlikely to respond to immunotherapy. Thus, we estimate that the maximal pathological response rate to an optimal immunotherapy would be 67% in this setting. Our objective would be to induce a pathological response in half of the candidate responders to M7824 that are not responding to anti-PD1/PDL1 alone (calculation: (67%-33%)/2= +17%). Therefore, the fixed target improvement will be of 17% corresponding to a target ORR for M7824 of 33+17 = 50,0%.

Sample size determination
For Cohort A, the objective is efficacy determination with sufficient power, to compare to the historical control of neoadjuvant pembrolizumab mentioned above.

We will use the two-stage Minimax design described by Simon et al. *(12)* with an unacceptable rate of pathological response of 30% or less and a hypothesized actual pathological response rate of 50% or more.

The sample size was determined by testing the null hypothesis H0: p ≤ 30% versus the alternative H1: p ≥ 50% at a one-sided significance level of 0.1 and a power of 0.9. In the first stage, 28 patients will be accrued and the study will conclude to inefficacy and should be stopped if the observed number of patients with a pathological response is 7 or less. If 8 or more patients present pathological response, then an additional 11 subjects will be accrued (second stage), bringing the total number of patients to n=39. The null hypothesis of p ≤ 30% will be rejected and M7824 will be considered

	effective if the total number of patients with a pathological response is 16 or more.
	To account for non-assessable patients (10%), we will include 4 additional patients.
	Required sample size is 43 for cohort A.
	For Cohort B, the objective is to estimate the rate of response with a limited width of confidence interval (CI).
	The sample size estimation for cohort B was completed by using the 95% CI method. We propose a sample size of 14. The half width of the 95% CI will be less than 25% if the response rate is at least 65%.
	To account for non-assessable patients (10%), we will include 2 additional patients.
	Required sample size is 16 for cohort B.
Number of patients	43 patients in cohort A and 16 in cohort B: 59 patients
Duration of the trial	1/ Enrollment period: 24 months 2/ Treatment: 2 weeks 3/ Follow-up: 6 months 4/ Duration of the study: 31 months The HPV status, which might need different duration to be obtained in the various centers, will not have to be determined at the time of the inclusion, since it does not influence the treatment protocol, in order to avoid surgical delays. Patient will be enrolled in the study as they come, independently of the HPV status. The accrual will be monitored continuously in order to respect the number of patients planned per cohort. More precisely, 2 situations might be encountered: Case 1: accrual of cohort B (n = 16) is completed before cohort A. From then, only patients with non-oropharyngeal SCC or with oropharyngeal SCC and smokers > 10PY will be enrolled. Knowledge of p16 status will still not be necessary for any new inclusion. Case 2: accrual of cohort A (n = 43) is completed before cohort B. From then, only patients with oropharyngeal SCC and non-smoker or smoker < 10PY will be registered. The HPV status, determined as per p16 staining by immunohistochemistry, will have to be obtained within 6 days after the baseline endoscopy, in order to be able to include the patient and start the treatment no longer than 7 days after the baseline endoscopy. This is due to guaranty the absence of surgical delay related to the need of the HPV status determination and to respect the recommended maximum duration between baseline endoscopy and the day of surgery (<45days). Centers that cannot not offer to obtain p16 results within this timeframe should stop enrolling patients.
Rationale for this study per objective	**Anti-tumor activity** M7824 is an innovative first-in-class bifunctional fusion protein composed of a human IgG1 mAb against PDL1 fused with 2

extracellular domains of TGF-β receptor II (a TGF-β"trap") and has shown promising antitumor activity and manageable safety in phase 1 trials, including as 2L treatment for NSCLC and HPV+ HNSCC (1), (7), (13).

Anti-PD1/PDL1 agents have shown antitumor activity in recurrent and/or metastatic HNSCC (14), (15), and in primary tumors in the preoperative setting (10), (11). However, the majority of patients do not respond to PD-1 /PDL1 antagonists used as single agents. Research aimed at identifying biomarker of response have highlighted the role of tumor mutational load, the intensity of intra-tumoral CD8+ T cell infiltrates, interferon gamma (IFNg) signature, and tumor and immune cell PDL1 expression (4) (16) (17) (18). Additionally, another signature of resistance, corresponding to the transforming growth factor β (TGF-β) pathway, associated with cancer associated fibroblasts (CAF), has been identified in 2 different pre-clinical models (urothelial and microsatellite-stable colorectal cancer) and in patients with metastatic urothelial cancer who were resistant to an anti-PDL1 agent (atezolizumab) (19). The role of TGF-β in treatment resistance has also been observed in HNSCC *in vitro* (20). Therefore, there is a strong rationale to inhibit both the PD-1/PDL1 axis and the TGF-β signaling in cancer patients, namely in tumor types showing both evidence of anti-tumor activity of PD-1/PDL1 inhibitors and high levels of primary resistance, such as HNSCC.

M7824 is aimed at neutralizing the TGFb, a pleiotropic cytokine that is overexpressed in HNSCC (21). TGFb is implicated in the epithelial-to-mesenchymal transition, invasion, and metastases of tumor cells, in fibroblast activation and deposition of collagenous extra-cellular matrix, and favors immunosuppression (22), (23), (24). Indeed, TGFb suppresses IFNg expression by T cells, inhibits CD8 effectors cells cytotoxicity, inhibits the differentiation of central memory cells (25), (26), and skews the differentiation of CD4 T cells away from Th1 polarization towards regulatory T cells (Treg) (27).

Additionally, M7824 is an IgG1 antibody has structural similarities to Avelumab and as shown to be able to induce ADCC (9), an additional mechanism of anti-tumor activity (28).

Therefore, the rationale for this fusion protein is the couple: (i) negative checkpoint blockade by targeting PDL1 on tumor cells and immune cells, (ii) TGFb targeting, in order to inhibit its immunosuppressive effects and and pro-tumoral effect on stroma and extra-cellular matrix (29), (iii) NK-mediated anti-tumor effect via ADCC. In a pre-clinical model, this fusion protein has shown to be more efficient than anti-PDL1 antibodies alone (Figure1) (8).
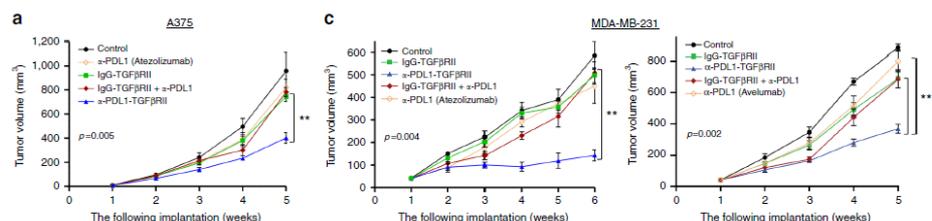
Figure 1: adapted from Ravi et al., Nature Comm, 2018 *(8)*.

Evaluation of alternative outputs of anti-tumor activity

Given the limited number of windows-of-opportunity trials in the pre-operative setting, the appropriate criteria of evaluation of anti-tumor activity remains unknown, in particular for immunotherapy: although tumor shrinkage occurred in almost half of patients, few patients experienced an objective response in the Pembrolizumab and Nivolumab pre-operative trials. In the present study, the threshold of 10% tumor necrosis has been defined as primary endpoint, similarly to the study with neoadjuvant Pembrolizumab. This low threshold is adapted to these very short durations of treatment. However, some patient showed 50% of even 90% pathological response rates even after a single injection (30). Therefore, analysis of the pathological response with the 50% and 90% tumor necrosis thresholds, and of the tumor size reduction per RECIST v1.1 will complete our evaluation of anti-tumor response.

Safety

Limited data on the safety of M7824 are available to date. In the NCT02517398 and NCT02517398 trials, 3/16 (19%) and 20/80 (25%) of the patients experienced grade 3 or 4 adverse events respectively (6), (7). No treatment-related death as been reported to date.

Usefulness of having inked the tumor margins during baseline endoscopy in avoiding surgical plan changes

Any neoadjuvant treatment, even given for a short period such as in window-of-opportunity pre-operative trials, lead to the risk of downgrading surgical plans in case of significant tumor size decrease. However, to date, primary surgery for head and neck cancers needs to be performed according to baseline tumor size, disregarding the effect of any neoadjuvant therapy, because the safety of considering the new margins as not been assessed. Therefore, we believe that inking the tumor margins during baseline endoscopy will help to prevent this risk of surgical under-treatment. This procedure will be evaluated in the present trial.

Identification of biomarkers

Identification of predictive and PD biomarker of response to M7824 is key to appropriately select the patients that will benefit from the treatment in future phase III trials and beyond.

For anti-PD1/PDL1 targeting, baseline levels of PDL1, intra-tumor CD8 T cells infiltrate, IFNg signature and tumor mutation burden are proposed predictive biomarkers, but their sensitivity and specificity remain limited (31).

For M7824, no predictive biomarker has been identified to date, and the addition of this TGFb "trap" significantly influences the mechanisms of action as compared to anti-PD1/PDL1 targeting alone, therefore requiring further efforts to identify the appropriate biomarkers.

Several studies have shown that whereas pre-treatment biopsies were unable to identify responders, the biopsies done after 1 or 2 treatment doses were much more informative (32), (33), (34), (35), (36). These early post-treatment biopsies match exactly with the design of the present pre-operative trial.

Translational research	**Translational research**
	Immuno-monitoring and genomic analysis will be performed on pre- and post-treatment blood and tumor samples. Pre-treatment tumor samples will come from additional biopsies done during baseline endoscopy, and post-treatment tumor samples will come from additional biopsies done immediately before the removal of the surgical specimen.
	Rationale and axes of research
	The aim of the proposed biological analysis is to address specific scientific questions related to potential predictive biomarkers of efficacy and the mechanism of action of the anti-tumor immune response in the context of the treatment by M7824:
	. Which biomarkers are specifically associated with a/o predictive of tumor response to treatment versus resistance to treatment?
	. Are these biomarkers present at baseline?, or only measurable after one cycle of treatment?, or only relevant when measured as an intra-patient variation between baseline and after one cycle of treatment?
	This multiparametric evaluation, including dynamical changes along treatment, will allow identifying differential parameters between responders and non-responders (supervised analysis), which will be coupled to unsupervised analysis.
	The main axis of research will be:
	. Targets: TGF-β & PDL1 expression
	. Immune microenvironment: immune subsets proportions, characteristics (other checkpoint expression, spatial distribution…) and dynamical changes
	. Cancer cell related parameters: TMB, molecular class, checkpoint expression, RNA expression
	. Fibrosis: ECM remodeling, CAF
	. ADCC, ADCP: Fc receptors balance and polymorphism
	. Specific immune response towards tumor antigens
	Biological sample collection
	Tumor tissue and blood sample collection will be performed at baseline and on the day of surgery.
	<u>Blood</u>
	30ml of blood will be collected from each patient in EDTA tubes and processed to obtain samples of peripheral blood monolayer cells (PBMC), plasma, and for genomic analysis. Additionally, each time a sufficient amount of tissue will be available to perform FACS on fresh tumor (see below), a fraction of fresh PBMC will be also analyzed by FACS.
	The procedures for blood sampling and processing will be described in greater detail in a separate Laboratory Manual. Processed samples will be stored on site at -80°C until such a time as the Sponsor request transfer to the central storage center.
	<u>Tumor</u>
	At least two core biopsies are to be collected at each time point.

One sample will be fixed in formalin and embedded in paraffin (FFPE). This sample will be transferred to the central laboratory for IHC analysis of biomarker expression levels.

One sample will be frozen in nitrogen or fixed using the optimum cutter temperature (OCT) compound method, and stored at -80°C. This sample will be used for whole genome and/or RNA sequencing analyses.

If the tumor lesion volume is not sufficient to obtain two biopsy cores, priority will be given to the FFPE biopsy.

If the tumor lesion volume is sufficient for one or two additional biopsies, they will be transferred in CO_2 independent medium, at 4°C, within 24h, to the laboratory of the center of immunotherapy in Institut Curie, Paris, in order to perform immune-monitoring by flow-cytometry.

The procedures for tumor tissue processing will be described in greater detail in a separate Laboratory Manual. FFPE and frozen samples will be stored on site at -80°C until such a time as the Sponsor request transfer to the central storage center. Only fresh tumor tissue, when available, will be shipped immediately as mentioned above.

Analysis planned

Blood (all delayed analysis)

1) biobanking of plasma, in order to perform soluble biomarkers analysis at a later date, such as measurement of serum levels of TGF-β, soluble PDL1, cytokines, etc...
2) biobanking of frozen PBMC, in order to study the TCR clonality, the sub-populations of the innate immune system of the lymphocyte sub-populations with analysis of their activation and expression of positive and negative immune checkpoints
3) whole blood will be processed to obtain DNA and RNA for delayed genomic analysis

Tumor
Real-time analysis
Fresh tumor samples, when available, will be analyzed by flow-cytometry and/or single cell sequencing according to the budget and the availability of pre- and post-treatment samples.

4) Immuno-monitoring with flow cytometry on digested fresh tumor samples at baseline (pre-treatment) and at surgery (post-treatment) (for information purposes, (a) 15 to 20 color panel(s) may include the following markers: CD45; CD3; CD8; CD4; CD56; CD25; CD127; CD27; CD39; CD69; CD103; CD29; FAP; CD15; EPCAM; PD1; PDL1; ICOSL; CD14; CD16; BDCA1; CD11c; HLADR; Live dead)
5) Gene expression analysis by single cell sequencing on fresh samples on sorted CD45+ cells. Ideally, we would perform a 5' sequencing together with TCR sequencing in order to obtain both information on targets and pathways of immune cells at the single cell level and information on the specific immune response towards tumor antigens (identification of the recurrent TCR that amplify under treatment, differentially between responders and non-responders). Taking into account the cost of such analysis and the supplemental amount of samples required, it should be limited to a small number of patients with pre and post-treatment comparisons.

	Delayed analysis 6) Immunohistochemistry (1 FFPE sample): single or multicolor panels, that may include, but are not limited to: HPV status for non-oropharyngeal tumors (p16) **Panel 1** (Pre-ttt and post-ttt*): TGFb, PDL1, CK, CD4, CD8 (Targets + hot/excluded/cold tumor identification); (*Post-ttt panel may be adapted with regard to the potential negativity of TGFb and PDL1 staining after treatment). **Panel 2** (Pre and post-ttt): TGFb pathway baseline activation status and effect of the M7824: (i) receptor: TBRII, (ii) canonical pathway: p-SMAD2, p-SMAD5, (iii) non canonical pathway: TAK1, p-p65, (iv) negative feedback: SMAD7 **Panel 3** (Pre and post-ttt): Collagen remodeling; **Panel 4** (Pre and post-ttt): Fc Receptors CD32a, CD32b 7) Gene expression analysis, that will be performed, according to the budget and technology development, by: . Targeted sequencing, OR . RNAseq (1 frozen sample): we will perform unsupervised analyzes to determine predictive signatures of treatment response, and test published signatures, a/o . RNAseq of microdissected stroma and epithelium (1FFPE sample; eg. DSP Nanostring® or Spatial transcriptomics®). Supervised analysis will be performed and explore tumor cell, checkpoints, EMT signature, immune subsets signatures & cell proportions and signaling pathways. Unsupervised analysis will be performed in order to identify a novel and M7824 specific response signature. 8) Tumor mutation burden evaluation (same frozen sample than RNAseq) We will prioritize these analyzes to adapt to the quantity of material available and to the budget.
Timeline	

Milestones	First Proposed Plan
CSA - Concept Sheet (Proposal) Approval	Jan-2019
FPA - Final Protocol Approved	May-2019
Research Ethics Committee Review	Jun/Jul-2019
FSFV - First Subject Signed ICF	Sep-2019
30 pc - 30 percent of subjects consented	Jun-2020
60 pc – 60 percent of subjects consented / Interim Analysis	Jan-2021

	LSFV - Last Subject Signed ICF	Sep-2021
	LSLV - Last Subject Last Visit	Oct/Nov-2021
	Key Stats - Key Stats Available	Dec-2021
	CTR - Clinical Trial Report Approved	Apr-2022
	Long term follow-up	
	LTFU - Last Subject Last Visit	Apr-2022
	DB Lock - Database Lock	Apr-2022
	LTFU - Full Stats Available	Jun-2022
	LTFU - Clinical Trial Report-Addendum Approved	Apr-2023
List of centers	**Comprehensive cancer centers** 1/ Institut Curie, 26 rue Ulm, 75005 PARIS PI: Christophe LE TOURNEAU (Med.O) & Caroline HOFFMANN (Surg.O) 2/ Centre Antoine Lacassagne, 227 av de la Lanterne, 06000 NICE PI: Joel Guigay (Med.O) & Alexandre BOZEC (Surg.O) 3/ Institut Gustave Roussy, 114 Rue Edouard Vaillant, 94800 VILLEJUIF PI: Caroline Even (Med.O) & Philippe GORPHE (Surg.O) 4/ Institut de cancérologie de Lorraine, 6 Avenue de Bourgogne, 54519 VANDŒUVRE-LÈS-NANCY PI: Gilles DOLIVET (Surg.O) 5/ Institut de Cancérologie de l'Ouest, 15 Rue André Boquel, 49100 ANGERS PI: frederic.rolland@ico.unicancer.fr 6/ Institut Claudius Regaud, 1 Av. Irène Joliot-Curie, 31100 TOULOUSE PI: Jean-Pierre Delord (Med.O) & Dupret-Bories.Agnes@iuct-oncopole.fr; 7/ Centre Léon Bérard: PI : Jerôme FAYETTE (Med.O) & Pierre-Eric ROUX (Surg.O) 8/ ICM Montpellier: PI: Didier CUPISSOL (Med.O) & Renaud GARREL (Surg.O) 9/ Centre Becquerel, rue d'Amiens, 76038 Rouen cedex PI : Florian Clatot (Med. O) florian.clatot@chb.unicancer.fr & Rais Obongo (Surg. O) **Academic Hospital**	

	10/ BORDEAUX PI: Amaury DASTE (Med.O) & Erwan DE-MONES-DEL-PUJOL (Surg.O) 11/ CHU Marseille: PI : Sebastien SALAS (Med.O) (sebastien.salas@ap-hm.fr) & Nicolas FAKHRY (Surg.O) (nicolas.fakhry@ap-hm.fr)
References	1. Huang SH, Xu W, Waldron J, Siu L, Shen X, Tong L, et al. Refining American Joint Committee on Cancer/Union for International Cancer Control TNM stage and prognostic groups for human papillomavirus-related oropharyngeal carcinomas. J Clin Oncol Off J Am Soc Clin Oncol. 2015 Mar 10;33(8):836–45. 2. Ferris RL. Immunology and Immunotherapy of Head and Neck Cancer. J Clin Oncol Off J Am Soc Clin Oncol. 2015 Oct 10;33(29):3293–304. 3. Lyford-Pike S, Peng S, Young GD, Taube JM, Westra WH, Akpeng B, et al. Evidence for a role of the PD-1:PDL1 pathway in immune resistance of HPV-associated head and neck squamous cell carcinoma. Cancer Res. 2013 Mar 15;73(6):1733–41. 4. Seiwert TY, Burtness B, Mehra R, Weiss J, Berger R, Eder JP, et al. Safety and clinical activity of pembrolizumab for treatment of recurrent or metastatic squamous cell carcinoma of the head and neck (KEYNOTE-012): an open-label, multicentre, phase 1b trial. Lancet Oncol. 2016 Jul;17(7):956–65. 5. B.C. Cho, A. Daste, A. Ravaud, S. Salas, N. Isambert, E. McClay5, A. Awada, C. Borel, L.S. Ojalvo, C. Helwig, P.A. Rolfe, J.L. Gulley, N. Penel. M7824 (MSB0011359c), a bifunctional fusion protein targeting TGF-β and PDL1, in patients with advanced SCCHN: results from a phase 1 cohort. ESMO congress, Munich 2018. In. 6. Strauss J, Margaret Elena Gatti-Mays, Jason Redman, Ravi Amrit Madan, Elizabeth Lamping, Michell Manu, Andrea Burmeister, Jennifer L. Marte, Lisa M. Cordes, Laureen Ojalvo, Christoph Helwig, Jeffrey Schlom, James L. Gulley. Safety and activity of M7824, a bifunctional fusion protein targeting PDL1 and TGF-β, in patients with HPV associated cancers. In: J Clin Oncol 36, 2018 (suppl; abstr 3007). 7. Paz-Ares LG, Tae Min Kim, David Vicente Baz, Enriqueta Felip, Dae Ho Lee, Ki Hyeong Lee, Chia-Chi Lin, Massimo A. Di Nicola, Rosa Maria Alvarez Alvarez, Isabelle Dussault, Christoph Helwig, Laureen Ojalvo, James L. Gulley, Byoung Chul Cho. Results from a second-line (2L) NSCLC cohort treated with M7824 (MSB0011359C), a bifunctional fusion protein targeting TGF-β and PDL1. In: J Clin Oncol 36, 2018 (suppl; abstr 9017). 8. Ravi R, Noonan KA, Pham V, Bedi R, Zhavoronkov A, Ozerov IV, et al. Bifunctional immune checkpoint-targeted antibody-ligand traps that simultaneously disable TGFβ enhance the efficacy of cancer immunotherapy. Nat Commun. 2018 21;9(1):741. 9. Jochems C, Tritsch SR, Pellom ST, Su Z, Soon-Shiong P, Wong HC, et al.

Analyses of functions of an anti-PDL1/TGFβR2 bispecific fusion protein (M7824). Oncotarget. 2017 Sep 26;8(43):75217–31.

10. Uppaluri R, Zolkind P, Lin T, Nussenbaum B, Jackson RS, Rich J. Neoadjuvant pembrolizumab in surgically resectable, locally advanced HPV negative head and neck squamous cell carcinoma (HNSCC). In: J Clin Oncol 35, 2017 (suppl; abstr 6012).

11. Ferris RL, Gonçalves A, Baxi S, Martens A, Gauthier H, Langenberg M et al. An Open-label, Multicohort, Phase 1/2 Study in Patients With Virus-Associated Cancers (CheckMate 358): Safety and Efficacy of Neoadjuvant Nivolumab in Squamous Cell Carcinoma of the Head and Neck. In: Poster LBA46, ESMO 2017.

12. Simon R. Optimal two-stage designs for phase II clinical trials. Control Clin Trials. 1989 Mar;10(1):1–10.

13. Vugmeyster Y, Justin Wilkins, Eleanor Harrison-Moench, Wanping Geng, Andre Koenig, Liang Cao, James L. Gulley, Isabelle Dussault, Akash Khandelwal. Selection of the recommended phase 2 dose (RP2D) for M7824 (MSB0011359C), a bifunctional fusion protein targeting TGF-β and PDL1. In: J Clin Oncol 36, 2018 (suppl; abstr 2566).

14. Ferris RL, Blumenschein G, Fayette J, Guigay J, Colevas AD, Licitra L, et al. Nivolumab for Recurrent Squamous-Cell Carcinoma of the Head and Neck. N Engl J Med. 2016 Nov 10;375(19):1856–67.

15. Chow LQM, Haddad R, Gupta S, Mahipal A, Mehra R, Tahara M, et al. Antitumor Activity of Pembrolizumab in Biomarker-Unselected Patients With Recurrent and/or Metastatic Head and Neck Squamous Cell Carcinoma: Results From the Phase Ib KEYNOTE-012 Expansion Cohort. J Clin Oncol Off J Am Soc Clin Oncol. 2016 Nov 10;34(32):3838–45.

16. Chow LQM, Mehra R, Haddad RI. Biomarkers and response to pembrolizumab (pembro) in recurrent/metastatic head and neck squamous cell carcinoma (R/M HNSCC). In: J Clin Oncol 2016;34(15 Suppl):6010.

17. Zolkind P, Uppaluri R. Checkpoint immunotherapy in head and neck cancers. Cancer Metastasis Rev. 2017 Sep;36(3):475–89.

18. Haddad RI, Seiwert TY, Chow LQM. Genomic determinants of response to pembrolizumab in head and neck squamous cell carcinoma (HNSCC). In: J Clin Oncol 2017 Abstract 6009.

19. Mariathasan S, Turley SJ, Nickles D, Castiglioni A, Yuen K, Wang Y, et al. TGFβ attenuates tumour response to PDL1 blockade by contributing to exclusion of T cells. Nature. 2018 Feb 14;554(7693):544–8.

20. Bates AM, Lanzel EA, Qian F, Abbasi T, Vali S, Brogden KA. Cell genomics and immunosuppressive biomarker expression influence PDL1 immunotherapy treatment responses in HNSCC-a computational study. Oral Surg Oral Med Oral Pathol Oral Radiol. 2017 Aug;124(2):157–64.

21. Lu S-L, Reh D, Li AG, Woods J, Corless CL, Kulesz-Martin M, et al. Overexpression of Transforming Growth Factor β1 in Head and Neck

Epithelia Results in Inflammation, Angiogenesis, and Epithelial Hyperproliferation. Cancer Res. 2004 Jul 1;64(13):4405–10.

22. Pickup M, Novitskiy S, Moses HL. The roles of TGFβ in the tumour microenvironment. Nat Rev Cancer. 2013 Nov;13(11):788–99.

23. David CJ, Massagué J. Contextual determinants of TGFβ action in development, immunity and cancer. Nat Rev Mol Cell Biol. 2018 Apr 11;

24. Caja L, Dituri F, Mancarella S, Caballero-Diaz D, Moustakas A, Giannelli G, et al. TGF-β and the Tissue Microenvironment: Relevance in Fibrosis and Cancer. Int J Mol Sci. 2018 Apr 26;19(5):1294.

25. Thomas DA, Massagué J. TGF-beta directly targets cytotoxic T cell functions during tumor evasion of immune surveillance. Cancer Cell. 2005 Nov;8(5):369–80.

26. Takai S, Schlom J, Tucker J, Tsang KY, Greiner JW. Inhibition of TGF-β1 signaling promotes central memory T cell differentiation. J Immunol Baltim Md 1950. 2013 Sep 1;191(5):2299–307.

27. Liu VC, Wong LY, Jang T, Shah AH, Park I, Yang X, et al. Tumor evasion of the immune system by converting CD4+CD25- T cells into CD4+CD25+ T regulatory cells: role of tumor-derived TGF-beta. J Immunol Baltim Md 1950. 2007 Mar 1;178(5):2883–92.

28. Wang W, Erbe AK, Hank JA, Morris ZS, Sondel PM. NK Cell-Mediated Antibody-Dependent Cellular Cytotoxicity in Cancer Immunotherapy. Front Immunol. 2015;6:368.

29. David JM, Dominguez C, McCampbell KK, Gulley JL, Schlom J, Palena C. A novel bifunctional anti-PDL1/TGF-β Trap fusion protein (M7824) efficiently reverts mesenchymalization of human lung cancer cells. OncoImmunology. 2017 Oct 3;6(10):e1349589.

30. Wise-Draper TM, Matthew O. Old, Francis P. Worden, Paul E. O'Brien, Ezra E.W. Cohen, Neal Dunlap, Michelle Lynn Mierzwa, Keith Casper, Sarah Palackdharry, Benjamin Hinrichs, Alfredo Molinolo, Vinita Takiar, Jonathan Mark, Alice Tang, Muhammad Kashif Riaz, John Charles Morris, Nooshin Hashemi Sadraei, Changchun Xie, Maura L. Gillison. Phase II multi-site investigation of neoadjuvant pembrolizumab and adjuvant concurrent radiation and pembrolizumab with or without cisplatin in resected head and neck squamous cell carcinoma. In: ASCO 2018, abstract 6017.

31. Morrison C, Pabla S, Conroy JM, Nesline MK, Glenn ST, Dressman D, et al. Predicting response to checkpoint inhibitors in melanoma beyond PDL1 and mutational burden. J Immunother Cancer. 2018 May 9;6(1):32.

32. Bell R Bryan. Neoadjuvant anti-OX40 (MEDI6469) prior to surgery in head and neck squamous cell carcinoma. In: J Clin Oncol 36, 2018 (suppl; abstr 6011).

33. Iijima Y, Hirotsu Y, Amemiya K, Ooka Y, Mochizuki H, Oyama T, et al. Very early response of circulating tumour-derived DNA in plasma predicts

efficacy of nivolumab treatment in patients with non-small cell lung cancer. Eur J Cancer Oxf Engl 1990. 2017;86:349–57.

34. Nonomura Y, Otsuka A, Nakashima C, Seidel JA, Kitoh A, Dainichi T, et al. Peripheral blood Th9 cells are a possible pharmacodynamic biomarker of nivolumab treatment efficacy in metastatic melanoma patients. Oncoimmunology. 2016;5(12):e1248327.

35. Tumeh PC, Harview CL, Yearley JH, Shintaku IP, Taylor EJM, Robert L, et al. PD-1 blockade induces responses by inhibiting adaptive immune resistance. Nature. 2014 Nov 27;515(7528):568–71.

36. Chen P-L, Roh W, Reuben A, Cooper ZA, Spencer CN, Prieto PA, et al. Analysis of Immune Signatures in Longitudinal Tumor Samples Yields Insight into Biomarkers of Response and Mechanisms of Resistance to Immune Checkpoint Blockade. Cancer Discov. 2016;6(8):827–37.

5.3   Plasmacytoid pre-dendritic cells (pDC) from molecular pathways to function and disease association.

Personal implementation: I have authored the chapter on pDC function in cancer.

Solana Alculumbre[1], Salvatore Raieli[1], Caroline Hoffmann[1], Rabie Chelbi[1], François-Xavier Danlos[1], Vassili Soumelis[2]

1 Institut Curie, PSL Research University, Institut National de la Santé et de la Recherche Médicale (INSERM), U932, F-75005 Paris, France

2 Institut Curie, PSL Research University, Institut National de la Santé et de la Recherche Médicale (INSERM), U932, F-75005 Paris, France. Vassili.soumelis@curie.fr

Abstract: Plasmacytoid pre-dendritic cells (pDC) are a specialized DC population with a great potential to produce large amounts of type I interferon (IFN). pDC are involved in the initiation of antiviral immune responses through their interaction with innate and adaptive immune cell populations. In a context-dependent manner, pDC activation can induce their differentiation into mature DC able to induce both T cell activation or tolerance. In this review, we described pDC functions during immune responses and their implication in the clearance or pathogenicity of human diseases during infection, autoimmunity, allergy and cancer. We discuss recent advances in the field of pDC biology and their implication for future studies.

pDC: a history of mysteries

Plasmacytoid pre-dendritic cells (pDC) were first described in 1958 by pathologists Lennert K, and Remmele W, as a plasmacytoid cell (i.e harboring morphological/cytological features similar to plasma cells) located in the T cell areas of secondary lymphoid tissue[1]. The long road from that seminal discovery to our current understanding of pDC biology was paved with mysteries. Many of them have been solved in the past 20 years[2]: why would plasma-like cells be present in the T cell area of lymph nodes? Why would these plasmacytoid cells express the CD4 T cell-associated marker and not B cell markers? Why would pDC express high levels of MHC class II and differentiate into bona fide dendritic cells (DC)? What is their antigen presenting capacity? Are pDC just DC precursors or do they have an important function as plasmacytoid cells? Which proteins are being produced in large amounts by pDC, as suggested by their plasmacytoid morphology and very well developed rough endoplasmic reticulum? Some of them still remain, at least partially, unsolved: What is the respective contribution of innate versus adaptive functions of pDC in physiology and pathology? Which are the factors evoking immune activating versus immunoregulatory functions of pDC? Are PDC protective or pathogenic in some diseases, and is there a therapeutic potential in targeting pDC?

Some important landmarks in solving those mysteries were i) the ability to purify human pDC from secondary lymphoid tissue and peripheral blood, which allowed for molecular and functional studies[3–5], ii) the serendipitous discovery of type I interferon (IFN) production as the main function of primary pDC[6,7], iii) the discovery of mouse pDC[8], which allowed in vivo analysis of pDC function, iv) the association of pDC with a number of infectious and inflammatory diseases, which sometimes provided a proof of concept for their pathogenicity

[9], but most of the time raised numerous additional questions regarding their role in the context of complex and dynamic inflammatory environments.

In this review, we will describe established features that are considered today as characteristic of pDC biology, and also discuss more recent and sometimes controversial work on pDC function and contribution to various types of disease. The pDC field has been very confusing at times, as illustrated by the number of names that pDC have been given (T-associated plasma cells, plasmacytoid T cells, plasmacytoid monocytes, pre-DC2, IPC: Interferon-Producing Cells, plasmacytoid pre-dendritic cells, plasmacytoid dendritic cells). This, together with the morphological, phenotypical, and functional plasticity of pDC, extended the confusion to even their very nature, in particular their link to DC [10]. This prompted us to insist on definitions, and clarity when referring to pDC in a resting/primary (plasmacytoid) versus activated state.

As the field has significantly moved towards the study of pDC in human diseases, raising a number of important questions, we will devote approximately half of this review to pathological settings, such as infection, autoimmunity, allergy, and cancer. We will also discuss the value of systems biology approaches for the study of human pDC, which will complement other reviews in this issue.

Focusing a review on human pDC is an additional reason to discuss more in depth the link with human pathology, which may differ in many aspects from mouse disease models. Also, there are a number of phenotypic and functional differences between human and mouse pDC, which may significantly impact their contribution to immune regulation in health and disease: i) mouse pDC express the B-cell marker B220, and the DC marker CD11c, both lacking from human pDC; ii) mouse pDC produce IL-12 in response to microbial stimulation, which is not the case for human pDC ([11] and see below). In most of the chapters below, we will essentially discuss studies specifically performed in the human system. We refer the readers to other reviews on pDC biology for more thorough information on mouse pDC (References [12,13]).

What are the defining features of human pDC

Since their discovery, pDC have been defined by a combination of characteristics, none of them being sufficient individually to discriminate them from other immune cells. PDC-defining features should clearly differentiate those that are absolutely required, and are linked to pDC "identity", and those that represent characteristics of variable specificity, depending on activation state, and/or anatomical location. The first defining feature for pDC is there plasmacytoid morphology that is very easily recognized by any cyto-pathologist: round shape, excentered nucleus, strongly basophilic peripheral cytoplasm, and a pale Golgi zone named the acroplasm[10]. This very peculiar morphological feature was the basis for the initial description of pDC in secondary lymphoid tissue[1], and should be seen as a required defining criterion, as illustrated by its presence in naming pDC ("plasmacytoid"). However, it is far from being 100% specific (and hence sufficient), since normal and malignant B cells can adopt a plasma cell like morphology[14], and so are some other rare urothelial malignancies[15]. The second defining feature is the ability of pDC to produce very large amounts of type I IFN[16]. This should really be seen as a "potential", since the actual triggering of IFN production is highly dependent on the nature of the activating signals

received by pDC ([16] and see below). However, immune cells not having the potential to produce type I IFN in large amounts under the appropriate stimulatory conditions are not pDC. The third type of defining criteria are surface markers, as well as some other functional molecules that characterize pDC in certain anatomical locations. MHC class II molecules are always constitutively expressed by pDC, and are upregulated following activation[16], this being shared by all antigen-presenting cells (APC). Granzyme B was shown to be one of the most pDC-specific markers in normal peripheral blood[17], although this marker is not specific in other contexts, in particular during inflammation, when other cells may express it. BDCA2 was identified as a pDC-specific marker in healthy donors peripheral blood[4], but was very recently shown to be also expressed by another rare DC subset, as revealed by single cell RNAseq [17,18]. BDCA4 (Neuropilin-1) is expressed by resting blood pDC[4], but can also be expressed by activated T cells and dendritic cells [19,20]. Last, there are a number of "negative" pDC markers that help differentiate them from other related cells, for example CD11c (negative on pDC, and positive on other human DC and monocyte/macrophages), and the more recently described AXL (negative on pDC and positive on AS-DC/DC5) [17]. In summary, the plasmacytoid morphology, and potential to produce large amounts of type I IFN in response to viral stimulation, are the two most robust and conserved defining features of human pDC. These should be assessed before concluding on the nature of any cell type suspected to correspond to pDC. Surface markers have been very useful to purify and quantify pDC in different settings, but should be used very cautiously because of their promiscuity (the same marker may be expressed by different cell types), and their variable expression levels during inflammation. We believe that the combined evaluation of several parameters is required to undoubtedly define a cell as pDC, and the selection of pDC-defining surface markers should be done very carefully, and integrate the latest single cell level studies in the field[17,18].

A specialized sensing machinery links innate stimuli to function

To understand pDC functions during immune responses, it is essential to characterize their sensing abilities. We will distinguish two main categories of receptors: i) pathogen sensors, located in intracellular compartments and; ii) endogenous (host-derived) factor receptors located on the cell surface.

Intracellular receptors for pathogen sensing

Among the pathogen-sensing receptors, high baseline expression of the endosomal Toll-Like Receptor (TLR)7 and 9 is one of the main features of human pDC [21,22]. Through TLR7, pDC recognize single-stranded viral RNA, synthetic imidazoquinolines (imiquimod, resiquimod, i.e R848) [23,24] and endogenous (self) RNA [25]; TLR9 allows the sensing of single stranded (ss)DNA viruses rich in CpG motives, such as herpes simplex virus 1 (HSV-1), HSV-2, as well as synthetic oligodeoxinucleotides (ODN) rich in unmethylated CpG motives [26]. The ability to sense ssDNA viruses through TLR9 distinguishes human pDC from other DC subsets [22]. In contrast, human pDC lack expression of TLR3, a feature of blood BDCA-3 DC, impeding recognition of double stranded RNA viruses through the endosomal pathway. Triggering of TLR7 and 9 from early endosomes activates the MyD88-IRF7 pathway, leading to the production of large amounts of type I IFN [26]. Constitutive high expression of the transcription factor IRF7 [27] is one of the mechanisms that endow pDC with their strong type I IFN production potential [16,17]. Alternatively, TLR-ligand recognition from late

endosomes, induces the activation of the MyD88-NFkB pathway, stimulating the production of pro-inflammatory cytokines and chemokines, as well as upregulation of costimulatory immune checkpoints [26]. In addition to the TLR-dependent sensing of nucleic acids, pDC can sense cytosolic DNA through the helicases DHX36 and DHX9 [28], members of the RIG-I-like receptors superfamily. This response is MyD88-dependent and can trigger both IFN and pro-inflammatory cytokines production [28]. It has been suggested as well that upon activation through TLR ligands, pDC can upregulate the expression of the cytosolic dsRNA sensor RIG-I and respond to 5'-triphosphate dsRNA [29]. Another study showed that pDC can sense cytoplasmic RNA from replicating viruses in yellow fever live vaccine YF-17D infection through RIG-I leading to IRF3 activation and IFN production [30]. In addition, it has been proposed for mouse [31] and human pDC [32] the presence of a functional cGAS-STING pathway sensing cytosolic DNA and inducing type I IFN production. Both TLRs and cytosolic sensors have the potential to initiate a strong type I IFN response by pDCs, and require prior internalization of the microbial nucleic acids by mechanisms such as endocytosis [12], autophagy [33], or LC3-associated phagocytosis (LAP) [34]. The use of intra-cellular microbial sensing receptors in human pDC has several implications: i) it restrains the IFN production to specific intracellular pathogens, mostly viruses, which are themselves a target of IFN anti-viral effects; ii) it creates a specialization of pDC among other innate immune cells; iii) it prevents pDC activation by extra-cellular nucleic acids, which can be produced physiologically in certain forms of inflammatory cell death, especially from neutrophils [35]. Access of autologous nucleic acids to endosomal pDC compartments contributes to breaking tolerance to self-antigens, and development of auto-immunity [26] (*See below*)

Environmental sensing by surface receptors
PDC surface receptors can induce pDC activation and differentiation into mature DC capable of T cell priming, or can modulate pDC responses to TLR ligands. PDC express the IL-3R, whose specific α-chain CD123 has been largely used as a very sensitive (albeit non-specific) pDC marker [16]. PDC activation through IL-3 induces the upregulation of costimulatory checkpoint molecules such as CD80 and CD86 and their differentiation into mature DC capable of stimulating CD4+ T cell proliferation [3]. PDC also express the GM-CSFR, which shares the common β chain with the IL-3R, and respond to GM-CSF activation in a similar manner [36]. Both IL-3 and GM-CSF promote pDC survival and activation, without inducing IFN secretion. At a different level, autocrine/paracrine TNF-α can increase pDC maturation into DC when it is present in combination with a pDC survival factor [37]. PDC also express other cytokine receptors that can modulate their responses but do not function as a primary activating stimulus. PDC-derived IFN-α/β act through the IFN receptor (IFNAR) in an autocrine manner, establishing a positive feedback for IFN production [38]. On the other hand, IL-10 and TGF-β have been shown to diminish pDC-IFN secretion in response to TLR ligands [39,40]. Other cytokines that modulate pDC functions are IL-2, increasing TNF-α secretion on CD40L-activated pDC [41], and IL-18 promoting pDC chemotaxis [42].
Since IFNs are pleiotropic cytokines that can potentially induce exacerbated inflammation, their production should be tightly regulated. PDC express several inhibitory surface receptors that regulate type I IFN production by interfering with TLR7 and 9 signaling. Human pDC express the ITAM-associated receptors ILT7 [43,44], BDCA-2 [45], FcεRIα[46] and, upon activation with IL-3, NKp44[47]. The ITAM receptors need association with an adapter molecule for signal transduction, and human pDC express the adapters DAP12 and

the γ chain of Fc receptor ε (FcεRΙγ). Another group of inhibitory receptors contain the intracellular ITIM domain, and human pDC express CD300 [48] and DCIR [49].

Although pDC activation in response to pathogens depends on intracellular sensing, its function can be regulated by numerous surface receptors. This allows controlling pDC responses by secreted host-derived factors, in order to support an orchestrated and properly regulated immune response.

PDC modulate immune responses through type I IFN

PDC have been named "Professional type I IFN producing cells" [16]. Within 6 hours of viral activation, 60% of human pDC transcriptome corresponds to type I IFN genes. They can produce up to 1000 times more IFN than any other blood cell [6,7]. Along with their robust production of type I IFNs, including IFN-α, IFN-β and IFN-ϖ, pDC can also express type III IFNS IL-28a (IFN-λ2), IL-28b (IFN-λ3) and IL-29 (IFN-λ1) in response to TLR7 or 9 ligands [50].

During viral infections, pDC-derived IFNs can directly act on infected cells, as well as surrounding neighbors through the ubiquitously expressed IFNAR. Downstream signaling from IFNAR induce the expression of IFN-stimulated genes (ISGs) participating in the control of viral replication and spread [51]. Furthermore, pDC-derived type I IFN has a critical role in modulating the innate and adaptive immune responses by inducing activation and maturation of several immune cell populations. IFN type I stimulates myeloid DC (mDC) maturation, as well as monocyte-derived DC differentiation promoting a Th1 type of immune response [52,53]. IFN enhances NK cell maturation and cytolytic activity, as well as IFN-γ secretion [54] and, together with pDC-secreted IL-6, promotes B cell differentiation into plasma cells [55]. In addition, pDC-derived type I IFN stimulates mDC and pDC antigen cross-presentation to CD8+T cells [56,57], and promotes CD4+ T cell polarization into Th1 cells [37,58] (Figure 1)

PDC differentiation into mature DC

Before the association between pDCs and "the natural type I IFN-producing cells" [16], pDC were shown to differentiate into mature DC in response to IL-3, or IL-3+CD40L [3]. Since then, this pDC functionality has been largely studied, and led to the understanding that pDC role as APC is absolutely dependent on the type of stimulation, and surrounding microenvironment. Steady state pDC express intermediate levels of MHC II molecules that are highly upregulated upon activation, together with costimulatory molecules, and allow antigen presentation to CD4+T cells [58]. In the presence of IL-3, pDC-derived DC upregulate the costimulatory molecules CD40, CD80, CD86, CD83, and OX40L, among others, and preferentially drive regulatory Th2 responses from naïve CD4+ T cells [59]. GM-CSF-activated pDC induced a similar pattern of T cell-derived cytokines although producing more IFN-γ and less IL-10 [36]. In contrast, viral or CpG ODN-mediated pDC activation promotes a strong naïve CD4+T cell polarization towards Th1 cells [37,58,59]. This Th1 priming was shown to be promoted by type I IFN, in an IL-12-independent manner [16]. Furthermore, TLR-activated pDC can induce the generation of T regulatory (Treg) cells, a process favored by the expression of ICOSL [60,61]. This tolerogenic response has emerged as a way to prevent excessive inflammation that could be detrimental to the host during infection, but may also be involved during thymus Treg development [62] (Figure 1).

PDC express MHC I and MHC II and are capable of presenting both endogenous and virus-derived antigens to CD4+ and CD8+ T cells [63]. However, their low antigen internalization ability mediated by micropinocytosis and phagocytosis, together with their lower MHC II expression, make them less efficient than mDC with regard to presentation of exogenous antigens [63]. Several studies on human pDC indicated that they are effective in cross-presenting antigens to CD8+ T cells [64,65], to a similar extent as BDCA1+ and BDCA3+ DC subsets [66].

Hence, pDC harbor key functions in both innate and adaptive immunity, controlled by complex, and highly context- and stimulus-dependent mechanisms. This has led to some controversies on whether adaptive pDC functions are being evoked in vivo in different physiopathological contexts, as opposed to IFN production being the main function of pDC [67,68]. We believe this is mainly due to the various contexts, stimuli, and disease models studied, rather than a cell-intrinsic exclusive involvement of pDC in innate versus adaptive immunity.

The multiple roles of pDC in infection

PDC are involved in different types of infections (such as virus, bacteria and fungi), their response being tightly linked to the underlying sensing mechanisms and downstream functional impact (*See above*).

PDC function against viruses is extremely important in the acute phase of the infection, to inhibit viral replication and prevent viral spreading, as for example in herpes simplex virus infection [69]. As the infection progresses, other host cell types, such as DC, monocytes, and macrophages, take part in IFN production [70]. Remarkably, individuals carrying mutations in the IRF7 gene, resulting in impaired pDC responses, are more susceptible to influenza virus infection [71]. However, type I IFN production by pDC may not be always beneficial during influenza infection, as shown by a mouse model wherein pDC over-activation induced massive and deleterious inflammation [72]. Whether this may contribute to pathology in severe forms of human influenza virus infections is not known.

In chronic viral infections, the role of pDC is more debated. During HIV infection, pDC may contribute to disease progression by recruiting T cells through chemokines, such as CCL3 and CCL4 [73], and producing Type I IFN [74]. Notably, *in vitro* HIV-stimulated pDCs induce T cell apoptosis trough TRAIL expression, and promote Treg development through the IDO pathway [75]. However, recent studies also highlight the beneficial role of pDC-derived IFN in the early stages of HIV infection in the simian model, and their recruitment in the gut of elite controllers during HIV infection, suggesting a contribution to protective anti-viral immunity [76,77]. PDC were also studied in the context of other chronic viral infections. A common feature is the absence or low IFN levels induced by hepatitis B (HBV) [78,79] and C (HCV) viruses [80,81], as well as human papilloma virus[82]. The amount of type I IFN induced by a given virus may be critical to promote viral control versus chronic infection (Figure 2A), in addition to virus-related features.

The role of pDC has been less characterized in bacterial infection. PDC are recruited to the lymph node T-cell zone in Mycobacterium tuberculosis patients where they are producing granzyme B [83]. The pathological role of Type I IFN observed in mycobacterial infections [84] point to a possible detrimental role of pDCs. However, the link between pDC, type I IFN,

and mycobacterial infection was not specifically addressed. Various reports indicate that pDC are present in human tonsils where they are in contact with bacteria [85]. Moreover, pDCs are able to sense and respond to Gram-positive and negative bacteria, with an upregulation of co-stimulatory molecules, and IFN production [85]. They can interact directly with B cells to induce IL-10 production in response to Staphylococus aureus. [86]. Hence, pDC influence both innate and adaptive immunity in bacterial infection, but their impact on the outcome of the infection remains unclear.

Intriguingly, latest studies highlight a role for pDCs in fungal infections. In the presence of *Aspergillus fumigatus hyphae*, pDCs play a protective role indirectly by producing IFN and TNF-α[87], and directly by killing fungi through the secretion of calprotectin and lactoferrin, capable of chelating divalent cations necessary for fungal growth[88]. Furthermore, in the presence of *A. fumigatus,* pDC secreted "pDC extracellular traps" (pETs) formed by DNA and citrullinated histone H3, with a structure similar to neutrophil extracellular traps (NETs)[89]. These traps are generally assembled with antimicrobial peptides leading to the killing of microbes that cannot be phagocytosed.

In parasitic infection, the role of pDCs was mostly studied in malaria, where pDCs were not activated in the context of *Plasmodium falciparum* blood-stage[90]. However, TLR7-dependent induction of IFN showed a protective role in early infection stages in the mouse[91]. More studies are needed to clarify the role of pDC and IFN in malaria and other parasitic infections.

In conclusion, the complexity of pDC functions in innate and adaptive immunity is reflected in their intricated beneficial or detrimental roles in infection. Factors such as pDC activation state, microbial and tissue context, and timing (early/acute versus late/chronic stages) all influence the ultimate impact on the outcome of the infection.

PDC are major players in autoimmune and allergic diseases.

Through their ability to secrete high amounts of type I IFN, pDC have been identified early on as a potential player in SLE, and other inflammatory and auto-immune diseases[92,93]. Important studies shed light on the signals that may induce pDC activation in such non-microbial/sterile inflammation. In SLE, circulating immune complexes (IC), formed by auto-antibodies (Ab) and autologous DNA/RNA, are internalized into pDC endosomes through FcγRII (CD32) and sensed by TLR7 and TLR9[94]. In psoriasis, antimicrobial peptides such as LL-37 trigger IFN production after binding extracellular DNA to form molecular complexes that are shuttled to, and retained within, early endocytic compartments in pDCs to trigger TLR-9[95]. Through these mechanisms, pDC may break tolerance to self-antigens in SLE and psoriasis (Figure 2B).

PDC can be actively recruited to inflamed tissues[96,97]. In early psoriasis plaque, fibroblasts, mast cells, and endothelial cells express chemerin and promote pDC recruitment through chem23R[98]. PDC interact with other immune cells to promote and exacerbate inflammation. Circulating neutrophils from SLE patients may release NETs and induce pDC activation[35] (Figure 2B). NK cells may promote pDC activation via MIP-1β secretion and LFA-mediated cell-cell contact[99]. In SLE, pDC-derived IFN-α and CD40 expression increase

plasmablast differentiation, auto-antibody production, and fail to induce regulatory B cells[100].

PDC pathogenicity may also be influenced by genetic predisposition to deregulation in the type I IFN pathway. Susceptibility loci to SLE and autoimmune diseases have been identified by genome-wide association studies[101]. Some of them could promote pDC activation and type I IFN production by alteration of immune complex clearance (FCGR2A, FCGR3A, ITGAM, CRP, C4A, C4B, C2, C1Q) and increased TLR7-9/IFN pathway (IRAK1, IRF5, IRF7, SPP1, STAT4, TREX1, ATG5). Studies have shown that some of these polymorphisms, in particular in the IRF-5, IRF-7, and ILT3 genes, may have a direct functional impact on type I IFN secretion by pDC[102–104].

Besides SLE, an "interferon signature" is associated to other active autoimmune diseases: Sjögren's syndrome, dermatomyositis and systemic sclerosis[105]. PDC have been involved in dermatomyositis lesional skin[106]. Circulating IC with auto-Ab to topoisomerase I, Jo-1, and Ro 52/60 may act as endogenous type I IFN inducers production in pDC[107,108]. In pDC from patients with systemic sclerosis, an upregulation of miR-618 influence pDC development and increase the expression of mRNA encoding IFN-responsive gene[109]. Future studies may reveal additional pDC-activating mechanisms underlying a dysregulation of innate immunity. Interestingly, pDC adaptive functions have been less studied in the context of autoimmunity, and it remains unclear whether they may also contribute to disease pathogenesis through excessive T cell activation.

Because of their clear disease association and pathogenic role, pDC are an important therapeutic target in autoimmunity. Hydroxychloroquine, an antimalarial agent, which inhibits type I IFN production by pDC, is the cornerstone of SLE management [110,111]. Development of drugs targeting the IFN pathway, such as the monoclonal antibody anifrolumab (anti type I IFN receptor Ab), or Janus kinase (JAK) and signal transducer and activator of transcription (STAT) pathway inhibitors, are promising compounds in SLE and autoimmune diseases associated with IFN signature and pDC dyregulation[112,113].

Besides auto-immunity, pDC are implicated in allergic diseases such as asthma, atopic dermatitis and allergic rhinitis, all being associated with chronic and dysregulated inflammation. They are characterized by an increased Th2 polarization, allergen-induced production of IgE by plasma cells and hypersensitivity mediated by basophils and FcεRI/II. PDC are being recruited in nasal mucosa and sputum from allergic patients, and involved in allergic inflammation[114,115]. In children with atopy, relative deficiency of circulating pDC appears to be a risk factor for future development of asthma[116] (Figure 2B). In asthma, pDC express higher CD40, CD62L, CD64 and FcεRIα, but TLR7-mediated IFN-α secretion is significantly reduced[117,118]. Interestingly, in healthy individuals, pDC-derived IFN-α selectively constrain Th2 cytokine synthesis following rhinovirus exposure[119]. This negative regulatory mechanism between IFN-α and Th2 polarization may be defective in allergy, explaining the possibility of a viral infection triggering or aggravating asthma exacerbations[120] (Figure 2B). Overall, evidence from human studies mostly points at a pathogenic role of pDC in allergy through Th2 priming. Mouse models in that context have brought controversial results, supporting either a protective effect through Treg

induction[121], or a pro-allergic effect through Th2 (V. Andreakos et al, unpublished). It will be important to specifically study pDC in a diversity of clinico-pathological forms of allergy, based on age, anatomical site, co-infections, chronicity, which may dictate opposite pDC functions through a different inflammatory micro-environment. This may have direct implications on designing relevant pDC-targeting strategies in allergy.

PDC function in cancer: from physiopathology to immunotherapy

The clinical benefit of type I IFN therapy in hematologic malignancies and melanoma, and the observation of pDC infiltrating multiple tumor types [122–126], have raised the question of the role of pDC in cancer.

Considering the innate-sensing receptors expressed by pDC, an important question was their possible ligands in the context of the tumor microenvironment (TME). Necrotic tumor cells release damage associated molecular patterns (DAMPs), such as high-mobility group box-1 protein (HMGB1) and mitochondrial DNA, which stimulate TLR9[127], and may activate pDC. The presence of GM-CSF in the TME is well documented in multiple cancers, supporting an activation of tumor-infiltratin (Ti) pDC through constitutively expressed GM-CSF receptor[128]. However, the expression of maturation markers such as CD40 and CD80 on TipDC obtained from human tumor biopsies seems to vary among tumor types, either absent in lung cancer [129] or upregulated as compared to blood pDC in melanoma [126], breast[130], or ovarian cancer[124], making it unclear whether endogenous tumor-derived signals are effectively activating pDC.

Interestingly, the same studies all showed that TipDC have a decreased capacity to produce IFN under TLR stimulation in vitro as compared to blood or healthy tonsil pDC, regardless of the expression of maturation markers before stimulation. This impairment in IFN production suggested a tolerogenic phenotype of TipDC, further supported by an ability to expand Treg cells and induce a Th2 differentiation, through the ICOSL and OX40L pathways, respectively [126,128]. In melanoma, the expression of Indoleamine 2,3-dioxygenase (IDO), another well-known immunosuppressive molecule, has been predominantly detected in pDC among the different DC subsets[131]. The importance of this mechanism was confirmed by the enhancement of Ag presentation and Ag-specific cytotoxic T lymphocyte induction, following IDO inhibition by Toho-1 in a human leukemic pDC line[132].

Studies have shown that IFN production under TLR stimulation of pDC was significantly decreased by the addition of head and neck[122] or breast tumor-derived supernatants[130]. Since then, an ever-growing list of molecules, such as TGF-β, TNF-α[133], IL-10[134], Prostanglandin E2 (PGE2)[135] or IL-3[125], were shown to contribute to this tolerogenic phenotype of TipDC. The role of TGF-β and IL-10 suggests a potential paracrine loop between pDC and regulatory T cells (Figure 2B). Another mechanism that could reduce TipDC activation is the tumor-induced down-regulation of TLR9[122] . The induction of a Th2 differentiation of tumor infiltrating T cells by TipDC may be induced by GM-CSF, as shown in breast cancer[128] or TARC/CCL17, MDC/CCL22 and MMP-2, as suggested in melanoma[126].

Beside their tolerogenic effect, in vitro cytotoxicity assays with blood pDC acting on tumor cell lines suggested that TipDC may also have a direct cytotoxic effect on tumor cells in a TRAIL-dependent manner, but also via Granzyme B secretion, and Fas-Fas ligand interaction[136]. However, in these studies, blood pDC were artificially stimulated with TLR ligands and outnumber by 20 to 100 fold their targets, two conditions that do not reproduce the TME context and limit the extrapolation of these data. Hence, although pDC expression of Granzyme B and TRAIL was shown by many studies[137], and confirmed on "pure pDC", defined as HLA-DR+CD123+AXL-CD2- DC[17], the role of these molecules in the tumor context remains controversial.

Despite pDC functional plasticity, and their expression of death molecules, most studies suggest that pDC may function predominantly as promoting tumor development through Treg induction [138]. These mechanistic observations are in line with the clinical correlation of high levels of TipDC with bad prognosis in several cancer types, such as breast cancer[123], ovarian cancer[124], multiple myeloma[125], and melanoma[126]. Thus, TipDC may be considered as a potential target for anti-cancer therapy. A first approach would be to deplete pDC. SL-401 targets IL-3 receptor (IL-3R) and efficiently depletes pDC in a mouse model of multiple myeloma[125].

A second approach would be to reprogram pDC phenotype from tolerogenic to anti-tumoral pDC through TipDC stimulation. It is one of the modes of action of the TLR7 agonist Imiquimod, which is routinely used to treat basal-cell carcinoma and HPV-associated cutaneous tumors, and under investigation in melanoma[139] (Figure 2B). However, apoptosis induction of tumor cells in a Bcl-2[140] or p53-dependent manner[141], has been described.
A last approach is to exploit the T cell priming capacity of pDC. A vaccine, consisting of intranodal injections of pDCs previously activated and loaded with tumor antigens[142] has been tested in melanoma patients and was able to induce specific CD4 and CD8 responses. However, clinical response rates were limited to a small proportion of patients. To overcome this limited efficacy, the most recent approach is to combine DC-based vaccines, which include both pDC and myeloid DC, with targeted therapies[143], or to directly deliver intravenously RNA lipoplexes, which are internalized by pDC but also CD11c+ conventional DC and macrophages[144] (Figure 2B).
In summary, pDC are actively explored as targets for cancer immunotherapy, despite a complex function, and remaining controversies on their contribution to tumor development versus control. As for allergy, we propose that specific studies of pDC in various tumor types and stages, may uncover clinical settings and patient groups which would predominantly benefit from pDC targeting.

Systems biology approaches redefine human pDC biology
Systems biology often involves the generation and the analysis of high dimensional data, offering a unique opportunity to explore biological processes at high resolution, and to get insight into the organization/structure of the data, which would reflect important biological features[145]. This interdisciplinary field provided crucial insights into the complexity and identity of human pDC.

High dimensional methods including single-cell RNA-seq and quantitative mass-spectrometry have contributed to the unbiased characterization of human blood pDC. Recent work using single-cell mRNA sequencing and cytometry by time of flight (CyTOF) described a novel population of pre-DC, which shares markers previously thought to be pDC-specific, such as BDCA-2[18]. Another single-cell RNAseq study delineated human blood DC heterogeneity, and identified a new DC subset named AS DC/DC5 (AXL+ BDCA2+) sharing a transcriptional signature with pDC (AXL-, BDCA2+) including for example IL3RA, IGJ, NRP1, MZB1, but more potently activating T cells[17]. These recently deciphered DC populations invite us to reconsider earlier findings such as pDC expression of costimulatory molecules[64,146], pDC ability to exhibit Ag presentation, and their potency in mediating Th1 immunity via IL-12 and IFN production[58,146]. It was already shown that some of these molecular and functional features may be due to contamination of pDC with myeloid DC populations, for example for IL-12 production [11]. The recent single cell RNAseq studies bring additional and objective knowledge in order to precisely assign functional features to well defined DC subsets.

Systems approaches can also be useful to unravel the complexity of multiple signal integration by immune cells. We have developed a high-resolution analysis framework to analyze the integration of endogenous and microbial signals by human pDC based on large-scale transcriptomics data[147]. This established the concept of multimodality in signal integration, meaning that the two same signals can be integrated according to multiple modes for different cellular outputs. Our study also revealed that a microbial stimulus (influenza virus) may inhibit the response to an endogenous factor (IL-3).

Because of the complex physiopathology of autoimmune diseases, large scale data analysis approaches have been broadly carried out[148]. The analysis of pDCs from lupus mice with RNAseq technology led to conclude that pDC present an altered transcriptional signature in early stages of the disease[149,150]. Using RNAseq technology, gene loci were associated with IFN production in human pDC in systemic lupus erythematosus patients[102]. Gene expression profile of human primary pDC stimulated with CpGB showed overexpression of MYC via TLR9 agonist, which is a novel target that modulates human pDC[151]. Large-scale proteomics analysis was used to elucidate the role of pDC in priming the immune response upon viral challenge. The shift of pDC response upon TLR stimulation from type I IFN to IL-1b may avoid disproportionate inflammation response[152].

Numerous perspectives are offered by the broad range of possible applications of systems biology approaches. Currently, mostly transcriptomics based approaches have been exploited. Epigenetic modifications are critical to a diversity of autoimmune diseases[153], and could be addressed in future studies. Innovative schemes and experimental designs will be needed to integrate the complexity of PDC function, molecular regulation, heterogeneity, and adaptation to various inflammatory microenvironments.

Conclusions and perspectives
Although major progress was made in our understanding of pDC biology, many aspects remain unclear, and the complexity of pDC functions constitute a future challenge. A clear pDC definition needs to be used, putting at the forefront cytological and functional features,

surface markers being essential tools to identify and purify pDC but difficult to use as defining criteria because of their variable sensitivity, specificity and stability in different steady state and inflammatory microenvironments. In that area, important new knowledge was recently generated by single cell RNAseq studies, which now needs to be integrated in pDC purification and monitoring protocols.

A number of molecular mechanisms have been identified and characterized regulating pDC function: how they work together is now the challenge. How multiple signals are being integrated? Which of activating versus inhibitory receptors are dominant when co-triggered? The implication of pDC in several human diseases is well established, but the detailed understanding of their contribution to disease pathogenesis and physiopathology is lacking in most cases. The complexity here rises from the several ways pDC may adapt to various and dynamic inflammatory microenvironments. This is complicated by additional genetic factors.

Addressing all these levels of complexity is expected to derive exciting new biology, and to help deciphering inflammatory diseases, because of the numerous interactions between pDC and other molecular and cellular inflammatory players. Ultimately, this will be the only way to rationale pDC-targeting strategies, which may rarely be of general benefit in a given disease entity, but should most of the time benefit only a subset of patients with specific disease characteristics.

Figure legends

Figure 1. PDC activation and modulation of the immune response

PDC activation through endosomal TLR7/9 ssRNA or dsDNA viruses, or CpG ODNs leads to high type I IFN secretion and pDC maturation into mature DC. PDC-derived IFN-I induce an antiviral response on immune and non-immune cells through the upregulation of interferon stimulated genes (ISGs) that prevent viral replication and spread. IFN-I induces NK cells cytotoxic activity and IFN-γ secretion; APC functions by stimulating mDC maturation and crosspresentation and, monocyte differentiation into DC and; favors B cell differentiation into plasma cells. pDC-derived DC and IFN-I can prime naïve CD4+T cells differentiation into regulatory Th1 cells and crosspresent Ag to CD8+Tcells. Alternatively, TLR-independent pDC activation through IL-3 or GM-CSF, induces their differentiation into mature DC capable of priming Th2 responses without IFN secretion.

Figure 2. PDC involvement in human diseases

A. During acute viral infections, pDC-derived type I IFN plays a critical role in the viral clearance by preventing replication and spread. IFN-I induces innate and adaptive immune cells activation. Viral-induced pDC-derived DC prime naïve CD4+T cells to differentiate into Th1 and T regs. During chronic viral infections, pDC may be reduced in the circulation or producing low IFN-I, failing in controlling the viral spread. Bacteria can trigger pDC activation. In Mycobacterial infections, pDC-derived IFN-I has a negative impact on the disease severity. Both Gram+ and Gram- bacteria can induce pDC activation, IFN-I secretion and upregulation of costimulatory immunecheckpoints. Fungal infections, as A. fumigatus, can stimulate IFN-I and TNF-α secretion as well molecules acting in directly killing the fungi as calprotectin, lactoferrin and pDC extracellular traps (pETs). It has been proposed that pDC may produce IFN-I upon triggering by parasites as malaria. B. In autoimmune diseases, as systemic lupus erythematosus (SLE), the presence of autoantibodies and neutrophils

extracellular traps (NETs) complexes with self-nucleic acids induce pDC activation and type I IFN secretion that contributes to increase inflammation and disease pathology. Treatments include hydroxychloroquine, a drug inhibiting endosomal acidification and TLR activation; and anti IFNAR antibodies. In psoriasis, pDCs are recruited to the skin plaques by chemerins, where cationic antimicrobial peptides such as LL37 can complex with self-DNA and activate pDC though TLR9 to induce IFN-I secretion. In cancer, the presence of Treg cytokines as IL-10 and TGF-β can stimulate a tolerogenic pDC state that contributes to the generation of Tregs through the expression of ICOSL and IDO, constituting a pDC-Treg feedback. Treatments with imiquimod aim to induce pDC activation through TLR7 to rescue their IFN-producing capacity. The use of RNA-lipoplexes (RNA-LPX) can trigger pDC IFN secretion and DC maturation and antigen presentation. In allergy, pDC role is debated, some studies showing a pDC contribution to the allergic inflammation by the induction of Th2 cells and, others suggesting a beneficial effect by the induction of Tregs contributing to the tolerance.

References:

[1]   K. LENNERT, W. REMMELE, [Karyometric research on lymph node cells in man. I. Germinoblasts, lymphoblasts & lymphocytes]., Acta Haematol. 19 (1958) 99–113.

[2]   Y.-J. Liu, Uncover the mystery of plasmacytoid dendritic cell precursors or type 1 interferon producing cells by serendipity, Hum. Immunol. 63 (2002) 1067–1071. doi:10.1016/S0198-8859(02)00744-9.

[3]   G. Grouard, M.C. Rissoan, L. Filgueira, I. Durand, J. Banchereau, Y.J. Liu, The enigmatic plasmacytoid T cells develop into dendritic cells with interleukin (IL)-3 and CD40-ligand., J. Exp. Med. 185 (1997) 1101–11.

[4]   a. Dzionek, a. Fuchs, P. Schmidt, S. Cremer, M. Zysk, S. Miltenyi, D.W. Buck, J. Schmitz, BDCA-2, BDCA-3, and BDCA-4: Three Markers for Distinct Subsets of Dendritic Cells in Human Peripheral Blood, J. Immunol. 165 (2000) 6037–6046. doi:10.4049/jimmunol.165.11.6037.

[5]   S. Alculumbre, L. Pattarini, Purification of Human Dendritic Cell Subsets from Peripheral Blood, in: E. Segura, N. Onai (Eds.), Dendritic Cell Protoc., Springer New York, New York, NY, 2016: pp. 153–167. doi:10.1007/978-1-4939-3606-9_11.

[6]   F.P. Siegal, The Nature of the Principal Type 1 Interferon-Producing Cells in Human Blood, Science (80-.). 284 (1999) 1835–1837. doi:10.1126/science.284.5421.1835.

[7]   M. Cella, D. Jarrossay, F. Facchetti, O. Alebardi, H. Nakajima, a Lanzavecchia, M. Colonna, Plasmacytoid monocytes migrate to inflamed lymph nodes and produce large amounts of type I interferon., Nat. Med. 5 (1999) 919–923. doi:10.1038/11360.

[8]   C. Asselin-Paturel, a Boonstra, M. Dalod, I. Durand, N. Yessaad, C. Dezutter-Dambuyant, a Vicari, a O'Garra, C. Biron, F. Brière, G. Trinchieri, Mouse type I IFN-producing cells are immature APCs with plasmacytoid morphology., Nat. Immunol. 2 (2001) 1144–1150. doi:10.1038/ni736.

[9]   R. Lande, M. Gilliet, Plasmacytoid dendritic cells: key players in the initiation and regulation of immune responses., Ann. N. Y. Acad. Sci. 1183 (2010) 89–103. doi:10.1111/j.1749-6632.2009.05152.x.

[10]   V. Soumelis, Y.-J. Liu, From plasmacytoid to dendritic cell: morphological and functional switches during plasmacytoid pre-dendritic cell differentiation., Eur. J. Immunol. 36 (2006) 2286–92. doi:10.1002/eji.200636026.

[11] T. Ito, H. Kanzler, O. Duramad, W. Cao, Y. Liu, Specialization, kinetics, and repertoire of type 1 interferon responses by human plasmacytoid predendritic cells., Blood. 107 (2006) 2423–31. doi:10.1182/blood-2005-07-2709.

[12] M. Swiecki, M. Colonna, The multifaceted biology of plasmacytoid dendritic cells, Nat. Rev. Immunol. (2015). doi:10.1038/nri3865.

[13] B. Reizis, A. Bunin, H.S. Ghosh, K.L. Lewis, V. Sisirak, Plasmacytoid dendritic cells: recent progress and open questions., Annu. Rev. Immunol. 29 (2011) 163–83. doi:10.1146/annurev-immunol-031210-101345.

[14] M. Clavio, S. Quintino, C. Venturino, F. Ballerini, R. Varaldo, S. Gatto, V. Galbusera, A. Garrone, R. Grasso, L. Canepa, M. Miglino, I. Pierri, M. Gobbi, Lymphoplasmacytic lymphoma/immunocytoma: towards a disease-targeted treatment?, J. Exp. Clin. Cancer Res. 20 (2001) 351–8.

[15] Y. Shao, C. Kao, S. Tang, T. Cha, C. Tsao, E. Meng, D. Yu, G. Sun, S. Wu, Unusual presentation of direct intraperitoneal metastases complicated with massive ascites from plasmacytoid variant of bladder cancer and adenocarcinoma of colon: A case report and literature review., Medicine (Baltimore). 96 (2017) e5816. doi:10.1097/MD.0000000000005816.

[16] Y.-J. Liu, IPC: professional type 1 interferon-producing cells and plasmacytoid dendritic cell precursors., Annu. Rev. Immunol. 23 (2005) 275–306. doi:10.1146/annurev.immunol.23.021704.115633.

[17] A.-C. Villani, R. Satija, G. Reynolds, S. Sarkizova, K. Shekhar, J. Fletcher, M. Griesbeck, A. Butler, S. Zheng, S. Lazo, L. Jardine, D. Dixon, E. Stephenson, E. Nilsson, I. Grundberg, D. McDonald, A. Filby, W. Li, P.L. De Jager, O. Rozenblatt-Rosen, A.A. Lane, M. Haniffa, A. Regev, N. Hacohen, Single-cell RNA-seq reveals new types of human blood dendritic cells, monocytes, and progenitors, Science (80-.). 356 (2017) eaah4573. doi:10.1126/science.aah4573.

[18] P. See, C.-A. Dutertre, J. Chen, P. Günther, N. McGovern, S.E. Irac, M. Gunawan, M. Beyer, K. Händler, K. Duan, H.R. Bin Sumatoh, N. Ruffin, M. Jouve, E. Gea-Mallorquí, R.C.M. Hennekam, T. Lim, C.C. Yip, M. Wen, B. Malleret, I. Low, N.B. Shadan, C.F.S. Fen, A. Tay, J. Lum, F. Zolezzi, A. Larbi, M. Poidinger, J.K.Y. Chan, Q. Chen, L. Renia, M. Haniffa, P. Benaroch, A. Schlitzer, J.L. Schultze, E.W. Newell, F. Ginhoux, Mapping the human DC lineage through the integration of high-dimensional techniques, Science (80-.). 3009 (2017). doi:10.1126/science.eaag3009.

[19] B. Chaudhary, Y.S. Khaled, B.J. Ammori, E. Elkord, Neuropilin 1: Function and therapeutic potential in cancer, Cancer Immunol. Immunother. 63 (2014) 81–99. doi:10.1007/s00262-013-1500-0.

[20] R. Tordjman, Y. Lepelletier, V. Lemarchandel, M. Cambot, P. Gaulard, O. Hermine, P.-H. Roméo, A neuronal receptor, neuropilin-1, is essential for the initiation of the primary immune response, Nat. Immunol. 3 (2002). doi:10.1038/ni789.

[21] N. Kadowaki, S. Ho, S. Antonenko, R.W. Malefyt, R. a Kastelein, F. Bazan, Y.J. Liu, Subsets of human dendritic cell precursors express different toll-like receptors and respond to different microbial antigens., J. Exp. Med. 194 (2001) 863–869. doi:10.1084/jem.194.6.863.

[22] D. Jarrossay, G. Napolitani, M. Colonna, F. Sallusto, A. Lanzavecchia, Specialization and complementarity in microbial molecule recognition by human myeloid and plasmacytoid dendritic cells, Eur. J. Immunol. 31 (2001) 3388–3393. doi:10.1002/1521-4141(200111)31:11<3388::AID-IMMU3388>3.0.CO;2-Q.

[23] S.S. Diebold, T. Kaisho, H. Hemmi, S. Akira, C. Reis e Sousa, Innate antiviral responses by means of TLR7-mediated recognition of single-stranded RNA., Science. 303 (2004) 1529–1531. doi:10.1126/science.1093616.

[24] J.M. Lund, L. Alexopoulou, A. Sato, M. Karow, N.C. Adams, N.W. Gale, A. Iwasaki, R. a Flavell, Recognition of single-stranded RNA viruses by Toll-like receptor 7., Proc. Natl. Acad. Sci. U. S. A. 101 (2004) 5598–5603. doi:10.1073/pnas.0400937101.

[25] U. Bave, M. Magnusson, M.-L. Eloranta, A. Perers, G. V. Alm, L. Ronnblom, Fc RIIa Is Expressed on Natural IFN- -Producing Cells (Plasmacytoid Dendritic Cells) and Is Required for the IFN- Production Induced by Apoptotic Cells Combined with Lupus IgG, J. Immunol. 171 (2003) 3296–3302. doi:10.4049/jimmunol.171.6.3296.

[26] M. Gilliet, W. Cao, Y.-J. Liu, Plasmacytoid dendritic cells: sensing nucleic acids in viral infection and autoimmune diseases., Nat. Rev. Immunol. 8 (2008) 594–606. doi:10.1038/nri2358.

[27] K. Vasquez, K. Sigrist, R. Kucherlapati, P. Demant, W.F. Dietrich, S. Agoulnik, S. Plus, IRF-7 is the master regulator of, Nature. 434 (2005) 772–777. doi:10.1038/nature03419.1.

[28] T. Kim, S. Pazhoor, M. Bao, Z. Zhang, S. Hanabuchi, V. Facchinetti, L. Bover, J. Plumas, L. Chaperot, J. Qin, Y.-J. Liu, Aspartate-glutamate-alanine-histidine box motif (DEAH)/RNA helicase A helicases sense microbial DNA in human plasmacytoid dendritic cells., Proc. Natl. Acad. Sci. U. S. A. 107 (2010) 15181–6. doi:10.1073/pnas.1006539107.

[29] A. Szabo, Z. Magyarics, K. Pazmandi, L. Gopcsa, E. Rajnavolgyi, A. Bacsi, TLR ligands upregulate RIG-I expression in human plasmacytoid dendritic cells in a type I IFN-independent manner, Immunol. Cell Biol. 92 (2014) 671–678. doi:10.1038/icb.2014.38.

[30] D. Bruni, M. Chazal, L. Sinigaglia, L. Chauveau, O. Schwartz, P. Despres, N. Jouvenet, Viral entry route determines how human plasmacytoid dendritic cells produce type I interferons, Sci. Signal. 8 (2015) ra25-ra25. doi:10.1126/scisignal.aaa1552.

[31] H. Ishikawa, Z. Ma, G.N. Barber, STING regulates intracellular DNA-mediated, type I interferon-dependent innate immunity, Nature. 461 (2009) 788–792. doi:10.1038/nature08476.

[32] C. Bode, M. Fox, P. Tewary, A. Steinhagen, R.K. Ellerkmann, D. Klinman, G. Baumgarten, V. Hornung, F. Steinhagen, Human plasmacytoid dentritic cells elicit a Type I Interferon response by sensing DNA via the cGAS-STING signaling pathway, Eur. J. Immunol. 46 (2016) 1615–1621. doi:10.1002/eji.201546113.

[33] H.K. Lee, J.M. Lund, B. Ramanathan, N. Mizushima, A. Iwasaki, Autophagy-dependent viral recognition by plasmacytoid dendritic cells., Science. 315 (2007) 1398–401. doi:10.1126/science.1136880.

[34] J. Henault, J. Martinez, J.M. Riggs, J. Tian, P. Mehta, L. Clarke, M. Sasai, E. Latz, M.M. Brinkmann, A. Iwasaki, A.J. Coyle, R. Kolbeck, D.R. Green, M. a Sanjuan, Noncanonical autophagy is required for type I interferon secretion in response to DNA-immune complexes., Immunity. 37 (2012) 986–97. doi:10.1016/j.immuni.2012.09.014.

[35] R. Lande, D. Ganguly, V. Facchinetti, L. Frasca, C. Conrad, J. Gregorio, S. Meller, G. Chamilos, R. Sebasigari, V. Riccieri, R. Bassett, H. Amuro, S. Fukuhara, T. Ito, Y.-J. Liu, M. Gilliet, Neutrophils Activate Plasmacytoid Dendritic Cells by Releasing Self-DNA-Peptide Complexes in Systemic Lupus Erythematosus, Sci. Transl. Med. 3 (2011) 73ra19-73ra19. doi:10.1126/scitranslmed.3001180.

[36] C. Ghirelli, R. Zollinger, V. Soumelis, Systematic cytokine receptor profiling reveals GM-CSF as a novel TLR-independent activator of human plasmacytoid predendritic cells., Blood. 115 (2010) 5037–40. doi:10.1182/blood-2010-01-266932.

[37] N. Kadowaki, S. Antonenko, J.Y. Lau, Y.J. Liu, Natural interferon alpha/beta-producing cells link innate and adaptive immunity., J. Exp. Med. 192 (2000) 219–226. doi:10.1084/jem.192.2.219.

[38] C. Asselin-Paturel, G. Brizard, K. Chemin, A. Boonstra, A. O'Garra, A. Vicari, G. Trinchieri, Type I interferon dependence of plasmacytoid dendritic cell activation and migration., J. Exp. Med. 201 (2005) 1157–67. doi:10.1084/jem.20041930.

[39] O. Duramad, K.L. Fearon, J.H. Chan, H. Kanzler, J.D. Marshall, R.L. Coffman, F.J. Barrat, IL-10 regulates plasmacytoid dendritic cell response to CpG-containing immunostimulatory sequences., Blood. 102 (2003) 4487–92. doi:10.1182/blood-2003-07-2465.

[40] L. Li, S. Liu, T. Zhang, W. Pan, X. Yang, X. Cao, Splenic Stromal Microenvironment Negatively Regulates Virus-Activated Plasmacytoid Dendritic Cells through TGF- , J. Immunol. 180 (2008) 2951–2956. doi:10.4049/jimmunol.180.5.2951.

[41] M. Naranjo-Gómez, H. Oliva, N. Climent, M.A. Fernández, M. Ruiz-Riol, M. Bofill, J.M. Gatell, T. Gallart, R. Pujol-Borrell, F.E. Borràs, Expression and function of the IL-2 receptor in activated human plasmacytoid dendritic cells, Eur. J. Immunol. 37 (2007) 1764–1772. doi:10.1002/eji.200636980.

[42] A. Kaser, S. Kaser, N.C. Kaneider, B. Enrich, C. J, H. Tilg, Interleukin-18 attracts plasmacytoid dendritic cells (DC2) and promotes Th1 induction by DC2 through IL - 18 receptor expression, Hematology. 103 (2003) 648–656. doi:10.1182/blood-2002-07-2322.

[43] W. Cao, D.B. Rosen, T. Ito, L. Bover, M. Bao, G. Watanabe, Z. Yao, L. Zhang, L.L. Lanier, Y.-J. Liu, Plasmacytoid dendritic cell-specific receptor ILT7-Fc epsilonRI gamma inhibits Toll-like receptor-induced interferon production., J. Exp. Med. 203 (2006) 1399–405. doi:10.1084/jem.20052454.

[44] W. Cao, L. Bover, Signaling and ligand interaction of ILT7: Receptor-mediated regulatory mechanisms for plasmacytoid dendritic cells, Immunol. Rev. 234 (2010) 163–176. doi:10.1111/j.0105-2896.2009.00867.x.

[45] a Dzionek, Y. Sohma, J. Nagafune, M. Cella, M. Colonna, F. Facchetti, G. Günther, I. Johnston, a Lanzavecchia, T. Nagasaka, T. Okada, W. Vermi, G. Winkels, T. Yamamoto, M. Zysk, Y. Yamaguchi, J. Schmitz, BDCA-2, a novel plasmacytoid dendritic cell-specific type II C-type lectin, mediates antigen capture and is a potent inhibitor of interferon alpha/beta induction., J. Exp. Med. 194 (2001) 1823–1834. doi:10.1084/jem.194.12.1823.

[46] J.T. Schroeder, a P. Bieneman, H. Xiao, K.L. Chichester, K. Vasagar, S. Saini, M.C. Liu, TLR- and FceRi-Mediated Responses Opposed One Another in Plasmacytoid Dendritic Cells by Down-Regulating Receptor Expression, J.Immunol. 175 (2005) 5724–5731. doi:10.4049/jimmunol.175.9.5724.

[47] A. Fuchs, M. Cella, T. Kondo, M. Colonna, Paradoxic inhibition of human natural interferon-producing cells by the activating receptor NKp44., Blood. 106 (2005) 2076–82. doi:10.1182/blood-2004-12-4802.

[48] X. Ju, M. Zenke, D.N.J. Hart, G.J. Clark, CD300a/c regulate type I interferon and TNF-alpha secretion by human plasmacytoid dendritic cells stimulated with TLR7 and TLR9 ligands., Blood. 112 (2008) 1184–94. doi:10.1182/blood-2007-12-127951.

[49] F. Meyer-Wentrup, D. Benitez-Ribas, P.J. Tacken, C.J. a Punt, C.G. Figdor, I.J.M. de Vries, G.J. Adema, Targeting DCIR on human plasmacytoid dendritic cells results in antigen presentation and inhibits IFN-alpha production., Blood. 111 (2008) 4245–53. doi:10.1182/blood-2007-03-081398.

[50] E.M. Coccia, M. Severa, E. Giacomini, D. Monneron, M.E. Remoli, I. Julkunen, M. Cella, R. Lande, G. Uzé, Viral infection and Toll-like receptor agonists induce a differential expression of type I and lambda interferons in human plasmacytoid and monocyte-derived dendritic cells., Eur. J. Immunol. 34 (2004) 796–805. doi:10.1002/eji.200324610.

[51] W.M. Schneider, M.D. Chevillotte, C.M. Rice, Interferon-stimulated genes: a complex web of host defenses., Annu. Rev. Immunol. 32 (2014) 513–45. doi:10.1146/annurev-immunol-032713-120231.

[52] T. Luft, K.C. Pang, E. Thomas, P. Hertzog, D.N. Hart, J. Trapani, J. Cebon, Type I IFNs enhance the terminal differentiation of dendritic cells., J. Immunol. 161 (1998) 1947–53.

[53] S.M. Santini, C. Lapenta, M. Logozzi, S. Parlato, M. Spada, T. Di Pucchio, F. Belardelli, Type I Interferon as a Powerful Adjuvant for Monocyte-derived Dendritic Cell Development and Activity In Vitro and in Hu-PBL-SCID Mice, J. Exp. Med. 51200 (2000) 1777–1788. doi:10.1084/jem.191.10.1777.

[54] T.S.M.M. Mathan, C.G. Figdor, S.I. Buschow, Human plasmacytoid dendritic cells: from molecules to intercellular communication network., Front. Immunol. 4 (2013) 372. doi:10.3389/fimmu.2013.00372.

[55] G. Jego, A.K. Palucka, J.-P.J. Blanck, C. Chalouni, V. Pascual, J. Banchereau, Plasmacytoid dendritic cells induce plasma cell differentiation through type I interferon and interleukin 6, Immunity. 19 (2003) 225–234. doi:S1074761303002085 [pii].

[56] A. Le Bon, N. Etchart, C. Rossmann, M. Ashton, S. Hou, D. Gewert, P. Borrow, D.F. Tough, Cross-priming of CD8+ T cells stimulated by virus-induced type I interferon., Nat. Immunol. 4 (2003) 1009–1015. doi:10.1038/ni978.

[57] P. Fitzgerald-Bocarsly, D. Feng, The role of type I interferon production by dendritic cells in host defense., Biochimie. 89 (2009) 843–55. doi:10.1016/j.biochi.2007.04.018.

[58] M. Cella, F. Facchetti, a Lanzavecchia, M. Colonna, Plasmacytoid dendritic cells activated by influenza virus and CD40L drive a potent TH1 polarization., Nat. Immunol. 1 (2000) 305–310. doi:10.1038/79747.

[59] M.C. Rissoan, V. Soumelis, N. Kadowaki, G. Grouard, F. Briere, R. de Waal Malefyt, Y.J. Liu, Reciprocal control of T helper cell and dendritic cell differentiation., Science. 283 (1999) 1183–1186. doi:10.1126/science.283.5405.1183.

[60] E.A. Moseman, X. Liang, A.J. Dawson, A. Panoskaltsis-Mortari, A.M. Krieg, Y.-J. Liu, B.R. Blazar, W. Chen, Human plasmacytoid dendritic cells activated by CpG oligodeoxynucleotides induce the generation of CD4+CD25+ regulatory T cells., J. Immunol. 173 (2004) 4433–42.

[61] T. Ito, M. Yang, Y.-H. Wang, R. Lande, J. Gregorio, O. a Perng, X.-F. Qin, Y.-J. Liu, M. Gilliet, Plasmacytoid dendritic cells prime IL-10-producing T regulatory cells by inducible costimulator ligand., J. Exp. Med. 204 (2007) 105–115. doi:10.1084/jem.20061660.

[62] S. Hanabuchi, T. Ito, W.-R. Park, N. Watanabe, J.L. Shaw, E. Roman, K. Arima, Y.-H. Wang, K.S. Voo, W. Cao, Y.-J. Liu, Thymic Stromal Lymphopoietin-Activated

Plasmacytoid Dendritic Cells Induce the Generation of FOXP3+ Regulatory T Cells in Human Thymus, J. Immunol. 184 (2010) 2999–3007. doi:10.4049/jimmunol.0804106.

[63] J. a. Villadangos, L. Young, Antigen-Presentation Properties of Plasmacytoid Dendritic Cells, Immunity. 29 (2008) 352–361. doi:10.1016/j.immuni.2008.09.002.

[64] G. Hoeffel, A.C. Ripoche, D. Matheoud, M. Nascimbeni, N. Escriou, P. Lebon, F. Heshmati, J.G. Guillet, M. Gannagé, S. Caillat-Zucman, N. Casartelli, O. Schwartz, H. De la Salle, D. Hanau, A. Hosmalin, C. Marañón, Antigen Crosspresentation by Human Plasmacytoid Dendritic Cells, Immunity. 27 (2007) 481–492. doi:10.1016/j.immuni.2007.07.021.

[65] T. Di Pucchio, B. Chatterjee, A. Smed-Sörensen, S. Clayton, A. Palazzo, M. Montes, Y. Xue, I. Mellman, J. Banchereau, J.E. Connolly, Direct proteasome-independent cross-presentation of viral antigen by plasmacytoid dendritic cells on major histocompatibility complex class I, Nat. Immunol. 9 (2008) 551–557. doi:10.1038/ni.1602.

[66] E. Segura, M. Durand, S. Amigorena, Similar antigen cross-presentation capacity and phagocytic functions in all freshly isolated human lymphoid organ-resident dendritic cells., J. Exp. Med. 210 (2013) 1035–47. doi:10.1084/jem.20121103.

[67] B. Reizis, M. Colonna, G. Trinchieri, F. Barrat, M. Gilliet, Plasmacytoid dendritic cells: one-trick ponies or workhorses of the immune system?, Nat. Rev. Immunol. 11 (2011) 558–65. doi:10.1038/nri3027.

[68] L. Galibert, C.R. Maliszewski, S. Vandenabeele, Plasmacytoid monocytes/T cells: a dendritic cell lineage?, Semin. Immunol. 13 (2001) 283–289. doi:10.1006/smim.2001.0324.

[69] M. Swiecki, Y. Wang, S. Gilfillan, M. Colonna, Plasmacytoid Dendritic Cells Contribute to Systemic but Not Local Antiviral Responses to HSV Infections, PLoS Pathog. 9 (2013) 2–11. doi:10.1371/journal.ppat.1003728.

[70] Y. Wang, M. Swiecki, S. a. McCartney, M. Colonna, dsRNA sensors and plasmacytoid dendritic cells in host defense and autoimmunity, Immunol. Rev. 243 (2011) 74–90. doi:10.1111/j.1600-065X.2011.01049.x.

[71] M.J. Ciancanelli, S.X.L. Huang, P. Luthra, H. Garner, Y. Itan, S. Volpi, F.G. Lafaille, C. Trouillet, M. Schmolke, R.A. Albrecht, E. Israelsson, H.K. Lim, M. Casadio, T. Hermesh, L. Lorenzo, L.W. Leung, V. Pedergnana, B. Boisson, S. Okada, C. Picard, B. Ringuier, F. Troussier, D. Chaussabel, L. Abel, I. Pellier, L.D. Notarangelo, A. Garcia-Sastre, C.F. Basler, F. Geissmann, S.-Y. Zhang, H.-W. Snoeck, J.-L. Casanova, Life-threatening influenza and impaired interferon amplification in human IRF7 deficiency, Science (80-.). 348 (2015) 448–453. doi:10.1126/science.aaa1578.

[72] S. Davidson, S. Crotta, T.M. McCabe, A. Wack, Pathogenic potential of interferon αβ in acute influenza infection, Nat. Commun. 5 (2014). doi:10.1038/ncomms4864.

[73] Q. Li, J.D. Estes, P.M. Schlievert, L. Duan, A.J. Brosnahan, P.J. Southern, C.S. Reilly, M.L. Peterson, N. Schultz-Darken, K.G. Brunner, K.R. Nephew, S. Pambuccian, J.D. Lifson, J. V. Carlis, A.T. Haase, Glycerol monolaurate prevents mucosal SIV transmission, Nature. 458 (2009) 1034–1038. doi:10.1038/nature07831.

[74] M. O'Brien, O. Manches, R.L. Sabado, S.J. Baranda, Y. Wang, I. Marie, L. Rolnitzky, M. Markowitz, D.M. Margolis, D. Levy, N. Bhardwaj, Spatiotemporal trafficking of HIV in human plasmacytoid dendritic cells defines a persistently IFN-α-producing and partially matured phenotype, J. Clin. Invest. 121 (2011) 1088–1101. doi:10.1172/JCI44960.

[75] O. Manches, M.V. Fernandez, J. Plumas, L. Chaperot, N. Bhardwaj, Activation of the noncanonical NF-κB pathway by HIV controls a dendritic cell immunoregulatory phenotype., Proc. Natl. Acad. Sci. U. S. A. 109 (2012) 14122–7. doi:10.1073/pnas.1204032109.

[76] H. Li, P. Goepfert, R.K. Reeves, Plasmacytoid Dendritic Cells from HIV-1 Elite Controllers Maintain a Gut-Homing Phenotype Associated with Immune Activation., AIDS Res. Hum. Retroviruses. 30 (2014) 1–3. doi:10.1089/aid.2014.0174.

[77] N.G. Sandler, S.E. Bosinger, J.D. Estes, R.T.R. Zhu, G.K. Tharp, E. Boritz, D. Levin, S. Wijeyesinghe, K.N. Makamdop, G.Q. del Prete, B.J. Hill, J.K. Timmer, E. Reiss, G. Yarden, S. Darko, E. Contijoch, J.P. Todd, G. Silvestri, M. Nason, R.B. Norgren, B.F. Keele, S. Rao, J.A. Langer, J.D. Lifson, G. Schreiber, D.C. Douek, Type I interferon responses in rhesus macaques prevent SIV infection and slow disease progression., Nature. 511 (2014) 601–5. doi:10.1038/nature13554.

[78] X.Z. Duan, M. Wang, H.W. Li, H. Zhuang, D. Xu, F.S. Wang, Decreased frequency and function of circulating plasmocytoid dendritic cells (pDC) in hepatitis B virus infected humans, J. Clin. Immunol. 24 (2004) 637–646. doi:10.1007/s10875-004-6249-y.

[79] A.M. Woltman, M.L. Op den Brouw, P.J. Biesta, C.C. Shi, H.L. a Janssen, Hepatitis B virus lacks immune activating capacity, but actively inhibits plasmacytoid dendritic cell function., PLoS One. 6 (2011) e15324. doi:10.1371/journal.pone.0015324.

[80] N.L. Yonkers, B. Rodriguez, K. a Milkovich, R. Asaad, M.M. Lederman, P.S. Heeger, D.D. Anthony, TLR ligand-dependent activation of naive CD4 T cells by plasmacytoid dendritic cells is impaired in hepatitis C virus infection., J. Immunol. 178 (2007) 4436–44. doi:10.4049/jimmunol.178.7.4436.

[81] S. Zhang, K. Kodys, G.J. Babcock, G. Szabo, CD81/CD9 tetraspanins aid plasmacytoid dendritic cells in recognition of hepatitis C virus-infected cells and induction of interferon-alpha., Hepatology. 58 (2013) 940–9. doi:10.1002/hep.25827.

[82] P. Lenz, D. Lowy, J. Schiller, Papillomavirus virus-like particles induce cytokines characteristic of innate immune responses in plasmacytoid dendritic cells, Eur. J. Immunol. 35 (2005) 1548–1556. doi:10.1002/eji.200425547.

[83] L. Lozza, M. Farinacci, M. Bechtle, M. Stäber, U. Zedler, A. Baiocchini, F. Del Nonno, S.H.E. Kaufmann, Communication between Human Dendritic Cell Subsets in Tuberculosis: Requirements for Naive CD4(+) T Cell Stimulation., Front. Immunol. 5 (2014) 324. doi:10.3389/fimmu.2014.00324.

[84] R.M.B. Teles, T.G. Graeber, S.R. Krutzik, D. Montoya, M. Schenk, D.J. Lee, E. Komisopoulou, K. Kelly-Scumpia, R. Chun, S.S. Iyer, E.N. Sarno, T.H. Rea, M. Hewison, J.S. Adams, S.J. Popper, D.A. Relman, S. Stenger, B.R. Bloom, G. Cheng, R.L. Modlin, Type I interferon suppresses type II interferon-triggered human anti-mycobacterial responses., Science. 339 (2013) 1448–53. doi:10.1126/science.1233665.

[85] P. Michea, P. Vargas, M.-H. Donnadieu, M. Rosemblatt, M.R. Bono, G. Duménil, V. Soumelis, Epithelial control of the human pDC response to extracellular bacteria., Eur. J. Immunol. 43 (2013) 1264–73. doi:10.1002/eji.201242990.

[86] M. Parcina, M.A. Miranda-Garcia, S. Durlanik, S. Ziegler, B. Over, P. Georg, S. Foermer, S. Ammann, D. Hilmi, K.-J. Weber, M. Schiller, K. Heeg, W. Schneider-Brachert, F. Götz, I. Bekeredjian-Ding, Pathogen-triggered activation of plasmacytoid dendritic cells induces IL-10-producing B cells in response to Staphylococcus aureus., J. Immunol. 190 (2013) 1591–602. doi:10.4049/jimmunol.1201222.

[87] Z.G. Ramirez-Ortiz, C.A. Specht, J.P. Wang, C.K. Lee, D.C. Bartholomeu, R.T. Gazzinelli,

S.M. Levitz, Toll-like receptor 9-dependent immune activation by unmethylated CpG motifs in Aspergillus fumigatus DNA., Infect. Immun. 76 (2008) 2123–9. doi:10.1128/IAI.00047-08.

[88] Z.G. Ramirez-Ortiz, C.K. Lee, J.P. Wang, L. Boon, C.A. Specht, S.M. Levitz, A nonredundant role for plasmacytoid dendritic cells in host defense against the human fungal pathogen Aspergillus fumigatus., Cell Host Microbe. 9 (2011) 415–24. doi:10.1016/j.chom.2011.04.007.

[89] F. V Loures, M. Röhm, C.K. Lee, E. Santos, J.P. Wang, C.A. Specht, V.L.G. Calich, C.F. Urban, S.M. Levitz, Recognition of Aspergillus fumigatus hyphae by human plasmacytoid dendritic cells is mediated by dectin-2 and results in formation of extracellular traps., PLoS Pathog. 11 (2015) e1004643. doi:10.1371/journal.ppat.1004643.

[90] J.R. Loughland, G. Minigo, D.S. Sarovich, M. Field, P.E. Tipping, M. Montes de Oca, K.A. Piera, F.H. Amante, B.E. Barber, M.J. Grigg, T. William, M.F. Good, D.L. Doolan, C.R. Engwerda, N.M. Anstey, J.S. McCarthy, T. Woodberry, Plasmacytoid dendritic cells appear inactive during sub-microscopic Plasmodium falciparum blood-stage infection, yet retain their ability to respond to TLR stimulation., Sci. Rep. 7 (2017) 2596. doi:10.1038/s41598-017-02096-2.

[91] X. Yu, B. Cai, M. Wang, P. Tan, X. Ding, J. Wu, J. Li, Q. Li, P. Liu, C. Xing, H.Y. Wang, X. Su, R.-F. Wang, Cross-Regulation of Two Type I Interferon Signaling Pathways in Plasmacytoid Dendritic Cells Controls Anti-malaria Immunity and Host Mortality., Immunity. 45 (2016) 1093–1107. doi:10.1016/j.immuni.2016.10.001.

[92] A. Bengtsson, G. Sturfelt, L. Truedsson, J. Blomberg, G. Alm, H. Vallin, L. Rönnblom, Activation of type I interferon system in systemic lupus erythematosus correlates with disease activity but not with antiretroviral antibodies, Lupus. 9 (2000) 664–671. doi:10.1191/096120300674499064.

[93] L. Rönnblom, G. V Alm, A pivotal role for the natural interferon alpha-producing cells (plasmacytoid dendritic cells) in the pathogenesis of lupus., J. Exp. Med. 194 (2001) F59–F63. doi:10.1084/jem.194.12.f59.

[94] T.K. Means, E. Latz, F. Hayashi, M.R. Murali, D.T. Golenbock, A.D. Luster, Human lupus autoantibody-DNA complexes activate DCs through cooperation of CD32 and TLR9, J. Clin. Invest. 115 (2005) 407–417. doi:10.1172/JCI200523025.

[95] D. Ganguly, G. Chamilos, R. Lande, J. Gregorio, S. Meller, V. Facchinetti, B. Homey, F.J. Barrat, T. Zal, M. Gilliet, Self-RNA-antimicrobial peptide complexes activate human dendritic cells through TLR7 and TLR8., J. Exp. Med. 206 (2009) 1983–94. doi:10.1084/jem.20090480.

[96] L. Farkas, K. Beiske, F. Lund-Johansen, P. Brandtzaeg, F.L. Jahnsen, Plasmacytoid Dendritic Cells (Natural Interferon- α/β-Producing Cells) Accumulate in Cutaneous Lupus Erythematosus Lesions, Am. J. Pathol. 159 (2001) 237–243. doi:10.1016/S0002-9440(10)61689-6.

[97] N. Fiore, G. Castellano, A. Blasi, C. Capobianco, A. Loverre, V. Montinaro, S. Netti, D. Torres, C. Manno, G. Grandaliano, E. Ranieri, F.P. Schena, L. Gesualdo, Immature myeloid and plasmacytoid dendritic cells infiltrate renal tubulointerstitium in patients with lupus nephritis, Mol. Immunol. 45 (2008) 259–265. doi:10.1016/j.molimm.2007.04.029.

[98] C. Albanesi, C. Scarponi, S. Pallotta, R. Daniele, D. Bosisio, S. Madonna, P. Fortugno, S. Gonzalvo-Feo, J.-D. Franssen, M. Parmentier, O. De Pità, G. Girolomoni, S. Sozzani,

Chemerin expression marks early psoriatic skin lesions and correlates with plasmacytoid dendritic cell recruitment, J. Exp. Med. 206 (2009). doi:10.1084/jem.20080129.

[99] N. Hagberg, O. Berggren, D. Leonard, G. Weber, Y.T. Bryceson, G. V Alm, M.-L. Eloranta, L. Rönnblom, IFN-α production by plasmacytoid dendritic cells stimulated with RNA-containing immune complexes is promoted by NK cells via MIP-1β and LFA-1., J. Immunol. 186 (2011) 5085–94. doi:10.4049/jimmunol.1003349.

[100] M. Menon, P. Blair, D. Isenberg, C. Mauri, A Regulatory Feedback between Plasmacytoid Dendritic Cells and Regulatory B Cells Is Aberrant in Systemic Lupus Erythematosus, Immunity. 44 (2016) 683–697. doi:10.1016/j.immuni.2016.02.012.

[101] I.T.W. Harley, K.M. Kaufman, C.D. Langefeld, J.B. Harley, J.A. Kelly, Genetic susceptibility to SLE: new insights from fine mapping and genome-wide association studies, Nat. Rev. Genet. 10 (2009) 285–290. doi:10.1038/nrg2571.

[102] O. Berggren, A. Alexsson, D.L. Morris, K. Tandre, G. Weber, T.J. Vyse, A.-C. Syvänen, L. Rönnblom, M.-L. Eloranta, IFN-α production by plasmacytoid dendritic cell associations with polymorphisms in gene loci related to autoimmune and inflammatory diseases., Hum. Mol. Genet. 24 (2015) 3571–81. doi:10.1093/hmg/ddv095.

[103] Q. Fu, J. Zhao, X. Qian, J.L.H. Wong, K.M. Kaufman, C.Y. Yu, M.Y. Mok, J.B. Harley, J.M. Guthridge, Y.W. Song, S.-K. Cho, S.-C. Bae, J.M. Grossman, B.H. Hahn, F.C. Arnett, N. Shen, B.P. Tsao, Association of a functional IRF7 variant with systemic lupus erythematosus, Arthritis Rheum. 63 (2011) 749–754. doi:10.1002/art.30193.

[104] M. Rossato, A.J. Affandi, S. Thordardottir, C.G.K. Wichers, M. Cossu, J.C.A. Broen, F.M. Moret, L. Bossini-Castillo, E. Chouri, L. van Bon, F. Wolters, W. Marut, M. van der Kroef, S. Silva-Cardoso, C.P.J. Bekker, H. Dolstra, J.M. van Laar, J. Martin, J.A.G. van Roon, K.A. Reedquist, L. Beretta, T.R.D.J. Radstake, Expression of miR-618 in plasmacytoid dendritic cells from systemic sclerosis patients is associated with their altered frequency and activation, Arthritis Rheumatol. 72 (2017) 596 LP-601. doi:10.1002/art.40163.

[105] B.W. Higgs, Z. Liu, B. White, W. Zhu, W.I. White, C. Morehouse, P. Brohawn, P.A. Kiener, L. Richman, D. Fiorentino, S.A. Greenberg, B. Jallal, Y. Yao, Patients with systemic lupus erythematosus, myositis, rheumatoid arthritis and scleroderma share activation of a common type I interferon pathway, Ann. Rheum. Dis. 70 (2011) 2029 LP-2036.

[106] S. Shrestha, B. Wershil, J.F. Sarwark, T.B. Niewold, T. Philipp, L.M. Pachman, Lesional and nonlesional skin from patients with untreated juvenile dermatomyositis displays increased numbers of mast cells and mature plasmacytoid dendritic cells, Arthritis Rheum. 62 (2010) 2813–2822. doi:10.1002/art.27529.

[107] M.-L. Eloranta, S. Barbasso Helmers, A.-K. Ulfgren, L. R?nnblom, G. V Alm, I.E. Lundberg, A possible mechanism for endogenous activation of the type I interferon system in myositis patients with anti?Jo-1 or anti?Ro 52/anti?Ro 60 autoantibodies, Arthritis Rheum. 56 (2007) 3112–3124. doi:10.1002/art.22860.

[108] D. Kim, A. Peck, D. Santer, P. Patole, S.M. Schwartz, J.A. Molitor, F.C. Arnett, K.B. Elkon, Induction of interferon?? by scleroderma sera containing autoantibodies to topoisomerase I: Association of higher interferon?? activity with lung fibrosis, Arthritis Rheum. 58 (2008) 2163–2173. doi:10.1002/art.23486.

[109] M. Rossato, A.J. Affandi, S. Thordardottir, C.G.K. Wichers, M. Cossu, J.C.A. Broen, F.M.

Moret, L. Bossini-Castillo, E. Chouri, L. van Bon, F. Wolters, W. Marut, M. van der Kroef, S. Silva-Cardoso, C.P.J. Bekker, H. Dolstra, J.M. van Laar, J. Martin, J.A.G. van Roon, K.A. Reedquist, L. Beretta, T.R.D.J. Radstake, Expression of miR-618 in plasmacytoid dendritic cells from systemic sclerosis patients is associated with their altered frequency and activation., Arthritis Rheumatol. (Hoboken, N.J.). 11 (2017) 300–308. doi:10.1002/art.40163.

[110] K. Sacre, L.A. Criswell, J.M. Mccune, Hydroxychloroquine is associated with impaired interferon-alpha and tumor necrosis factor-alpha production by plasmacytoid dendritic cells in systemic lupus erythematosus, (2012). doi:10.1186/ar3895.

[111] N. Costedoat-Chalumeau, Z. Amoura, J.-S. Hulot, G. Aymard, G. Leroux, D. Marra, P. Lechat, J.-C. Piette, Very low blood hydroxychloroquine concentration as an objective marker of poor adherence to treatment of systemic lupus erythematosus., Ann. Rheum. Dis. 66 (2007) 821–824. doi:10.1136/ard.2006.067835.

[112] D.M. Schwartz, M. Bonelli, M. Gadina, J.J. O'Shea, Type I/II cytokines, JAKs, and new strategies for treating autoimmune diseases, Nat. Rev. Rheumatol. 12 (2015) 25–36. doi:10.1038/nrrheum.2015.167.

[113] R. Furie, M. Khamashta, J.T. Merrill, V.P. Werth, K. Kalunian, P. Brohawn, G.G. Illei, J. Drappa, L. Wang, S. Yoo, Anifrolumab, an Anti–Interferon-α Receptor Monoclonal Antibody, in Moderate-to-Severe Systemic Lupus Erythematosus, Arthritis Rheumatol. 69 (2017) 376–386. doi:10.1002/art.39962.

[114] F.L. Jahnsen, F. Lund-Johansen, J.F. Dunne, L. Farkas, R. Haye, P. Brandtzaeg, Experimentally Induced Recruitment of Plasmacytoid (CD123high) Dendritic Cells in Human Nasal Allergy, J. Immunol. 165 (2000) 4062–4068. doi:10.4049/jimmunol.165.7.4062.

[115] B. Dua, R.M. Watson, G.M. Gauvreau, P.M. O'Byrne, B. de Saint-Vis, K. Franz-Bacon, et al., Myeloid and plasmacytoid dendritic cells in induced sputum after allergen inhalation in subjects with asthma., J. Allergy Clin. Immunol. 126 (2010) 133–9. doi:10.1016/j.jaci.2010.04.006.

[116] J.W. Upham, G. Zhang, A. Rate, S.T. Yerkovich, M. Kusel, P.D. Sly, P.G. Holt, Plasmacytoid dendritic cells during infancy are inversely associated with childhood respiratory tract infections and wheezing., J. Allergy Clin. Immunol. 124 (2009) 707–13.e2. doi:10.1016/j.jaci.2009.07.009.

[117] K. Bratke, C. Prieschenk, K. Garbe, M. Kuepper, M. Lommatzsch, J.C. Virchow, Plasmacytoid dendritic cells in allergic asthma and the role of inhaled corticosteroid treatment, Clin. Exp. Allergy. 43 (2013) 312–321. doi:10.1111/cea.12064.

[118] J.R. Tversky, T. V. Le, A.P. Bieneman, K.L. Chichester, R.G. Hamilton, J.T. Schroeder, Human blood dendritic cells from allergic subjects have impaired capacity to produce interferon-? via toll-like receptor 9, Clin. Exp. Allergy. 38 (2008) 781–788. doi:10.1111/j.1365-2222.2008.02954.x.

[119] A.L. Pritchard, M.L. Carroll, J.G. Burel, O.J. White, S. Phipps, J.W. Upham, Innate IFNs and Plasmacytoid Dendritic Cells Constrain Th2 Cytokine Responses to Rhinovirus: A Regulatory Mechanism with Relevance to Asthma, J. Immunol. 188 (2012) 5898–5905. doi:10.4049/jimmunol.1103507.

[120] A. Froidure, O. Vandenplas, V. D'Alpaos, G. Evrard, C. Pilette, Defects in Plasmacytoid Dendritic Cell Expression of Inducible Costimulator Ligand and IFN-α Are Associated in Asthma with Disease Persistence, Am. J. Respir. Crit. Care Med. 192 (2015) 392–395. doi:10.1164/rccm.201503-0479LE.

[121] H.J. de Heer, H. Hammad, T. Soullié, D. Hijdra, N. Vos, M.A.M. Willart, H.C. Hoogsteden, B.N. Lambrecht, Essential Role of Lung Plasmacytoid Dendritic Cells in Preventing Asthmatic Reactions to Harmless Inhaled Antigen, J. Exp. Med. 200 (2004) 89–98. doi:10.1084/jem.20040035.

[122] E. Hartmann, B. Wollenberg, S. Rothenfusser, M. Wagner, D. Wellisch, B. Mack, T. Giese, O. Gires, S. Endres, G. Hartmann, B. W, Identification and Functional Analysis of Tumor-Infiltrating Plasmacytoid Dendritic Cells in Head and Neck Cancer 1, (2003) 6478–6487.

[123] I. Treilleux, Dendritic Cell Infiltration and Prognosis of Early Stage Breast Cancer, Clin. Cancer Res. 10 (2004) 7466–7474. doi:10.1158/1078-0432.CCR-04-0684.

[124] S.I. Labidi-Galy, V. Sisirak, P. Meeus, M. Gobert, I. Treilleux, A. Bajard, J.D. Combes, J. Faget, F. Mithieux, A. Cassignol, O. Tredan, I. Durand, C. M??n??trier-Caux, C. Caux, J.Y. Blay, I. Ray-Coquard, N. Bendriss-Vermare, Quantitative and functional alterations of plasmacytoid dendritic cells contribute to immune tolerance in ovarian cancer, Cancer Res. 71 (2011) 5423–5434. doi:10.1158/0008-5472.CAN-11-0367.

[125] A. Ray, D.S. Das, Y. Song, V. Macri, P. Richardson, C.L. Brooks, D. Chauhan, K.C. Anderson, A novel agent SL-401 induces anti-myeloma activity by targeting plasmacytoid dendritic cells, osteoclastogenesis, and cancer stem-like cells, Nat. Publ. Gr. (2017) 1–9. doi:10.1038/leu.2017.135.

[126] C. Aspord, M.-T. Leccia, J. Charles, J. Plumas, Plasmacytoid Dendritic Cells Support Melanoma Progression by Promoting Th2 and Regulatory Immunity through OX40L and ICOSL, Cancer Immunol. Res. 1 (2013) 402–415. doi:10.1158/2326-6066.CIR-13-0114-T.

[127] Y. Liu, G. Zeng, Cancer and innate immune system interactions: translational potentials for cancer immunotherapy., J. Immunother. 35 (2012) 299–308. doi:10.1097/CJI.0b013e3182518e83.

[128] C. Ghirelli, F. Reyal, M. Jeanmougin, R. Zollinger, P. Sirven, P. Michea, C. Caux, N. Bendriss-Vermare, M.H. Donnadieu, M. Caly, V. Fourchotte, A. Vincent-Salomon, B. Sigal-Zafrani, X. Sastre-Garau, V. Soumelis, Breast cancer cell-derived GM-CSF licenses regulatory Th2 induction by plasmacytoid predendritic cells in aggressive disease subtypes, Cancer Res. 75 (2015) 2775–2787. doi:10.1158/0008-5472.CAN-14-2386.

[129] I. Perrot, D. Blanchard, N. Freymond, S. Isaac, B. Guibert, Y. Pacheco, S. Lebecque, Dendritic Cells Infiltrating Human Non-Small Cell Lung Cancer Are Blocked at Immature Stage, J. Immunol. 178 (2007) 2763–2769. doi:10.4049/jimmunol.178.5.2763.

[130] V. Sisirak, J. Faget, M. Gobert, N. Goutagny, N. Vey, I. Treilleux, S. Renaudineau, G. Poyet, S.I. Labidi-Galy, S. Goddard-Leon, I. Durand, I. Le Mercier, A. Bajard, T. Bachelot, A. Puisieux, I. Puisieux, J.Y. Blay, C. M??n??trier-Caux, C. Caux, N. Bendriss-Vermare, Impaired IFN-?? production by plasmacytoid dendritic cells favors regulatory T-cell expansion that may contribute to breast cancer progression, Cancer Res. 72 (2012) 5188–5197. doi:10.1158/0008-5472.CAN-11-3468.

[131] I. Chevolet, R. Speeckaert, M. Schreuer, B. Neyns, O. Krysko, C. Bachert, B. Hennart, D. Allorge, N. van Geel, M. Van Gele, L. Brochez, Characterization of the in vivo immune network of IDO, tryptophan metabolism, PD-L1, and CTLA-4 in circulating immune cells in melanoma., Oncoimmunology. 4 (2015) e982382. doi:10.4161/2162402X.2014.982382.

[132] A. Yamahira, M. Narita, M. Iwabuchi, T. Uchiyama, S. Iwaya, R. Ohiwa, Y. Nishizawa, T.

Suzuki, Y. Yokoyama, S. Hashimoto, J. Takizawa, H. Sone, M. Takahashi, Activation of the leukemia plasmacytoid dendritic cell line PMDC05 by Toho-1, a novel IDO inhibitor, Anticancer Res. 34 (2014) 4021–4028.

[133] V. Sisirak, N. Vey, N. Goutagny, S. Renaudineau, M. Malfroy, S. Thys, I. Treilleux, S.I. Labidi-Galy, T. Bachelot, C. Dezutter-Dambuyant, C. Ménétrier-Caux, J.-Y. Blay, C. Caux, N. Bendriss-Vermare, Breast cancer-derived transforming growth factor-β and tumor necrosis factor-α compromise interferon-α production by tumor-associated plasmacytoid dendritic cells., Int. J. Cancer. 133 (2013) 771–8. doi:10.1002/ijc.28072.

[134] S. Beckebaum, X. Zhang, X. Chen, Z. Yu, A. Frilling, G. Dworacki, H. Grosse-Wilde, C.E. Broelsch, G. Gerken, V.R. Cicinnati, Increased levels of interleukin-10 in serum from patients with hepatocellular carcinoma correlate with profound numerical deficiencies and immature phenotype of circulating dendritic cell subsets, Clin. Cancer Res. 10 (2004) 7260–7269. doi:10.1158/1078-0432.CCR-04-0872.

[135] I. Bekeredjian-Ding, M. Schäfer, E. Hartmann, R. Pries, M. Parcina, P. Schneider, T. Giese, S. Endres, B. Wollenberg, G. Hartmann, Tumour-derived prostaglandin E 2 and transforming growth factor-β synergize to inhibit plasmacytoid dendritic cell-derived interferon-α, Immunology. 128 (2009) 439–450. doi:10.1111/j.1365-2567.2009.03134.x.

[136] J. Tel, S. Anguille, C.E.J. Waterborg, E.L. Smits, C.G. Figdor, I.J.M. de Vries, Tumoricidal activity of human dendritic cells, Trends Immunol. 35 (2014) 38–46. doi:10.1016/j.it.2013.10.007.

[137] T. Matsui, J.E. Connolly, M. Michnevitz, D. Chaussabel, C.-I. Yu, C. Glaser, S. Tindle, M. Pypaert, H. Freitas, B. Piqueras, J. Banchereau, a K. Palucka, CD2 distinguishes two subsets of human plasmacytoid dendritic cells with distinct phenotype and functions., J. Immunol. 182 (2009) 6815–23. doi:10.4049/jimmunol.0802008.

[138] B.M. Matta, A. Castellaneta, A.W. Thomson, Tolerogenic plasmacytoid DC, Eur. J. Immunol. 40 (2010) 2667–2676. doi:10.1002/eji.201040839.

[139] S. Kobold, G. Wiedemann, S. Rothenfußer, S. Endres, Modes of action of TLR7 agonists in cancer therapy, Immunotherapy. 6 (2014) 1085–1095. doi:10.2217/imt.14.75.

[140] M.P. Schön, B.G. Wienrich, C. Drewniok, A.B. Bong, J. Eberle, C.C. Geilen, H. Gollnick, M. Schön, Death receptor-independent apoptosis in malignant melanoma induced by the small-molecule immune response modifier imiquimod, J. Invest. Dermatol. 122 (2004) 1266–1276. doi:10.1111/j.0022-202X.2004.22528.x.

[141] S.-W. Huang, S.-H. Chang, S.-W. Mu, H.-Y. Jiang, S.-T. Wang, J.-K. Kao, J.-L. Huang, C.-Y. Wu, Y.-J. Chen, J.-J. Shieh, Imiquimod activates p53-dependent apoptosis in a human basal cell carcinoma cell line, J. Dermatol. Sci. 81 (2016) 182–191. doi:10.1016/j.jdermsci.2015.12.011.

[142] J. Tel, E.H.J.G. Aarntzen, T. Baba, G. Schreibelt, B.M. Schulte, D. Benitez-Ribas, O.C. Boerman, S. Croockewit, W.J.G. Oyen, M. van Rossum, G. Winkels, P.G. Coulie, C.J.A. Punt, C.G. Figdor, I.J.M. de Vries, Natural Human Plasmacytoid Dendritic Cells Induce Antigen-Specific T-Cell Responses in Melanoma Patients, Cancer Res. 73 (2013) 1063–1075. doi:10.1158/0008-5472.CAN-12-2583.

[143] J. Tel, R. Koornstra, N. de Haas, V. van Deutekom, H. Westdorp, S. Boudewijns, N. van Erp, S. Di Blasio, W. Gerritsen, C.G. Figdor, I.J.M. de Vries, S. V. Hato, Preclinical exploration of combining plasmacytoid and myeloid dendritic cell vaccination with BRAF inhibition, J. Transl. Med. 14 (2016) 88. doi:10.1186/s12967-016-0844-6.

[144] L.M. Kranz, M. Diken, H. Haas, S. Kreiter, C. Loquai, K.C. Reuter, M. Meng, D. Fritz, F.

Vascotto, H. Hefesha, C. Grunwitz, M. Vormehr, Y. Hüsemann, A. Selmi, A.N. Kuhn, J. Buck, E. Derhovanessian, R. Rae, S. Attig, J. Diekmann, R.A. Jabulowsky, S. Heesch, J. Hassel, P. Langguth, S. Grabbe, C. Huber, Ö. Türeci, U. Sahin, Systemic RNA delivery to dendritic cells exploits antiviral defence for cancer immunotherapy, Nature. 534 (2016) 396–401. doi:10.1038/nature18300.

[145] D.E. Zak, V.C. Tam, A. Aderem, Systems-level analysis of innate immunity., Annu. Rev. Immunol. 32 (2014) 547–77. doi:10.1146/annurev-immunol-032713-120254.

[146] A. Krug, S. Rothenfusser, V. Hornung, B. Jahrsdrfer, S. Blackwell, Z.K. Ballas, S. Endres, A.M. Krieg, G. Hartmann, Identification of CpG oligonucleotide sequences with high induction of IFN-??/?? in plasmacytoid dendritic cells, Eur. J. Immunol. 31 (2001) 2154–2163. doi:10.1002/1521-4141(200107)31:7<2154::AID-IMMU2154>3.0.CO;2-U.

[147] A. Cappuccio, R. Zollinger, M. Schenk, A. Walczak, N. Servant, E. Barillot, P. Hupé, R.L. Modlin, V. Soumelis, Combinatorial code governing cellular responses to complex stimuli, Nat. Commun. 6 (2015) 6847. doi:10.1038/ncomms7847.

[148] H.Y. Kim, H.R. Kim, S.H. Lee, Advances in systems biology approaches for autoimmune diseases, Immune Netw. 14 (2014) 73–80. doi:10.4110/in.2014.14.2.73.

[149] X. Liao, S. Li, R.E. Settlage, S. Sun, J. Ren, A.M. Reihl, H. Zhang, S. V. Karyala, C.M. Reilly, S.A. Ahmed, X.M. Luo, Cutting Edge: Plasmacytoid Dendritic Cells in Late-Stage Lupus Mice Defective in Producing IFN-α, J. Immunol. 195 (2015) 4578–4582. doi:10.4049/jimmunol.1501157.

[150] V. Sisirak, D. Ganguly, K.L. Lewis, C. Couillault, L. Tanaka, S. Bolland, V. D'Agati, K.B. Elkon, B. Reizis, Genetic evidence for the role of plasmacytoid dendritic cells in systemic lupus erythematosus., J. Exp. Med. 211 (2014) 1969–76. doi:10.1084/jem.20132522.

[151] T.W. Kim, S. Hong, Y. Lin, E. Murat, H. Joo, T. Kim, V. Pascual, Y.-J. Liu, Transcriptional Repression of IFN Regulatory Factor 7 by MYC Is Critical for Type I IFN Production in Human Plasmacytoid Dendritic Cells, J. Immunol. 197 (2016) 3348–3359. doi:10.4049/jimmunol.1502385.

[152] K. Worah, T.S.M. Mathan, T.P. Vu Manh, S. Keerthikumar, G. Schreibelt, J. Tel, T. Duiveman-de Boer, A.E. Sköld, A.B. van Spriel, I.J.M. de Vries, M.A. Huynen, H.J. Wessels, J. Gloerich, M. Dalod, E. Lasonder, C.G. Figdor, S.I. Buschow, Proteomics of Human Dendritic Cell Subsets Reveals Subset-Specific Surface Markers and Differential Inflammasome Function, Cell Rep. 16 (2016) 2953–2966. doi:10.1016/j.celrep.2016.08.023.

[153] J.J. Powell, J. Van De Water, M.E. Gershwin, Evidence for the role of environmental agents in the initiation or progression of autoimmune conditions, Environ. Health Perspect. 107 (1999) 667–672. doi:10.1289/ehp.99107s5667.

Figure 1
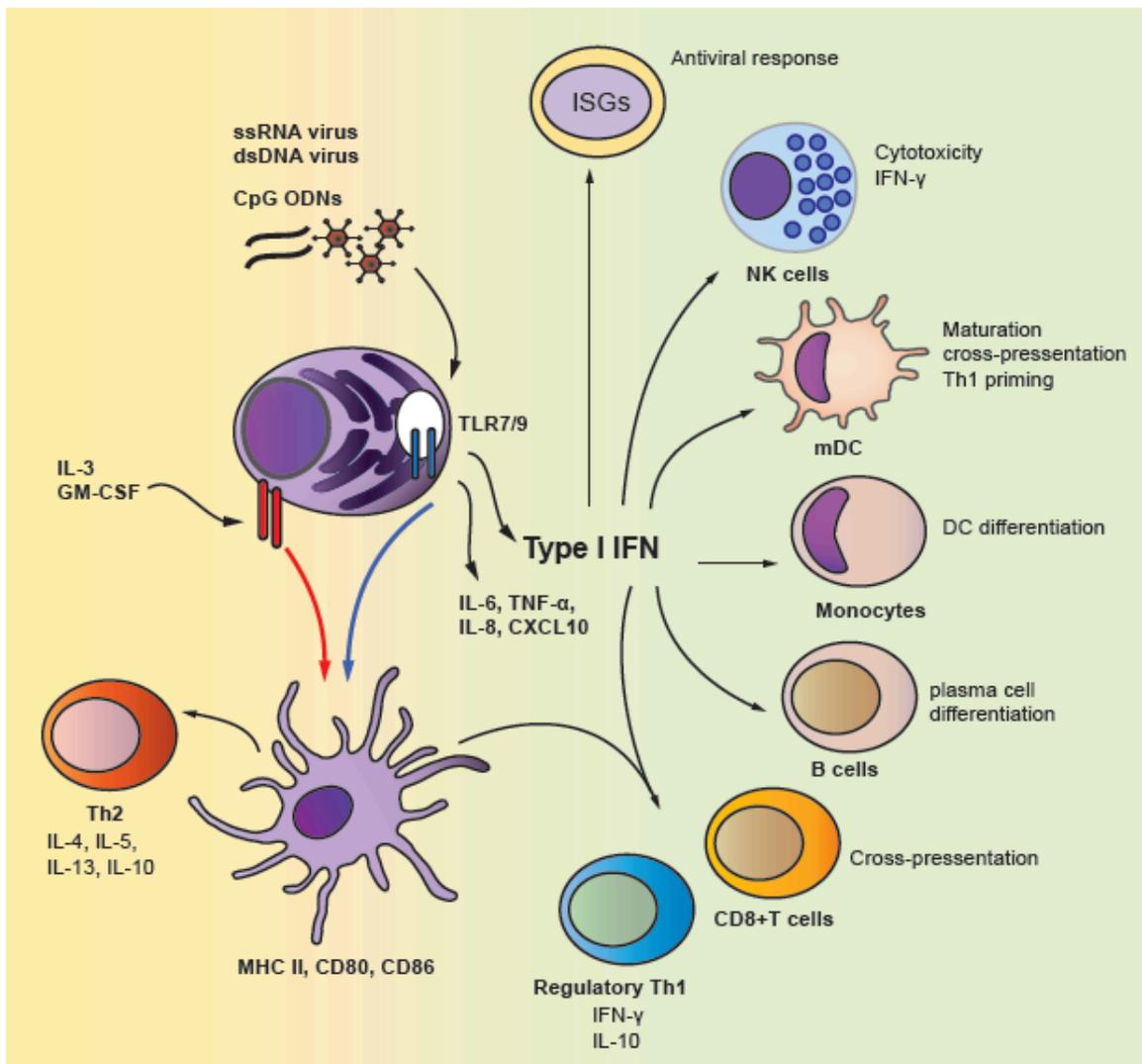
Figure 2
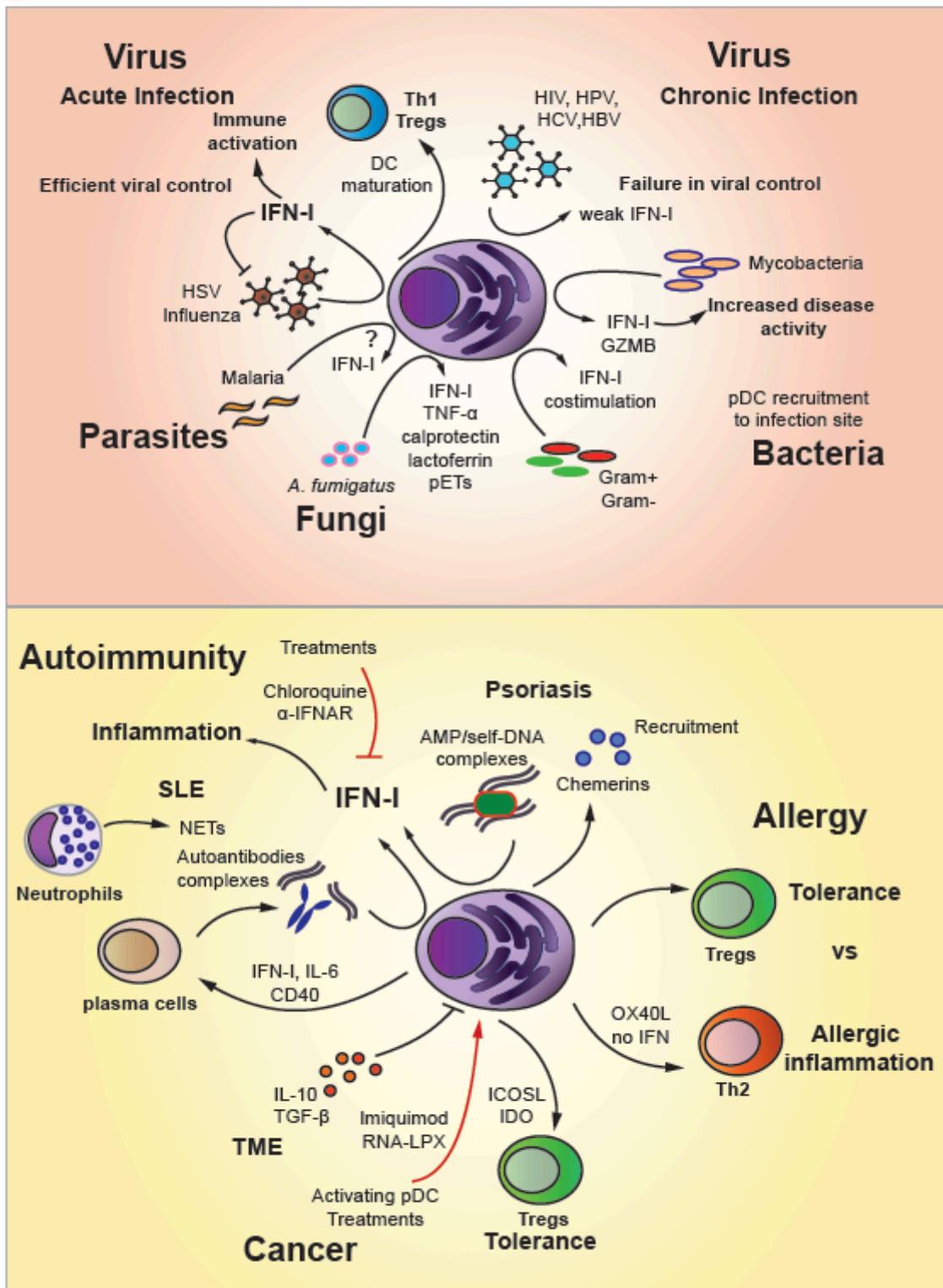
5.4 Anti-NKG2A mAb is a checkpoint inhibitor that promotes anti-tumor immunity by unleashing both T and NK cells

Personal implementation

During my PhD, I participated to an industrial collaboration with the company Innate Pharma located in Marseille. Together with Olivier Lantz and Ana Lalanne, we performed deep immune-monitoring of HNSCC and skin SCC samples and their paired juxtatumor, blood and draining lymph node from 26 patients, with the goal of identifying and quantifying immune targets and NK cell receptors in particular. Some results on 19 patients are presented in figure 4 of this paper.

Abstract

Immuno-oncology, including checkpoint inhibitors targeting the PD-1/PDL1 (PD-x) axis in particular, has revolutionized cancer treatment. However, only a minority of patients respond to these immunotherapies, and the development of drug resistance is frequent. Here, we report that the blocking of the inhibitory NKG2A receptor enhances tumor immunity by promoting both Natural Killer (NK) and CD8$^+$ T-cell effector functions in mice and humans. Monalizumab, a humanized anti-NKG2A antibody, enhanced NK cell activity against various tumor cells and rescued CD8$^+$ T-cell function in combination with PD-x axis blockade. Monalizumab also stimulated NK-cell activity against antibody-coated target cells. We also established proof-of-principle for the use of combined immunotherapy with monalizumab and cetuximab, in a phase II clinical trial for squamous cell carcinoma of the head and neck (SCCHN), in which the combination gave a better response rate than cetuximab alone. NKG2A targeting with monalizumab is thus a novel checkpoint inhibitory mechanism promoting anti-tumor immunity by enhancing the activity of both T and NK cells, which may complement the first-generation immunotherapies against cancer.

ANTI-NKG2A MAB IS A CHECKPOINT INHIBITOR THAT PROMOTES ANTI-TUMOR IMMUNITY BY UNLEASHING BOTH T AND NK CELLS

Pascale André[1], Caroline Denis[1], Caroline Soulas[1], Clarisse Bourbon[1], Julie Lopez[1], Thomas Arnoux[1], Mathieu Bléry[1], Cécile Bonnafous[1], Romain Remark[1], Violette Breso[1], Elodie Bonnet[1], Ana Lalanne[2], Caroline Hoffman[2,3], Olivier Lantz[2], Jérôme Fayette[4], Agnès Boyer-Chammard[1], Robert Zerbib[1], Pierre Dodion[1], Hormas Ghadially[5], Maria Jure-Kunkel[6], Ronald Herbst[6], Emilie Narni-Mancinelli[7], Roger B. Cohen[8], Eric Vivier[1,7,9*]

[1] Innate Pharma, Marseille, France

[2] Unité INSERM U932, Immunité et Cancer, Institut Curie, Paris, France.

[3] Service ORL et Chirurgie cervico-faciale, Institut Curie, Paris, France

[4] Centre Léon Bérard, Lyon, France

[5] MedImmune, Ltd, Aaron Klugg Building, Granta Park, Cambridge, UK

[6] MedImmune, LLC, One MedImmune Way, Gaithersburg, MD 20817 7 Aix Marseille Université, INSERM, CNRS, Centre d'Immunologie de Marseille-Luminy, Marseille, France

[8] Abramson Cancer Center, Philadelphia, PA, USA

[9] Service d'Immunologie, Marseille Immunopole, Hôpital de la Timone, Assistance Publique-Hôpitaux de Marseille, Marseille, France

* Correspondence: pascale.andre@innate-pharma.fr, eric.vivier@innate-pharma.fr,

Introduction

Immuno-oncology has revolutionized cancer treatment (Baumeister et al., 2016; Fridman et al., 2017; Schreiber et al., 2011; Schumacher and Schreiber, 2015; Sharma and Allison, 2015a, b). Unprecedented improvements in tumor control have been achieved by the use of therapeutic monoclonal antibodies (mAbs) that block immune inhibitory ('checkpoint') receptors. In particular, mAbs directed against the PD-1 (programmed-cell death protein 1)/PDL1 (programmed -cell death ligand 1) axis (PDx) in monotherapy or combination therapy have been approved for the treatment of several indications including metastatic melanoma, non-small cell lung cancer, kidney cancer, bladder cancer, oral cancer, Hodgkin lymphoma, and solid tumors that are microsatellite instability-high or mismatched repair-deficient. Such treatment often yields durable benefits and, in most patients, toxicity can be controlled. However, only a minority of the patients treated with antibodies specific for PD-1 or PDL1 display a strong response, and the cancers of a substantial fraction of patients are resistant to these immune checkpoint inhibitors (ICI). One of the major challenge in immuno-oncology is, therefore, understanding the mechanisms of resistance to ICI, to increase the proportion of patients benefiting from such treatment and to control treatment toxicity. One approach that could be used is to identify novel molecular targets, the modulation of which boosts anti-tumor immunity. Blocking inhibitory pathways of effector lymphocytes, such as T cells and NK cells, are attracting considerable research interest in this context.

Cell-surface receptors harboring intracytoplasmic tyrosine-based inhibitory motifs (ITIMs) are particularly relevant in this respect. These motifs are phosphorylated and recruit the phosphatases (SHP-1/2 or SHIP) responsible for transmitting the inhibition signal to immune effector cells (Daeron et al., 2008). Bioinformatics analyses of the human genome have predicted the presence of more than 300 type I and type II integral membrane proteins containing at least one ITIM domain (Daeron et al., 2008), but only a few of these receptors are currently targeted in therapeutic approaches.

NKG2A is an ITIM-bearing receptor expressed on both T and NK cells. NKG2A is expressed as a heterodimer with CD94 in humans and mice and recognizes the non-classical Class I major histocompatibility complex (MHC-I) molecules HLA-E in humans and Qa-1[b] in mice. The binding of NKG2A/CD94 to its cognate ligand inhibits T and NK cell effector functions (Le Drean et al., 1998; Rapaport et al., 2015). This inhibition is dependent on the recruitment of the SHP-1 tyrosine phosphatase to the tyrosine-phosphorylated form of NKG2A (Viant et al., 2014).

We show here, that NKG2A blockade enhances the anti-tumor immunity mediated by NK and CD8^{+} T cells. We developed a humanized anti-NKG2A IgG4 blocking mAb (monalizumab) and we describe its anti-tumor efficacy*, in vitro* and *in vivo* when used as a single agent or in combination with other therapeutic antibodies, such as durvalumab, blocking PDL1, or cetuximab, directed against EGFR expressed by tumor cells.

Results

NKG2A blockade promotes anti-tumor immunity

We assessed the impact of NKG2A on cytotoxic lymphocyte activity, by using BALB/c B cell lymphoma A20 cells, which express the non-classical MHC-I Qa-1^b molecule, the mouse homologue of HLA-E, and generating the corresponding Qa-1^b-knock-out cells (**Figure S1A**). The growth rates of parental and Qa-1^b-deficient A20 cells were similar *in vitro* (data not shown). As expected, the frequency of cytotoxic NKG2A$^+$ NK cells — assessed on the basis of the expression of CD107a, a degranulation marker — was higher in cocultures with Qa-1^b-deficient A20 cells than in cocultures with parental cells (data not shown). Following their subcutaneous injection into syngeneic BALB/c mice, wild-type A20 B-cell lymphoma cells grew progressively in all mice (**Figure 1A, left panel**). By contrast, 70% of the mice into which genetically engineered Qa-1^b-deficient A20 cells were injected did not display tumor growth (**Figure 1A, right panel**). Both NK cells and CD8$^+$ T cells were required to control tumor growth, because the administration of anti-asialo-GM1 and anti-CD8a antibodies, respectively, into tumor-bearing mice abolished the control of parental and Qa-1^b-deficient tumor growth and led to premature death (**Figures 1B and 1C**).

These results validate Qa-1^b as a potentially useful target. We then dissected the immune response to A20 in the tumor bed, by analyzing tumor-infiltrating lymphocytes (TILs). A20 tumors were found to be infiltrated with NK and CD8$^+$ T cells. As in the spleen, ~60% of NK TILs expressed the NKG2A receptor (**Figure 2A**). We also monitored PD-1 expression, because the immune control of A20 tumors has been reported to be partially dependent on PD-1 (Sagiv-Barfi et al., 2015). The expression of PD-1, either alone or together with NKG2A, was barely detectable on the surface of NK TILs. We did not observe NKG2A expression on the surface of CD8$^+$ T cells from the spleen, and few cells expressed PD-1 (~4%) (**Figure 2A**). However, PD-1$^+$ CD8$^+$ T cells accounted for ~44% of TILs. Importantly, NKG2A was also expressed on the surface of half the PD-1$^+$ CD8$^+$ TILs. In this model, we also observed that double-positive PD-1$^+$ NKG2A$^+$ CD8$^+$ TILs displayed higher levels of PD-1 and NKG2A expression at their surface than cells positive only for PD-1 or for NKG2A (**Figure 2A**). Very few CD8$^+$ TILs (~2%) expressed NKG2A without PD-1.

We then investigated whether NKG2A blockade could promote anti-tumor immunity. We generated a recombinant mouse version of the rat anti-NKG2A antibody, 20d5 (Vance et al., 1999). We confirmed that the blockade of NKG2A *in vitro* promoted the expression of CD107a by NK cells cocultured with Qa-1b$^+$ A20 tumors but not with Qa-1b$^-$ YAC-1 target cells (**Figure S1B**). When used as single agents *in vitro*, anti-NKG2A or anti-PDL1 mAbs only modestly improved *ex vivo* tumor-infiltrating CD8$^+$ T-cell effector activities after restimulation with A20 cells (**Figure S1C**). By contrast, the use of anti-NKG2A and anti-PDL1 mAbs in combination, increased the frequency of CD107a-expressing NKG2A$^+$ PD-1$^+$ CD8$^+$ TILs.

We further investigated the effects of immunotherapy with anti-NKG2A and anti-PDL1 antibodies by treating A20 tumor-bearing mice with anti-NKG2A mAb, anti-PDL1 mAb or a combination of these two blocking reagents (**Figure 2B**). In this experimental setting, anti-

NKG2A mAb did not rescue mice from death when used as a single agent when compared to control group. By contrast, anti-PDL1 mAb rescued ~40% of tumor-bearing mice from death, as shown by comparison with untreated mice. Interestingly, a combination of anti-NKG2A and anti-PDL1 mAbs had a synergistic effect, improving the control of tumor growth and rescuing ~60% of the mice from death (**Figure 2B)**. The results obtained for mice treated with anti-asialo-GM1 or anti-CD8a antibodies also demonstrated that the anti-tumor effect of the anti-NKG2A/PDL1 mAb combination therapy was dependent on both NK and CD8^{+} T cells (**Figure 2C**). Thus, the combination of an anti-NKG2A mAb with an anti-PDL1 mAb had a therapeutic anti-tumor effect, because it unleashed NK cells and CD8^{+} T cells in the A20 model Similar results were obtained with a combination of anti-NKG2A/PD-1 mAbs (**Figure S2**).

Combined blockade of NKG2A and PDL1 promotes the generation of protective anti-tumor memory

We investigated the anti-tumor therapeutic properties of the anti-NKG2A mAb further, by using this antibody to treat C57BL/6 mice bearing another tumor, subcutaneously injected RMA-Rae-1β T lymphoma. Like A20 cells, RMA-Rae-1β tumor cells express Qa-1[b] and PDL1 (**Figure S3**). The frequency of NKG2A^{+} NK cells in the tumor was higher than that in the spleen, but NK TILs did not express PD-1, as observed in the A20 model (**Figure 3A**). We found that ~21% of total CD8^{+} TILs expressed NKG2A but not PD-1, ~14% expressed both these molecules and ~21% expressed PD-1 but not NKG2A (**Figure 3A**). Anti-NKG2A mAb or anti-PDL1 monotherapy was not effective in RMA-Rae-1b tumor-bearing mice (**Figure 3B**). However, treatment with a combination of mAbs against NKG2A and PDL1 resulted in tumor growth control in 45% of the tumor-bearing mice, which were rescued from death. The combination therapy acted through the release of CD8^{+} T-cell but not NK cell inhibition, as the injection of a depleting anti-CD8a mAb but not anti-NK1.1 antibodies abolished tumor growth control and impaired mouse survival (**Figure 3C**).

We observed the generation of CD62L^{-} CD44^{+} effector memory CD8^{+} T cells in the spleens of mice in which RMA-Rae-1b tumors were implanted and then cured by immunotherapy, but not in the spleens of untreated mice (**Figure 3D**). Accordingly, RMA-Rae-1β tumor cells were completely rejected when injected into mice that had already been injected with the tumor and cured by treatment with anti-NKG2A and anti-PDL1 mAbs, whereas the injection of these cells led to unchecked tumor growth in untreated mice (**Figure 3D**). Therefore, in addition to curing mice of their implanted tumors, blocking NKG2A in combination with another ICI can promote durable protective anti-tumor CD8^{+} T-cell memory response in a preclinical mouse model.

HLA-E and NKG2A expression in human tumors

We then monitored the expression of NKG2A and HLA-E at the surface of several tumors, to identify the indications for which anti-NKG2A therapeutic blocking mAbs might promote anti-tumor immunity in cancer patients. HLA-E was found to be widely expressed on the surfaces of several human tumors. We observed HLA-E expression in lung, pancreas, stomach, colon, head and neck and liver tumor tissues (**Figure 4**). By contrast, PDL1 expression was

restricted to some lung, stomach and colon tissue tumors (**Figure S4**). HLA-E was strongly expressed by SCCHN and colorectal carcinoma (**Figure 4A and B**), in which we also detected NKG2A-positive cells. NKG2A-positive cells and HLA-E expression were also found in ovarian, endometrial and cervical cancers (**Figure 4B**). NKp46$^+$ NK (**Figure 4B**) and CD8$^+$ TILs were also present in all these tumors. We investigated SCCHN more closely by flow cytometry and detected high frequencies of CD8$^+$ TILs expressing PD-1 and co-expressing both PD-1 and NKG2A in the tumor (**Figure 4C**). NKG2A-expressing NK cells were also present at high frequency, and some of these cells had a PD-1$^+$ NKG2A$^+$ phenotype. Similar results were obtained for CRC and lung tumors (data not shown). Thus, several tumors expressed HLA-E and were infiltrated with NK and CD8$^+$ TILs expressing NKG2A. We therefore reasoned that NKG2A blockade, either alone or together with the use of other checkpoint inhibitors, such as anti-PD-1/PDL1 antibodies, might improve the anti-tumor efficacy of NK and CD8$^+$ TILs in cancer patients.

Generation and characterization of a chimeric blocking mAb directed against human NKG2A

A murine anti-human NKG2A IgG1 monoclonal antibody clone, Z270, was generated in a previous study (Sivori et al., 1996). We humanized this antibody by fusion with an IgG$_4$ with a single point mutation in the Fc heavy chain to prevent the formation of half-antibodies and screened the selected humanized clones for binding to CD94-NKG2A with an affinity similar to that of the original murine monoclonal antibody. The selected humanized clone was named monalizumab (IPH2201/NNC141-0100). Importantly unlike other anti-NKG2A mAbs described to date, monalizumab is specific for human NKG2A, as it bound human NKG2A$^+$ cells, but not Ba/F3 transfected cells expressing human NKG2C, the activating isoform of NKG2A **(Figure S5A**). The EC$_{50}$ calculated by whole blood titration was 4.5 ng/ml for NKG2A$^+$ NK cells and 11.4 ng/ml for NKG2A$^+$ CD8$^+$ T cells (**Figure S5B**). Finally, another critical feature of monalizumab resided in its capacity to inhibit the binding of HLA-E tetramers to human NK cells expressing NKG2A (**Figure S5C**).

Monalizumab promotes the anti-tumor cell activities of human NK cells and CD8$^+$ T cells

We then sought to assess the blocking activity of monalizumab on effector cells, by monitoring the production of CD107 by NKG2A$^+$ NK cells cocultured with K562 tumor target cells expressing HLA-E (**Figure 5A**). The prototypic K562 cells, which lack HLA-E, activated NK cells, but forced HLA-E expression decreased the frequency of CD107$^+$ NKG2A$^+$ NK cells. The addition of monalizumab to the assay restored the production of CD107 by NKG2A$^+$ NK cells to the levels observed with parental K562 targets. We then assessed the anti-tumor efficacy of monalizumab in co-cultures of NK cells with tumor cell lines with different levels of HLA-E expression (**Figure S6**). Monalizumab increased the frequency of activated NKG2A$^+$ NK cells, as assessed by measuring the cell-surface induction of CD107 and CD137 (4-1BB), an activation-induced costimulatory molecule, in co-cultures with three different SCCHN cell lines and three different ovarian tumor cell lines, although this stimulation was weaker for the CAL-27 and Caov-2 cell lines (**Figure S6**).

The anti-NKG2A mAb and the anti-PDL1 mAb had synergistic effects in our preclinical mouse tumor models. We therefore assessed the effects of a combination of the anti-human NKG2A mAb monalizumab and the anti-human PDL1 mAb durvalumab on NK cell activity against K562 cells co-expressing HLA-E and PDL1 *in vitro*. NKG2A$^+$ PD-1$^+$ NK cells were generated by chronically stimulating various donor PBMCs with IL-15 (**Figure 5B**). The anti-NKG2A monalizumab, used as a single agent, increased the frequencies of CD107$^+$ NKG2A$^+$ PD-1$^-$ NK cells in cocultures with K562-HLA-E or K562-HLA-E PDL1 cells (**Figure 5C**). Addition of the anti-PDL1 antibody durvalumab did not improve NK-cell reactivity in this assay. When used as a single agent, monalizumab also improved CD107 expression by NKG2A$^+$ PD-1$^+$ NK cells cocultured with K562-HLA-E targets. The use of monalizumab or durvalumab as single agents only modestly increased the reactivity of NKG2A$^+$ PD-1$^+$ NK cells cocultured with K562-HLA-E PDL1 cells, whereas these two antibodies had additive effects when used in combination. Thus, monalizumab efficiently released the inhibition conferred by the engagement of the inhibitory receptor NKG2A. In combination with other ICI, monalizumab has additive effects, promoting NK-cell effector functions.

We assessed the boosting effect of monalizumab on CD8$^+$ T-cell functions in more detail because, in our preclinical model, many CD8$^+$ TILs expressed NKG2A (**Figures 2A and 3A**). We aimed to generate antigen-specific NKG2A$^+$ CD8$^+$ T cells *in vitro* through chronic stimulation with IL-15, monocytes and antigenic peptides derived from human influenza virus (Flu) (**Figure 5D**). The Flu-specific CD8$^+$ T cells obtained after nine days of culture harbored different phenotypes. In addition to PD-1$^+$ NKG2A$^-$ Flu-specific CD8$^+$ T cells, a substantial fraction of the Flu-specific CD8$^+$ T cells co-expressed PD-1 and NKG2A (**Figure 5D**). Cells were then cocultured with Flu peptide-pulsed K562-HLA-A2 cells expressing or not expressing the inhibitory ligands HLA-E and PDL1. The addition of monalizumab or durvalumab modestly increased the frequency of CD107$^+$NKG2A$^+$ Flu-specific-CD8$^+$ T cells (**Figure 5E**). However, the combination of monalizumab with durvalumab improved CD8$^+$ T-cell activity. Thus, monalizumab can promote activation and effector functions of both NK cells and CD8$^+$ T cells, and this effect is more marked when it is used in combination with durvalumab.

Monalizumab promotes human NK-cell antibody-dependent cell-mediated cytotoxicity (ADCC)

Blockade of the NKG2A/Qa-1 axis added with PD-1/PDL1 blockade to boost NK-cell cytotoxicity. We then evaluated the potential of monalizumab to promote NK-cell effector functions when combined with other commonly used anti-tumor reagents, such as those promoting ADCC (**Figure 6**). The anti-epidermal growth factor (EGF-R) mAb cetuximab is used to treat advanced and recurrent and/or metastatic SCCHN and metastatic CRC (Ferris et al., 2018). Cetuximab mobilizes adaptive and innate immunity against tumor cells, partly by promoting ADCC (Ferris et al., 2018). HLA-E membrane expression in CRC could inhibit cetuximab-mediated cellular cytotoxicity (Levy et al., 2009). We used a combination of monalizumab and cetuximab to stimulate NK cells against an SCCHN cell line *in vitro* (**Figure 6A**, left panel), and the induction of CD137 as a marker of NK cell activation including ADCC. This combination of antibodies amplified the anti-tumor efficacy of NK cells, as shown by the higher frequencies of CD137$^+$ NK cells. Monalizumab also enhanced the NK cell-mediated ADCC by the anti-CD20 mAb obinutuzumab in cocultures with B cell lines

expressing MHC class I (**Figure 6A**, right panel). Thus, the anti-NKG2A mAb monalizumab can amplify the beneficial effects of other IO treatments, such as those promoting ADCC.

In vivo tumor control by a combination of monalizumab and cetuximab in patients with SCCHN

We found that combinations of NKG2A-blocking mAbs with other IO treatments, such as anti-PD-1 mAbs, anti-PDL1 mAbs or cetuximab, had additive effects on anti-tumor immunity in preclinical experimental settings *in vitro* and *in vivo*. These results provide a scientific rationale for evaluations of the efficacy and safety of monalizumab in cancer patients. SCCHN tumors were strongly positive for HLA-E and were infiltrated with CD8+ T cells and NK cells, which may express NKG2A (**Figures 4A-C**). Cetuximab is used in the standard care regimen for SCCHN. We therefore assessed the safety and efficacy of the combination of monalizumab and cetuximab in patients with previously treated recurrent or metastatic (R/M) SCCHN in a phase II clinical trial (NCT02643550). We evaluated five doses of monalizumab (0.4, 1, 2, 4, 10 mg/kg every 2 weeks) in combination with the approved dose of cetuximab (400 mg/m² loading dose and then 250 mg/m² weekly). The maximum tolerated dose was not reached and the highest dose of monalizumab tested (10 mg/kg) was used for expansion of the phase II cohort. We used a one-stage Fleming design with futility analysis after the first 11 patients; the overall phase II study will include 40 patients. The characteristics of the patients are shown in **Table 1**. As of March 9, 2018, thirty-one patients with R/M SCCHN were treated and evaluable for safety, of which 26 patients to date are evaluable for efficacy and remaining patients were studied too early for baseline assessment. All 31 patients had been previously treated with platinum-based chemotherapy, and 24 patients received one or two systemic treatment regimens. Fourteen patients had already received IO, and three had been already treated with cetuximab for locally advanced disease and had been free from progressive disease for at least four months. Safety was the primary endpoint of the part I and objective response rate (ORR) of this part II. The combination was well tolerated. Most of the adverse events (AE) observed (93%) were of grade 1-2 severity, rapidly reversible and easily manageable. The most common monalizumab-related AEs were fatigue (17%), pyrexia (13%) and headache (10%). The most frequent AEs reported for cetuximab in previous studies (7) were skin disorders (rash 49%, acne 26%, nail disorders 16%, dry skin 14%), and these effects were not exacerbated by monalizumab. No infusion-related reactions were observed (patients received premedication for cetuximab as specified on the label). No treatment-related deaths were reported. No new or unusual signs suggestive of poor safety were observed with the combination of monalizumab and cetuximab. We thus concluded that the safety profile of the combination was similar to that for the two single agents.

Interim treatment efficacy results for the phase II trial showed that treatment with the monalizumab and cetuximab combination resulted in a confirmed RECIST partial response in 8 of 26 patients (31%), stable disease (SD) in 14 of 26 (54%) and progressive disease (PD) in 3 of 26 (11%) patients and one patient died from progressive disease at week 8 without post-baseline imaging **(Figure 6B-D)**. The lesion disappeared in one patient, as shown in **Figure 6D**. Assuming an ORR of 25%, using 10% as the cutoff for inactivity, α =0.05, and a power of 0.76, the predefined number of eight responses required to declare a positive result for the trial has already been reached. Two of the eight patients with confirmed responses

had previously received immunotherapy. The median response duration was not reached; six responding patients were still on treatment. Median follow-up time was 129 days: 17 patients (55%) were still on treatment, 14 patients (45%) had stopped treatment, due to progressive disease in 12 (38%), and adverse event in one and on the decision of the investigator in the final case Overall, these data showed that the combination therapy of monalizumab with cetuximab has promise for the treatment of patients with SCCHN with exptected toxicity profile of either agent alone.

Discussion

Immuno-oncology is an emerging field that has revolutionized cancer treatment. Immune checkpoint inhibitors have greatly improved the control of several types of cancer, but there is a need to improve the efficacy of these treatments further, and to control their toxicity. One way of achieving this goal would be to identify critical immune checkpoints other than PD-1 and CTLA-4 for targeting by therapeutic antibodies to promote effective immune responses to cancers. Most immunomodulatory strategies to date have focused on enhancing T-cell responses, but there has been a recent surge of interest in harnessing the relatively underexplored natural killer (NK) cell compartment for therapeutic interventions (Cerwenka and Lanier, 2018; Guillerey and Smyth, 2016; Rautela et al., 2018; Vivier et al., 2012). The manipulation of NK cells in cancer is designed to initiate a multilayered immune response culminating in protective and long-lasting immunity to tumors based on a number of different cell types, including T cells.

We focus here on the NKG2A receptor, a well-known ITIM-bearing inhibitory receptor expressed on both T and NK cells (Moretta et al., 2001), emitting inhibitory signals transduced via the protein tyrosine phosphatase SHP-1 (Viant et al., 2014). The abundance of $NKG2A^+CD8^+$ T cells is low in human blood, but NKG2A expression can be induced at the surface of $CD8^+$ T cells upon activation (Braud et al., 2003). The targeting of NKG2A with a monoclonal blocking antibody would therefore have the unique advantage of enhancing T- and NK cell responses. Another advantage of targeting NKG2A is the safety of this approach, as no abnormalities have been reported in mouse strains lacking CD94 (Vance et al., 1999), which forms a heterodimer with NKG2A. These mice therefore lack cell-surface NKG2A expression.

One critical point for such an approach is the expression of NKG2A and HLA-E during cancer. We have shown that the NKG2A receptor is expressed on NK and T cells in the tumor bed in many human cancers and we have also shown that its ligand, HLA-E, is frequently overexpressed in tumors. By contrast, classical MHC-I expression is often weak on tumor cells, and this downregulation has been recognized as a major mechanism by which tumor cells escape T-cell control (Garrido et al., 2017; Sharma et al., 2017). Unlike classical HLA class I molecules, HLA-E continues to be expressed on the surface of tumor cells, sometimes even more strongly than on healthy cells, in 50–80% of patients with solid tumors or leukemia/lymphoma (Benson et al., 2012; Mamessier et al., 2011; Platonova et al., 2011; Talebian Yazdi et al., 2016). This conservation of expression likely results from the dependence of cell-surface HLA-E expression on the leader peptides of HLA-A, B or C. Downregulation therefore would require the elimination of three types of HLA molecule. Our data for NKG2A expression are consistent with earlier reports on tumor-infiltrating NK and T cells in melanoma, breast and cervical cancers (Mamessier et al., 2011; Sheu et al., 2005).

One of the key findings of our studies is the demonstration that NKG2A is often co-expressed with PD-1 on $CD8^+$ T cells. PD-1 expression is a hallmark of exhausted $CD8^+$ T cells (Hashimoto et al., 2018). This result therefore suggested that NKG2A expression might constitute an additional brake on release, for reversing $CD8^+$ T-cell exhaustion. The regulation of NKG2A expression on both NK and $CD8^+$ T cells remains to be dissected in detail. Nevertheless, unlike PD-1 expression, which can be observed on the surface of $CD8^+$

T cells from whole blood or lymph nodes from cancer patients, NKG2A-expressing CD8^{+} T cells are found selectively localized in the tumor bed or adjacent tissue. These results suggest that signals derived specifically from the tumor would be required to induce, or, more probably, to sustain NKG2A expression.

We also found that HLA-E was more frequently expressed than PDL1 in several types of cancer. This finding is consistent with previous suggestions that HLA-E expression may account for some of the lack of responsiveness to anti-PDx observed in Merkel cell carcinoma (Paulson et al., 2018) and in an *in vivo* CRISPR screening program that identified Qa-1[b] (the mouse HLA-E ortholog) as a cancer immunotherapy target, because Qa-1[b] loss-of-function increased the efficacy of immunotherapy by PD-1 blockade (Manguso et al., 2017). These data support the use of a combination of monoclonal antibodies blocking the PDx and NKG2A:HLA-E inhibitory pathways. Our results for mice indicate that NKG2A pathway blockade does indeed improve tumor control when combined with a blockade of the PD-1/PDL1 inhibitory pathway. We also demonstrated the generation of protective memory CD8^{+} T cells in mice into which RMA-Rae-1β tumors were implanted and then cured by combined PDL1 and NKG2A blockade. Thus, our preclinical results provide a rationale for combining monalizumab and durvalumab into a novel immunotherapy for cancer patients. Importantly, such a clinical trial is ongoing (NCT02671435) and very recently preliminary safety and efficacy data were reported (Segal et al., 2018). Briefly, the dose escalation part of the study demonstrated the feasibility of combining the two agents with no new safety signals noted beyond the known safety profile for each individual agent. The initial clinical activity data from a cohort expansion in pretreated (median of three previous lines of systemic therapy) microsatellite stable colorectal cancer (MSS CRC; n=39) demonstrated an ORR of 8% (median duration of response of 16.1 weeks) and a disease control rate (DCR) at 16 weeks of 31% (Segal et al., 2018). Although these results are very preliminary, they are an example of potential therapeutic opportunities for immunotherapy in MSS CRC, a setting where immune checkpoint-based therapy has so far failed to demonstrate any consistent and meaningful clinical benefit.

Combining a blockade of inhibitory signals with the delivery of activating signals should improve the efficacy of immunotherapies. Many possible approaches of this type are being tested, including the triggering of innate immunity via the delivery of TLR ligands (Du et al., 2016), activation of the STING pathway at the tumor bed (Corrales et al., 2016), treatment with antibodies targeting activating cell surface receptors (Callahan et al., 2016; Muntasell et al., 2017) and the use of engineered forms of cytokines, such pegylated IL-2 (Charych et al., 2017; Charych et al., 2016), and IL-2 variants (Sockolosky et al., 2018). Antibodies directed against tumor cells could also be used to stimulate the immune response to tumor cells, thereby helping to eliminate cancer. The mode of action of these treatments differs between antibodies, but efficacy is partly dependent on ADCC, as for rituximab, an anti–CD20 mAb used to treat non-Hodgkin lymphoma and chronic lymphocytic leukemia (Cartron and Watier, 2017). Other antibodies are also used to stimulate the immune system via ADCC. One such antibody is cetuximab, which is used in metastatic CRC and SCCHN. We showed *in vitro* that NKG2A blockade with monalizumab boosts NK cell-mediated ADCC against cetuximab-coated SCCHN tumor cells. Consistent with these data, treatment with a combination of monalizumab and cetuximab was found to be potentially effective and expected toxicity profile in a phase II clinical trial for SCCHN. These encouraging results require consolidation in further clinical trials, but they constitute a key step towards the use of monalizumab in

combination treatments against cancer, and are consistent with the improvement in tumor control achieved by NKG2A blockade, through the activation of NK cells via ADCC.

In conclusion, we report here the full characterization of a first-in-class immune checkpoint inhibitor, monalizumab. This therapeutic antibody has several key features. First, it enhances the antitumor activities of both T and NK cells, by blocking the inhibitory function of NKG2A, which forms heterodimers on both NK cells and CD8$^+$ T cells. Second, the ligand of NKG2A is the non-classical MHC class I molecule HLA-E, which is frequently overexpressed on human tumors, providing a mechanism of resistance to lymphocyte activation in the tumor bed. Third, monalizumab is well-tolerated in humans and has yielded encouraging efficacy results in clinical trials assessing its use in combination with cetuximab in SCCHN, and in combination with durvalumab in MSS CRC, two clinical conditions with low ORRs, for which no major response is observed in many patients. Anti-NKG2A mAb is, therefore, a promising checkpoint inhibitor that promotes antitumor immunity by enhancing the activities of both T and NK cells. Interestingly, NKG2A has been shown to contribute to the inhibition HIV-infected target cell clearance by NK cells (Ramsuran et al., 2018). The therapeutic blockade of HLA-E:NKG2A interaction by monalizumab may, therefore, be beneficial in patients with HIV disease, in addition to those with cancer.

Figures
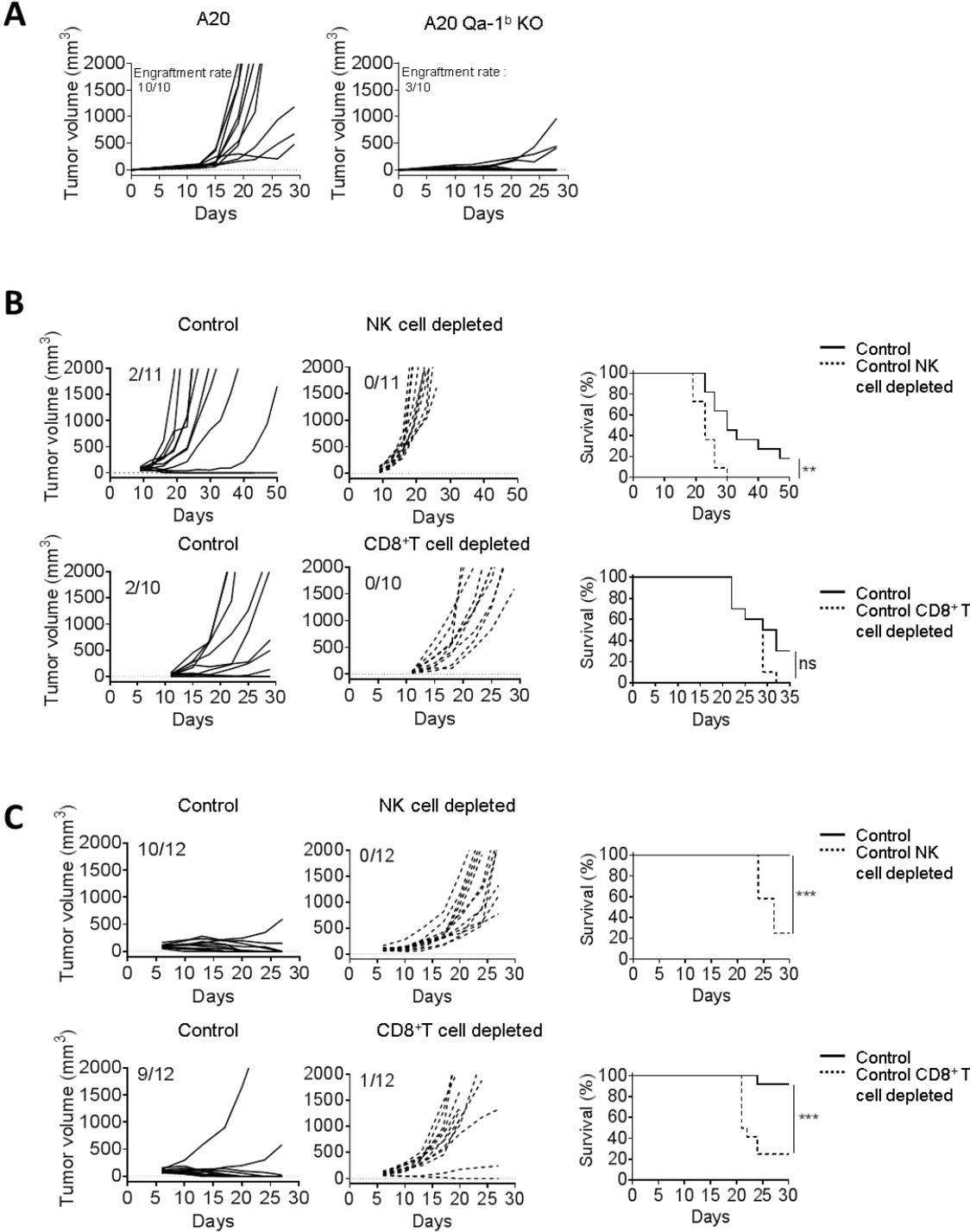
André et al., Fig. 1

Figure 1. NKG2A is an inhibitory receptor that blocks the anti-tumor efficacy of NK and CD8^{+} T cells

(**A**) Qa-1[b]-sufficient or -deficient A20 tumor cells were engrafted subcutaneously in BALB/c mice. Effective engraftment was quantified by measuring tumor volumes.

(**B**) BALB/c mice were left untreated or treated with an anti-asialo-GM1 pAbs to deplete NK cells or an anti-CD8a mAb to deplete CD8^{+} T cells and then subcutaneously engrafted with A20 tumor cells. Graphs show tumor growth in each individual and combined survival curves. Complete regressions are indicated. Log-rank test, **p=0.0020, ns: no significant.

(**C**) Experiment similar to that in (**B**), but with Qa-1[b] KO A20 tumor cells. Log-rank test, ***p=0.0002 (NK cell depletion) and ***p=0.0006 (CD8^{+} T cell depletion).
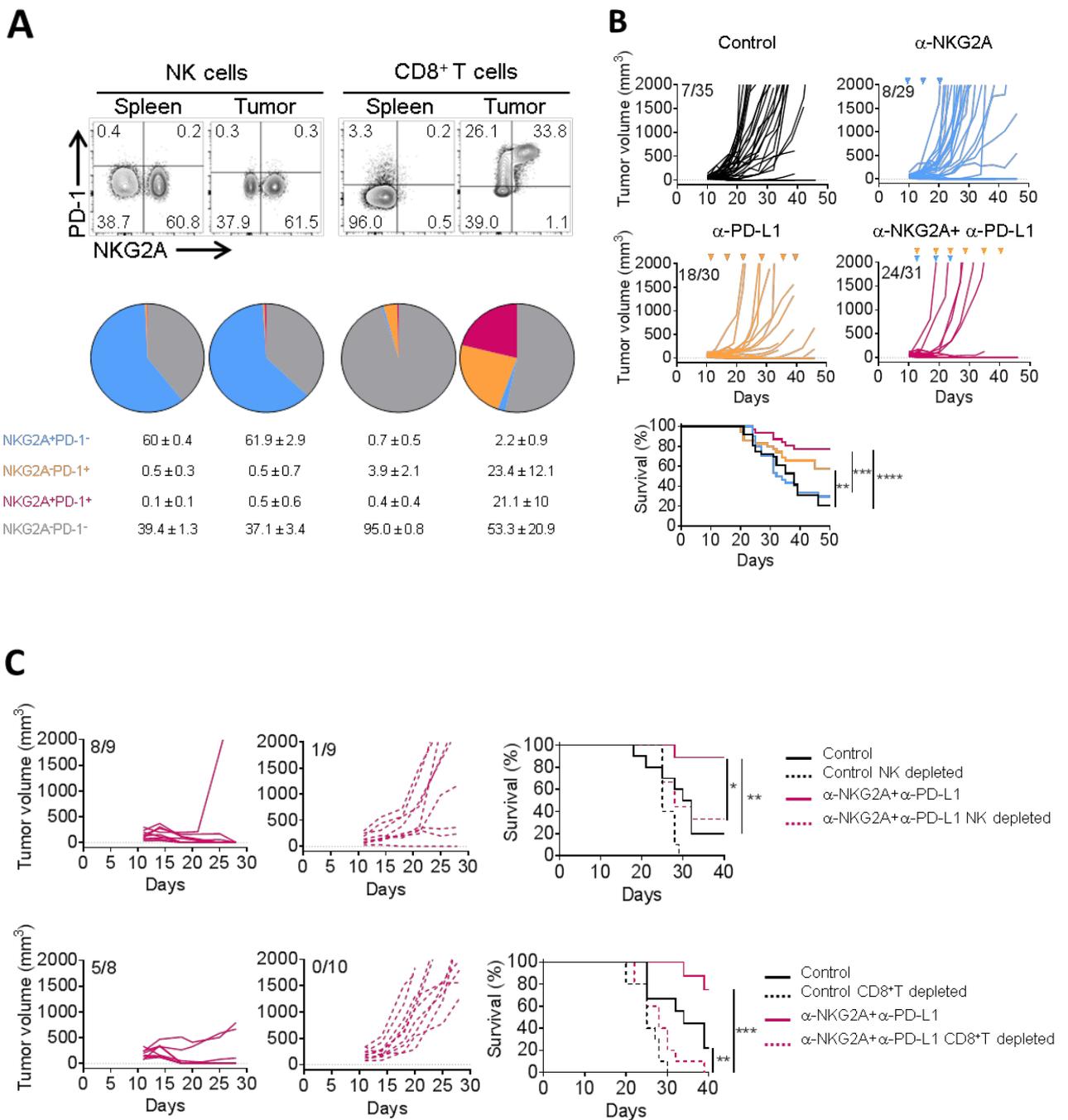
Figure 2. The combined blockade of NKG2A and PD-1/PDL1 promotes anti-tumor immunity in A20 tumor-bearing BALB/c mice

(**A**) Flow cytometry characterization of NK and CD8^{+} TILs 19 days after the injection of A20 tumor cells. The spleen was used as the standard. Upper panels: representative FACS profiles of PD-1 and NKG2A expression at the surface of NK and CD8^{+} T cells in the spleen and the tumor bed. Lower panels: Pie chart analysis (mean ±SD). The data presented are the pooled results of three independent experiments (*n*=12).

(**B**) A20 tumor cells were engrafted in BALB/c mice. Tumor-bearing mice were then treated at three- to four-day intervals with isotype control (IC) antibody, anti-NKG2A antibody, anti-PDL1 antibody or a combination of these last two antibodies. Graphs show tumor growth in each individual and combined survival curves. The data presented are the pooled results of three independent experiments. Log-rank test, ***p=0.0087, ***p*=0.0001, ****p*<0.0001.

 (**C**) Experiment similar to that described in (**B**) but with treatment of the mice with an anti-asialo-GM1 pAbs or an anti-CD8a mAb one day before the initiation of immunotherapy. Graphs show tumor growth in each individual and combined survival curves. Log Rank test, *p<0.0016, ***p<0.01, ***p*=0.0001.
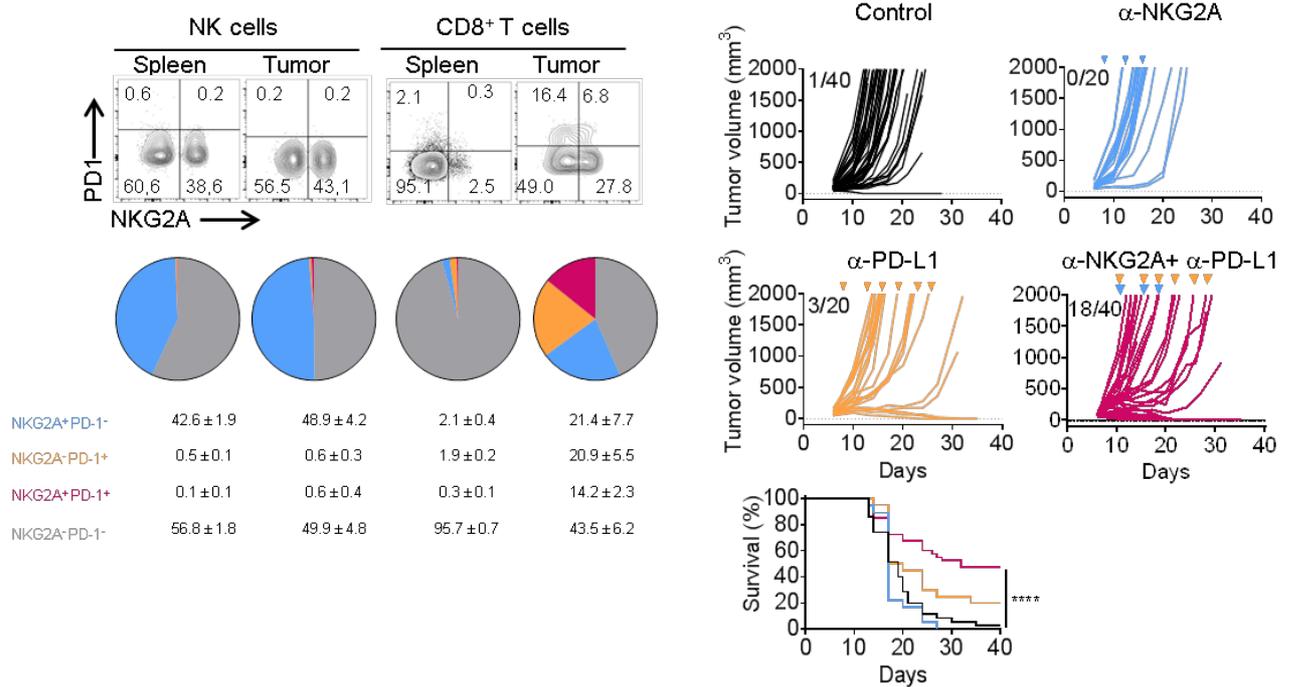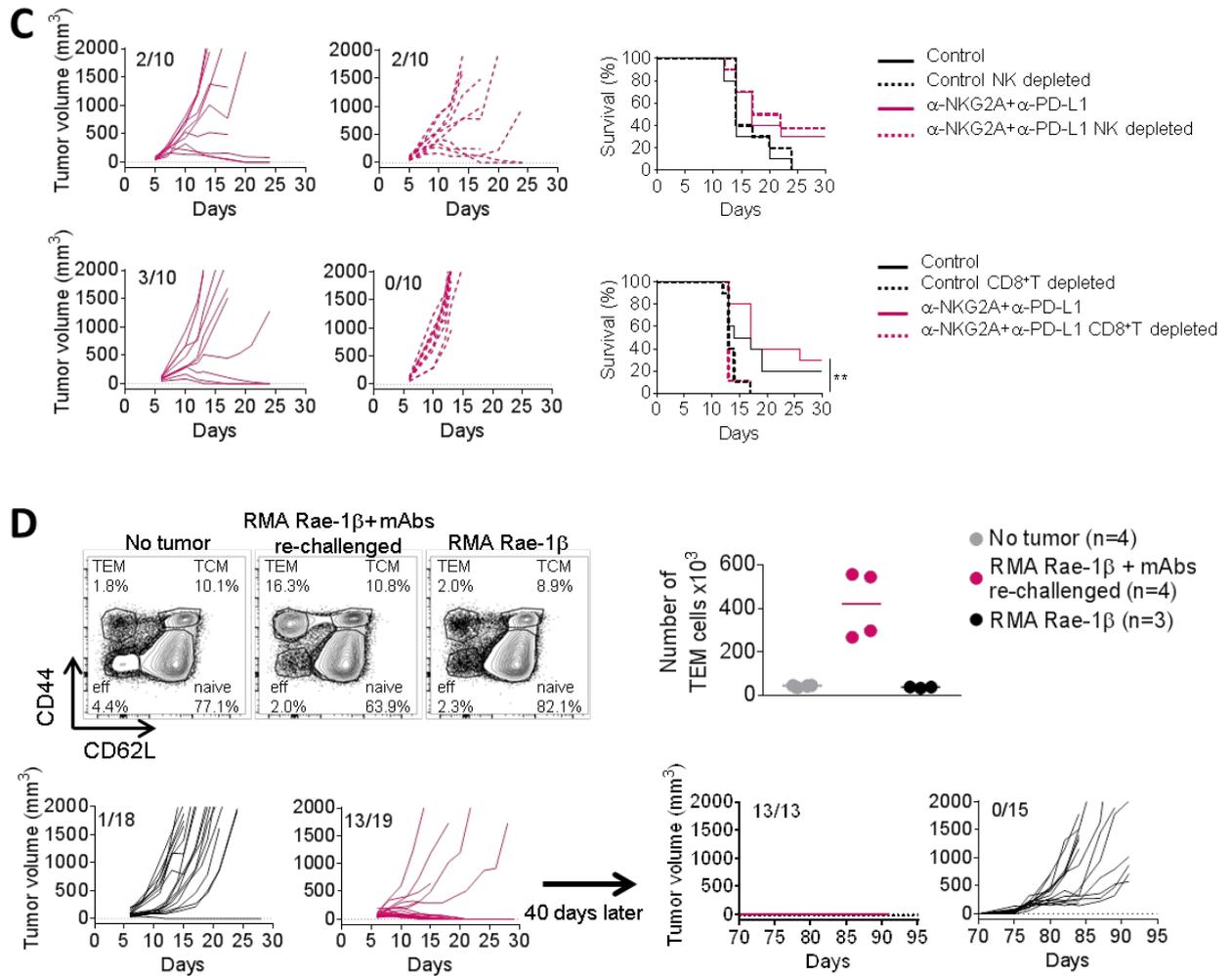
Figure 3. The combined blockade of NKG2A and PD-1/PDL1 promotes anti-tumor immunity in RMA Rae-1β tumor-bearing C57BL/6J mice.

(**A**) RMA Rae-1β tumor cells were injected subcutaneously into C57BL/6J mice. Flow cytometry characterization of NK and CD8^{+} TILs 12 days post-injection, with the spleen used as the standard. Upper panels: representative FACS profiles of PD-1 and NKG2A expression at the surface of NK and CD8^{+} T cells in the spleen and the tumor bed. Lower panels: Pie chart analysis (mean ±SD). The data presented are the pooled results of two independent experiments (*n*=8 mice).

(**B**) RMA Rae-1β tumor-bearing C57BL/6J mice were treated with IC antibodies, anti-NKG2A, anti-PDL1 mAbs or a combination of these last two antibodies, as indicated. Graphs show tumor growth in each individual and combined survival curves. The data presented are the pooled results of four independent experiments. Log-rank test, *****p*<0.0001.

(**C**) Experiment similar to that in (**D**), except that the mice were treated with anti-NK1.1 mAb or anti-aCD8a mAb one day before the initiation of immunotherapy. Graphs show tumor growth in each individual and combined survival curves. Log-rank test, ***p*=0.0024.

(**D**) Upper left panels: FACS profiles of CD44 and CD62L expression on the surface of CD8^{+} T cells in the spleen of naive (no tumor) mice, mice receiving their first injection of RMA Rae-1β tumor cells (RMA Rae-1β) and mice previously injected with RMA Rae-1β tumors, cured

by immunotherapy and re-challenged (RMA Rae-1β + mAbs re-challenged). Percentages of naive (CD44⁻CD62L⁺), central memory (TCM, CD44⁺CD62L⁺), effector memory (TEM, CD44⁺CD62L⁻) and effector CD8⁺ T cells (eff, CD44⁻CD62L⁻) are indicated. Upper right panel: Absolute numbers of effector memory CD8⁺ T cells in the spleen are shown. Lines represent medians. Lower panels: RMA Rae-1β tumor-bearing C57BL/6J mice were treated with IC antibody or with a combination of anti-NKG2A and anti-PDL1 mAbs. Mice cured by immunotherapy (*n*=13) were re-challenged subcutaneously with RMA-Rae-1β tumor cells after 70 days. Untreated C57BL/6J mice (*n*=15) also received injections of RMA-Rae-1β cells as a control. The graphs show tumor growth in each individual. The data presented are the pooled results of two independent experiments.
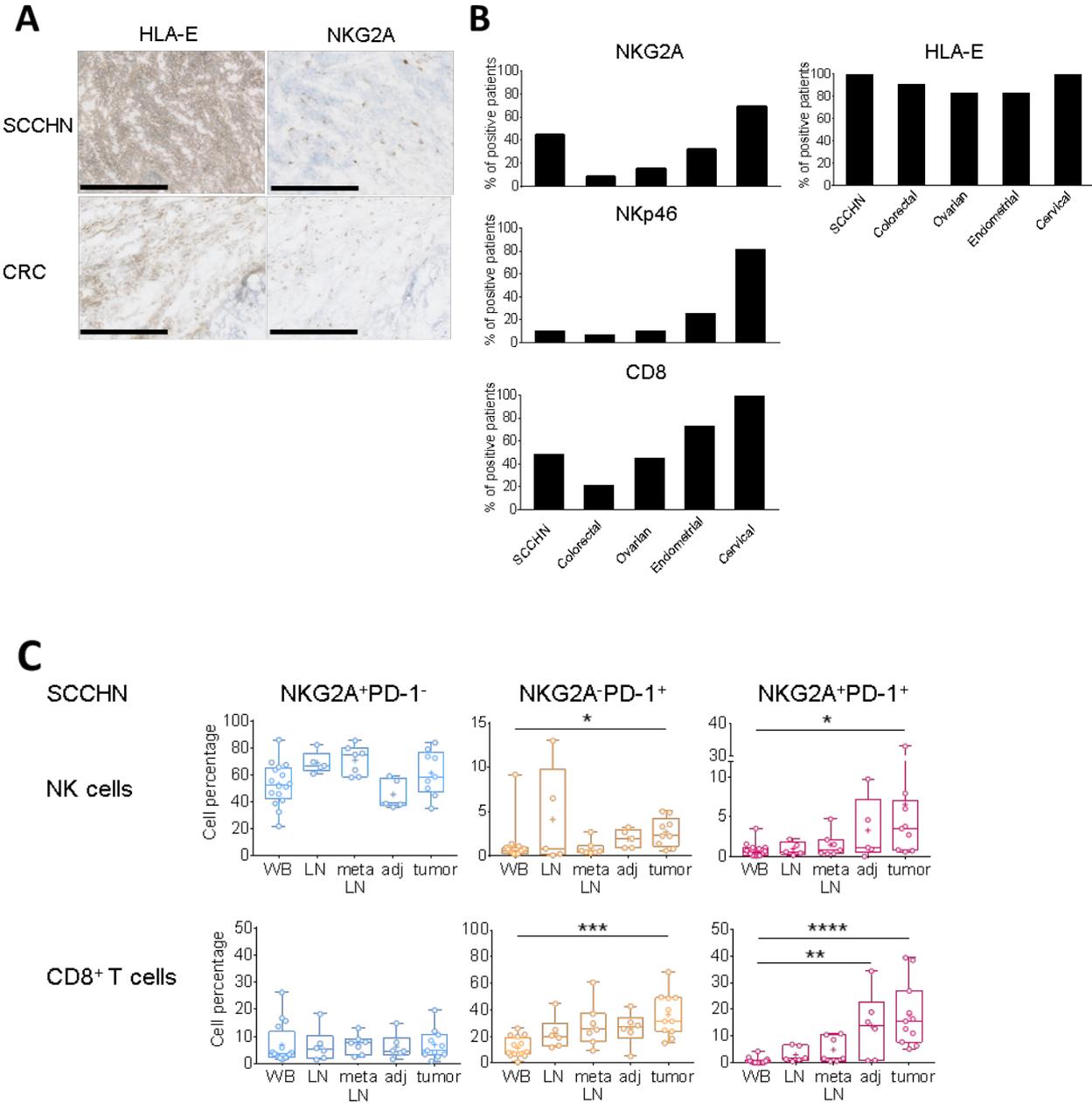
Figure 4. CD8$^+$, NKp46$^+$ or NKG2A$^+$ immune cells are present in several types of HLA-E-expressing solid cancers

(**A**) Representative example of HLA-E and NKG2A expression on frozen sections from head and neck (SCCHN) and colorectal (CRC) cancer samples. Scale bars correspond to 250 µm.

(**B**) Semi-quantitative analysis of NKG2A-, NKp46-, and CD8-positive cells and of HLA-E expression on frozen human cancer samples. SCCHN (*n*=23), colorectal cancer (*n*=48), ovarian cancer (*n*=40), endometrial cancer (*n*=40) and cervical cancer (*n*=17). CD8, NKp46 and NKG2A cells were quantified in the tumor bed. HLA-E expression was assessed on the surface of cancer cells.

(**C**) Percentages of NK cells (upper panels) and CD8$^+$ T cells (lower panels) expressing NKG2A and PD-1 in SCCHN cancer samples. Cells from WB (whole blood, *n*=16), LN (normal lymph node, *n*=5), meta LN (metastatic lymph node, *n*=7), Adj (healthy tissue adjacent to the tumor, *n*=5) and tumor (*n*=9) were analyzed by flow cytometry. Box and whiskers plot, in which the means are indicated by crosses. Kruskal-Wallis analysis followed by Dunn's multiple comparisons test. * $p<0.05$, ** $p≤0.001$, ****$p<0.0001$.

Patients characteristics for FACS analysis Fig 4.C

Patient Characteristics N=19		N (%)
Age, median [range]		65 [51-94]
Sex	Female	5 (26%)
	Male	14 (74%)
HPV status	Positive	4 (21%)
	Negative	11 (58%)
	To be determined	5 (26%)
Tobacco	Never	4 (21%)
	Former	3 (16%)
	Current	10 (53%)
Tumor site	Oral cavity	6 (31%)
	Oropharynx	2 (11%)
	Larynx	3 (16%)
	Hypopharynx	2 (11%)
	Cutaneous	6 (31%)
History of radiotherapy (overall)	Yes	10 (53%)
	No	9 (47%)
Systemic therapy (last 6 months)	Platinum	2 (11%)
	IO	3 (16%)
	Cetuximab	1 (5%)
	Nivo+Iiri	1 (5%)

A NKG2A⁺ NK

B Day 0 / Day 9

C NKG2A⁺ PD-1⁻ / NKG2A⁺ PD-1⁺

D

E NKG2A⁻ / NKG2A⁺
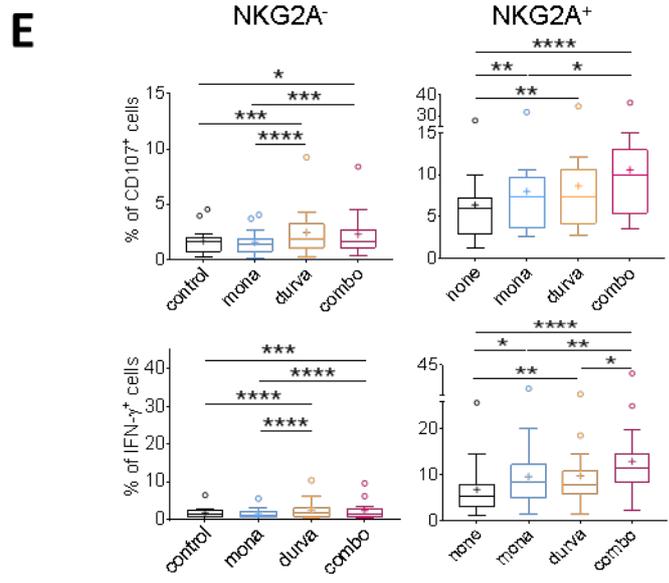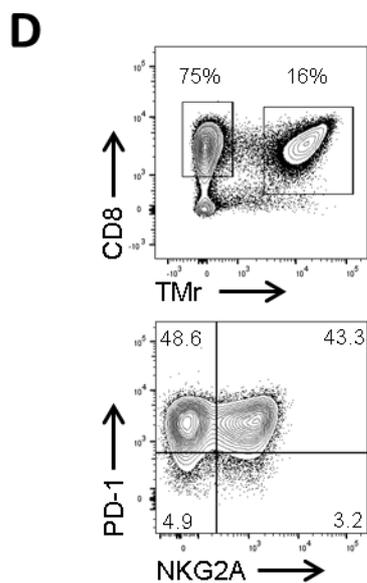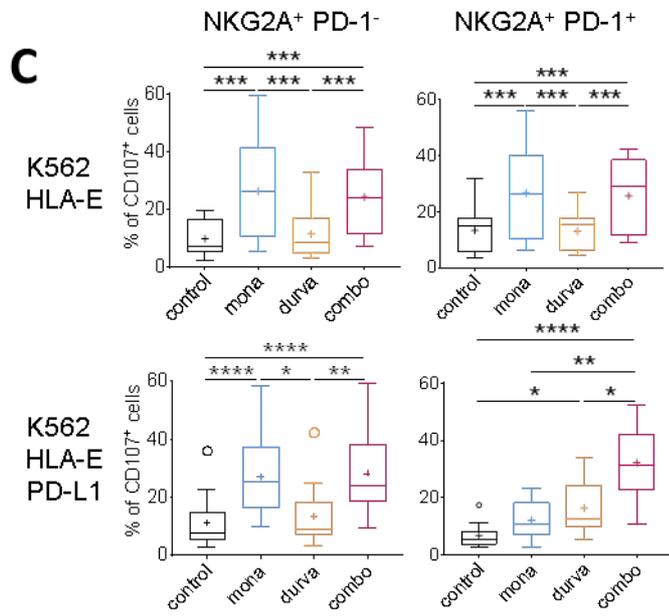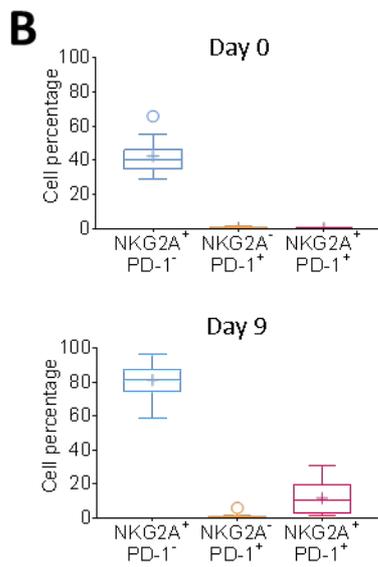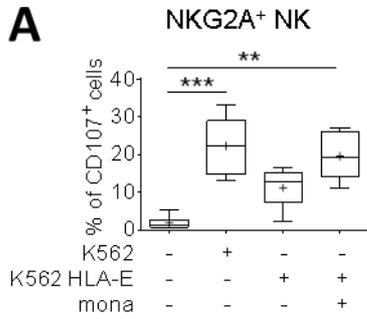
Figure 5. Monalizumab and durvalumab unleash NK and CD8$^+$ T-cell function *in vitro*

(**A**) NK cells were co-cultured with K562 or K562 cells expressing HLA-E in the presence or absence of monalizumab. The frequencies of CD107-producing NK cells are shown. Box and whiskers plot, with the means indicated by crosses. *N*=8. The whiskers are drawn down to the 25th percentile minus 1.5 times IQR (interquartile range) and up to the 75th percentile plus 1.5 times IQR. Friedman analysis followed by Dunn's multiple comparisons test. ** *p*=0.006, ****p*=0.0001.

(**B**) NK cells were stimulated *in vitro* with IL-15 for 9 days. The data shown are the frequencies of NK cells expressing NKG2A or PD-1 before (day 0) and after (day 9) culture.

(**C**) The NK cells generated in (**B**) were co-cultured with K562 cells expressing HLA-E or co-expressing HLA-E and PDL1 without (control) or with monalizumab (mona), durvalumab (durva) or both these antibodies (combo). The data shown are the frequencies of CD107-expressing NKG2A$^+$ PD-1$^+$ or PD-1$^-$ NK cells. Box and whiskers plot, with the means indicated by crosses. *N*=13 donors. The whiskers are drawn down to the 25th percentile minus 1.5 times IQR and up to the 75th percentile plus 1.5 times IQR. Friedman analysis followed by Dunn's multiple comparisons test. * *p*<0.05, ** *p*<0.01, ****p*<0.001, *****p*<0.0001.

(**D**) CD8$^+$ T cells were co-cultured *in vitro* with monocytes in the presence of IL-15 and Flu-peptide for 9 days. Top panel: one representative dot plot showing the frequency of tetramer (TMr$^+$)CD8$^+$ T cells after culture (n=14). Bottom panel: frequencies of NKG2A$^+$ and/or PD-1$^+$ cells after gating on TMr$^+$ CD8$^+$ T cells (*n*=14).

(**E**) The CD8$^+$ T cells generated in (**D**) were co-cultured with flu peptide-pulsed K562 cells expressing PDL1, HLA-E and HLA-A2 without (control) or with monalizumab (mona), durvalumab (durva) or both antibodies (combo). The data shown are the frequencies of CD107-expressing (upper panels) and IFN-γ-secreting (lower panels) NKG2A$^+$ or NKG2A$^-$ CD8$^+$ T cells. The whiskers are drawn down to the 25th percentile minus 1.5 times IQR and up to the 75th percentile plus 1.5 times IQR. Friedman followed by Dunn's test for multiple comparisons. * *p*≤0.05, ** *p*<0.01, ****p*<0.001, *****p*<0.0001.
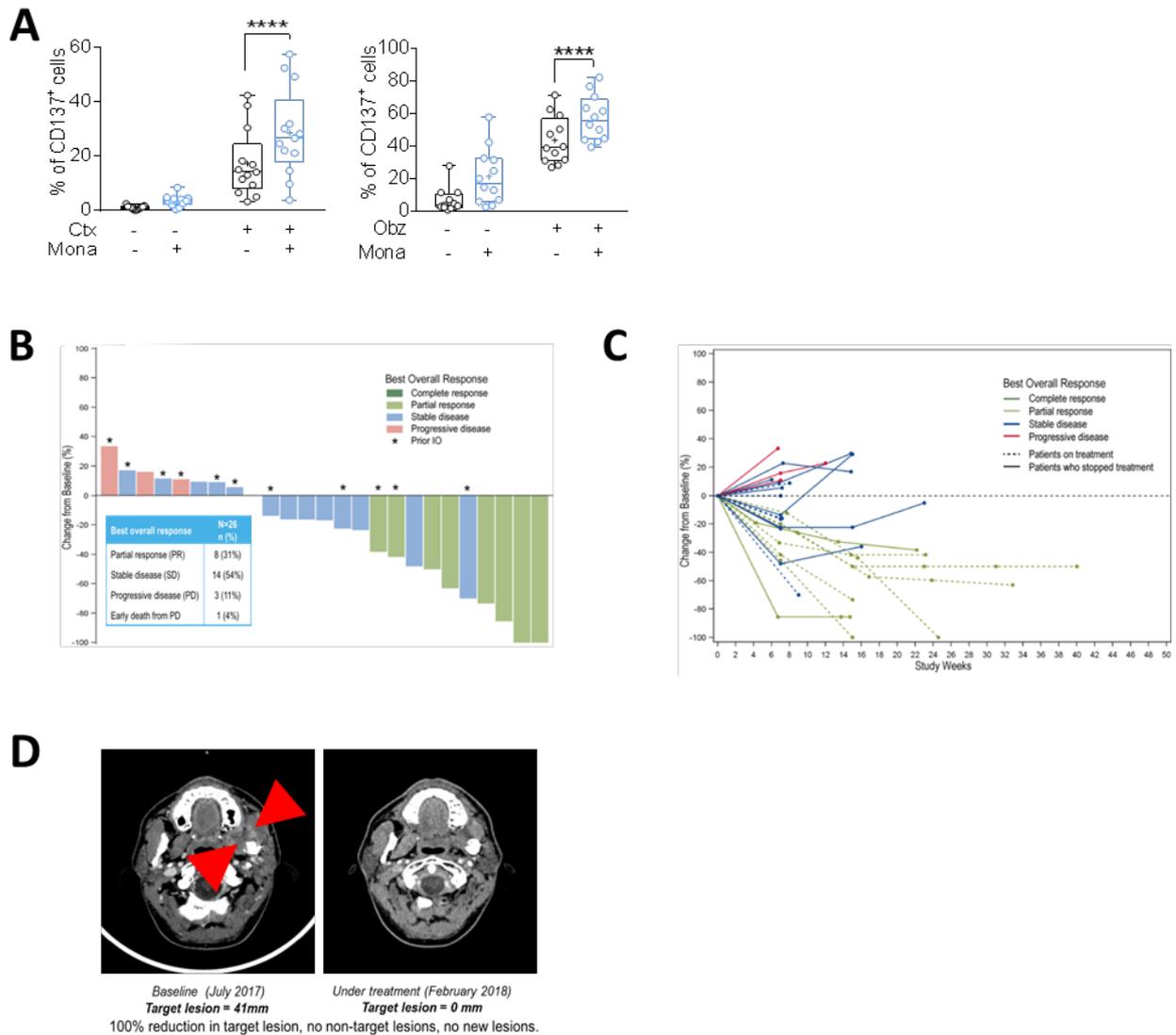
Figure 6. Monalizumab enhances human NK cell-mediated ADCC and anti-tumor activity of monalizumab and cetuximab

(A) Left panel: NK cells from healthy donors were co-cultured with the CAL-27 SCCHN cell line in the presence or absence of monalizumab (Mona) or cetuximab (Ctx). The data shown are the frequencies of CD137-expressing NKG2A$^+$ NK cells after 24 hours of co-culture. N=13. Student t-test comparing Mona+Ctx combination with Ctx as single agent ****p<0.0001. Right panel: NK cells from healthy donors were co-cultured with 721.221 cells expressing HLA-Cw3 and HLA-Cw4 in the presence or absence of monalizumab (Mona) or obinutuzumab (Obz). The data shown are the frequencies of CD137-expressing NKG2A$^+$ NK cells after 24 hours of culture. N=12. Student t-test comparing Mona+Obz combination with Obz as single agent ****p<0.0001.

(**B**) Waterfall plot of target lesion reduction relative to baseline.

(**C**) Spider plot of target lesion reduction relative to baseline.

The patient who died early, due to disease progression, before the first assessment is not represented in these graphs. In accordance with RECIST 1.1, a confirmation of response was required.

(**D**) Example of a partial response after treatment with a combination of monalizumab and cetuximab in a patient with recurrent oral cavity cancer (left masticator space) previously treated by surgery, chemotherapy (cisplatin) and radiation therapy.

Table 1. Characteristics of the patients with recurrent or metastatic (R/M) SCCHN enrolled in the phase II clinical trial

Patient Characteristics N=31		n (%)
Age, median [range]		64 [34-76]
Sex	Female	10 (32%)
	Male	21 (68%)
ECOG	0	12 (39%)
	1	19 (61%)
HPV status	Positive	4 (13%)
	Negative	15 (48%)
	To be determined	12 (39%)
Tobacco	Never	6 (19%)
	Former	20 (65%)
	Current	5 (16%)
Tumor site	Oral cavity	14 (45%)
	Oropharynx	10 (32%)
	Larynx	4 (13%)
	Hypopharynx	2 (6%)
	Nasopharynx	1 (3%)
Type of recurrence	Local	18 (58%)
	Distant	13 (42%)
Prior lines of systemic therapy (overall)		
Number of previous lines		
1		16 (52%)
2		10 (32%)
3		5 (16%)
Prior platinum		31 (100%)
Prior IO		14 (45%)
Prior cetuximab		3 (10%)

References

Baumeister, S.H., Freeman, G.J., Dranoff, G., and Sharpe, A.H. (2016). Coinhibitory Pathways in Immunotherapy for Cancer. Annu Rev Immunol *34*, 539-573.

Benson, D.M., Jr., Hofmeister, C.C., Padmanabhan, S., Suvannasankha, A., Jagannath, S., Abonour, R., Bakan, C., Andre, P., Efebera, Y., Tiollier, J*., et al.* (2012). A phase 1 trial of the anti-KIR antibody IPH2101 in patients with relapsed/refractory multiple myeloma. Blood *120*, 4324-4333.

Braud, V.M., Aldemir, H., Breart, B., and Ferlin, W.G. (2003). Expression of CD94-NKG2A inhibitory receptor is restricted to a subset of CD8+ T cells. Trends Immunol *24*, 162-164.

Callahan, M.K., Postow, M.A., and Wolchok, J.D. (2016). Targeting T Cell Co-receptors for Cancer Therapy. Immunity *44*, 1069-1078.

Cartron, G., and Watier, H. (2017). Obinutuzumab: what is there to learn from clinical trials? Blood *130*, 581-589.

Cerwenka, A., and Lanier, L.L. (2018). Natural killers join the fight against cancer. Science *359*, 1460-1461.

Charych, D., Khalili, S., Dixit, V., Kirk, P., Chang, T., Langowski, J., Rubas, W., Doberstein, S.K., Eldon, M., Hoch, U*., et al.* (2017). Modeling the receptor pharmacology, pharmacokinetics, and pharmacodynamics of NKTR-214, a kinetically-controlled interleukin-2 (IL2) receptor agonist for cancer immunotherapy. PLoS One *12*, e0179431.

Charych, D.H., Hoch, U., Langowski, J.L., Lee, S.R., Addepalli, M.K., Kirk, P.B., Sheng, D., Liu, X., Sims, P.W., VanderVeen, L.A*., et al.* (2016). NKTR-214, an Engineered Cytokine with Biased IL2 Receptor Binding, Increased Tumor Exposure, and Marked Efficacy in Mouse Tumor Models. Clin Cancer Res *22*, 680-690.

Corrales, L., McWhirter, S.M., Dubensky, T.W., Jr., and Gajewski, T.F. (2016). The host STING pathway at the interface of cancer and immunity. J Clin Invest *126*, 2404-2411.

Daeron, M., Jaeger, S., Du Pasquier, L., and Vivier, E. (2008). Immunoreceptor tyrosine-based inhibition motifs: a quest in the past and future. Immunol Rev *224*, 11-43.

Du, B., Jiang, Q., Cleveland, J., Liu, B., and D., Z. (2016). Targeting Toll-like receptors against cancer J Cancer Metastasis Treat *2*, 463-470.

Ferris, R.L., Lenz, H.J., Trotta, A.M., Garcia-Foncillas, J., Schulten, J., Audhuy, F., Merlano, M., and Milano, G. (2018). Rationale for combination of therapeutic antibodies targeting tumor cells and immune checkpoint receptors: Harnessing innate and adaptive immunity through IgG1 isotype immune effector stimulation. Cancer Treat Rev *63*, 48-60.

Fridman, W.H., Zitvogel, L., Sautes-Fridman, C., and Kroemer, G. (2017). The immune contexture in cancer prognosis and treatment. Nat Rev Clin Oncol *14*, 717-734.

Garrido, F., Ruiz-Cabello, F., and Aptsiauri, N. (2017). Rejection versus escape: the tumor MHC dilemma. Cancer Immunol Immunother *66*, 259-271.

Guillerey, C., and Smyth, M.J. (2016). NK Cells and Cancer Immunoediting. Curr Top Microbiol Immunol *395*, 115-145.

Hashimoto, M., Kamphorst, A.O., Im, S.J., Kissick, H.T., Pillai, R.N., Ramalingam, S.S., Araki, K., and Ahmed, R. (2018). CD8 T Cell Exhaustion in Chronic Infection and Cancer: Opportunities for Interventions. Annu Rev Med *69*, 301-318.

Le Drean, E., Vely, F., Olcese, L., Cambiaggi, A., Guia, S., Krystal, G., Gervois, N., Moretta, A., Jotereau, F., and Vivier, E. (1998). Inhibition of antigen-induced T cell response and antibody-induced NK cell cytotoxicity by NKG2A: association of NKG2A with SHP-1 and SHP-2 protein-tyrosine phosphatases. Eur J Immunol *28*, 264-276.

Levy, E.M., Sycz, G., Arriaga, J.M., Barrio, M.M., von Euw, E.M., Morales, S.B., Gonzalez, M., Mordoh, J., and Bianchini, M. (2009). Cetuximab-mediated cellular cytotoxicity is inhibited by HLA-E membrane expression in colon cancer cells. Innate Immun *15*, 91-100.

Mamessier, E., Sylvain, A., Thibult, M.L., Houvenaeghel, G., Jacquemier, J., Castellano, R., Goncalves, A., Andre, P., Romagne, F., Thibault, G.*, et al.* (2011). Human breast cancer cells enhance self tolerance by promoting evasion from NK cell antitumor immunity. J Clin Invest *121*, 3609-3622.

Manguso, R.T., Pope, H.W., Zimmer, M.D., Brown, F.D., Yates, K.B., Miller, B.C., Collins, N.B., Bi, K., LaFleur, M.W., Juneja, V.R.*, et al.* (2017). In vivo CRISPR screening identifies Ptpn2 as a cancer immunotherapy target. Nature *547*, 413-418.

Moretta, A., Bottino, C., Vitale, M., Pende, D., Cantoni, C., Mingari, M.C., Biassoni, R., and Moretta, L. (2001). Activating receptors and coreceptors involved in human natural killer cell-mediated cytolysis. Annu Rev Immunol *19*, 197-223.

Muntasell, A., Ochoa, M.C., Cordeiro, L., Berraondo, P., Lopez-Diaz de Cerio, A., Cabo, M., Lopez-Botet, M., and Melero, I. (2017). Targeting NK-cell checkpoints for cancer immunotherapy. Curr Opin Immunol *45*, 73-81.

Paulson, K.G., Park, S.Y., Vandeven, N.A., Lachance, K., Thomas, H., Chapuis, A.G., Harms, K.L., Thompson, J.A., Bhatia, S., Stang, A.*, et al.* (2018). Merkel cell carcinoma: Current US incidence and projected increases based on changing demographics. J Am Acad Dermatol *78*, 457-463 e452.

Platonova, S., Cherfils-Vicini, J., Damotte, D., Crozet, L., Vieillard, V., Validire, P., Andre, P., Dieu-Nosjean, M.C., Alifano, M., Regnard, J.F.*, et al.* (2011). Profound coordinated alterations of intratumoral NK cell phenotype and function in lung carcinoma. Cancer Res *71*, 5412-5422.

Ramsuran, V., Naranbhai, V., Horowitz, A., Qi, Y., Martin, M.P., Yuki, Y., Gao, X., Walker-Sperling, V., Del Prete, G.Q., Schneider, D.K.*, et al.* (2018). Elevated HLA-A expression impairs HIV control through inhibition of NKG2A-expressing cells. Science *359*, 86-90.

Rapaport, A.S., Schriewer, J., Gilfillan, S., Hembrador, E., Crump, R., Plougastel, B.F., Wang, Y., Le Friec, G., Gao, J., Cella, M.*, et al.* (2015). The Inhibitory Receptor NKG2A Sustains Virus-Specific CD8(+) T Cells in Response to a Lethal Poxvirus Infection. Immunity *43*, 1112-1124.

Rautela, J., Souza-Fonseca-Guimaraes, F., Hediyeh-Zadeh, S., Delconte, R.B., Davis, M.J., and Huntington, N.D. (2018). Molecular insight into targeting the NK cell immune response to cancer. Immunol Cell Biol.

Sagiv-Barfi, I., Kohrt, H.E., Czerwinski, D.K., Ng, P.P., Chang, B.Y., and Levy, R. (2015). Therapeutic antitumor immunity by checkpoint blockade is enhanced by ibrutinib, an inhibitor of both BTK and ITK. Proc Natl Acad Sci U S A *112*, E966-972.

Schreiber, R.D., Old, L.J., and Smyth, M.J. (2011). Cancer immunoediting: integrating immunity's roles in cancer suppression and promotion. Science *331*, 1565-1570.

Schumacher, T.N., and Schreiber, R.D. (2015). Neoantigens in cancer immunotherapy. Science *348*, 69-74.

Segal, N.H., J., N., G., C., Patel, S., Sahebjam, S., Papadopoulos, K.P., Gordon, M.S., Wang, D., Rueda, A.G., Song, X.*, et al.* (2018). First-in-human dose escalation of monalizumab plus durvalumab, with expansion in patients with metastatic microsatellite-stable colorectal cancer. J Clin Oncol *36*.

Sharma, P., and Allison, J.P. (2015a). The future of immune checkpoint therapy. Science *348*, 56-61.

Sharma, P., and Allison, J.P. (2015b). Immune checkpoint targeting in cancer therapy: toward combination strategies with curative potential. Cell *161*, 205-214.

Sharma, P., Hu-Lieskovan, S., Wargo, J.A., and Ribas, A. (2017). Primary, Adaptive, and Acquired Resistance to Cancer Immunotherapy. Cell *168*, 707-723.

Sheu, B.C., Chiou, S.H., Lin, H.H., Chow, S.N., Huang, S.C., Ho, H.N., and Hsu, S.M. (2005). Up-regulation of inhibitory natural killer receptors CD94/NKG2A with suppressed intracellular perforin expression of tumor-infiltrating CD8+ T lymphocytes in human cervical carcinoma. Cancer Res *65*, 2921-2929.

Sivori, S., Vitale, M., Bottino, C., Marcenaro, E., Sanseverino, L., Parolini, S., Moretta, L., and Moretta, A. (1996). CD94 functions as a natural killer cell inhibitory receptor for different HLA class I alleles: identification of the inhibitory form of CD94 by the use of novel monoclonal antibodies. Eur J Immunol *26*, 2487-2492.

Sockolosky, J.T., Trotta, E., Parisi, G., Picton, L., Su, L.L., Le, A.C., Chhabra, A., Silveria, S.L., George, B.M., King, I.C.*, et al.* (2018). Selective targeting of engineered T cells using orthogonal IL-2 cytokine-receptor complexes. Science *359*, 1037-1042.

Talebian Yazdi, M., van Riet, S., van Schadewijk, A., Fiocco, M., van Hall, T., Taube, C., Hiemstra, P.S., and van der Burg, S.H. (2016). The positive prognostic effect of stromal CD8+ tumor-infiltrating T cells is restrained by the expression of HLA-E in non-small cell lung carcinoma. Oncotarget *7*, 3477-3488.

Vance, R.E., Jamieson, A.M., and Raulet, D.H. (1999). Recognition of the class Ib molecule Qa-1(b) by putative activating receptors CD94/NKG2C and CD94/NKG2E on mouse natural killer cells. J Exp Med *190*, 1801-1812.

Viant, C., Fenis, A., Chicanne, G., Payrastre, B., Ugolini, S., and Vivier, E. (2014). SHP-1-

mediated inhibitory signals promote responsiveness and anti-tumour functions of natural killer cells. Nat Commun *5*, 5108.

Vivier, E., Ugolini, S., Blaise, D., Chabannon, C., and Brossay, L. (2012). Targeting natural killer cells and natural killer T cells in cancer. Nat Rev Immunol *12*, 239-252.

SYNTHESE EN FRANÇAIS

6. SYNTHESE EN FRANÇAIS

Les cellules dendritiques dans le micro-environnement tumoral des cancers ORL : des mécanismes aux biomarqueurs

INTRODUCTION

Les carcinomes épidermoïdes des voies aéro-digestives supérieures

Les carcinomes épidermoïdes des voies aéro-digestives supérieures (CEVADS) sont les cancers O.R.L. les plus fréquents. Il existe quatre localisations principales de CEVADS : cavité buccale, oropharynx, larynx et hypopharynx. Les facteurs de risques de cancer O.R.L. sont le tabac et l'alcool, dans des proportions variées en fonction de ces localisations. Le papilloma virus humain (HPV) est également responsable de plus de la moitié des cancers de l'oropharynx, et ceux-ci sont plus sensibles à la radiothérapie et ont globalement un meilleur pronostic (6). Il existe plusieurs classifications moléculaires des CEVADS, mais celles-ci n'ont pas de valeur pronostique et restent peu utilisées. En dehors du virus HPV, dont la valeur pronostique est restreinte aux cancers de l'oropharynx, il n'existe pas de biomarqueur pronostic validé pour les autres types de CEVADS, et notamment ceux de la cavité buccale qui font l'objet du deuxième article de cette thèse. Le traitement habituel fait appel à la chirurgie, la radiothérapie et la chimiothérapie. L'ensemble de ses traitements entraîne une toxicité importante et des séquelles locales lourdes. Environ 25 % des cancers de la cavité buccale présentent des récidives précoces et sévères et aboutissants au décès lié à la maladie dans les premières années qui suivent le diagnostic (11) (15). L'immunothérapie par anticorps monoclonal anti-PD1 est un nouveau traitement validé en seconde ligne pour les CEVADS avancés et/ou métastatiques après échec du cisplatine. Les taux de réponses étaient de 13,3% et 14,6% dans les 2 études princeps CheckMate-141 (16) et Keynote-040 (17).
.

Nous faisons ainsi face à un double besoin médical : (i) améliorer les taux de réponse à l'immunothérapie : c'est le fondement du premier article de cette thèse via un travail sur les cellules dendritiques dont nous verrons l'importance dans ce cadre (ii) savoir dépister à l'avance les patients à haut risque de récidive sévère pour pouvoir leur proposer une intensification thérapeutique : c'est l'objectif du second article de cette thèse.

Bases d'immunologie

Il existe deux types de système immunitaires : le système inné et le système adaptatif. Le système inné reconnaît le non-soi de façon non spécifique par des motifs de microbiens redondants via des récepteurs « PRR ». Inversement, le système adaptatif reconnaît spécifiquement chaque antigène. Les cellules présentatrices d'antigènes font le lien entre ces deux systèmes. Elles capturent par endocytose, phagocytose ou macropinocytose les antigènes anormaux, les couplent aux molécules du complexe majeur d'histocompatibilité (MHC), et les présentent sous forme de complexe CMH- peptide à leur surface aux cellules du système immunitaire adaptatif et notamment les lymphocytes T. Les peptides associé au CMH de classe II sont présentés aux lymphocytes T CD4, dont le rôle est d'activer et moduler les lymphocytes T CD8 cytotoxiques : ce sont les T CD4 helper. Les peptides associé au CMH de classe I sont présentés aux lymphocytes T CD8, un processus nommé « cross-présentation », qui active directement et lymphocytes cytotoxiques, et serait particulièrement important dans l'immunité anti-tumorale (77), (223), (238).

Les cellules dendritiques (CD) sont des cellules immunitaires qui ont été découvertes par Ralph Steinman en 1973 (41). Elles furent rapidement identifiées comme étant les cellules présentatrice d'antigène les plus efficaces pour activer le système immunitaire adaptatif (44). Cette activation des lymphocytes T nécessite 3 signaux complémentaires. Le signal 1 correspond à la présentation du complexe CMH-peptide. Le signal 2 correspond à des molécules de costimulation membranaires qui vont interagir avec des récepteurs sur les lymphocytes T, tel que CD80/86 (CD) – CD28 (lymphocyte T). Le signal 3 correspond à des cytokines secrétées dans par les CD (45), (46).

Les CD sont issues d'un progéniteur commun dans la moelle osseuse, circulent dans le sang, et infiltrent la plupart des tissus, notamment les muqueuses. Il existe plusieurs sous-types de CD qui ont certaines divergences de fonction : les CD plasmacytoïdes « pDC », et les CD conventionnelles ou myéloïdes, elles même subdivisées en 3 sous-types principaux, les « cDC1 », « cDC2 », « cDC4 ». Dans les tissus, il existe aussi des CD inflammatoires issues des monocytes, exprimant CD14, et appelées « Mo-DC » ou « CD14+DC ». Les pDC sont spécialisées dans la sécrétion d'interféron de type I en réponse à des stimuli viraux essentiellement. Les cDC1 sont BDCA3highBDCA1- et sont les CD les plus efficaces pour la « cross-présentation » (72), (73), (74). Les cDC2 sont BDCA3lowBDCA1+, activent préférentiellement les lymphocytes CD4+ et sont les plus nombreuses (80). Les cDC4 sont BDCA3lowBDCA1- et ont moins été étudiées (64).

Les CD possèdent des récepteurs que l'on peut classer en 3 catégories : ceux qui détectent directement des pathogènes ou des signaux de danger, appelés « PRR », ceux détectant indirectement la présence d'une inflammation comme les récepteurs de cytokines et chemokines, et les récepteurs pour les autres fonctions des DC, notamment homéostatiques. Les « PRR » comprennent les récepteurs Toll-like « TLR », les récepteurs lectine de type C « CLR », les senseurs cytosoliques et les récepteurs de signaux de danger « DAMP ». Les voies de signalisation intra-cellulaires aboutissent à l'activation des facteurs de transcriptions NFkb, AP1, CREB, IRF (102). Les récepteurs de cytokines signalent principalement par la voie Jak/STAT(122). Même si les voies de signalisation sont très redondantes d'un récepteur à l'autre, et que le nombre de récepteurs différents est limité, chaque stimulus, présent à une dose et à une durée définie va engendrer une combinaison précise de niveau d'activation de chaque voie pour aboutir à une réponse cellulaire spécifique. Cette notion est importante pour le second article de cette thèse.

La maturation des cellules dendritiques

La liaison d'un ligand sur les récepteurs senseurs directs ou indirect de pathogènes, de danger et d'inflammation entraîne des modifications notables de la CD, regroupées sous le terme de maturation. Les principaux évènements sont : (i) l'augmentation de la présentation antigénique, allant de pair avec la diminution de capacité d'endocytose et de macropinocytose (156), (158) ; (ii) l'augmentation de l'expression de molécules de costimulation (45), (159), (160), (161); (iii) l'augmentation de la production de cytokines et chemokines (166) ; (iv) l'acquisition de la capacité de migration vers le ganglion drainant associée à l'expression du récepteur CCR7 (47); (v) l'augmentation en nombre et en taille des protrusions cellulaires ou « dendrites » ayant donné leur nom à la cellule (181). Il faut noter que les CD peuvent également exprimer des molécules de surface et des cytokines à effet immunosuppresseurs pour les lymphocytes T, tels que PDL1 et IL-10 (159), (160), (161).

Ainsi, selon la combinaison de molécules de surface et de cytokines produites, on distingue plusieurs nuances de maturation dénommées dans la littérature comme mature immunogéniques, matures tolérogéniques, semi-matures, immatures tolérogéniques, matures homéostatique, etc (187)… Grossièrement, les CD sont dites immunogéniques quand elles favorisent une réponse T cytotoxiques et tolérogéniques quand elles favorisent une immunosuppression et soit l'anergie des lymphocytes T, soit l'induction de lymphocytes T régulateurs. Les réponse immunogéniques sont elles-mêmes nuancées selon la polarisation des lymphocytes T CD4 (ex: Th1, Th2…) (54).

Les cellules dendritiques infiltrant les cancers

Les CD sont des cellules clefs de la réponse immunitaire anti-tumorale. Les différents sous-types de CD infiltrent les cancers (71).. Les CD sont recrutées à partir du sang en réponse aux signaux de dommages tissulaires issus de la destruction du tissu normal ou de la mort des cellules cancéreuses(230). De nombreuses évidences supportent le rôle anti-tumoral des CD, notamment des cDC1 et de la « cross-présentation » (72), (77), (223), (238), mais aussi des cDC2 (237), (243), (244), (245), (246). Le rôle des pDC est présenté en annexe 5.3 et ne sera pas détaillé. Inversement, d'autres études relèvent le rôle pro-tumoral des CD infiltrant les tumeurs, qui seraient préférentiellement tolérogéniques (251), (252), (253). Finalement, des données de transcriptomique issues de CD humaines infiltrant ses tumeurs du sein et de l'amygdale humaines ont noté une co-expression de molécules immunogéniques et immunosuppressives (71), (236).

Les CD peuvent être utilisées comme immunothérapie anti-cancéreuse, en thérapie cellulaire après modulation *in vitro* de leur maturation (274), (287). Egalement, les CD intra-tumorales ou du sang peuvent aussi être activées par le biais de stimuli administrés dans les tumeurs ou en adjuvant de vaccins peptidiques (40), (207), (278), (281).

OBJECTIFS DE LA THESE

La biologie des CD est un domaine de recherche relativement récent mais à présent très riche de connaissance. Cependant, il persiste certaines incertitudes concernant les états de maturation des CD, en particulier dans le contexte du cancer. Des données pré-cliniques et cliniques ont montré que les CD sont une cible intéressante pour l'immunothérapie et que les états de maturation sont la clef de l'efficacité de ces traitements. Les données sur les CD infiltrant les tumeurs ORL sont limitées et ne permettent pas d'anticiper comment moduler les CD intra-tumorales à des fins thérapeutiques.

L'objectif de ma thèse était de décrire avec une résolution fine l'état moléculaire des CD

infiltrant les cancers ORL, et leur relation au microenvironnement tumoral.

Nous voulions répondre à plusieurs questions :

- Quels sous-types de CD infiltrent les cancers ORL et dans quelles proportions ?
- Quels marqueurs de maturation et molécules immunostimulatrices ou immunosuppressives expriment-elles ?
- Quelle est la relation entre les CD et les autres cellules immunitaires infiltrant les tumeurs ?
- Quels mécanismes influencent l'état des CD dans les tumeurs ?
- Y-a-t-il des classes d'infiltration immunitaire tumorale ?
- Quel est le lien entre l'infiltrat immunitaire tumoral et le microenvironnement soluble ?
- Quels paramètres du microenvironnement sont associés au pronostique ?
- Pouvons-nous identifier des cibles thérapeutiques et des biomarqueurs prédictifs ?

RESULTATS

PDL1 et ICOSL distinguent les CD humaines « sécrétantes » et « aidantes »

En utilisant une large base de données de CD activées *in vitro* par 16 stimuli différents (130 observations), nous avons pu décrire 2 états d'activation des CD humaines. Les CD « sécrétantes » PDL1fortICOSLfaible/nul produisaient de grandes quantités de cytokines et de chemokines, mais induisaient très peu de sécrétion de cytokines T helper après co-culture avec les lymphocytes T CD4 naïfs ; inversement, les CD « aidantes » PDL1faibleICOSLfort sécrétaient peu elles-mêmes, mais induisaient une forte sécrétion de cytokines T helper, aussi bien Th1, Th2, Th9 et Treg. Par cytométrie en flux, puis par analyse transcriptomiques de CD infiltrant les cancers ORL, nous avons pu observer que celles infiltrant les tumeurs riches en lymphocytes T correspondaient au type de maturation « sécrétantes ». Elles exprimaient PDL1, mais aussi CD40, PVR, IL1B, TNF et CCL19. Les CD infiltrant les tumeurs pauvres en lymphocytes T étaient peu nombreuses et semblaient peu activées, proche des CD du sang. Nous proposons ainsi une nouvelle classification fonctionnelle des CD humaines avec un fort potentiel d'application en immunothérapie anti-cancéreuse.

MMP2 est un biomarqueur pronostic indépendant des cancers de la cavité buccale.

Nous avons observé dans l'article précédent que l'infiltrat lymphocytaire était associé à une plus forte infiltration de CD et un état d'activation spécifique. En étudiant le microenvironnement soluble de 18 cancers ORL, nous avons pu observer que CXCL9 et CXCL10 étaient fortement corrélées à l'infiltrat immunitaire. Dans une seconde cohorte de 37 patients atteints de cancers de la cavité buccale traités par chirurgie première, CXCL9, CXCL10 et 27 autres molécules sur les 49 mesurées étaient différentiellement exprimées dans les tumeurs par rapport aux tissus sains périphériques pairés. Parmi ces molécules, seul MMP2 soluble, était prédictif de mauvais pronostic, ce qui suggère un rôle pronostique fort de cette métalloprotéinase et moindre de l'infiltrat immunitaire dans ce contexte clinique.

Nous avons établi une cohorte de validation de 145 patients et analysé un panel de 30 gènes par RTqPCR à partir d'ARN extrait d'échantillons tumoraux congelés : MMP1, MMP2, MMP9, une signature de 18 gènes prédictive de la réponse au Pembrolizumab (anticorps anti-PD1) (304), et d'autres gènes associés à l'infiltrat immunitaire. En analyse univariée, des taux élevés MMP2 et CD276, et des taux faibles de CXCL10 et STAT1 étaient associés à un mauvais pronostique. En analyse multivariée, MMP2 (p=0.001) et l'effraction extra-capsulaire (EEC) (p=0.006) étaient des marqueurs indépendants de survie spécifique de la maladie (SSM). Ainsi, nous avons pu définir 4 groupes pronostiques avec des SSM à 5ans variant de 36% (MMP2fortEEC+) à 88% (MMP2faibleENE-). L'expression de la signature prédictive de réponse au pembrolizumab était similaire dans les différents groupes pronostiques, suggérant que les taux de réponse au traitement attendus devraient être similaires.

Le statut MMP2 définit en pré-opératoire ou en post-opératoire pourrait être utilisé pour un réaliser un essai clinique d'intensification thérapeutique dirigé par biomarqueurs. Les patients à haut risque pourraient recevoir une immunothérapie ou une chimiothérapie néoadjuvante en sus du traitement standard par chirurgie puis radio-chimiothérapie.

DISCUSSION

La maturation des cellules dendritiques : vers une nouvelle classification ?

Dans notre étude, nous avons observé que la plupart des stimuli différents induisaient l'une ou l'autre des 2 catégories de CD : « sécrétantes » ou « aidantes », bien que la plupart de ces stimuli agissent sur des récepteurs différents. Cette observation pose la question de l'universalité de cette classification. Il serait intéressant de déterminer si : (i) cette classification s'applique à tous les sous-types de CD, (ii) PDL1 et ICOSL sont toujours les meilleurs marqueurs de surface pour discriminer les sous-types d'activation ; (iii) cette classification s'applique à tous les stimuli, y compris des senseurs cytosolic comme le cGAMP.

De plus, les analyses transcriptomiques nous ont permis d'identifier les facteurs de transcription associés à l'un ou l'autre des types d'activation, mais le rôle des molécules mesurées (PDL1, ICOSL, IL12p40, IL10) ou non mesurées dans ce travail dans l'effet induit sur les lymphocytes T reste à éclaircir.

Utilisation de la classification « sécrétante » versus « aidantes » des cellules dendritiques comme une base pour l'utilisation de modulateurs en cancérologie

Les stimuli induisant des CD « sécrétantes » comme le R848 pourraient être utilisé pour augmenter le nombre de CD intra-tumorales dans les tumeurs peu infiltrées. On comprend cependant qu'il serait nécessaire d'y associer des anticorps anti-PD(L)1, voire un inhibiteur d'IL-10. Les essais cliniques en cours avec R848 n'ont pas prévu de telles combinaisons.

Nous n'avons pas observé *in vivo* de CD « sécrétantes », il serait intéressant de déterminer si elles existent spontanément dans d'autres contextes comme les maladies allergiques, inflammatoires et auto-immunes, ou si on pourrait les induire dans les tumeurs en utilisant les stimuli identifiés (TSLP, GM-CSF). Enfin, l'impact sur les cellules T et le bénéfice thérapeutique resterait à déterminer.

MMP2, vers un biomarqueur de routine pour les cancers de la cavité buccale ?

Deux étapes seront nécessaires pour poursuivre le développement de MMP2 comme biomarqueur prédictif de cancers de la cavité buccale résécables : le choix d'une technologie de mesure et l'uniformisation de celle-ci dans les différents centres de soins, et la réalisation

d'un essai clinique randomisé montrant la supériorité de la prise en charge orientée par biomarqueur par rapport à la prise en charge standard.

REFERENCES

7. REFERENCES

1. Pai SI, Faivre S, Licitra L, Machiels J-P, Vermorken JB, Bruzzi P, et al. Comparative analysis of the phase III clinical trials of anti-PD1 monotherapy in head and neck squamous cell carcinoma patients (CheckMate 141 and KEYNOTE 040). J Immunother Cancer. 2019 Apr 3;7(1):96.

2. Danny Rischin, Kevin J. Harrington, Richard Greil, Denis Soulieres, Makoto Tahara, Gilberto de Castro, Amanda Psyrri, Neus Baste, Prakash C. Neupane, Ase Bratland, Thorsten Fuereder, Brett Gordon Maxwell Hughes, Ricard Mesia, Nuttapong Ngamphaiboon, Tamara Rordorf, Wan Zamaniah Wan Ishak, Yayan Zhan. Protocol-specified final analysis of the phase 3 KEYNOTE-048 trial of pembrolizumab (pembro) as first-line therapy for recurrent/metastatic head and neck squamous cell carcinoma (R/M HNSCC). J Clin Oncol 37, 2019 (suppl; abstr 6000). In.

3. Trédan O, Wang Q, Pissaloux D, Cassier P, de la Fouchardière A, Fayette J, et al. Molecular screening program to select molecular-based recommended therapies for metastatic cancer patients: analysis from the ProfiLER trial. Ann Oncol Off J Eur Soc Med Oncol. 2019 May 1;30(5):757–65.

4. Fujiwara RJT, Burtness B, Husain ZA, Judson BL, Bhatia A, Sasaki CT, et al. Treatment guidelines and patterns of care in oral cavity squamous cell carcinoma: Primary surgical resection vs. nonsurgical treatment. Oral Oncol. 2017;71:129–37.

5. Siegel RL, Miller KD, Jemal A. Cancer statistics, 2018: Cancer Statistics, 2018. CA Cancer J Clin. 2018 Jan;68(1):7–30.

6. Ang KK, Harris J, Wheeler R, Weber R, Rosenthal DI, Nguyen-Tân PF, et al. Human Papillomavirus and Survival of Patients with Oropharyngeal Cancer. N Engl J Med. 2010 Jul;363(1):24–35.

7. Guigay J, Sâada-Bouzid E, Peyrade F, Michel C. Approach to the Patient with Recurrent/Metastatic Disease. Curr Treat Options Oncol. 2019 Jun 25;20(8):65.

8. NCCN. https://www.nccn.org/professionals/physician_gls/default.aspx.

9. Gañán L, López M, García J, Esteller E, Quer M, León X. Management of recurrent head and neck cancer: variables related to salvage surgery. Eur Arch Oto-Rhino-Laryngol Off J Eur Fed Oto-Rhino-Laryngol Soc EUFOS Affil Ger Soc Oto-Rhino-Laryngol - Head Neck Surg. 2016 Dec;273(12):4417–24.

10. Argiris A, Karamouzis MV, Raben D, Ferris RL. Head and neck cancer. Lancet Lond Engl. 2008 May 17;371(9625):1695–709.

11. Tam S, Araslanova R, Low T-HH, Warner A, Yoo J, Fung K, et al. Estimating Survival After Salvage Surgery for Recurrent Oral Cavity Cancer. JAMA Otolaryngol-- Head Neck Surg. 2017 01;143(7):685–90.

12. Ord RA, Kolokythas A, Reynolds MA. Surgical salvage for local and regional recurrence in oral cancer. J Oral Maxillofac Surg Off J Am Assoc Oral Maxillofac Surg. 2006 Sep;64(9):1409–14.

13. Liao C-T, Chang JT-C, Wang H-M, Ng S-H, Hsueh C, Lee L-Y, et al. Salvage therapy in relapsed squamous cell carcinoma of the oral cavity: how and when? Cancer. 2008 Jan 1;112(1):94–103.

14. Sacco AG, Cohen EE. Current Treatment Options for Recurrent or Metastatic Head and Neck Squamous Cell Carcinoma. J Clin Oncol Off J Am Soc Clin Oncol. 2015 Oct 10;33(29):3305–13.

15. Janot F, de Raucourt D, Benhamou E, Ferron C, Dolivet G, Bensadoun R-J, et al. Randomized trial of postoperative reirradiation combined with chemotherapy after salvage surgery compared with salvage surgery alone in head and neck carcinoma. J Clin Oncol Off J Am Soc Clin Oncol. 2008 Dec 1;26(34):5518–23.

16. Ferris RL, Blumenschein G, Fayette J, Guigay J, Colevas AD, Licitra L, et al. Nivolumab for Recurrent Squamous-Cell Carcinoma of the Head and Neck. N Engl J Med. 2016 Nov 10;375(19):1856–67.

17. Cohen EEW, Soulières D, Le Tourneau C, Dinis J, Licitra L, Ahn M-J, et al. Pembrolizumab versus methotrexate, docetaxel, or cetuximab for recurrent or metastatic head-and-neck squamous cell carcinoma (KEYNOTE-040): a randomised, open-label, phase 3 study. The Lancet. 2019 Jan;393(10167):156–67.

18. Zorat PL, Paccagnella A, Cavaniglia G, Loreggian L, Gava A, Mione CA, et al. Randomized phase III trial of neoadjuvant chemotherapy in head and neck cancer: 10-year follow-up. J Natl Cancer Inst. 2004 Nov 17;96(22):1714–7.

19. Bossi P, Lo Vullo S, Guzzo M, Mariani L, Granata R, Orlandi E, et al. Preoperative chemotherapy in advanced resectable OCSCC: long-term results of a randomized phase III trial. Ann Oncol Off J Eur Soc Med Oncol. 2014 Feb;25(2):462–6.

20. Forastiere A, Koch W, Trotti A, Sidransky D. Head and neck cancer. N Engl J Med. 2001 Dec 27;345(26):1890–900.

21. Bykov VJN, Eriksson SE, Bianchi J, Wiman KG. Targeting mutant p53 for efficient cancer therapy. Nat Rev Cancer. 2018;18(2):89–102.

22. Keck MK, Zuo Z, Khattri A, Stricker TP, Brown CD, Imanguli M, et al. Integrative Analysis of Head and Neck Cancer Identifies Two Biologically Distinct HPV and Three Non-HPV Subtypes. Clin Cancer Res. 2015 Feb 15;21(4):870–81.

23. TCGA Releases Head and Neck Cancer Data. Cancer Discov. 2015 Apr;5(4):340–1.

24. De Cecco L, Nicolau M, Giannoccaro M, Daidone MG, Bossi P, Locati L, et al. Head and neck cancer subtypes with biological and clinical relevance: Meta-analysis of gene-expression data. Oncotarget. 2015 Apr 20;6(11):9627–42.

25. Puram SV, Tirosh I, Parikh AS, Patel AP, Yizhak K, Gillespie S, et al. Single-Cell Transcriptomic Analysis of Primary and Metastatic Tumor Ecosystems in Head and Neck Cancer. Cell. 2017 Dec 14;171(7):1611-1624.e24.

26. Rivera C, Oliveira AK, Costa RAP, De Rossi T, Paes Leme AF. Prognostic biomarkers in oral squamous cell carcinoma: A systematic review. Oral Oncol. 2017;72:38–47.

27. McShane LM, Altman DG, Sauerbrei W, Taube SE, Gion M, Clark GM, et al. REporting recommendations for tumour MARKer prognostic studies (REMARK). Br J Cancer. 2005 Aug 22;93(4):387–91.

28. Hayes DF, Bast RC, Desch CE, Fritsche H, Kemeny NE, Jessup JM, et al. Tumor marker utility grading system: a framework to evaluate clinical utility of tumor markers. J Natl Cancer Inst. 1996 Oct 16;88(20):1456–66.

29. Simon RM, Paik S, Hayes DF. Use of archived specimens in evaluation of prognostic and predictive biomarkers. J Natl Cancer Inst. 2009 Nov 4;101(21):1446–52.

30. Dunkel J, Vaittinen S, Koivunen P, Laranne J, Mäkinen MJ, Tommola S, et al. Tumoral Expression of CD44 and HIF1α Predict Stage I Oral Cavity Squamous Cell Carcinoma Outcome. Laryngoscope Investig Otolaryngol. 2016;1(1):6–12.

31. Shen S, Wang G, Shi Q, Zhang R, Zhao Y, Wei Y, et al. Seven-CpG-based prognostic signature coupled with gene expression predicts survival of oral squamous cell carcinoma. Clin Epigenetics. 2017;9:88.

32. Lu C, Lewis JS, Dupont WD, Plummer WD, Janowczyk A, Madabhushi A. An oral cavity squamous cell carcinoma quantitative histomorphometric-based image classifier of nuclear morphology can risk stratify patients for disease-specific survival. Mod Pathol [Internet]. 2017 Aug 4 [cited 2017 Aug 13]; Available from: http://www.nature.com/doifinder/10.1038/modpathol.2017.98

33. National Cancer Institute. NCI Dictionary of Cancer Terms. 2011.

34. Thorsson V, Gibbs DL, Brown SD, Wolf D, Bortone DS, Ou Yang T-H, et al. The Immune Landscape of Cancer. Immunity. 2018 17;48(4):812-830.e14.

35. Mandal R, Şenbabaoğlu Y, Desrichard A, Havel JJ, Dalin MG, Riaz N, et al. The head and neck cancer immune landscape and its immunotherapeutic implications. JCI Insight. 2016 Oct 20;1(17):e89829.

36. Chakravarthy A, Furness A, Joshi K, Ghorani E, Ford K, Ward MJ, et al. Pan-cancer deconvolution of tumour composition using DNA methylation. Nat Commun. 2018 13;9(1):3220.

37. Fehniger TA, Cooper MA. Harnessing NK Cell Memory for Cancer Immunotherapy. Trends Immunol. 2016;37(12):877–88.

38. Zhu J. T Helper Cell Differentiation, Heterogeneity, and Plasticity. Cold Spring Harb Perspect Biol. 2018 01;10(10).

39. Van Voorhis WC, Hair LS, Steinman RM, Kaplan G. Human dendritic cells. Enrichment and characterization from peripheral blood. J Exp Med. 1982 Apr 1;155(4):1172–87.

40. Hossain MK, Wall KA. Use of Dendritic Cell Receptors as Targets for Enhancing Anti-Cancer Immune Responses. Cancers. 2019 Mar 24;11(3).

41. Steinman RM, Cohn ZA. Identification of a novel cell type in peripheral lymphoid organs of mice. I. Morphology, quantitation, tissue distribution. J Exp Med. 1973 May 1;137(5):1142–62.

42. Steinman RM, Witmer MD. Lymphoid dendritic cells are potent stimulators of the primary mixed leukocyte reaction in mice. Proc Natl Acad Sci U S A. 1978 Oct;75(10):5132–6.

43. Marques PE, Grinstein S, Freeman SA. SnapShot:Macropinocytosis. Cell. 2017 04;169(4):766-766.e1.

44. Steinman RM. Decisions about dendritic cells: past, present, and future. Annu Rev Immunol. 2012;30:1–22.

45. Curtsinger JM, Schmidt CS, Mondino A, Lins DC, Kedl RM, Jenkins MK, et al. Inflammatory cytokines provide a third signal for activation of naive CD4+ and CD8+ T cells. J Immunol Baltim Md 1950. 1999 Mar 15;162(6):3256–62.

46. Jain A, Pasare C. Innate Control of Adaptive Immunity: Beyond the Three-Signal Paradigm. J Immunol Baltim Md 1950. 2017 15;198(10):3791–800.

47. Worbs T, Hammerschmidt SI, Förster R. Dendritic cell migration in health and disease. Nat Rev Immunol. 2017;17(1):30–48.

48. Guermonprez P, Valladeau J, Zitvogel L, Théry C, Amigorena S. Antigen presentation and T cell stimulation by dendritic cells. Annu Rev Immunol. 2002;20:621–67.

49. Bevan MJ. Cross-priming for a secondary cytotoxic response to minor H antigens with H-2 congenic cells which do not cross-react in the cytotoxic assay. J Exp Med. 1976 May 1;143(5):1283–8.

50. Mosmann TR, Coffman RL. Two types of mouse helper T-cell clone Implications for immune regulation. Immunol Today. 1987;8(7–8):223–7.

51. Chalmin F, Humblin E, Ghiringhelli F, Végran F. Transcriptional Programs Underlying Cd4 T Cell Differentiation and Functions. Int Rev Cell Mol Biol. 2018;341:1–61.

52. Lutz MB. Induction of CD4(+) Regulatory and Polarized Effector/helper T Cells by Dendritic Cells. Immune Netw. 2016 Feb;16(1):13–25.

53. Yamane H, Paul WE. Early signaling events that underlie fate decisions of naive CD4(+) T cells toward distinct T-helper cell subsets. Immunol Rev. 2013 Mar;252(1):12–23.

54. Gaurav R, Agrawal DK. Clinical view on the importance of dendritic cells in asthma. Expert Rev Clin Immunol. 2013 Oct;9(10):899–919.

55. Sozzani S, Del Prete A, Bosisio D. Dendritic cell recruitment and activation in autoimmunity. J Autoimmun. 2017 Dec;85:126–40.

56. Gardner A, Ruffell B. Dendritic Cells and Cancer Immunity. Trends Immunol. 2016;37(12):855–65.

57. Vroman H, van den Blink B, Kool M. Mode of dendritic cell activation: the decisive hand in Th2/Th17 cell differentiation. Implications in asthma severity? Immunobiology. 2015 Feb;220(2):254–61.

58. Zernecke A. Dendritic cells in atherosclerosis: evidence in mice and humans. Arterioscler Thromb Vasc Biol. 2015 Apr;35(4):763–70.

59. Lapérine O, Blin-Wakkach C, Guicheux J, Beck-Cormier S, Lesclous P. Dendritic-cell-derived osteoclasts: a new game changer in bone-resorption-associated diseases. Drug Discov Today. 2016;21(9):1345–54.

60. Lechler RI, Batchelor JR. Restoration of immunogenicity to passenger cell-depleted kidney allografts by the addition of donor strain dendritic cells. J Exp Med. 1982 Jan 1;155(1):31–41.

61. Zhuang Q, Lakkis FG. Dendritic cells and innate immunity in kidney transplantation. Kidney Int. 2015 Apr;87(4):712–8.

62. Vremec D, Zorbas M, Scollay R, Saunders DJ, Ardavin CF, Wu L, et al. The surface phenotype of dendritic cells purified from mouse thymus and spleen: investigation of the CD8 expression by a subpopulation of dendritic cells. J Exp Med. 1992 Jul 1;176(1):47–58.

63. See P, Dutertre C-A, Chen J, Günther P, McGovern N, Irac SE, et al. Mapping the human DC lineage through the integration of high-dimensional techniques. Science. 2017 09;356(6342).

64. Villani A-C, Satija R, Reynolds G, Sarkizova S, Shekhar K, Fletcher J, et al. Single-cell RNA-seq reveals new types of human blood dendritic cells, monocytes, and progenitors. Science. 2017 Apr 21;356(6335).

65. Dutertre C-A, Becht E, Irac SE, Khalilnezhad A, Narang V, Khalilnezhad S, et al. Single-Cell Analysis of Human Mononuclear Phagocytes Reveals Subset-Defining Markers and Identifies Circulating Inflammatory Dendritic Cells. Immunity. 2019 Aug 27;

66. Günther P, Cirovic B, Baßler K, Händler K, Becker M, Dutertre CA, et al. A rule-based data-informed cellular consensus map of the human mononuclear phagocyte cell space. bioRxiv [Internet]. 2019 Jun 3 [cited 2019 Sep 14]; Available from: http://biorxiv.org/lookup/doi/10.1101/658179

67. Soumelis V, Liu Y-J. From plasmacytoid to dendritic cell: morphological and functional switches during plasmacytoid pre-dendritic cell differentiation. Eur J Immunol. 2006 Sep;36(9):2286–92.

68. Lin DS, Kan A, Gao J, Crampin EJ, Hodgkin PD, Naik SH. DiSNE Movie Visualization and Assessment of Clonal Kinetics Reveal Multiple Trajectories of Dendritic Cell Development. Cell Rep. 2018 06;22(10):2557–66.

69. Dzionek A, Fuchs A, Schmidt P, Cremer S, Zysk M, Miltenyi S, et al. BDCA-2, BDCA-3, and BDCA-4: three markers for distinct subsets of dendritic cells in human peripheral blood. J Immunol Baltim Md 1950. 2000 Dec 1;165(11):6037–46.

70. Cancel J-C, Crozat K, Dalod M, Mattiuz R. Are Conventional Type 1 Dendritic Cells Critical for Protective Antitumor Immunity and How? Front Immunol. 2019;10:9.

71. Abolhalaj M, Askmyr D, Sakellariou CA, Lundberg K, Greiff L, Lindstedt M. Profiling dendritic cell subsets in head and neck squamous cell tonsillar cancer and benign tonsils. Sci Rep. 2018 May 23;8(1):8030.

72. Jongbloed SL, Kassianos AJ, McDonald KJ, Clark GJ, Ju X, Angel CE, et al. Human CD141+ (BDCA-3)+ dendritic cells (DCs) represent a unique myeloid DC subset that cross-presents necrotic cell antigens. J Exp Med. 2010 Jun 7;207(6):1247–60.

73. Haniffa M, Shin A, Bigley V, McGovern N, Teo P, See P, et al. Human tissues contain CD141hi cross-presenting dendritic cells with functional homology to mouse CD103+ nonlymphoid dendritic cells. Immunity. 2012 Jul 27;37(1):60–73.

74. van der Aa E, Biesta PJ, Woltman AM, Buschow SI. Transcriptional patterns associated with BDCA3 expression on BDCA1+ myeloid dendritic cells. Immunol Cell Biol. 2018;96(3):330–6.

75. Watchmaker PB, Lahl K, Lee M, Baumjohann D, Morton J, Kim SJ, et al. Comparative transcriptional and functional profiling defines conserved programs of intestinal DC differentiation in humans and mice. Nat Immunol. 2013 Dec 1;15(1):98–108.

76. Collin M, Bigley V. Human dendritic cell subsets: an update. Immunology. 2018;154(1):3–20.

77. Hildner K, Edelson BT, Purtha WE, Diamond M, Matsushita H, Kohyama M, et al. Batf3 deficiency reveals a critical role for CD8alpha+ dendritic cells in cytotoxic T cell immunity. Science. 2008 Nov 14;322(5904):1097–100.

78. Poulin LF, Salio M, Griessinger E, Anjos-Afonso F, Craciun L, Chen J-L, et al. Characterization of human DNGR-1+ BDCA3+ leukocytes as putative equivalents of mouse CD8alpha+ dendritic cells. J Exp Med. 2010 Jun 7;207(6):1261–71.

79. Schulz O, Diebold SS, Chen M, Näslund TI, Nolte MA, Alexopoulou L, et al. Toll-like receptor 3 promotes cross-priming to virus-infected cells. Nature. 2005 Feb 24;433(7028):887–92.

80. Granot T, Senda T, Carpenter DJ, Matsuoka N, Weiner J, Gordon CL, et al. Dendritic Cells Display Subset and Tissue-Specific Maturation Dynamics over Human Life. Immunity. 2017 21;46(3):504–15.

81. Segura E, Valladeau-Guilemond J, Donnadieu M-H, Sastre-Garau X, Soumelis V, Amigorena S. Characterization of resident and migratory dendritic cells in human lymph nodes. J Exp Med. 2012 Apr 9;209(4):653–60.

82. Wylie B, Read J, Buzzai AC, Wagner T, Troy N, Syn G, et al. CD8+XCR1neg Dendritic Cells Express High Levels of Toll-Like Receptor 5 and a Unique Complement of Endocytic Receptors. Front Immunol. 2018;9:2990.

83. Persson EK, Uronen-Hansson H, Semmrich M, Rivollier A, Hägerbrand K, Marsal J, et al. IRF4 transcription-factor-dependent CD103(+)CD11b(+) dendritic cells drive mucosal T helper 17 cell differentiation. Immunity. 2013 May 23;38(5):958–69.

84. Hambleton S, Salem S, Bustamante J, Bigley V, Boisson-Dupuis S, Azevedo J, et al. IRF8 mutations and human dendritic-cell immunodeficiency. N Engl J Med. 2011 Jul 14;365(2):127–38.

85. Sontag S, Förster M, Qin J, Wanek P, Mitzka S, Schüler HM, et al. Modelling IRF8 Deficient Human Hematopoiesis and Dendritic Cell Development with Engineered iPS Cells. Stem Cells Dayt Ohio. 2017;35(4):898–908.

86. Krug A, Towarowski A, Britsch S, Rothenfusser S, Hornung V, Bals R, et al. Toll-like receptor expression reveals CpG DNA as a unique microbial stimulus for plasmacytoid dendritic cells which synergizes with CD40 ligand to induce high amounts of IL-12. Eur J Immunol. 2001 Oct;31(10):3026–37.

87. Murakami R, Denda-Nagai K, Hashimoto S, Nagai S, Hattori M, Irimura T. A unique dermal dendritic cell subset that skews the immune response toward Th2. PloS One. 2013;8(9):e73270.

88. Haniffa M, Collin M, Ginhoux F. Ontogeny and functional specialization of dendritic cells in human and mouse. Adv Immunol. 2013;120:1–49.

89. Segura E, Amigorena S. Inflammatory dendritic cells in mice and humans. Trends Immunol. 2013 Sep;34(9):440–5.

90. Goudot C, Coillard A, Villani A-C, Gueguen P, Cros A, Sarkizova S, et al. Aryl Hydrocarbon Receptor Controls Monocyte Differentiation into Dendritic Cells versus Macrophages. Immunity. 2017 19;47(3):582-596.e6.

91. Joffre OP, Segura E, Savina A, Amigorena S. Cross-presentation by dendritic cells. Nat Rev Immunol. 2012 Jul 13;12(8):557–69.

92. Alculumbre S, Raieli S, Hoffmann C, Chelbi R, Danlos F-X, Soumelis V. Plasmacytoid pre-dendritic cells (pDC): from molecular pathways to function and disease association. Semin Cell Dev Biol. 2019;86:24–35.

93. Lennert K, Remmele W. [Karyometric research on lymph node cells in man. I. Germinoblasts, lymphoblasts & lymphocytes]. Acta Haematol. 1958 Feb;19(2):99–113.

94. Grouard G, Rissoan MC, Filgueira L, Durand I, Banchereau J, Liu YJ. The enigmatic plasmacytoid T cells develop into dendritic cells with interleukin (IL)-3 and CD40-ligand. J Exp Med. 1997 Mar 17;185(6):1101–11.

95. Cella M, Jarrossay D, Facchetti F, Alebardi O, Nakajima H, Lanzavecchia A, et al. Plasmacytoid monocytes migrate to inflamed lymph nodes and produce large amounts of type I interferon. Nat Med. 1999 Aug;5(8):919–23.

96. Siegal FP, Kadowaki N, Shodell M, Fitzgerald-Bocarsly PA, Shah K, Ho S, et al. The nature of the principal type 1 interferon-producing cells in human blood. Science. 1999 Jun 11;284(5421):1835–7.

97. Asselin-Paturel C, Boonstra A, Dalod M, Durand I, Yessaad N, Dezutter-Dambuyant C, et al. Mouse type I IFN-producing cells are immature APCs with plasmacytoid morphology. Nat Immunol. 2001 Dec;2(12):1144–50.

98. Kadowaki N, Ho S, Antonenko S, Malefyt RW, Kastelein RA, Bazan F, et al. Subsets of human dendritic cell precursors express different toll-like receptors and respond to different microbial antigens. J Exp Med. 2001 Sep 17;194(6):863–9.

99. Villadangos JA, Young L. Antigen-presentation properties of plasmacytoid dendritic cells. Immunity. 2008 Sep 19;29(3):352–61.

100. Hoeffel G, Ripoche A-C, Matheoud D, Nascimbeni M, Escriou N, Lebon P, et al. Antigen crosspresentation by human plasmacytoid dendritic cells. Immunity. 2007 Sep;27(3):481–92.

101. Pandolfi F, Altamura S, Frosali S, Conti P. Key Role of DAMP in Inflammation, Cancer, and Tissue Repair. Clin Ther. 2016;38(5):1017–28.

102. Shekarian T, Valsesia-Wittmann S, Brody J, Michallet MC, Depil S, Caux C, et al. Pattern recognition receptors: immune targets to enhance cancer immunotherapy. Ann Oncol Off J Eur Soc Med Oncol. 2017 Aug 1;28(8):1756–66.

103. Cao L, Chang H, Shi X, Peng C, He Y. Keratin mediates the recognition of apoptotic and necrotic cells through dendritic cell receptor DEC205/CD205. Proc Natl Acad Sci U S A. 2016 22;113(47):13438–43.

104. Lim K-H, Staudt LM. Toll-like receptor signaling. Cold Spring Harb Perspect Biol. 2013 Jan 1;5(1):a011247.

105.   Jiménez-Dalmaroni MJ, Gerswhin ME, Adamopoulos IE. The critical role of toll-like receptors--From microbial recognition to autoimmunity: A comprehensive review. Autoimmun Rev. 2016 Jan;15(1):1–8.

106.   Dalod M, Chelbi R, Malissen B, Lawrence T. Dendritic cell maturation: functional specialization through signaling specificity and transcriptional programming. EMBO J. 2014 May 16;33(10):1104–16.

107.   Dambuza IM, Brown GD. C-type lectins in immunity: recent developments. Curr Opin Immunol. 2015 Feb;32:21–7.

108.   Martinez-Pomares L. The mannose receptor. J Leukoc Biol. 2012 Dec;92(6):1177–86.

109.   Iberg CA, Hawiger D. Advancing immunomodulation by in vivo antigen delivery to DEC-205 and other cell surface molecules using recombinant chimeric antibodies. Int Immunopharmacol. 2019 Aug;73:575–80.

110.   Guo M, Gong S, Maric S, Misulovin Z, Pack M, Mahnke K, et al. A monoclonal antibody to the DEC-205 endocytosis receptor on human dendritic cells. Hum Immunol. 2000 Aug;61(8):729–38.

111.   Geijtenbeek TB, Torensma R, van Vliet SJ, van Duijnhoven GC, Adema GJ, van Kooyk Y, et al. Identification of DC-SIGN, a novel dendritic cell-specific ICAM-3 receptor that supports primary immune responses. Cell. 2000 Mar 3;100(5):575–85.

112.   Mason CP, Tarr AW. Human lectins and their roles in viral infections. Mol Basel Switz. 2015 Jan 29;20(2):2229–71.

113.   Takeuchi O, Akira S. Pattern recognition receptors and inflammation. Cell. 2010 Mar 19;140(6):805–20.

114.   Miao EA, Rajan JV, Aderem A. Caspase-1-induced pyroptotic cell death. Immunol Rev. 2011 Sep;243(1):206–14.

115.   Kis-Toth K, Szanto A, Thai T-H, Tsokos GC. Cytosolic DNA-activated human dendritic cells are potent activators of the adaptive immune response. J Immunol Baltim Md 1950. 2011 Aug 1;187(3):1222–34.

116.   Takaoka A, Wang Z, Choi MK, Yanai H, Negishi H, Ban T, et al. DAI (DLM-1/ZBP1) is a cytosolic DNA sensor and an activator of innate immune response. Nature. 2007 Jul 26;448(7152):501–5.

117.   Corrales L, Matson V, Flood B, Spranger S, Gajewski TF. Innate immune signaling and regulation in cancer immunotherapy. Cell Res. 2017 Jan;27(1):96–108.

118.   Tammaro A, Derive M, Gibot S, Leemans JC, Florquin S, Dessing MC. TREM-1 and its potential ligands in non-infectious diseases: from biology to clinical perspectives. Pharmacol Ther. 2017 Sep;177:81–95.

119.   Sedlacek AL, Younker TP, Zhou YJ, Borghesi L, Shcheglova T, Mandoiu II, et al. CD91 on dendritic cells governs immunosurveillance of nascent, emerging tumors. JCI Insight. 2019 Apr 4;4(7).

120.   Wang T, Niu G, Kortylewski M, Burdelya L, Shain K, Zhang S, et al. Regulation of the innate and adaptive immune responses by Stat-3 signaling in tumor cells. Nat Med. 2004 Jan;10(1):48–54.

121.   Qian C, Cao X. Dendritic cells in the regulation of immunity and inflammation. Semin Immunol. 2018;35:3–11.

122.   Leonard WJ, Lin JX. Cytokine receptor signaling pathways. J Allergy Clin Immunol. 2000 May;105(5):877–88.

123.   Sabatté J, Maggini J, Nahmod K, Amaral MM, Martínez D, Salamone G, et al. Interplay of pathogens, cytokines and other stress signals in the regulation of dendritic cell function. Cytokine Growth Factor Rev. 2007 Apr;18(1–2):5–17.

124.   Li HS, Watowich SS. Diversification of dendritic cell subsets: Emerging roles for STAT proteins. JAK-STAT. 2013 Oct 1;2(4):e25112.

125.   Shi Z, Jiang W, Wang M, Wang X, Li X, Chen X, et al. Inhibition of JAK/STAT pathway restrains TSLP-activated dendritic cells mediated inflammatory T helper type 2 cell response in allergic rhinitis. Mol Cell Biochem. 2017 Jun;430(1–2):161–9.

126.   Wan C-K, Oh J, Li P, West EE, Wong EA, Andraski AB, et al. The cytokines IL-21 and GM-CSF have opposing regulatory roles in the apoptosis of conventional dendritic cells. Immunity. 2013 Mar 21;38(3):514–27.

127.   Villarino AV, Kanno Y, Ferdinand JR, O'Shea JJ. Mechanisms of Jak/STAT signaling in immunity and disease. J Immunol Baltim Md 1950. 2015 Jan 1;194(1):21–7.

128.   Ward-Kavanagh LK, Lin WW, Šedý JR, Ware CF. The TNF Receptor Superfamily in Co-stimulating and Co-inhibitory Responses. Immunity. 2016 17;44(5):1005–19.

129.   Caux C, Massacrier C, Vanbervliet B, Dubois B, Van Kooten C, Durand I, et al. Activation of human dendritic cells through CD40 cross-linking. J Exp Med. 1994 Oct 1;180(4):1263–72.

130.   De Trez C, Ware CF. The TNF receptor and Ig superfamily members form an integrated signaling circuit controlling dendritic cell homeostasis. Cytokine Growth Factor Rev. 2008 Aug;19(3–4):277–84.

131.   Regnault A, Lankar D, Lacabanne V, Rodriguez A, Théry C, Rescigno M, et al. Fcgamma receptor-mediated induction of dendritic cell maturation and major histocompatibility complex class I-restricted antigen presentation after immune complex internalization. J Exp Med. 1999 Jan 18;189(2):371–80.

132.   Pincetic A, Bournazos S, DiLillo DJ, Maamary J, Wang TT, Dahan R, et al. Type I and type II Fc receptors regulate innate and adaptive immunity. Nat Immunol. 2014 Aug;15(8):707–16.

133.   Boruchov AM, Heller G, Veri M-C, Bonvini E, Ravetch JV, Young JW. Activating and inhibitory IgG Fc receptors on human DCs mediate opposing functions. J Clin Invest. 2005 Oct;115(10):2914–23.

134.   Sjölin H, Robbins SH, Bessou G, Hidmark A, Tomasello E, Johansson M, et al. DAP12 signaling regulates plasmacytoid dendritic cell homeostasis and down-modulates their function during viral infection. J Immunol Baltim Md 1950. 2006 Sep 1;177(5):2908–16.

135.	Cao W, Zhang L, Rosen DB, Bover L, Watanabe G, Bao M, et al. BDCA2/Fc epsilon RI gamma complex signals through a novel BCR-like pathway in human plasmacytoid dendritic cells. PLoS Biol. 2007 Sep 11;5(10):e248.

136.	Rahim MMA, Tai L-H, Troke AD, Mahmoud AB, Abou-Samra E, Roy JG, et al. Ly49Q positively regulates type I IFN production by plasmacytoid dendritic cells in an immunoreceptor tyrosine-based inhibitory motif-dependent manner. J Immunol Baltim Md 1950. 2013 Apr 15;190(8):3994–4004.

137.	Jiménez-Reinoso A, Marin AV, Regueiro JR. Complement in basic processes of the cell. Mol Immunol. 2017;84:10–6.

138.	Murphy KM, Weaver C. Janeway Immunobiology 9th ed 2017, Garland Science. ISBN 978-0-8153-4505-3. In.

139.	Nussenzweig MC, Steinman RM. Contribution of dendritic cells to stimulation of the murine syngeneic mixed leukocyte reaction. J Exp Med. 1980 May 1;151(5):1196–212.

140.	Schuler G, Steinman RM. Murine epidermal Langerhans cells mature into potent immunostimulatory dendritic cells in vitro. J Exp Med. 1985 Mar 1;161(3):526–46.

141.	Inaba K, Steinman RM. Antibody responses to T-dependent antigens: contributions of dendritic cells and helper T lymphocytes. Adv Exp Med Biol. 1985;186:369–76.

142.	Weaver CT, Hawrylowicz CM, Unanue ER. T helper cell subsets require the expression of distinct costimulatory signals by antigen-presenting cells. Proc Natl Acad Sci U S A. 1988 Nov;85(21):8181–5.

143.	Koide S, Steinman RM. Induction of murine interleukin 1: stimuli and responsive primary cells. Proc Natl Acad Sci U S A. 1987 Jun;84(11):3802–6.

144.	Springer TA. Adhesion receptors of the immune system. Nature. 1990 Aug 2;346(6283):425–34.

145.	Larsen CP, Ritchie SC, Pearson TC, Linsley PS, Lowry RP. Functional expression of the costimulatory molecule, B7/BB1, on murine dendritic cell populations. J Exp Med. 1992 Oct 1;176(4):1215–20.

146.	Mellman I, Steinman RM. Dendritic cells: specialized and regulated antigen processing machines. Cell. 2001 Aug 10;106(3):255–8.

147.	Trombetta ES, Mellman I. Cell biology of antigen processing in vitro and in vivo. Annu Rev Immunol. 2005;23:975–1028.

148.	Randolph GJ, Angeli V, Swartz MA. Dendritic-cell trafficking to lymph nodes through lymphatic vessels. Nat Rev Immunol. 2005 Aug;5(8):617–28.

149.	Banchereau J, Steinman RM. Dendritic cells and the control of immunity. Nature. 1998 Mar 19;392(6673):245–52.

150.	Inaba K, Turley S, Iyoda T, Yamaide F, Shimoyama S, Reis e Sousa C, et al. The formation of immunogenic major histocompatibility complex class II-peptide ligands in lysosomal

compartments of dendritic cells is regulated by inflammatory stimuli. J Exp Med. 2000 Mar 20;191(6):927–36.

151.	Fiebiger E, Meraner P, Weber E, Fang IF, Stingl G, Ploegh H, et al. Cytokines regulate proteolysis in major histocompatibility complex class II-dependent antigen presentation by dendritic cells. J Exp Med. 2001 Apr 16;193(8):881–92.

152.	Pierre P, Mellman I. Developmental regulation of invariant chain proteolysis controls MHC class II trafficking in mouse dendritic cells. Cell. 1998 Jun 26;93(7):1135–45.

153.	Trombetta ES, Ebersold M, Garrett W, Pypaert M, Mellman I. Activation of lysosomal function during dendritic cell maturation. Science. 2003 Feb 28;299(5611):1400–3.

154.	Driessen C, Bryant RA, Lennon-Duménil AM, Villadangos JA, Bryant PW, Shi GP, et al. Cathepsin S controls the trafficking and maturation of MHC class II molecules in dendritic cells. J Cell Biol. 1999 Nov 15;147(4):775–90.

155.	Manoury B. Proteases: essential actors in processing antigens and intracellular toll-like receptors. Front Immunol. 2013 Sep 24;4:299.

156.	Cella M, Engering A, Pinet V, Pieters J, Lanzavecchia A. Inflammatory stimuli induce accumulation of MHC class II complexes on dendritic cells. Nature. 1997 Aug 21;388(6644):782–7.

157.	Turley SJ, Inaba K, Garrett WS, Ebersold M, Unternaehrer J, Steinman RM, et al. Transport of peptide-MHC class II complexes in developing dendritic cells. Science. 2000 Apr 21;288(5465):522–7.

158.	Vargas P, Maiuri P, Bretou M, Sáez PJ, Pierobon P, Maurin M, et al. Innate control of actin nucleation determines two distinct migration behaviours in dendritic cells. Nat Cell Biol. 2016 Jan;18(1):43–53.

159.	Pardoll DM. The blockade of immune checkpoints in cancer immunotherapy. Nat Rev Cancer. 2012 Mar 22;12(4):252–64.

160.	Ramsay AG. Immune checkpoint blockade immunotherapy to activate anti-tumour T-cell immunity. Br J Haematol. 2013 Aug;162(3):313–25.

161.	Mahoney KM, Rennert PD, Freeman GJ. Combination cancer immunotherapy and new immunomodulatory targets. Nat Rev Drug Discov. 2015 Aug;14(8):561–84.

162.	Korman AJ, Peggs KS, Allison JP. Checkpoint blockade in cancer immunotherapy. Adv Immunol. 2006;90:297–339.

163.	Tseng SY, Otsuji M, Gorski K, Huang X, Slansky JE, Pai SI, et al. B7-DC, a new dendritic cell molecule with potent costimulatory properties for T cells. J Exp Med. 2001 Apr 2;193(7):839–46.

164.	Bleijs DA, de Waal-Malefyt R, Figdor CG, van Kooyk Y. Co-stimulation of T cells results in distinct IL-10 and TNF-alpha cytokine profiles dependent on binding to ICAM-1, ICAM-2 or ICAM-3. Eur J Immunol. 1999;29(7):2248–58.

165. Wingren AG, Parra E, Varga M, Kalland T, Sjogren H-O, Hedlund G, et al. T Cell Activation Pathways: B7, LFA-3, and ICAM-1 Shape Unique T Cell Profiles. Crit Rev Immunol. 2017;37(2–6):463–81.

166. Hoshino K, Kaisho T, Iwabe T, Takeuchi O, Akira S. Differential involvement of IFN-beta in Toll-like receptor-stimulated dendritic cell activation. Int Immunol. 2002 Oct;14(10):1225–31.

167. Hoebe K, Janssen EM, Kim SO, Alexopoulou L, Flavell RA, Han J, et al. Upregulation of costimulatory molecules induced by lipopolysaccharide and double-stranded RNA occurs by Trif-dependent and Trif-independent pathways. Nat Immunol. 2003 Dec;4(12):1223–9.

168. Mattei F, Schiavoni G, Belardelli F, Tough DF. IL-15 is expressed by dendritic cells in response to type I IFN, double-stranded RNA, or lipopolysaccharide and promotes dendritic cell activation. J Immunol Baltim Md 1950. 2001 Aug 1;167(3):1179–87.

169. Mittal SK, Roche PA. Suppression of antigen presentation by IL-10. Curr Opin Immunol. 2015 Jun;34:22–7.

170. Hochrein H, O'Keeffe M, Luft T, Vandenabeele S, Grumont RJ, Maraskovsky E, et al. Interleukin (IL)-4 is a major regulatory cytokine governing bioactive IL-12 production by mouse and human dendritic cells. J Exp Med. 2000 Sep 18;192(6):823–33.

171. Maldonado-López R, De Smedt T, Michel P, Godfroid J, Pajak B, Heirman C, et al. CD8alpha+ and CD8alpha- subclasses of dendritic cells direct the development of distinct T helper cells in vivo. J Exp Med. 1999 Feb 1;189(3):587–92.

172. Ohl L, Mohaupt M, Czeloth N, Hintzen G, Kiafard Z, Zwirner J, et al. CCR7 governs skin dendritic cell migration under inflammatory and steady-state conditions. Immunity. 2004 Aug;21(2):279–88.

173. Tal O, Lim HY, Gurevich I, Milo I, Shipony Z, Ng LG, et al. DC mobilization from the skin requires docking to immobilized CCL21 on lymphatic endothelium and intralymphatic crawling. J Exp Med. 2011 Sep 26;208(10):2141–53.

174. Rescigno M, Martino M, Sutherland CL, Gold MR, Ricciardi-Castagnoli P. Dendritic cell survival and maturation are regulated by different signaling pathways. J Exp Med. 1998 Dec 7;188(11):2175–80.

175. Wendland M, Willenzon S, Kocks J, Davalos-Misslitz AC, Hammerschmidt SI, Schumann K, et al. Lymph node T cell homeostasis relies on steady state homing of dendritic cells. Immunity. 2011 Dec 23;35(6):945–57.

176. Nakano H, Burgents JE, Nakano K, Whitehead GS, Cheong C, Bortner CD, et al. Migratory properties of pulmonary dendritic cells are determined by their developmental lineage. Mucosal Immunol. 2013 Jul;6(4):678–91.

177. Zigmond E, Varol C, Farache J, Elmaliah E, Satpathy AT, Friedlander G, et al. Ly6C hi monocytes in the inflamed colon give rise to proinflammatory effector cells and migratory antigen-presenting cells. Immunity. 2012 Dec 14;37(6):1076–90.

178. Yi T, Cyster JG. EBI2-mediated bridging channel positioning supports splenic dendritic cell homeostasis and particulate antigen capture. eLife. 2013 May 14;2:e00757.

179.   Saeki H, Wu MT, Olasz E, Hwang ST. A migratory population of skin-derived dendritic cells expresses CXCR5, responds to B lymphocyte chemoattractant in vitro, and co-localizes to B cell zones in lymph nodes in vivo. Eur J Immunol. 2000 Oct;30(10):2808–14.

180.   Pattarini L, Trichot C, Bogiatzi S, Grandclaudon M, Meller S, Keuylian Z, et al. TSLP-activated dendritic cells induce human T follicular helper cell differentiation through OX40-ligand. J Exp Med. 2017 01;214(5):1529–46.

181.   Benvenuti F. The Dendritic Cell Synapse: A Life Dedicated to T Cell Activation. Front Immunol. 2016;7:70.

182.   Torres-Bacete J, Delgado-Martín C, Gómez-Moreira C, Simizu S, Rodríguez-Fernández JL. The Mammalian Sterile 20-like 1 Kinase Controls Selective CCR7-Dependent Functions in Human Dendritic Cells. J Immunol Baltim Md 1950. 2015 Aug 1;195(3):973–81.

183.   Faure-André G, Vargas P, Yuseff M-I, Heuzé M, Diaz J, Lankar D, et al. Regulation of dendritic cell migration by CD74, the MHC class II-associated invariant chain. Science. 2008 Dec 12;322(5908):1705–10.

184.   Heuzé ML, Vargas P, Chabaud M, Le Berre M, Liu Y-J, Collin O, et al. Migration of dendritic cells: physical principles, molecular mechanisms, and functional implications. Immunol Rev. 2013 Nov;256(1):240–54.

185.   Knight SC, Mertin J, Stackpoole A, Clark J. Induction of immune responses in vivo with small numbers of veiled (dendritic) cells. Proc Natl Acad Sci U S A. 1983 Oct;80(19):6032–5.

186.   Dustin ML, Baldari CT. The Immune Synapse: Past, Present, and Future. Methods Mol Biol Clifton NJ. 2017;1584:1–5.

187.   Dudek AM, Martin S, Garg AD, Agostinis P. Immature, Semi-Mature, and Fully Mature Dendritic Cells: Toward a DC-Cancer Cells Interface That Augments Anticancer Immunity. Front Immunol. 2013 Dec 11;4:438.

188.   Flavell RA, Sanjabi S, Wrzesinski SH, Licona-Limón P. The polarization of immune cells in the tumour environment by TGFbeta. Nat Rev Immunol. 2010 Aug;10(8):554–67.

189.   Li Q, Guo Z, Xu X, Xia S, Cao X. Pulmonary stromal cells induce the generation of regulatory DC attenuating T-cell-mediated lung inflammation. Eur J Immunol. 2008 Oct;38(10):2751–61.

190.   Stary G, Bangert C, Tauber M, Strohal R, Kopp T, Stingl G. Tumoricidal activity of TLR7/8-activated inflammatory dendritic cells. J Exp Med. 2007 Jun 11;204(6):1441–51.

191.   Tkach M, Kowal J, Zucchetti AE, Enserink L, Jouve M, Lankar D, et al. Qualitative differences in T-cell activation by dendritic cell-derived extracellular vesicle subtypes. EMBO J. 2017 16;36(20):3012–28.

192.   Lutz MB, Schuler G. Immature, semi-mature and fully mature dendritic cells: which signals induce tolerance or immunity? Trends Immunol. 2002 Sep;23(9):445–9.

193.   Rissoan MC, Soumelis V, Kadowaki N, Grouard G, Briere F, de Waal Malefyt R, et al. Reciprocal control of T helper cell and dendritic cell differentiation. Science. 1999 Feb 19;283(5405):1183–6.

194.   Weber C, Meiler S, Döring Y, Koch M, Drechsler M, Megens RTA, et al. CCL17-expressing dendritic cells drive atherosclerosis by restraining regulatory T cell homeostasis in mice. J Clin Invest. 2011 Jul;121(7):2898–910.

195.   Hammad H, Lambrecht BN. Dendritic cells and epithelial cells: linking innate and adaptive immunity in asthma. Nat Rev Immunol. 2008 Mar;8(3):193–204.

196.   Spörri R, Reis e Sousa C. Inflammatory mediators are insufficient for full dendritic cell activation and promote expansion of CD4+ T cell populations lacking helper function. Nat Immunol. 2005 Feb;6(2):163–70.

197.   Schulz O, Edwards AD, Schito M, Aliberti J, Manickasingham S, Sher A, et al. CD40 triggering of heterodimeric IL-12 p70 production by dendritic cells in vivo requires a microbial priming signal. Immunity. 2000 Oct;13(4):453–62.

198.   Langenkamp A, Messi M, Lanzavecchia A, Sallusto F. Kinetics of dendritic cell activation: impact on priming of TH1, TH2 and nonpolarized T cells. Nat Immunol. 2000 Oct;1(4):311–6.

199.   Kapsenberg ML. Dendritic-cell control of pathogen-driven T-cell polarization. Nat Rev Immunol. 2003 Dec;3(12):984–93.

200.   Stary G, Olive A, Radovic-Moreno AF, Gondek D, Alvarez D, Basto PA, et al. VACCINES. A mucosal vaccine against Chlamydia trachomatis generates two waves of protective memory T cells. Science. 2015 Jun 19;348(6241):aaa8205.

201.   Sandoval F, Terme M, Nizard M, Badoual C, Bureau M-F, Freyburger L, et al. Mucosal imprinting of vaccine-induced CD8$^+$ T cells is crucial to inhibit the growth of mucosal tumors. Sci Transl Med. 2013 Feb 13;5(172):172ra20.

202.   Mitchison NA. Graft rejection, the histocompatibility complex and the Langerhans' cell. Clin Exp Dermatol. 1979 Dec;4(4):489–93.

203.   Nossal GJ. Negative selection of lymphocytes. Cell. 1994 Jan 28;76(2):229–39.

204.   Li MO, Flavell RA. TGF-beta: a master of all T cell trades. Cell. 2008 Aug 8;134(3):392–404.

205.   Miller JF, Morahan G. Peripheral T cell tolerance. Annu Rev Immunol. 1992;10:51–69.

206.   Jonuleit H, Schmitt E, Schuler G, Knop J, Enk AH. Induction of interleukin 10-producing, nonproliferating CD4(+) T cells with regulatory properties by repetitive stimulation with allogeneic immature human dendritic cells. J Exp Med. 2000 Nov 6;192(9):1213–22.

207.   Dhodapkar MV, Steinman RM, Krasovsky J, Munz C, Bhardwaj N. Antigen-specific inhibition of effector T cell function in humans after injection of immature dendritic cells. J Exp Med. 2001 Jan 15;193(2):233–8.

208.   Mahnke K, Qian Y, Knop J, Enk AH. Induction of CD4+/CD25+ regulatory T cells by targeting of antigens to immature dendritic cells. Blood. 2003 Jun 15;101(12):4862–9.

209.   Zou T, Caton AJ, Koretzky GA, Kambayashi T. Dendritic cells induce regulatory T cell proliferation through antigen-dependent and -independent interactions. J Immunol Baltim Md 1950. 2010 Sep 1;185(5):2790–9.

210.   Peron G, de Lima Thomaz L, Camargo da Rosa L, Thomé R, Cardoso Verinaud LM. Modulation of dendritic cell by pathogen antigens: Where do we stand? Immunol Lett. 2018;196:91–102.

211.   Schülke S. Induction of Interleukin-10 Producing Dendritic Cells As a Tool to Suppress Allergen-Specific T Helper 2 Responses. Front Immunol. 2018;9:455.

212.   Liang X, Lu L, Chen Z, Vickers T, Zhang H, Fung JJ, et al. Administration of dendritic cells transduced with antisense oligodeoxyribonucleotides targeting CD80 or CD86 prolongs allograft survival. Transplantation. 2003 Aug 27;76(4):721–9.

213.   Zheng X, Suzuki M, Ichim TE, Zhang X, Sun H, Zhu F, et al. Treatment of autoimmune arthritis using RNA interference-modulated dendritic cells. J Immunol Baltim Md 1950. 2010 Jun 1;184(11):6457–64.

214.   Coates PT, Krishnan R, Kireta S, Johnston J, Russ GR. Human myeloid dendritic cells transduced with an adenoviral interleukin-10 gene construct inhibit human skin graft rejection in humanized NOD-scid chimeric mice. Gene Ther. 2001 Aug;8(16):1224–33.

215.   Penna G, Amuchastegui S, Giarratana N, Daniel KC, Vulcano M, Sozzani S, et al. 1,25-Dihydroxyvitamin D3 selectively modulates tolerogenic properties in myeloid but not plasmacytoid dendritic cells. J Immunol Baltim Md 1950. 2007 Jan 1;178(1):145–53.

216.   Sato K, Yamashita N, Matsuyama T. Human peripheral blood monocyte-derived interleukin-10-induced semi-mature dendritic cells induce anergic CD4(+) and CD8(+) T cells via presentation of the internalized soluble antigen and cross-presentation of the phagocytosed necrotic cellular fragments. Cell Immunol. 2002 Feb;215(2):186–94.

217.   Geissmann F, Revy P, Regnault A, Lepelletier Y, Dy M, Brousse N, et al. TGF-beta 1 prevents the noncognate maturation of human dendritic Langerhans cells. J Immunol Baltim Md 1950. 1999 Apr 15;162(8):4567–75.

218.   Geissmann F, Revy P, Brousse N, Lepelletier Y, Folli C, Durandy A, et al. Retinoids regulate survival and antigen presentation by immature dendritic cells. J Exp Med. 2003 Aug 18;198(4):623–34.

219.   Rutella S, Bonanno G, Procoli A, Mariotti A, de Ritis DG, Curti A, et al. Hepatocyte growth factor favors monocyte differentiation into regulatory interleukin (IL)-10++IL-12low/neg accessory cells with dendritic-cell features. Blood. 2006 Jul 1;108(1):218–27.

220.   Jiang A, Bloom O, Ono S, Cui W, Unternaehrer J, Jiang S, et al. Disruption of E-cadherin-mediated adhesion induces a functionally distinct pathway of dendritic cell maturation. Immunity. 2007 Oct;27(4):610–24.

221.   Gonzalez-Rey E, Chorny A, Fernandez-Martin A, Ganea D, Delgado M. Vasoactive intestinal peptide generates human tolerogenic dendritic cells that induce CD4 and CD8 regulatory T cells. Blood. 2006 May 1;107(9):3632–8.

222.   Baron C, Raposo G, Scholl SM, Bausinger H, Tenza D, Bohbot A, et al. Modulation of MHC class II transport and lysosome distribution by macrophage-colony stimulating factor in human dendritic cells derived from monocytes. J Cell Sci. 2001 Mar;114(Pt 5):999–1010.

223.   Gerner MY, Mescher MF. Antigen processing and MHC-II presentation by dermal and tumor-infiltrating dendritic cells. J Immunol Baltim Md 1950. 2009 Mar 1;182(5):2726–37.

224.   Iliev ID, Mileti E, Matteoli G, Chieppa M, Rescigno M. Intestinal epithelial cells promote colitis-protective regulatory T-cell differentiation through dendritic cell conditioning. Mucosal Immunol. 2009 Jul;2(4):340–50.

225.   Denning TL, Norris BA, Medina-Contreras O, Manicassamy S, Geem D, Madan R, et al. Functional specializations of intestinal dendritic cell and macrophage subsets that control Th17 and regulatory T cell responses are dependent on the T cell/APC ratio, source of mouse strain, and regional localization. J Immunol Baltim Md 1950. 2011 Jul 15;187(2):733–47.

226.   Karumuthil-Melethil S, Perez N, Li R, Vasu C. Induction of innate immune response through TLR2 and dectin 1 prevents type 1 diabetes. J Immunol Baltim Md 1950. 2008 Dec 15;181(12):8323–34.

227.   Depaolo RW, Tang F, Kim I, Han M, Levin N, Ciletti N, et al. Toll-like receptor 6 drives differentiation of tolerogenic dendritic cells and contributes to LcrV-mediated plague pathogenesis. Cell Host Microbe. 2008 Oct 16;4(4):350–61.

228.   Wenink MH, Santegoets KCM, Roelofs MF, Huijbens R, Koenen HJPM, van Beek R, et al. The inhibitory Fc gamma IIb receptor dampens TLR4-mediated immune responses and is selectively up-regulated on dendritic cells from rheumatoid arthritis patients with quiescent disease. J Immunol Baltim Md 1950. 2009 Oct 1;183(7):4509–20.

229.   Gil-Pulido J, Zernecke A. Antigen-presenting dendritic cells in atherosclerosis. Eur J Pharmacol. 2017 Dec 5;816:25–31.

230.   Zelenay S, Reis e Sousa C. Adaptive immunity after cell death. Trends Immunol. 2013 Jul;34(7):329–35.

231.   Spranger S, Bao R, Gajewski TF. Melanoma-intrinsic β-catenin signalling prevents anti-tumour immunity. Nature. 2015 Jul 9;523(7559):231–5.

232.   Pasparakis M, Vandenabeele P. Necroptosis and its role in inflammation. Nature. 2015 Jan 15;517(7534):311–20.

233.   Galluzzi L, Buqué A, Kepp O, Zitvogel L, Kroemer G. Immunogenic cell death in cancer and infectious disease. Nat Rev Immunol. 2017;17(2):97–111.

234.   Aoto K, Mimura K, Okayama H, Saito M, Chida S, Noda M, et al. Immunogenic tumor cell death induced by chemotherapy in patients with breast cancer and esophageal squamous cell carcinoma. Oncol Rep. 2018 Jan;39(1):151–9.

235.   Engelhardt JJ, Boldajipour B, Beemiller P, Pandurangi P, Sorensen C, Werb Z, et al. Marginating dendritic cells of the tumor microenvironment cross-present tumor antigens and stably engage tumor-specific T cells. Cancer Cell. 2012 Mar 20;21(3):402–17.

236.   Michea P, Noël F, Zakine E, Czerwinska U, Sirven P, Abouzid O, et al. Adjustment of dendritic cells to the breast-cancer microenvironment is subset specific. Nat Immunol. 2018;19(8):885–97.

237.   Lavin Y, Kobayashi S, Leader A, Amir E-AD, Elefant N, Bigenwald C, et al. Innate Immune Landscape in Early Lung Adenocarcinoma by Paired Single-Cell Analyses. Cell. 2017 04;169(4):750-765.e17.

238.	Salmon H, Idoyaga J, Rahman A, Leboeuf M, Remark R, Jordan S, et al. Expansion and Activation of CD103(+) Dendritic Cell Progenitors at the Tumor Site Enhances Tumor Responses to Therapeutic PD-L1 and BRAF Inhibition. Immunity. 2016 Apr 19;44(4):924–38.

239.	Bachem A, Güttler S, Hartung E, Ebstein F, Schaefer M, Tannert A, et al. Superior antigen cross-presentation and XCR1 expression define human CD11c+CD141+ cells as homologues of mouse CD8+ dendritic cells. J Exp Med. 2010 Jun 7;207(6):1273–81.

240.	Crozat K, Guiton R, Contreras V, Feuillet V, Dutertre C-A, Ventre E, et al. The XC chemokine receptor 1 is a conserved selective marker of mammalian cells homologous to mouse CD8alpha+ dendritic cells. J Exp Med. 2010 Jun 7;207(6):1283–92.

241.	Spranger S, Dai D, Horton B, Gajewski TF. Tumor-Residing Batf3 Dendritic Cells Are Required for Effector T Cell Trafficking and Adoptive T Cell Therapy. Cancer Cell. 2017 08;31(5):711-723.e4.

242.	Segura E, Durand M, Amigorena S. Similar antigen cross-presentation capacity and phagocytic functions in all freshly isolated human lymphoid organ–resident dendritic cells. J Exp Med. 2013 May 6;210(5):1035–47.

243.	Gerner MY, Casey KA, Mescher MF. Defective MHC class II presentation by dendritic cells limits CD4 T cell help for antitumor CD8 T cell responses. J Immunol Baltim Md 1950. 2008 Jul 1;181(1):155–64.

244.	Broz ML, Binnewies M, Boldajipour B, Nelson AE, Pollack JL, Erle DJ, et al. Dissecting the tumor myeloid compartment reveals rare activating antigen-presenting cells critical for T cell immunity. Cancer Cell. 2014 Nov 10;26(5):638–52.

245.	Bedoui S, Heath WR, Mueller SN. CD4(+) T-cell help amplifies innate signals for primary CD8(+) T-cell immunity. Immunol Rev. 2016;272(1):52–64.

246.	Kim H-J, Cantor H. CD4 T-cell subsets and tumor immunity: the helpful and the not-so-helpful. Cancer Immunol Res. 2014 Feb;2(2):91–8.

247.	Fuertes MB, Kacha AK, Kline J, Woo S-R, Kranz DM, Murphy KM, et al. Host type I IFN signals are required for antitumor CD8+ T cell responses through CD8{alpha}+ dendritic cells. J Exp Med. 2011 Sep 26;208(10):2005–16.

248.	Diamond MS, Kinder M, Matsushita H, Mashayekhi M, Dunn GP, Archambault JM, et al. Type I interferon is selectively required by dendritic cells for immune rejection of tumors. J Exp Med. 2011 Sep 26;208(10):1989–2003.

249.	Roberts EW, Broz ML, Binnewies M, Headley MB, Nelson AE, Wolf DM, et al. Critical Role for CD103(+)/CD141(+) Dendritic Cells Bearing CCR7 for Tumor Antigen Trafficking and Priming of T Cell Immunity in Melanoma. Cancer Cell. 2016 08;30(2):324–36.

250.	Dieu-Nosjean M-C, Antoine M, Danel C, Heudes D, Wislez M, Poulot V, et al. Long-term survival for patients with non-small-cell lung cancer with intratumoral lymphoid structures. J Clin Oncol Off J Am Soc Clin Oncol. 2008 Sep 20;26(27):4410–7.

251.	Zhang X, Huang H, Yuan J, Sun D, Hou W-S, Gordon J, et al. CD4-8- dendritic cells prime CD4+ T regulatory 1 cells to suppress antitumor immunity. J Immunol Baltim Md 1950. 2005 Sep 1;175(5):2931–7.

252.   Ghiringhelli F, Puig PE, Roux S, Parcellier A, Schmitt E, Solary E, et al. Tumor cells convert immature myeloid dendritic cells into TGF-beta-secreting cells inducing CD4+CD25+ regulatory T cell proliferation. J Exp Med. 2005 Oct 3;202(7):919–29.

253.   Dumitriu IE, Dunbar DR, Howie SE, Sethi T, Gregory CD. Human dendritic cells produce TGF-beta 1 under the influence of lung carcinoma cells and prime the differentiation of CD4+CD25+Foxp3+ regulatory T cells. J Immunol Baltim Md 1950. 2009 Mar 1;182(5):2795–807.

254.   Liu VC, Wong LY, Jang T, Shah AH, Park I, Yang X, et al. Tumor evasion of the immune system by converting CD4+CD25- T cells into CD4+CD25+ T regulatory cells: role of tumor-derived TGF-beta. J Immunol Baltim Md 1950. 2007 Mar 1;178(5):2883–92.

255.   Chen Y-X, Man K, Ling GS, Chen Y, Sun B-S, Cheng Q, et al. A crucial role for dendritic cell (DC) IL-10 in inhibiting successful DC-based immunotherapy: superior antitumor immunity against hepatocellular carcinoma evoked by DC devoid of IL-10. J Immunol Baltim Md 1950. 2007 Nov 1;179(9):6009–15.

256.   Munn DH, Sharma MD, Mellor AL. Ligation of B7-1/B7-2 by human CD4+ T cells triggers indoleamine 2,3-dioxygenase activity in dendritic cells. J Immunol Baltim Md 1950. 2004 Apr 1;172(7):4100–10.

257.   Fallarino F, Asselin-Paturel C, Vacca C, Bianchi R, Gizzi S, Fioretti MC, et al. Murine plasmacytoid dendritic cells initiate the immunosuppressive pathway of tryptophan catabolism in response to CD200 receptor engagement. J Immunol Baltim Md 1950. 2004 Sep 15;173(6):3748–54.

258.   Flies DB, Higuchi T, Harris JC, Jha V, Gimotty PA, Adams SF. Immune checkpoint blockade reveals the stimulatory capacity of tumor-associated CD103(+) dendritic cells in late-stage ovarian cancer. Oncoimmunology. 2016 Aug;5(8):e1185583.

259.   Kuipers H, Muskens F, Willart M, Hijdra D, van Assema FBJ, Coyle AJ, et al. Contribution of the PD-1 ligands/PD-1 signaling pathway to dendritic cell-mediated CD4+ T cell activation. Eur J Immunol. 2006 Sep;36(9):2472–82.

260.   Krempski J, Karyampudi L, Behrens MD, Erskine CL, Hartmann L, Dong H, et al. Tumor-infiltrating programmed death receptor-1+ dendritic cells mediate immune suppression in ovarian cancer. J Immunol Baltim Md 1950. 2011 Jun 15;186(12):6905–13.

261.   Oderup C, Cederbom L, Makowska A, Cilio CM, Ivars F. Cytotoxic T lymphocyte antigen-4-dependent down-modulation of costimulatory molecules on dendritic cells in CD4+ CD25+ regulatory T-cell-mediated suppression. Immunology. 2006 Jun;118(2):240–9.

262.   Ruffell B, Chang-Strachan D, Chan V, Rosenbusch A, Ho CMT, Pryer N, et al. Macrophage IL-10 Blocks CD8+ T Cell-Dependent Responses to Chemotherapy by Suppressing IL-12 Expression in Intratumoral Dendritic Cells. Cancer Cell. 2014 Nov;26(5):623–37.

263.   Reis M, Mavin E, Nicholson L, Green K, Dickinson AM, Wang X-N. Mesenchymal Stromal Cell-Derived Extracellular Vesicles Attenuate Dendritic Cell Maturation and Function. Front Immunol. 2018;9:2538.

264.   Kaliński P, Hilkens CM, Snijders A, Snijdewint FG, Kapsenberg ML. IL-12-deficient dendritic cells, generated in the presence of prostaglandin E2, promote type 2 cytokine production in maturing human naive T helper cells. J Immunol Baltim Md 1950. 1997 Jul 1;159(1):28–35.

265.   Gabrilovich DI, Chen HL, Girgis KR, Cunningham HT, Meny GM, Nadaf S, et al. Production of vascular endothelial growth factor by human tumors inhibits the functional maturation of dendritic cells. Nat Med. 1996 Oct;2(10):1096–103.

266.   Lo AS, Gorak-Stolinska P, Bachy V, Ibrahim MA, Kemeny DM, Maher J. Modulation of dendritic cell differentiation by colony-stimulating factor-1: role of phosphatidylinositol 3'-kinase and delayed caspase activation. J Leukoc Biol. 2007 Dec;82(6):1446–54.

267.   Zhou Z, Li W, Song Y, Wang L, Zhang K, Yang J, et al. Growth differentiation factor-15 suppresses maturation and function of dendritic cells and inhibits tumor-specific immune response. PloS One. 2013;8(11):e78618.

268.   Demoulin SA, Somja J, Duray A, Guénin S, Roncarati P, Delvenne PO, et al. Cervical (pre)neoplastic microenvironment promotes the emergence of tolerogenic dendritic cells via RANKL secretion. Oncoimmunology. 2015 Jun;4(6):e1008334.

269.   Gottfried E, Kunz-Schughart LA, Ebner S, Mueller-Klieser W, Hoves S, Andreesen R, et al. Tumor-derived lactic acid modulates dendritic cell activation and antigen expression. Blood. 2006 Mar 1;107(5):2013–21.

270.   Cubillos-Ruiz JR, Bettigole SE, Glimcher LH. Molecular Pathways: Immunosuppressive Roles of IRE1α-XBP1 Signaling in Dendritic Cells of the Tumor Microenvironment. Clin Cancer Res Off J Am Assoc Cancer Res. 2016 May 1;22(9):2121–6.

271.   Hwang SL, Chung NP-Y, Chan JK-Y, Lin C-LS. Indoleamine 2, 3-dioxygenase (IDO) is essential for dendritic cell activation and chemotactic responsiveness to chemokines. Cell Res. 2005 Mar;15(3):167–75.

272.   Youlin K, Weiyang H, Simin L, Xin G. Prostaglandin E2 Inhibits Prostate Cancer Progression by Countervailing Tumor Microenvironment-Induced Impairment of Dendritic Cell Migration through LXRα/CCR7 Pathway. J Immunol Res. 2018;2018:5808962.

273.   Constantino J, Gomes C, Falcão A, Neves BM, Cruz MT. Dendritic cell-based immunotherapy: a basic review and recent advances. Immunol Res. 2017;65(4):798–810.

274.   Kantoff PW, Higano CS, Shore ND, Berger ER, Small EJ, Penson DF, et al. Sipuleucel-T immunotherapy for castration-resistant prostate cancer. N Engl J Med. 2010 Jul 29;363(5):411–22.

275.   Mohammadzadeh M, Shirmohammadi M, Ghojazadeh M, Nikniaz L, Raeisi M, Aghdas SAM. Dendritic cells pulsed with prostate-specific membrane antigen in metastatic castration-resistant prostate cancer patients: a systematic review and meta-analysis. Prostate Int. 2018 Dec;6(4):119–25.

276.   Tel J, Aarntzen EHJG, Baba T, Schreibelt G, Schulte BM, Benitez-Ribas D, et al. Natural human plasmacytoid dendritic cells induce antigen-specific T-cell responses in melanoma patients. Cancer Res. 2013 Feb 1;73(3):1063–75.

277.   Schreibelt G, Bol KF, Westdorp H, Wimmers F, Aarntzen EHJG, Duiveman-de Boer T, et al. Effective Clinical Responses in Metastatic Melanoma Patients after Vaccination with Primary Myeloid Dendritic Cells. Clin Cancer Res Off J Am Assoc Cancer Res. 2016 01;22(9):2155–66.

278.   Deng L, Liang H, Xu M, Yang X, Burnette B, Arina A, et al. STING-Dependent Cytosolic DNA Sensing Promotes Radiation-Induced Type I Interferon-Dependent Antitumor Immunity in Immunogenic Tumors. Immunity. 2014 Nov 20;41(5):843–52.

279.   Woo S-R, Fuertes MB, Corrales L, Spranger S, Furdyna MJ, Leung MYK, et al. STING-dependent cytosolic DNA sensing mediates innate immune recognition of immunogenic tumors. Immunity. 2014 Nov 20;41(5):830–42.

280.   Corrales L, McWhirter SM, Dubensky TW, Gajewski TF. The host STING pathway at the interface of cancer and immunity. J Clin Invest. 2016 01;126(7):2404–11.

281.   Ho NI, Huis In 't Veld LGM, Raaijmakers TK, Adema GJ. Adjuvants Enhancing Cross-Presentation by Dendritic Cells: The Key to More Effective Vaccines? Front Immunol. 2018;9:2874.

282.   Cerboni S, Jeremiah N, Gentili M, Gehrmann U, Conrad C, Stolzenberg M-C, et al. Intrinsic antiproliferative activity of the innate sensor STING in T lymphocytes. J Exp Med. 2017 05;214(6):1769–85.

283.   Hammerich L, Marron TU, Upadhyay R, Svensson-Arvelund J, Dhainaut M, Hussein S, et al. Systemic clinical tumor regressions and potentiation of PD1 blockade with in situ vaccination. Nat Med. 2019;25(5):814–24.

284.   Desch AN, Gibbings SL, Clambey ET, Janssen WJ, Slansky JE, Kedl RM, et al. Dendritic cell subsets require cis-activation for cytotoxic CD8 T-cell induction. Nat Commun. 2014 Aug 19;5:4674.

285.   Kawarada Y, Ganss R, Garbi N, Sacher T, Arnold B, Hämmerling GJ. NK- and CD8(+) T cell-mediated eradication of established tumors by peritumoral injection of CpG-containing oligodeoxynucleotides. J Immunol Baltim Md 1950. 2001 Nov 1;167(9):5247–53.

286.   Heckelsmiller K, Rall K, Beck S, Schlamp A, Seiderer J, Jahrsdörfer B, et al. Peritumoral CpG DNA elicits a coordinated response of CD8 T cells and innate effectors to cure established tumors in a murine colon carcinoma model. J Immunol Baltim Md 1950. 2002 Oct 1;169(7):3892–9.

287.   Wilgenhof S, Corthals J, Heirman C, van Baren N, Lucas S, Kvistborg P, et al. Phase II Study of Autologous Monocyte-Derived mRNA Electroporated Dendritic Cells (TriMixDC-MEL) Plus Ipilimumab in Patients With Pretreated Advanced Melanoma. J Clin Oncol Off J Am Soc Clin Oncol. 2016 Apr 20;34(12):1330–8.

288.   Ma Y, Adjemian S, Mattarollo SR, Yamazaki T, Aymeric L, Yang H, et al. Anticancer chemotherapy-induced intratumoral recruitment and differentiation of antigen-presenting cells. Immunity. 2013 Apr 18;38(4):729–41.

289.   Gupta A, Probst HC, Vuong V, Landshammer A, Muth S, Yagita H, et al. Radiotherapy promotes tumor-specific effector CD8+ T cells via dendritic cell activation. J Immunol Baltim Md 1950. 2012 Jul 15;189(2):558–66.

290.   Bockel S, Durand B, Deutsch E. Combining radiation therapy and cancer immune therapies: From preclinical findings to clinical applications. Cancer Radiother J Soc Francaise Radiother Oncol. 2018 Oct;22(6–7):567–80.

291.   Levy A, Nigro G, Sansonetti PJ, Deutsch E. Candidate immune biomarkers for radioimmunotherapy. Biochim Biophys Acta Rev Cancer. 2017 Aug;1868(1):58–68.

292.   Cao M-D, Chen Z-D, Xing Y. Gamma irradiation of human dendritic cells influences proliferation and cytokine profile of T cells in autologous mixed lymphocyte reaction. Cell Biol Int. 2004;28(3):223–8.

293.   Grandclaudon M, Perrot-Dockès M, Trichot C, Mostafa-Abouzid O, Abou-Jaoudé W, Berger F, Hupé P, Thieffry D, Sansonnet L, Chiquet J, Levy-Leduc C, Soumelis V. A Quantitative Multivariate Model of Human Dendritic Cell-T Helper Cell Communication. Available at SSRN: https://ssrn.com/abstract=3353217. Accepted in Cell in July 2019.

294.   Alculumbre SG, Saint-André V, Di Domizio J, Vargas P, Sirven P, Bost P, et al. Diversification of human plasmacytoid predendritic cells in response to a single stimulus. Nat Immunol. 2018 Jan;19(1):63–75.

295.   Taghavi M, Mortaz E, Khosravi A, Vahedi G, Folkerts G, Varahram M, et al. Zymosan attenuates melanoma growth progression, increases splenocyte proliferation and induces TLR-2/4 and TNF-α expression in mice. J Inflamm Lond Engl. 2018;15:5.

296.   Hasegawa M, Fujimoto M, Matsushita T, Hamaguchi Y, Takehara K. Augmented ICOS expression in patients with early diffuse cutaneous systemic sclerosis. Rheumatol Oxf Engl. 2013 Feb;52(2):242–51.

297.   Marinelli O, Nabissi M, Morelli MB, Torquati L, Amantini C, Santoni G. ICOS-L as a Potential Therapeutic Target for Cancer Immunotherapy. Curr Protein Pept Sci. 2018;19(11):1107–13.

298.   Amatore F, Gorvel L, Olive D. Inducible Co-Stimulator (ICOS) as a potential therapeutic target for anti-cancer therapy. Expert Opin Ther Targets. 2018;22(4):343–51.

299.   Sato T, Kanai T, Watanabe M, Sakuraba A, Okamoto S, Nakai T, et al. Hyperexpression of inducible costimulator and its contribution on lamina propria T cells in inflammatory bowel disease. Gastroenterology. 2004 Mar;126(3):829–39.

300.   Fan X, Quezada SA, Sepulveda MA, Sharma P, Allison JP. Engagement of the ICOS pathway markedly enhances efficacy of CTLA-4 blockade in cancer immunotherapy. J Exp Med. 2014 Apr 7;211(4):715–25.

301.   Cheng N, Watkins-Schulz R, Junkins RD, David CN, Johnson BM, Montgomery SA, et al. A nanoparticle-incorporated STING activator enhances antitumor immunity in PD-L1-insensitive models of triple-negative breast cancer. JCI Insight. 2018 Nov 15;3(22).

302.   Yang X, Chu Y, Wang Y, Zhang R, Xiong S. Targeted in vivo expression of IFN-gamma-inducible protein 10 induces specific antitumor activity. J Leukoc Biol. 2006 Dec;80(6):1434–44.

303.   Gorbachev AV, Kobayashi H, Kudo D, Tannenbaum CS, Finke JH, Shu S, et al. CXC chemokine ligand 9/monokine induced by IFN-gamma production by tumor cells is critical for T cell-mediated suppression of cutaneous tumors. J Immunol Baltim Md 1950. 2007 Feb 15;178(4):2278–86.

304.   Cristescu R, Mogg R, Ayers M, Albright A, Murphy E, Yearley J, et al. Pan-tumor genomic biomarkers for PD-1 checkpoint blockade-based immunotherapy. Science. 2018 12;362(6411).

305.   Verweij J, Hendriks HR, Zwierzina H, Cancer Drug Development Forum. Innovation in oncology clinical trial design. Cancer Treat Rev. 2019 Mar;74:15–20.

306.   Burns PB, Rohrich RJ, Chung KC. The levels of evidence and their role in evidence-based medicine. Plast Reconstr Surg. 2011 Jul;128(1):305–10.

307.   Amin, M.B., Edge, S., Greene, F., Byrd, D.R., Brookland, R.K., Washington, M.K., Gershenwald, J.E., Compton, C.C., Hess, K.R., Sullivan, D.C., Jessup, J.M., Brierley, J.D., Gaspar, L.E., Schilsky, R.L., Balch, C.M., Winchester, D.P., Asare, E.A., Madera, M., Gress, D.M., Meyer, L.R. AJCC cancer staging manual. 8th ed. New York: Springer; 2017.

308.   Duffy MJ, McGowan PM, Harbeck N, Thomssen C, Schmitt M. uPA and PAI-1 as biomarkers in breast cancer: validated for clinical use in level-of-evidence-1 studies. Breast Cancer Res BCR. 2014 Aug 22;16(4):428.

309.   Look MP, van Putten WLJ, Duffy MJ, Harbeck N, Christensen IJ, Thomssen C, et al. Pooled analysis of prognostic impact of urokinase-type plasminogen activator and its inhibitor PAI-1 in 8377 breast cancer patients. J Natl Cancer Inst. 2002 Jan 16;94(2):116–28.

310.   Gontarz M, Wyszyńska-Pawelec G, Zapała J, Czopek J, Lazar A, Tomaszewska R. Immunohistochemical predictors in squamous cell carcinoma of the tongue and floor of the mouth. Head Neck. 2016;38 Suppl 1:E747-753.

311.   Chen C-H, Chien C-Y, Huang C-C, Hwang C-F, Chuang H-C, Fang F-M, et al. Expression of FLJ10540 is correlated with aggressiveness of oral cavity squamous cell carcinoma by stimulating cell migration and invasion through increased FOXM1 and MMP-2 activity. Oncogene. 2009 Jul 30;28(30):2723–37.

312.   Mehnert JM, Monjazeb AM, Beerthuijzen JMT, Collyar D, Rubinstein L, Harris LN. The Challenge for Development of Valuable Immuno-oncology Biomarkers. Clin Cancer Res Off J Am Assoc Cancer Res. 2017 01;23(17):4970–9.

313.   Xu D, Peltz G. Can Humanized Mice Predict Drug "Behavior" in Humans? Annu Rev Pharmacol Toxicol. 2016;56:323–38.

314.   De La Rochere P, Guil-Luna S, Decaudin D, Azar G, Sidhu SS, Piaggio E. Humanized Mice for the Study of Immuno-Oncology. Trends Immunol. 2018;39(9):748–63.

315.   Hadad SM, Coates P, Jordan LB, Dowling RJO, Chang MC, Done SJ, et al. Evidence for biological effects of metformin in operable breast cancer: biomarker analysis in a pre-operative window of opportunity randomized trial. Breast Cancer Res Treat. 2015 Feb;150(1):149–55.

316.   Gomez-Roca C, Even C, Tourneau CL, Rotllan NB, Delord J-P, Sarini J, et al. Abstract 5001: Open-label, non-randomized, exploratory pre-operative window-of-opportunity trial to investigate the pharmacokinetics and pharmacodynamics of the smac mimetic Debio 1143 in patients with resectable squamous cell carcinoma of the head and neck. In: Clinical Research (Excluding Clinical Trials) [Internet]. American Association for Cancer Research; 2019 [cited 2019 Aug 7]. p. 5001–5001. Available from: http://cancerres.aacrjournals.org/lookup/doi/10.1158/1538-7445.SABCS18-5001

317.   Stachura J, Wachowska M, Kilarski WW, Güç E, Golab J, Muchowicz A. The dual role of tumor lymphatic vessels in dissemination of metastases and immune response development. Oncoimmunology. 2016 Jul;5(7):e1182278.

318.   Fransen MF, Schoonderwoerd M, Knopf P, Camps MG, Hawinkels LJ, Kneilling M, et al. Tumor-draining lymph nodes are pivotal in PD-1/PD-L1 checkpoint therapy. JCI Insight. 2018 06;3(23).

319.   Teichgraeber JF, Clairmont AA. The incidence of occult metastases for cancer of the oral tongue and floor of the mouth: treatment rationale. Head Neck Surg. 1984 Oct;7(1):15–21.

320.   de Bree R, Takes RP, Castelijns JA, Medina JE, Stoeckli SJ, Mancuso AA, et al. Advances in diagnostic modalities to detect occult lymph node metastases in head and neck squamous cell carcinoma. Head Neck. 2015 Dec;37(12):1829–39.

ACKNOWLEDGEMENTS

8. ACKNOWLEDGEMENTS

which will be a transition between my PhD and my upcoming post-doc.

Future? It's all here: the next generation dual-cell therapy producing heart-shaped cancer-cell killing mediators!

Titre: Les cellules dendritiques dans le micro-environnement tumoral des cancers ORL : des mécanismes aux biomarqueurs

Mots clés : Microenvironnement tumoral ; Carcinomes épidermoïdes des voies aéro-digestives supérieures ; Cellules dendritiques ; Analyse intégrée ; Biomarqueurs

Résumé : L'objectif de ce travail était de comprendre l'état moléculaire des cellules dendritiques (CD) dans le micro-environnement tumoral. En intégrant l'analyse de tumeurs humaines par cytométrie en flux, de transcriptome, de secretome tumoral et l'analyse d'une base de données d'interaction CD-lymphocyte T générées in vitro, j'ai obtenu 2 résultats majeurs. Tout d'abord, nous proposons une nouvelle classification de CD activées humaines, qui sont soit « sécrétantes », c'est-à-dire spécialisées dans la production de cytokines et chemokines, soit « aidantes » c'est-à-dire spécialisées dans l'induction de la sécrétion de nombreuses cytokines T helper après co-culture. Les CD infiltrant les tumeurs ORL inflammées correspondaient au type « sécrétantes ».

Au-delà du nouveau concept biologique, cette classification est base théorique importante pour l'immunothérapie à base d'adjuvants. Deuxièmement, nous avons montré que l'inflammation tumorale n'était pas un facteur pronostic majeur des cancers ORL, mais que MMP2 et l'effraction extra-capsulaire étaient des facteurs pronostiques indépendants de la survie liée à la maladie. Nous avons pu classer les patients en 4 niveaux de risque et montré qu'ils avaient des chances équivalentes de réponse à l'immunothérapie. Nos données sont une base pour un essai clinique dirigé par biomarqueur, proposant de la chimiothérapie ou de l'immunothérapie néoadjuvantes, dans le but de diminuer le pourcentage de patients présentant des récidives sévères et précoces.

Title: Dendritic cells in Head and Neck cancer microenvironment: from mechanisms to biomarkers

Keywords: Tumor microenvironment; Head and neck squamous cell cancer; Dendritic cells ; Integrated analysis; Biomarker

Abstract: The objective of the thesis was to decipher the molecular state of tumor infiltrating dendritic cell (DC) and their relation to the tumor microenvironment. By combining the analysis of human tumor samples by flow cytometry and RNA sequencing, of tumor secretome and of a large dataset of in vitro DC- T cell interactions I obtained 2 main findings. First, we reported a novel classification of human activated DC, that are either "secretory" that is specialized in secreting cytokines and chemokines, or "helper" that is specialized at inducing the secretion of a broad range of T helper cytokines after cell co-culture. DC infiltrating inflamed human head and neck cancer matched the "secretory" phenotypic and transcriptomic signatures. Beyond this novel

biological concept, this classification is of importance as a theoretical basis for adjuvant-based immunotherapy. Secondly, we showed that tumor inflammation was not the main prognostic factor for oral cavity cancer (OCC) patients, but that MMP2 and the presence of extra-nodal extension were independent predictors of reduced disease-specific survival. We could stratify OCC into 4 prognostic groups and showed that they had similar expected rates of response to immunotherapy. Our data may serve to design a biomarker-driven clinical trial proposing neoadjuvant chemotherapy or immunotherapy to high-risk patients, with the goal of reducing the percentage of OCC patients that will present with early and severe recurrences.